The Roles of Histone Deacetylases and Histone Phosphorylation in Transcription and Nucleotide Excision Repair in *Saccharomyces cerevisiae*

by

Charlotte O'Connell

Thesis submitted in partial fulfilment of the requirements for the degree of Doctor of Philosophy

School of Medicine,

Cardiff University

ProQuest LLC
789 East Eisenhower Parkway
P.O. Box 1346
Ann Arbor, MI 48106-1346

Declaration

This work has not previously been accepted in substance for any degree and is not concurrently submitted in candidature for any degree.

Signed ..... (candidate) Date 08/02/07

Statement 1

This thesis is being submitted in partial fulfilment of the requirements for the degree of PhD.

Signed ..... (candidate) Date 08/02/07

Statement 2

This thesis is the result of my own investigation, except where otherwise stated. Other sources are acknowledged by explicit references.

Signed ..... (candidate) Date 08/02/07

Statement 3

I hereby give consent for my thesis, if accepted, to be available for photocopying and for inter-library loan, and for the title and summary to be made available to outside organisations.

Signed ..... (candidate) Date 08/02/07

ACKNOWLEDGEMENTS

First and foremost I would like to specially thank my supervisor Professor Ray Waters for his inspiring dedication and enthusiasm in the field, his full support, invaluable advice, and unbelievable patience throughout this study. It has not been an easy few years, with professional and personal relocations and upheavals, and the unwavering support from Ray has (and always will be) greatly appreciated.

I am also indebted to my second supervisor Dr. Yachuan Yu who has taught me so much and has been an invaluable source of new ideas, advice and support over the past few years. He showed remarkable patience whilst teaching me experimental techniques and without his help, this study would have been far more difficult. I have worked with a very talented group of researchers who have helped me immensely through their professional support and friendship, and would like to give many thanks to Dr. Yumin Teng, Dr. Shirong Yu, Dr. Simon Reed, Dr. Hairong Liu and others at the Cardiff University School of Medicine.

I would like to thank my husband Jason and my family for their continued love and support over the past few years which has helped me to persevere through difficult times, keep in view the light at the end of the tunnel, and keep myself motivated. Finally, a very special mention must also be given to my beautiful daughter Isabelle who has brought so much love and happiness into my life, always making me smile despite any stress or difficulties I may be facing, and who makes everything I do worthwhile.

Thanks again to everyone who has supported me throughout the past few years and has each played a part in helping me to get as far as I have.

SUMMARY

Repair of UV-induced damage in the cell is crucial to maintain genome integrity and stability. Acetylation of the histone amino-terminal tails plays key roles in transcription and DNA repair pathways. Acetylation states are determined by a balance between the activities of histone acetyltransferases (HATs) and histone deacetylases (HDACs). This study examined the roles of histone deacetylation in transcription and nucleotide excision repair (NER) in *Saccharomyces cerevisiae* using mutant strains defective in one or more of the genes encoding the deacetylases Rpd3, Hda1, Hos1, Hos2 and Hos3.

Single mutations in the genes *RPD3* and *HDA1* and the various tested combinations of triple mutations did not cause any detectable loss of transcriptional repression of the model *MFA2* gene. *rpd3* and *hda1* mutants were not found to confer a significant change in sensitivity to UV radiation, however all triple mutations tested resulted in increased UV sensitivity of the cells. Examination of the removal of UV-induced cyclobutane pyrimidine dimers from the genome overall revealed that combined mutations in *RPD3*, *HOS1* and *HOS2* or in *RPD3*, *HOS1* and *HDA1* resulted in enhanced NER, which intriguingly appears to contradict the UV sensitivity effects. Enhanced NER was also observed at the repressed *MFA2* gene for the same triple mutations, indicating roles for the histone deacetylase genes in chromatin alteration during both global and local NER. The NER effects were only observed upon deletion of multiple genes, suggesting a degree of functional redundancy among the deacetylase proteins.

Increasing evidence for an epigenetic histone code and interplay between post-translational histone modifications led to speculation that histone phosphorylation may also play a role in NER. Increased UV sensitivity was conferred by specific mutations in the tails of histone H2A and H2B. Genome-wide analysis in a histone mutant with the H2B tail truncated at serine position 125 suggested that any roles for this site in NER are likely to be specific to certain regions of the genome rather than involved in global NER.

ABBREVIATIONS

AP	Apurinic / Apyrimidinic
BER	Base excision repair
CPD	Cyclobutane pyrimidine dimer
CS	Cockayne Syndrome
DDB	Damaged DNA-binding (protein)
DNA	Deoxyribonucleic Acid
dsDNA	Double-stranded DNA
Endo III (IV)	Endonuclease III (IV)
ERCC	Excision repair cross complementing
HAT	Histone acetyltransferases
HAST	Hda1-Affected SubTelomeric
HDAC	Histone deacetylase
ML endo	*Micrococcus luteus* CPD endonuclease
MMS	Methyl methane sulphonate
MPC	Magnetic particle concentrator
MTHF	5, 10-Methenyl tetrahydrofolate
mRNA	Messenger RNA
NER	Nucleotide excision repair
NTS	Non-transcribed strand
ORF	Open reading frame
PCR	Polymerase chain reaction
Pol I (II)	Polymerase I (II)
6-4 photoproducts	Pyrimidine-pyrimidone (6-4) photoproducts
PR	Photoreactivation
PRTF	Pheromone receptor transcription factor
RNA	Ribonucleic acid
ROS	Reactive oxygen species
RPA	Replication protein A
r.t.	Room temperature
RT-PCR	Reverse-Transcription PCR
SGD	*Saccharomyces cerevisiae* Genome Database
ssDNA	Single-stranded DNA
TAF	TBP associated factor
TBP	TATA box binding protein
TCR	Transcription coupled repair
TFII	RNA polymerase II transcription factor
TRCF	Transcription-repair coupling factor
tRNA	Transfer RNA
TS	Transcribed strand
UAS	Upstream activation sequence
UES	Upstream essential sequence
URS	Upstream repressing sequence
UV	Ultraviolet (light)
WT	Wild type
XP	Xeroderma pigmentosum
YPD	Yeast extract/Peptone/Dextrose Medium

CONTENTS

Acknowledgements
Summary
Abbreviations
Contents

Chapter 1

General Introduction 1

1.1 DNA Damage 1
1.1.1 UV Radiation and DNA Damage 2
1.1.2 Cellular Responses to DNA Damage 7
1.1.3 Cell Cycle Responses to DNA Damage 8

1.2 DNA Repair Mechanisms 13
1.2.1 DNA Repair by Reversal of Damage 14
1.2.2 DNA Repair by the Excision of Damage 17
1.2.2.1 Mismatch repair (MMR) 19
1.2.2.2 Base excision repair (BER) 20
1.2.2.3 Nucleotide excision repair (NER) 22
1.2.2.4 NER in prokaryotes 22
1.2.2.5 NER in eukaryotes 24
1.2.2.6 Heterogeneity of NER in the genome 34
1.2.2.7 Human consequences of NER deficiencies 38

1.3 DNA Repair and Transcription 42
1.3.1 TFIIH 43

1.4 Chromatin Implications in Transcription and DNA Repair 45
1.4.1 Chromatin structure 45
1.4.2 Implications of chromatin structure 47
1.4.2.1 Chromatin and the formation of UV-induced damage 47
1.4.2.2 Chromatin and DNA-mediated processes 48
1.4.3 Histone acetylation 49
1.4.3.1 Histone acetyltransferases (HATs) 50
1.4.3.2 Histone deacetylases (HDACs) 51
1.4.3.3 Histone acetylation and transcription regulation 52
1.4.4 NER in a chromatin environment 54
1.4.4.1 Histone acetylation and NER in chromatin 56

1.5 The *S. cerevisiae MFA2* Gene 58
1.5.1 *MFA2* is an a-cell specific gene 58
1.5.2 Regulation of *MFA2* 59
1.5.3 *MFA2* as a model gene 62

1.6 The Present Study 64

Chapter 2

Materials and Methods 67

2.1 Yeast strains used 67

2.2 Growth and storage conditions 68

2.3 Analysis of UV sensitivity – Cell survival 69

2.4 UV irradiation of cells for repair analysis 70

2.5 Extraction of yeast DNA 72

2.6 Non-denaturing agarose gel electrophoresis 74

2.7 Detection of repair in the overall yeast genome 75

2.8 Studying DNA repair at gene resolution 77
2.8.1 DNA digestion with restriction endonuclease 80
2.8.2 Incision of DNA at the sites of CPDs 81
2.8.3 Denaturing gel electrophoresis and Southern blotting 81
2.8.4 Hybridisation of the membrane with a radioactive probe 83
2.8.5 Analysis of the radiolabelling results 84

2.9 Preparation of Strand-specific Radiolabelled Probes 85
2.9.1 PCR amplification of the sequence of interest 87
2.9.2 Preparation of the radiolabelled probe 88

2.10 Studying DNA Repair at Nucleotide Resolution 89
2.10.1 DNA digestion with restriction and CPD-specific enzymes 91
2.10.2 Purification of CPD-incised single stranded DNA fragments 92
2.10.3 End-labelling the fragments with α-[^{32}P] dATP 93
2.10.4 Denaturing polyacrylamide gel electrophoresis 93
2.10.5 Quantification and repair analysis 95

2.11 Analysis of Gene Expression 96
2.11.1 Extraction of total yeast RNA 96
2.11.2 Northern Blotting technique 97
2.11.2.1 Formaldehyde-agarose (FA) gel electrophoresis 98
2.11.2.2 Northern blotting, detection and analysis of RNA 98
2.11.3 Quantitative PCR (qPCR) 100
2.11.3.1 Reverse transcription (RT) to create cDNA 100
2.11.3.2 Quantitative real-time PCR analysis 101

Chapter 3

Histone Deacetylases and Transcription at Yeast *MFA2* 104

3.1 Introduction 104

3.2 Materials and Methods 110

3.3 Results 118

3.3.1 Construction of the *rpd3Δ* and *hda1Δ* strains....118
3.3.2 Effects of HDAC deletions upon *MFA2* transcription....119
3.3.2.1 Northern analysis of mRNA levels....120
3.3.2.2 qPCR analysis of mRNA levels....121
3.3.2.3 Quantification of qPCR data....121

3.4 Discussion....124

Chapter 4

The Roles of Histone Deacetylases in Nucleotide Excision Repair at the Yeast *MFA2* Gene....129

4.1 Introduction....129

4.2 Materials and Methods....135

4.3 Results....136
4.3.1 Analysis of UV sensitivity....136
4.3.2 Global repair of CPDs in genomic DNA is enhanced by the deletion of multiple histone deacetylase genes....139
4.3.3 Multiple HDAC deletions result in an increased rate of repair at *MFA2*....142
4.3.4 HDACs in repair of CPDs at nucleotide resolution....145
4.4 Discussion....152

Chapter 5

The Role of Histone Phosphorylation in Nucleotide Excision Repair at the Yeast *MFA2* Gene....163

5.1 Introduction....163

5.2 Materials and Methods....167

5.3 Results....172
5.3.1 Mutations at certain sites of histone phosphorylation result in mild UV sensitivity....172
5.3.2 Northern blotting to detect transcription of MFA2 to verify mating type....175
5.3.3 Global repair of CPDs in genomic DNA is not affected by the mutation of serine position 125 of the histone H2B tail....176
5.3.4 Mutation of the serine residue at position 125 of the H2B tail does not cause a change in the rate of NER at MFA2 in mating type a cells....177

5.4 Discussion....179

Chapter 6

Discussion and Future Experiments.....184

Appendices and References

Appendix I.....195

Appendix II.....203

Appendix III.....208

Appendix IV.....237

References.....250

Chapter 1

General Introduction

1.1 DNA Damage

DNA is the biomolecule that governs genetic inheritance from one generation to the next and provides a blueprint for the operation of any individual cell. Genetic stability and maintenance are therefore imperative in order to prevent DNA damage accumulating and resulting in mutations which can ultimately cause cancer, hereditary disease and cell death. Conversely, however, DNA damage is an essential occurrence for the maintenance of life as it enables genetic variation to arise, the fundamental basis for adaptation and Darwinian evolution. A delicate balance between the two outcomes therefore exists in order to enable genetic variation to arise whilst maintaining the integrity of genetic material (Friedberg, 2001, 2003). DNA is a dynamic molecule and vulnerable to constant attack from both exogenous and endogenous sources, resulting in a variety of forms of DNA damage which alter the structure and biochemistry of the DNA. If such damage is not removed or repaired, it may result in mutations which are passed on to the next cellular generation, or lead to cellular death (apoptosis).

The cell has to contend with a broad spectrum of different types of DNA damage, arising from both intra- and extra-cellular sources. Many forms of DNA damage can arise endogenously due to the spontaneous alterations of DNA bases (Lindahl, 1993; Friedberg *et al.*, 2005) or from essential DNA-mediated cellular activities such as recombination, replication and repair (Friedberg *et al.*, 2005), for example the semi conservative nature of DNA replication lends itself to the possibility of mispairing bases, deletions and insertions; and incomplete DNA repair can lead to

apurinic/apyrimidic (AP) sites in the DNA. Types of alterations to the DNA bases include deamination of adenine, guanine or cytosine to form xanthine, hypoxanthine and uracil, respectively; hydrolysis of the *N*-glycosydic bond between purines or pyrimidines and the deoxyribose backbone of DNA, forming AP sites; and base alterations formed by reactive oxygen species (ROS) (Friedberg *et al.*, 2005; Balajee and Bohr, 2000). Exogenous DNA damage arises through exposure of the cell to environmental agents such as ionising radiation and certain chemicals with mutagenic or carcinogenic properties such as alkylating agents. Types of DNA damage varying from simple base methylation to complex bulky lesions and DNA-protein crosslinks can result (Balajee and Bohr, 2000). Ionising radiation can be absorbed by living cells and induce DNA damage either directly, by causing breaks in the DNA strands, or indirectly by generating ROS during the hydrolysis of water. This study focuses on DNA damage induced by ultraviolet (UV) light. The implications of exposure to UV light will thus be discussed in further detail.

1.1.1 UV Radiation and DNA Damage

Early work using UV radiation as an experimental tool resulted in the accidental discoveries of the fact that living cells could recover from the effects of DNA damage induced by the UV (Kelner, 1949; Dulbecco, 1949). UV radiation has since become the best characterised and most extensively studied model system to investigate DNA damage and repair. It is also a highly relevant model as life on Earth has always had to contend with the incidence and effects of solar radiation. The UV radiation spectrum consists of three distinct wavelength bands, namely UV-A (400 to 320 nm), UV-B (320 to 290 nm) and UV-C (290 to 100 nm). Solar radiation reaching Earth consists mainly of UV-A and UV-B, as wavelengths below 320 nm are largely

filtered out by the atmospheric ozone layer. In contrast to many other DNA damage-inducing agents which cause an array of different types of DNA damage (Friedberg *et al.*, 2005; Balajee and Bohr, 2000), UV radiation induces mainly two types of photoproduct which are bulky, helix-distorting lesions and responsible for the mutagenic and tumorigenic effects of UV. Cyclobutane pyrimidines dimers (CPDs) and pyrimidine-pyrimidone (6-4) photoproducts (6-4 PPs) account for the vast majority of all UV-induced lesions and result from the covalent linking of adjacent pyrimidines (Mitchell, 1988). Purines absorb UV less efficiently and consequently constitute less than 1% of UV-induced lesions (Friedberg *et al.*, 2005).

Cyclobutane Pyrimidine Dimers (CPDs)

A germicidal UV lamp delivers UV radiation at a wavelength of about 254 nm. This is close to the absorption maximum of DNA, about 260 nm, and can result in two adjacent pyrimidines utilising the UV energy to become covalently bonded as a dimer structure. The thymine-thymine (T-T) dimer was first identified by Setlow in the 1960s as a stable and naturally occurring DNA lesion resulting from exposure of cells to sunlight which caused considerable distortion of the DNA structure, impacting upon processes such as replication and transcription (Setlow and Carrier, 1964). The formation of the namely cyclobutane pyrimidine dimers (CPDs) constitutes 70-85% of the total photoproducts induced by UV (Mitchell and Nairn, 1989).

The induction of CPDs is influenced by the flexibility of DNA, with sequences facilitating bending and unwinding appealing most for CPD formation (Thoma, 1999). The specific nucleotide composition of DNA also plays a vital role, with CPDs forming preferentially between two adjacent thymine residues (T-T), and further enhanced by the presence of a pyrimidine 5' to the dipyrimidine site (Gordon

and Haseltine, 1982). CPDs are formed at lower incidence at other dipyrimidine sites, with the ratio of T-T: C-T: T-C: C-C reported as 68:13:16:3 (Mitchell *et al.*, 1992). During the formation of a CPD, the normal C5=C6 double bond between carbon atoms C5 and C6 become saturated and rearranged into C5-C5 and C6-C6 single bonds. A four-membered (C5, C5, C6, C6) cyclobutyl ring structure results, linking the two pyrimidines as a dimer (see Figure 1.1). There are 12 theoretical isomeric forms of a CPD but only four exist in significant yields, with the configurations *cis-syn, cis-anti, trans-syn* and *trans-anti*. The *cis-syn* isoform is the most prevalent observed in double-stranded B-form DNA (Friedberg, 2005).

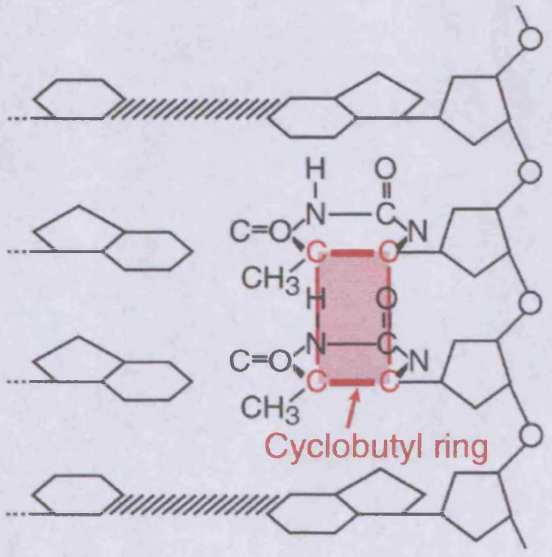

Figure 1.1. *Structure of a CPD.* A cyclobutane pyrimidine dimer (CPD) is formed between two adjacent pyrimidines in the same polynucleotide chain when the saturation of their respective 5,6 double bonds results in the four-membered ring structure covalently linking the pyrimidines as a dimer structure *(From Friedberg, 2005).*

CPDs are formed with an average distance of 10.3 bases apart and are positioned away from the histone interfaces (Pehrson, 1989). CPDs are traditionally considered as bulky helix-distorting lesions in the DNA, which can hinder sequence-

specific binding of proteins, thus seriously affecting DNA-mediated regulatory processes. However, some reports have indicated that *cis-syn* CPDs may also form without such major distortion (Taylor et al, 1981). CPDs can induce bends or kinks in the DNA of 7-9° (Husain *et al.*, 1988; Wang and Taylor, 1991; Kim *et al.*, 1995; Friedberg *et al.*, 2005) although bends of up to 30° have also been reported (Park *et al.*, 2002). The induction of CPDs is further affected by the compacting of DNA into chromatin and the nature of interactions of the DNA with histones and other proteins. These aspects will be considered further in later chapters.

Pyrimidine-Pyrimidone (6-4) Photoproducts (6-4 PPs)

In addition to CPDs, UV radiation also induces 6-4 PPs which constitute 15-30% of the total UV-induced photoproducts (Mitchell and Nairn, 1989). These are preferentially formed in the linker regions, with a six-fold greater incidence, than in the core nucleosomal regions of chromatin, unlike CPDs which form in equal abundance in both regions (Mitchell *et al.*, 1990). The heterogeneity of each type of dimer formation is further evident at the TATA box, where the transcription factor TATA-box binding protein (TBP) promotes selective formation of 6-4 PPs in the TATA-box itself where DNA is bent, in contrast to CPDs which preferentially form at the edges and outside of the TATA-box, where the DNA is not bent (Thoma, 1999). This trend has been observed *in vitro* and in active yeast cells and it has been suggested that the structural distortion of DNA by TBP is the same *in vitro* and in the initiation complexes *in vivo*, highlighting the importance of protein-DNA interactions in the induction of UV-induced photoproducts (Thoma, 1999; Aboussekhra and Thoma, 1999).

6-4 PPs occur at positions of cytosine (and less frequently at positions of thymine) located 3' to pyrimidine nucleotides. The resultant dimer is achieved by the formation of a stable bond between the 5' C6 and the 3' C4 positions of the adjacent pyrimidines (see Figure 1.2). The most abundant type of 6-4 PP forms between thymine and cytosine bases (T-C), with bonds between C-C and T-T occurring less frequently (Mitchell *et al.*, 1990).

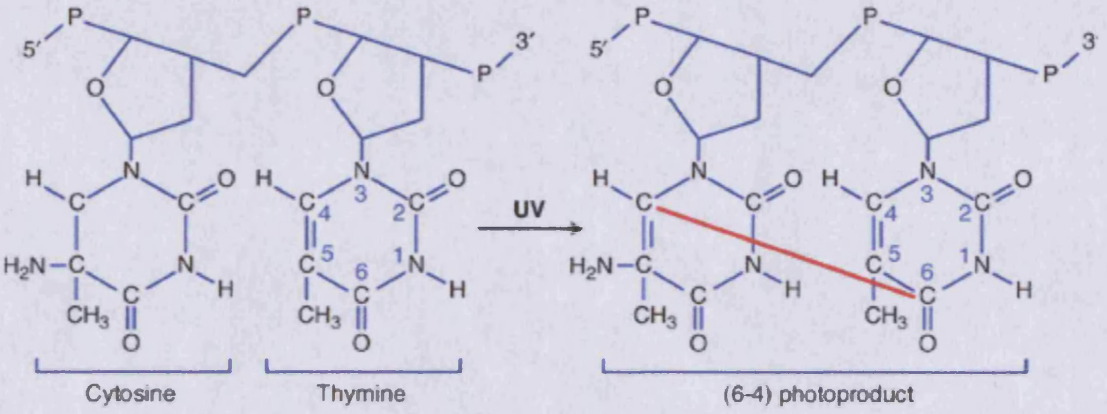

Figure 1.2. *Formation of a T-C Pyrimidine-Pyrimidone (6-4) Photoproduct.* UV can induce the formation of a crosslink between the C6 position of thymine and the C4 position of and adjacent cytosine residue. The formation of a 6-4 PP causes major distortion of the DNA double helix, much greater than that caused by CPD formation. *(From Matsumura and Ananthaswamy. 2002).*

Despite the formation of just a single bond linking the pyrimidines, 6-4 PPs induce extensive structural distortion of the DNA double helix. A DNA bend of up to 44° may be induced, much greater than that normally induced by CPD formation (Pearlman *et al.*, 1985). The plane of the 3' base moiety is shifted 90° relative to that of the 5' thymine (Friedberg *et al.*, 2005).

This study concerns the incidence and detection of UV-induced CPDs only, which can be detected specifically by using the crude extract from *Micrococcus luteus* (ML). The ML extract contains a UV endonuclease with CPD-DNA glycosylase /

abasic lyase activity that is strikingly similar in function to endonuclease V of phage T4 (Graftstrom *et al.*, 1982; Shiota and Nakayama, 1997; Friedberg *et al.*, 2005).

1.1.2 Cellular Responses to DNA Damage

Cells are constantly bombarded and under attack from a wide variety of damage-inducing sources. Since the 1930s it has been observed that living cells can recover from the lethal effects of UV radiation and other sources (Hollaender and Curtis, 1936), and in the 1940s the first clues to repair mechanisms were realised (Kelner, 1949; Dulbecco, 1949), even before the nature of DNA structure was elucidated by Watson and Crick (1953a). In order to maintain genetic integrity, the cell has evolved to develop an array of different responses and mechanisms to tolerate and repair the various forms of DNA damage, enabling cellular functions to proceed and promote viable transmission of genetic information from mother to daughter cells. The diverse nature of DNA damage is overcome by the varying specificity and redundancy of the different repair pathways and responses. When DNA damage is induced in eukaryotic cells, it apparently triggers a cascade of cellular responses, directed by signal transduction and collectively referred to as the 'DNA damage response' (Wang, 1998; Zhou and Elledge, 2000; Lowndes and Murguia, 2000; Walker, 2000; Abraham, 2001; Friedberg, 2001; Rouse and Jackson, 2002). Biological responses include (*i*) the activation of cell-cycle checkpoint pathways to slow or arrest progression of the cell cycle, thus enabling DNA repair pathways and other repair mechanisms to initiate; (*ii*) the operation of one or more enzymatic DNA repair pathways and (*iii*) the up-regulation of specific genes, often including some genes governing aspects of DNA repair. However, it is not always feasible to completely repair the DNA damage, particularly if it is extensive. In this instance, the

cell has two further possible responses: (*iv*) to activate mechanisms to tolerate mutations at a reasonable level, by operating biochemical processes to bypass DNA damage, despite the inevitability of resulting mutations; or (*v*) presumably as a 'last resort' when all other mechanisms are insufficient, the cell can activate pathways for programmed cell death (apoptosis). The above responses rarely operate independently but rather function cooperatively to complement and enhance the overall repair or tolerance of DNA damage by the cell. The precise combination of responses triggered is dependent upon the nature and severity of the DNA damage incurred. The specific nature of signals resulting from a given type of DNA damage is not fully understood, but it is thought that it may involve arrested DNA replication or the stalling of RNA polymerase II transcription which may initiate the signalling cascade to ultimately implement the described cellular responses (Friedberg, 2001).

1.1.3 Cell Cycle Responses to DNA Damage

The Cell Cycle

The somatic cell cycle consists of the series of events that occur from one mitotic cell division to the next. The period from the end of one mitosis to the start of the next is termed interphase and is divided into a number of different phases (Figure 1). S phase (synthetic period) refers to the phase when DNA is replicated, M phase refers to the period of actual division of the cell and nucleus (visible mitosis), the two intervening periods where no DNA synthesis occurs, but other processes such as transcription and translation occur, are termed gap phases G1 and G2. G0 denotes a non-dividing state called quiescence. The result of mitosis is the production of two identical diploid daughter cells, each of which then enter G1 of their own cell cycle.

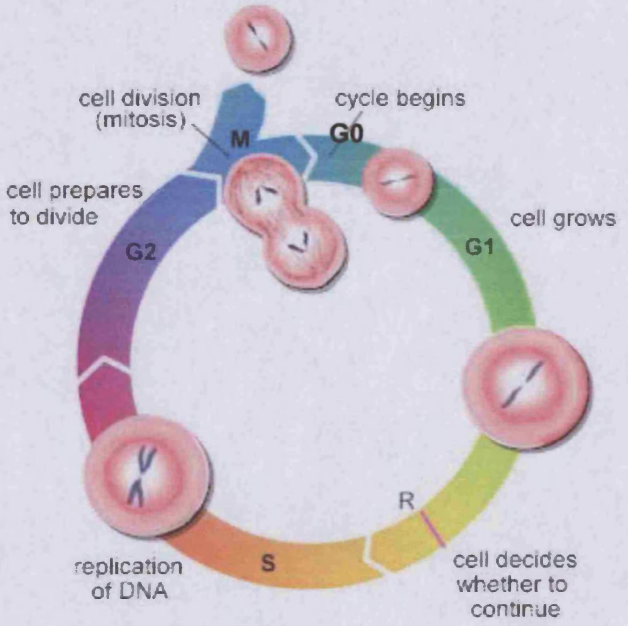

Figure 1.3. *The somatic cell cycle.* Interphase is divided up into the G1, S and G2 phases which prepare the cell for mitosis (M phase). A complete cycle in animal cells typically lasts about 18-24 hours and results in two diploid daughter cells which each enter their own cell cycle at G1 phase.
(From http://www.daviddarling.info/encyclopedia/C/cell_cycle.html)

During G1 phase, RNA and proteins are synthesised but no DNA replication occurs. The start of DNA replication represents the transition from G1 to S phase, which continues for the duration of DNA replication and culminates in the fully replicated DNA as two complete sets of diploid chromosomes ($4n$). During interphase, there is little visible change in the cell but during mitosis individual chromosomes become visible as they are segregated into separate daughter cells. The cell cycle typically takes 18-24 hours in animal somatic cells and G1 phase is usually the longest period, lasting typically between 6 and 12 hours. S phase varies depending on the time needed to replicate the entire genome, but typically lasts 6-8 hours. G2 is usually the shortest period of interphase and mitosis subsequently takes up to about 1 hour (Lewin, 2000).

Cell Cycle Progression

It is vital that the S phase and M phase are coordinated so that the genome is replicated accurately and fully but only once prior to mitosis. There are two major points during the cell cycle at which a decision is made to continue or arrest the cycle, considering the regulatory signals received by the cell and the current state of health of the cell in terms of DNA damage. Firstly, the cell commits to chromosome replication during G1 phase and if the checkpoint is 'passed' there is a lag period followed by entry to S phase (G1/S control). Second, the cell commits to mitosis at the end of G2 phase (G2/M control) and if the cell fails to divide at this point it remains with twice the normal diploid chromosome complement (4*n*). Internal cell cycle controls, termed checkpoints, ultimately ensure that the initiation of a later event in the cell cycle depends upon the successful completion of an earlier event.

G1/S control has been best defined for yeast cells, where it is termed START, and the analogous point in animal cells is termed the restriction point (denoted R in Figure 1). G1 control is the major control point for cultured animal cells and G2?M control is subsidiary. The length of G1 is adjusted in response to growth conditions, but when completed and the cultured cell enters G2, it will proceed to division. Some cell phenotypes do not divide and are considered to have 'left' the cell cycle. This non-dividing state is termed G0 and certain cells can be stimulated to leave or re-enter the cell cycle at this point which occurs before the restriction point (Lewin, 2000). The timing of S phase in yeast involves the assembly of pre-replication complexes (pre-RCs) which are converted to post-RCs as replication proceeds. The post-RCS are unable to initiate replication so prevent the cell re-copying the genome prior to mitosis (Stillman, 1996). The MCM family proteins Cdc6 and replication licensing

factors (RLFs) were first identified in yeast and have been implicated as components of pre-RCs. Homologues have also been identified in higher eukaryotes (Brown, 1999).

Cell cycle control is mediated largely by protein kinases which phosphorylate and activate enzymes, phosphatases which dephosphorylate enzymes and other proteins with specific functions within the cell cycle. The kinases are regulated themselves, partly by cyclin proteins which are present in the nucleus throughout the cell cycle. Other inhibitory proteins are also involved and the overall control of the cell cycle is very complex, depending on the abundance of various cyclins, kinases and other proteins (Brown, 1999; Lewin, 2000; Qin and Li, 2003; Woo and Poon, 2003).

Cell cycle checkpoints regulate replication and repair of DNA damage

The internal control points within the cell cycle are termed checkpoints and exist at various stages of the cell cycle to monitor events and initiate other cellular responses if needed. The two main checkpoints govern G1/S transition and G2/M transition, but there is also an intra-S-phase checkpoint.

The G1/S checkpoint prevents replication of damaged DNA which could lead to mutations or chromosomal breaks, subsequently leading to cancer. The DNA is checked for damage prior to replication, involving the recognition and response to both intrinsic and extrinsic forms of damage, thus damage sensors such as the RAS families of proteins and ATM/ATL proteins (Tel1/Mec1 in budding yeast), signal transducers such as the CHK kinase proteins and effector proteins which vary

depending on the stage of the cell cycle, are required in the checkpoint pathway. Cell cycle arrest at the G1/S checkpoint is mediated by the tumour suppressor protein p53 which acts as a DNA sequence-specific transcription factor. Its regulation involves multiple modification such as phosphorylation, dephosphorylation, acetylation and ubiquitination The role of p53 in cell cycle arrest is fairly well understood in terms of its action as a transcription factor affecting multiple target genes (Zhao *et al.*, 2000). Three key target genes are *p21*, *GADD45* and *14-3-3σ* . The induction of p21 arrests cells in G1 phase and prevents entry to S-phase whilst *GADD45* and *14-3-3σ* control the G2/M transition (Benchimol, 2001). None of these genes appear to play roles in p53-dependent apoptosis, another function of p53 thought to be important for its role as a tumour suppressor. Defects in cell cycle arrest are a major contributor to genetic instability in cancer cells, and over 50% of human cancers exhibit mutations in p53 or its regulators.

In addition to delaying cell cycle progression to enable time for DNA damage to be repaired, checkpoint pathways also help facilitate DNA repair pathways, for example, p53 has been widely implicated in the regulation of NER (Adimoolam and Ford, 2003; Benchimol, 2001) and also in BER (Zhou *et al.*, 2001), although the latter is less well understood.

The G2/M checkpoint monitors the completion of DNA replication and checks if the cell can safely initiate mitosis and successfully separate the sister chromatids. This checkpoint is activated by, and particularly important in the repair of, DNA damage due to ionising radiation. The G2/M checkpoint pathway can arrest the cell cycle using both p53 dependent and independent mechanisms, and defects in this pathway result in chromosomal abnormalities.

The S phase checkpoint was discovered when Paulovich and Hartwell (1995) showed that one response of yeast to DNA damage was to slow down or stop DNA replication, which was subsequently linked with the activation of certain genes involved in DNA repair (Elledge, 1996). S phase checkpoints prevent replication of DNA occurring if there are problems with the integrity of the DNA due to breaks or other forms of DNA damage. As with the regulation of entry to S phase, cyclin-dependent kinases are involved and may respond to damage-detection signals from proteins associated with the replication fork, such as the single strand binding factor RPA, accessory protein RFC and possibly polymerase ε (Waga and Stillman, 1998; Brown, 1999).

Overall, the highly complex system of checkpoints monitoring DNA repair, replication and cell division, collaboratively functioning to maintain the integrity of DNA, are an integral and vital part of the overall cellular response to genotoxic stress and multiple forms of DNA damage. An extremely sophisticated system of sensor molecules, signal transduction pathways and effector proteins help coordinate and regulate essential processes within the cell, including DNA repair, DNA replication and apoptosis, to ensure genomes are replicated accurately before dividing into daughter cells during mitosis. When cell cycle checkpoints and regulation does not function correctly, the consequences to the cell are often genetic instabilities which can ultimately lead to mutations and cancers.

1.2 DNA Repair Mechanisms

In order to protect the integrity of genetic information carried by the genome, the cell is well equipped with an arsenal of mechanisms to detect and repair the

diverse types of DNA damage from intracellular and environmental sources. DNA is the only biomolecule that is specifically repaired rather then replaced. There are three general modes of action to deal with DNA damage. The damage may be (*i*) directly reversed, (*ii*) physically excised from the DNA and a new portion inserted, or (*iii*) it may be tolerated by the cell and bypassed in cellular processes. Various mechanisms exist in the cell to enable these outcomes (see Table 1.1). Some of the repair processes will be briefly considered, but only those relevant to this study will be discussed in detail.

1.2.1 DNA Repair by Reversal of Damage

Table 1.1 Summary of cellular responses and mechanisms to process DNA damage

Cellular Response to DNA Damage	Repair / Tolerance Mechanism
Direct reversal of DNA damage	Enzymatic photoreactivation of CPDs, 6-4 PPs Repair of other photoproducts Repair of alkylated base damage Ligation of DNA strand breaks
Excision of DNA damage	Base Excision Repair (BER) Nucleotide Excision Repair (NER) Mismatch Repair (MMR)
Tolerance of DNA damage	Replicative bypass of template damage (gap formation and recombination) Translesion DNA synthesis

Cells possess mechanisms to increase the fidelity of DNA-mediated processes which inevitably introduce errors that would ultimately lead to mutations, such as the

indispensable 3' to 5' exonuclease activity of many DNA polymerases to monitor and rectify wrongly inserted bases during DNA synthesis (Friedberg *et al.*, 2005; Lodish *et al.*, 2000). However, such repair mechanisms are not infallible and can themselves induce further DNA damage. Additionally, mechanisms have evolved to directly reverse some forms of DNA damage such as base modifications induced by chemical agents and radiation. The direct reversal of DNA damage entails enzymatic reactions to restore the primary DNA structure to its correct sequence. The best studied example of damage reversal is the repair of CPDs during photoreactivation by the enzyme CPD photolyase.

Photoreactivation

Early studies (Dulbecco, 1949; Kelner, 1949) observing the capability of living cells to recover from the lethal effects of UV radiation led to the initial discovery of photoreactivation. In the late 1950's, studies using *E. coli* and *S. cerevisiae* showed that photoreactivation is an enzyme-catalysed reaction (Rupert *et al.*, 1958; Rupert, 1960). The mechanism involves photolyases (photoreactivating enzymes) which repair CPDs (CPD photolyase) or, less frequently, 6-4 PPs (6-4 PP photolyase) by monomerization of the dimers into their constituent pyrimidines, thereby reversing the damage (Sancar, 1990, 2000). Firstly, the target dimer is specifically recognised by the enzyme which binds to form a stable complex. The second stage of repair is a light-dependent reaction whereby the dimer is split by photolysis and the original pyrimidines are recovered. CPD photolyase contains two chromophores which absorb light energy. In all photolyases, one chromophore is $FADH^-$ and the other is either methenyl-tetrahydrofolate (MTHF) or 8-hydroxy-5-deazaflavin (8-HDF). MTHF and 8-HDF gather light and transfer the energy to

$FADH^-$, which is then used to split the dimer (Eker *et al.*, 1990; Malhotra *et al.*, 1992; Schleider *et al.*, 2005). CPD photolyases have been identified in bacteria, fungi, plants and many vertebrates, but not placental mammals (Yasui *et al.*, 1994; Yasui and Eker, 1998). 6-4 photolyases have been found in insects (Todo *et al.*, 1996), reptiles and amphibians (Todo *et al.*, 1997) but not in *E.* coli, yeast or mammals. However, despite limited evidence for photolyases in humans, light-dependent loss of pyrimidine dimers has been reported in living cells in culture and in intact human skin cells (Sutherland *et al.*, 1980; Wagner *et al.*, 1975).

Repair of Alkylation Damage

Some forms of alkylation are directly reversible by enzymes that can transfer the alkyl group from the damaged nucleotide to their own polypeptide chain. A common example of a chemical that can cause such damage is the alkylating agent *N*-methyl-*N'*-nitro-*N*-nitrosoguanidine (MNNG), which reacts with DNA to produce O-alkylated and N-alkylated products. O^6-alkylguanine and O^4-alkylthymine are potentially mutagenic and their repair by reversal of the damage has been extensively studied in *E. coli* (Friedberg *et al.*, 2005). The damage to specific bases is directly reversed by the activity of methyltransferase enzymes. O^6-alkylguanine-DNA alkyltransferases operate to reverse alkyl groups of varying size, from methyl to benzol. For example, the O^6-methylguanine-DNA methyltransferase enzyme (O^6-MTG) transfers a methyl group from the O^6 position of guanine in DNA to a cysteine residue in the protein to restore the native chemistry of guanine and directly reverse the base damage (Olsson and Lindahl, 1980; Friedberg *et al.*, 2005). However, once the alkyl group is transferred to the enzyme, the protein is permanently inactivated as

alkyl cysteine is very stable. Thus the synthesis of new repair molecules is required for additional repair.

Repair of single-strand DNA Breaks

Ionising radiation such as X-rays and gamma rays, and some chemical DNA-damaging agents, can induce breaks in one or both strands of DNA. Under certain conditions of a single-strand break, where there are two free ends of the DNA strand, no missing nucleotides and the presence of adjacent 3' hydroxyl and 5' phosphate termini, the damage can be repaired by simply rejoining the ends, catalysed by DNA ligase enzyme in a direct reversal of the break (Friedberg *et al.*, 2005). However, breaks which exceed simple breaks of a phosphodiester bond, with additional DNA backbone damage or base damage require more complex processing and repair, and cannot be reversed by simply sealing the nick.

1.2.2 DNA Repair by the Excision of Damage

To remove many diverse types of damage, including bulky, helix-distorting lesions from DNA, cells possess mechanisms to detect and excise the damage before resynthesising the affected portion of a DNA strand using the undamaged strand as a template and sealing the gap to restore the native structure of the DNA helix. These processes are termed 'excision repair' pathways and are essential for the removal of photoproducts induced by UV radiation such as CPDs. A general model for excision repair is illustrated in Figure 1.4.

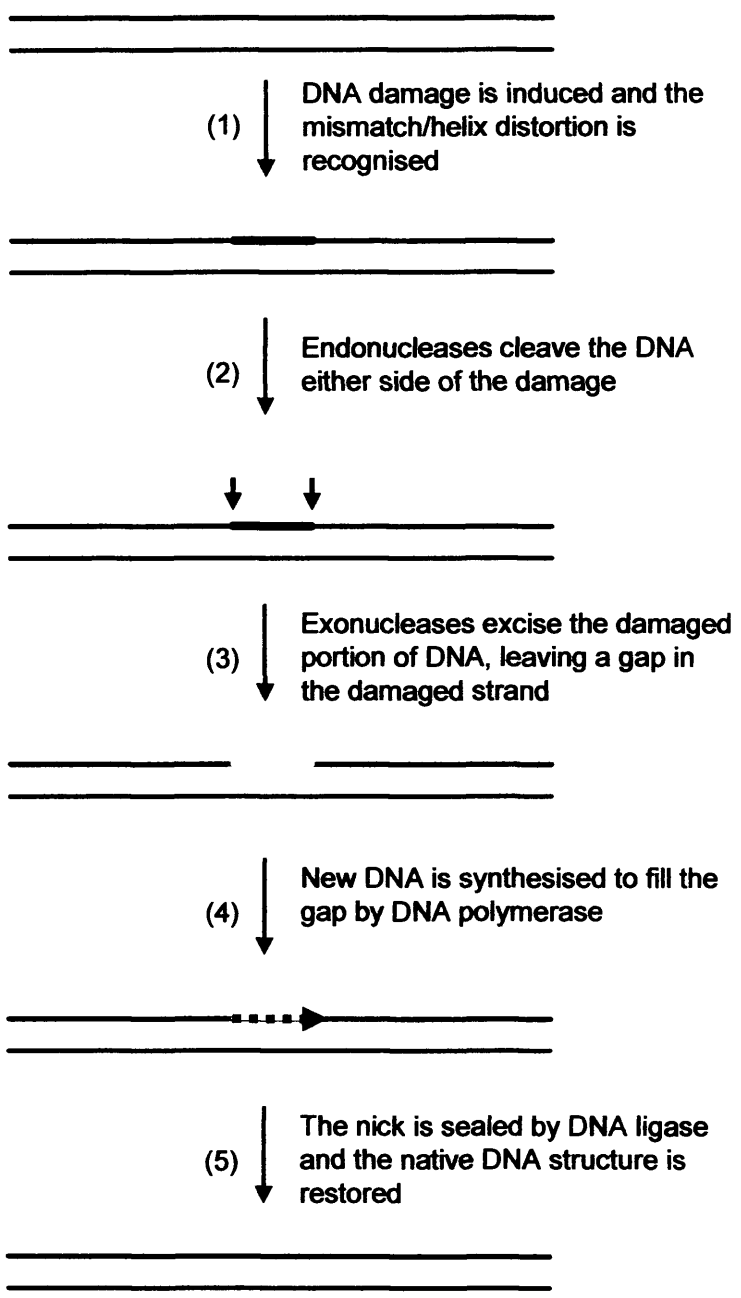

Figure 1.4. *General schematic model of excision repair mechanisms.* (1) DNA damage is induced by a variety of sources, resulting in a base pair mismatch or structural distortion of the DNA double helix. The cell possesses mechanisms to recognise such damage. (2) Endonucleases cleave the DNA strand containing the damage either side of the lesion. (3) The portion of DNA containing the damage is excised from the strand by exonucleases. (4) The resulting gap is filled by DNA polymerases synthesising new DNA. (5) The final nick is sealed by DNA ligase and the original DNA structure is restored.

1.2.2.1 Mismatch Repair (MMR)

Mismatched DNA bases can arise from various sources including DNA replication errors, recombination processes involving heteroduplex formations, or hairpin formations between imperfect palindromes (Friedberg *et al.*, 2005). Specific mismatch repair (MMR) mechanisms are required to correct such errors and serve to increase the fidelity of DNA replication by several orders of magnitude (Modrich and Lahue, 1996; Marti *et al.*, 2002; Jiricny, 2006). Other repair processes specifically recognise chemical abnormalities or base modifications, which are not produced as a result of mispaired bases – the bases are simply in the wrong position. MMR systems however, in addition to detecting some chemical errors, can detect the mispairing of chemically unaltered bases between the parent and daughter strands of DNA, consequently excising the mismatched portion of the daughter polynucleotide and resynthesising the gap in a similar way to other excision repair mechanisms (Brown, 1999; Friedberg *et al.*, 2005; Jiricny, 2006; Jun *et al.*, 2006).

MMR in *E. coli* is initiated by the action of three proteins. Firstly, MutS protein recognises various mismatches and binds the second protein, MutL, which subsequently activates MutH, an endonuclease, to cut the unmethylated daughter DNA strand containing the mispaired base. Uvr D, a DNA helicase II, then unwinds the DNA duplex from the nick generated by MutH. The precise nature of these protein interactions however remains unclear (Kunkel and Erie, 2005; Jun *et al.*, 2006). The activity of MutS in MMR is a critical step and important aspects of its function in mismatch recognition and initiation of MMR have recently been elucidated. MutS binds to mismatches and initiates repair in an ATP-dependent manner (Lamers *et al.*, 2003; Natrajan *et al.*, 2003). Two residues, phenylalanine (Phe) 36 and glutamate (Glu) 38, are involved in the recognition of various

mismatches: Phe 36 stacks onto a mismatched base, and a hydrogen bond is formed from the base to the Glu 38 residue (Natrajan *et al.*, 2003). The charge on Glu 38 is important in discriminating the mismatched base from the correctly paired base (Lebbink *et al.*, 2006). In addition to its role in recognition, the Glu 38 residue is further involved in the initiation of repair as the hydrogen bond formed induces intramolecular signalling events, leading to the inhibition of the ATPase activity of MutS and the formation of a stable MutS-ATP-DNA clamp, triggering further MMR events (Lebbink *et al.*, 2006).

The MMR system is conserved but is more complex in eukaryotes than the prokaryotic system (Kolodner, 1996; Jiricny, 2006; Jun *et al.*, 2006). Organisms from yeast to mammals possess five MutS homologues (MSH proteins) and four MutL homologues (MLH and post meiotic segregation, PMS, proteins), which function as heterodimers with multiple proteins (Mankovich *et al.*, 1989; Prolla *et al.*, 1994; Jun *et al.*, 2006, Waters, 2006). However, no orthologues of MutH or UvrD have been identified by genetic studies in yeast to date (Hafe and Robertson, 2000). Defective MMR in humans, particularly involving the proteins *hMSH2* and *hMLH1*, has been implicated in genetic diseases such as hereditary nonpolyposis colorectal cancer (HNPCC) (Gimble and Sauer, 1986; Leach *et al.*, 1993; Parsons *et al.*, 1993; Mandal *et al.*, 1993; Lynch and de la Chapelle, 1999; Heinen *et al.*, 2002; Li, 2003).

1.2.2.2 Base Excision Repair (BER)

Base excision repair (BER) involves the removal of a damaged nucleotide and the resynthesis of DNA to fill in the resulting apurinic/apyrimidimic (AP) site. The process operates on many types of modified nucleotide suffering relatively minor damage and is initiated by DNA glycosylases which cleave the β-*N*-glycosidic bond

between a damaged base and the deoxyribose-phosphate component of the nucleotide. DNA glycosylases are a diverse class of specific enzymes which each recognise a single or small subset of chemical alterations or mismatches of bases. Most organisms possess DNA glycosylases to successfully repair deaminated bases such as uracil or hypoxanthine; oxidation products such as thymine glycol, 8-oxo-7,8-dihydroguanine (8-oxoGua) and 5-hydroxycytosine; and methylated bases such as 2-methylcytosine and 7-methylguanine (Seeberg *et al.*, 1995; Krokan *et al.*, 1997; Barnes and Lindahl, 2004; Fromme and Verdine, 2004). They remove a damaged base by flipping the structure to a position outside of the DNA double helix and then detaching it from the polynucleotide chain (Kunkel and Wilson, 1996; Roberts and Cheng, 1998). Following recognition and cleavage by a DNA glycosylase, an AP endonuclease or AP lyase excises the AP site. This step may be achieved by various activities. Commonly, an AP endonuclease such as the *E. coli* endonuclease IV cuts the phosphodiester bond 5' to the AP site. The endonuclease alone may then also remove the deoxyribose component, or a separate phosphodiesterase may be required. Alternatively, some DNA glycosylases are able to cut the DNA at the 3' side of the AP site simultaneously to removing the damaged base, again followed by phosphodiesterase activity to completely remove the damaged nucleotide. The resulting nucleotide gap is subsequently resynthesised by a DNA polymerase (Pol β in mammals) using the intact strand as a template and finally, the gap is sealed by the insertion of a phosphodiester bond by DNA ligase (Seeberg *et al.*, 1995; Brown, 1999; Friedberg *et al.*, 2005).

In human cells, a major AP endonuclease is Ape1 which is involved in the repair of DNA single strand breaks containing 3'-phosphoglycolate (3'-PG) ends (Demple *et al.*, 1991; Parsons *et al.*, 2004). Further repair is then achieved through at

least two distinct BER subpathways, involving different subsets of enzymes, which result in the replacement of one nucleotide (short-patch BER), or two or more nucleotides (long-patch BER) (Sung and Demple, 2006).

1.2.2.3 Nucleotide Excision Repair (NER)

The mismatch repair and base excision repair systems have limited specificities in the types of DNA damage upon which they can operate. For more extensive types of damage, cells possess a nucleotide excision repair (NER) mechanism. NER responds to DNA damage which distorts the native helical structure and operates on a broad spectrum of different forms of damage, ranging from minor base alterations to intrastrand crosslinks and large bulky adducts which cause high degrees of helix distortion (Friedberg *et al.*, 2005; Balajee and Bohr, 2000; Friedberg, 2001). The UV-induced photoproducts cyclobutane pyrimidine dimers (CPDs) and 6-4 photoproducts (6-4 PPs) are among the common targets for NER.

1.2.2.4 NER in prokaryotes

NER has been extensively studied in prokaryotic systems, particularly *E. coli* (Van Houten, 1990; Sancar and Sancar, 1988; Friedberg *et al.*, 2005; Brown, 1999). The most common pathway is the 'short-patch' NER pathway (Figure 1.5), so called due to the relatively short oligonucleotide excised during repair, commonly 12 nucleotides in length although this is variable. This process is initiated by a multienzyme termed the UvrABC endonuclease, constituting the UvrA, UvrB and UvrC proteins (Howard-Flanders *et al.*, 1966). Initially, a trimer of two UvrA proteins and one UvrB protein specifically binds at the site of damage. The broad specificity of binding suggests that damage recognition is general, such as detection

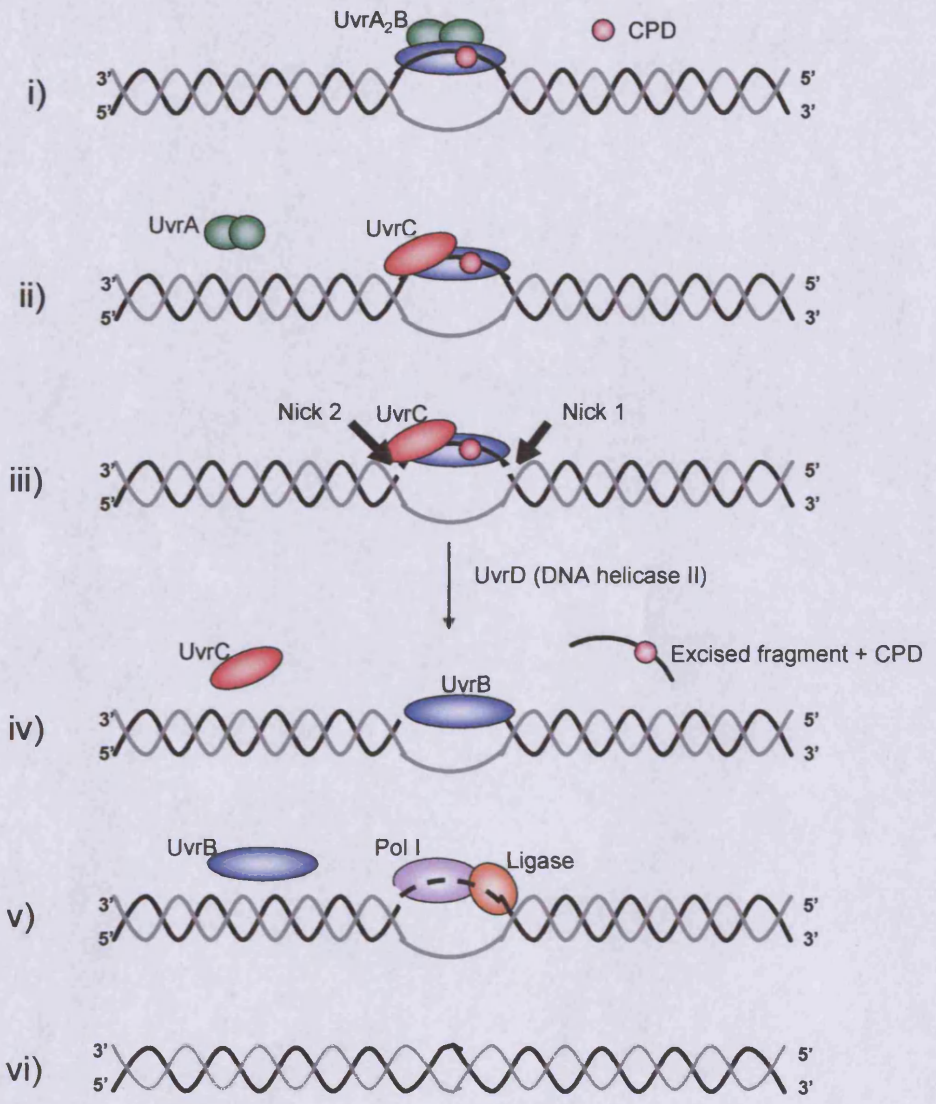

Figure 1.5. *Schematic model of short-patch NER in E. coli.* (i) Helix distortion due to DNA damage (CPD) is recognised, UvrA dimer and UvrB protein bind forming a stable UvrB-damage complex. (ii) The UvrA dimer dissociates and UvrC protein binds. (iii) UvrC induces a conformational change in UvrB enabling it to incise the DNA 4 nucleotides 3' to the damage to complete the bimodal incision step. UvrC then catalyses the incision of DNA 7 nucleotides 5' to the damage. (iv) Following incision, UvrD (DNA helicase II) is recruited to excise the oligonucleotide fragment containing the CPD, and to displace UvrC. (v) Repair synthesis by DNA Pol I resynthesises the DNA and UvrB is released. DNA ligase seals the final nick to join the newly synthesised DNA to the polynucleotide chain and complete the NER process. (vi) The native DNA is thus restored.

of the distortion of the DNA double helix, rather than detection of specific forms of DNA damage. Following the $UvrA_2B$ binding, UvrA dissociates and UvrC protein binds to form a UvrBC dimer. A conformational change is induced enabling the bound UvrB protein to cut the DNA 4 nucleotides 3' to the site of damage (e.g. a CPD). UvrC subsequently catalyses an incision in the DNA 7 nucleotides 5' to the damage to complete bimodal incision either side of the damage. Following incision, UvrD protein (helicase II) enables the dissociation of UvrC and the excision of the oligonucleotide containing the DNA lesion. UvrB apparently remains bound to the gapped DNA and is released during the repair synthesis reaction catalysed by DNA polymerase (Pol) I. The final step, catalysed by DNA ligase, seals the nick to complete NER, and restores the native undamaged DNA structure.

Less-well studied in *E. coli* is the 'long-patch' NER pathway which also employs the Uvr proteins but can result in repair synthesis patches of up to 2kb and additionally requires the activities of RecA and LexA proteins, which regulate the inducible NER 'SOS responses' whereby numerous genes are derepressed in an additional response to DNA damage (Cooper, 1982; Friedberg *et al.*, 2005). More extensive DNA degradation is observed in long patch NER, presumably to repair forms of DNA damage affecting a greater proportion of DNA than those repaired by short-patch NER.

1.2.2.5 NER in eukaryotes

Overall NER in eukaryotes resembles the process in prokaryotes but is far more complex, involving over 30 proteins and remains less well characterised, largely due to the increased genome sizes and complex packaging of nucleosomal DNA in eukaryotic cells. The proteins involved do not appear to be homologues of the *E. coli*

Uvr proteins. However, in eukaryotes, the mechanisms and proteins involved are highly conserved from yeast to higher eukaryotes including humans. Much of the current information known has been elucidated from studies involving human cells from patients suffering with Xeroderma pigmentosum (XP) and Cockayne Syndrome (CS), two hereditary disorders associated with defective NER pathways, in conjunction with studies utilising homologous yeast mutant strains (Balajee and Bohr, 2000; Friedberg *et al.*, 2005).

Eukaryotic NER may be referred to as 'long patch' but only about 25-30 nucleotides are usually replaced (Petit and Sancar, 1999; Prakash and Prakash, 2000) compared to the much longer patches observed in prokaryotes, and the term is simply used to distinguish NER from base excision repair (Brown, 1999).

NER in Saccharomyces cerevisiae

The genes involved in NER in yeast have been identified and can be classified into two groups depending on the magnitude of their requirement for NER and the degree of UV sensitivity inflicted upon cells due to the mutation of the genes. The first class are essential for NER and mutations confer high levels of UV sensitivity and profound defects in the incision step of NER. This class consists of the RAD genes *RAD1, RAD2, RAD4, RAD10* and *RAD14*, the genes encoding subunits of the RPA complex, namely *RFA1, RFA2* and *RFA3*, and the genes encoding subunits of core TFIIH, including *RAD3, RAD25/SSL2, SSL1, TBF1, TBF2, TBF3 TBF4* and *TBF5*) (Prakash *et al.*, 1993; Wang *et al.*, 1995; Lauder *et al.*, 1996). The second class consists of genes that are not essential for NER and mutations inflict moderate UV sensitivity and lesser effects upon the incision step of NER compared to those due

to mutations in class 1 NER genes (Prakash *et al.*, 1993; Prakash and Prakash, 2000). Class 2 genes include *RAD7, RAD16, RAD23* and *MMS19* (Lauder *et al.*, 1996).

Homologous NER proteins to those discovered in *S. cerevisiae* have been identified in other yeast species, lower animals such as *Drosophila melanogaster* and in mammals, including humans. The NER proteins in yeast and their human counterparts are summarised in Table 1.2.

Table 1.2 Yeast and human proteins required for nucleotide excision repair

	Yeast Protein	Human Protein	Likely Biochemical Activity
	Rad4	XPC	GGR (also repair of TS in yeast); works with Rad23/HR23B; binds damaged DNA and recruits other NER proteins
	Rad23	HR23B	Works in complex with Rad4/XPC as above
	Rad14	XPA	Binds and stabilises open complex, recognises DNA damage
RPA	Rfa1/Rpa1	RPAp70	
RPA	Rfa2/Rpa2	p32	RPA stabilises/protects ssDNA during formation of the open complex (with Rad14/XPA)
RPA	Rfa3/Rpa3	p14	
TFIIH	Rad3	XPD	5' to 3' DNA helicase
TFIIH	Rad25 / Ssl2	XPB	3' to 5' DNA helicase
TFIIH	Ssl1	GTF2H2/p44	Zn finger; DNA binding?
TFIIH	Tfb1	GTF2H1/p62	
TFIIH	Tfb2	GTF2H4/p52	
TFIIH	Tfb3 / Rig2	MAT1	CDK assembly factor
TFIIH	Tfb4	GTF2H3	Ring finger; DNA binding?
TFIIH	Tfb5	TFB5; TTD-A	Stabilization of TFIIH
TFIIH	Kin28	Cdk7	CDK; C-terminal domain kinase; CAK
TFIIH	Ccl1	CycH	Cyclin
	Rad1	XPF	Part of endonuclease (5' incision) in Rad1-Rad10 complex
	Rad10	ERCC1	Part of endonuclease (5' incision) in Rad1-Rad10 complex
	Rad2	XPG	Endonuclease (3' incision); stabilizes full open complex
	Rad7	unknown	DNA-dependent ATPase in Rad7-Rad16 complex
	Rad16	unknown	DNA-dependent ATPase in Rad7-Rad16 complex
	Abf1	unknown	DNA binding protein, possible chromatin-reorganizing activity Works as part of Rad7-Rad16 NER subcomplex
	Mms19	unknown	Possibly influences TFIIH as upstream regulatory element
	Rad26	CSB	DNA-dependent ATPase
	Rad28	CSA	

(Adapted from http://asajj.roswellpark.org/huberman/DNA_Repair/ner.html)

Biochemical studies have elucidated possible or likely roles for many NER proteins, although the activities of some remain to be determined. Many of the NER proteins work in complexes with one another or function closely alongside other proteins, and such associations are indicated in the table by the groupings of certain proteins together. A particularly important complex is the 10-subunit complex TFIIH which plays key roles in both NER and transcription (see Section 1.3.1).

Molecular mechanism of NER in eukaryotes

The general principles and basic steps of eukaryotic NER resemble those of prokaryotic systems but the overall process is far more complicated and requires the involvement of over 30 proteins. The nature of the protein interactions and sequential activities during NER has been extensively studied using both yeast and human proteins to reconstitute the NER process *in vitro*. A key question explored was how such a large number of proteins were organised and their complex interactions and activities regulated to enable effective NER. It has been reported that a large pre-assembled multiprotein complex or 'repairosome' exists prior to the incidence of DNA damage in yeast (Svejstrup *et al.*, 1995; Rodriguez *et al.*, 1998) and human cells (He and Ingles, 1997). However, most current widely-accepted models of NER support the alternative concept of a sequential, stepwise assembly of the NER proteins at the sites of DNA damage (Friedberg *et al.*, 2005; Guzder *et al.*, 1996b; Araujo and Wood, 1999; Prakash and Prakash, 2000; Araujo *et al.*, 2001; Friedberg, 2001; Volker *et al.*, 2001; Politi *et al.*, 2005).

The mechanism of NER can be described as five main sequential steps:

i. ***Recognition of DNA damage.*** It is postulated that the distortion of the DNA helix is recognised to initiate NER, rather than the specific modification or lesion itself.

ii. ***Open complex formation***. The DNA surrounding the damage is unwound by DNA helicase activities of proteins within the complex TFIIH to create a 'bubble' in the DNA, or an open complex. This affords repair proteins access to the DNA and lesion.

iii. ***Dual incision***. Endonucleases incise the DNA either side of the damage.

iv. ***Excision of damage***. An oligonucleotide, typically 25-30 nucleotides in length, containing the lesion, is excised from the DNA helix.

v. ***Repair synthesis and ligation***. New DNA is synthesised to replace the excised fragment, using the opposite intact strand as a template, and the final nick is sealed to join the new portion to the polynucleotide chain of the original DNA helix.

An overview of eukaryotic NER is illustrated in Figure 1.6. For simplicity, only the names of yeast proteins are given, although the process is conserved in mammalian cells and the homologous human NER proteins can be deduced using Table 1.2.

Recognition of DNA damage

NER is initiated by DNA damage recognition which is widely acknowledged as the rate-limiting step of the process (Sugasawa *et al.*, 1998; Thoma, 1999; Balajee and Bohr, 2000; Friedberg, 2001) and the binding of the recognition proteins to DNA may be affected by numerous factors such as the chemical nature of the lesion and the degree of helical distortion induced by a particular lesion (Van Hoffen *et al.*, 1995; Balajee *et al.*, 1999; Balajee and Bohr, 2000). NER can be classified into two sub-pathways, differing mainly in how damage is recognised. Global genomic repair (GGR) repairs DNA damage inflicted in the non-transcribed regions of the genome, including the non-transcribed strand (NTS) of active genes whereas transcription-coupled repair (TCR) removes damage at a faster rate from the actively transcribed

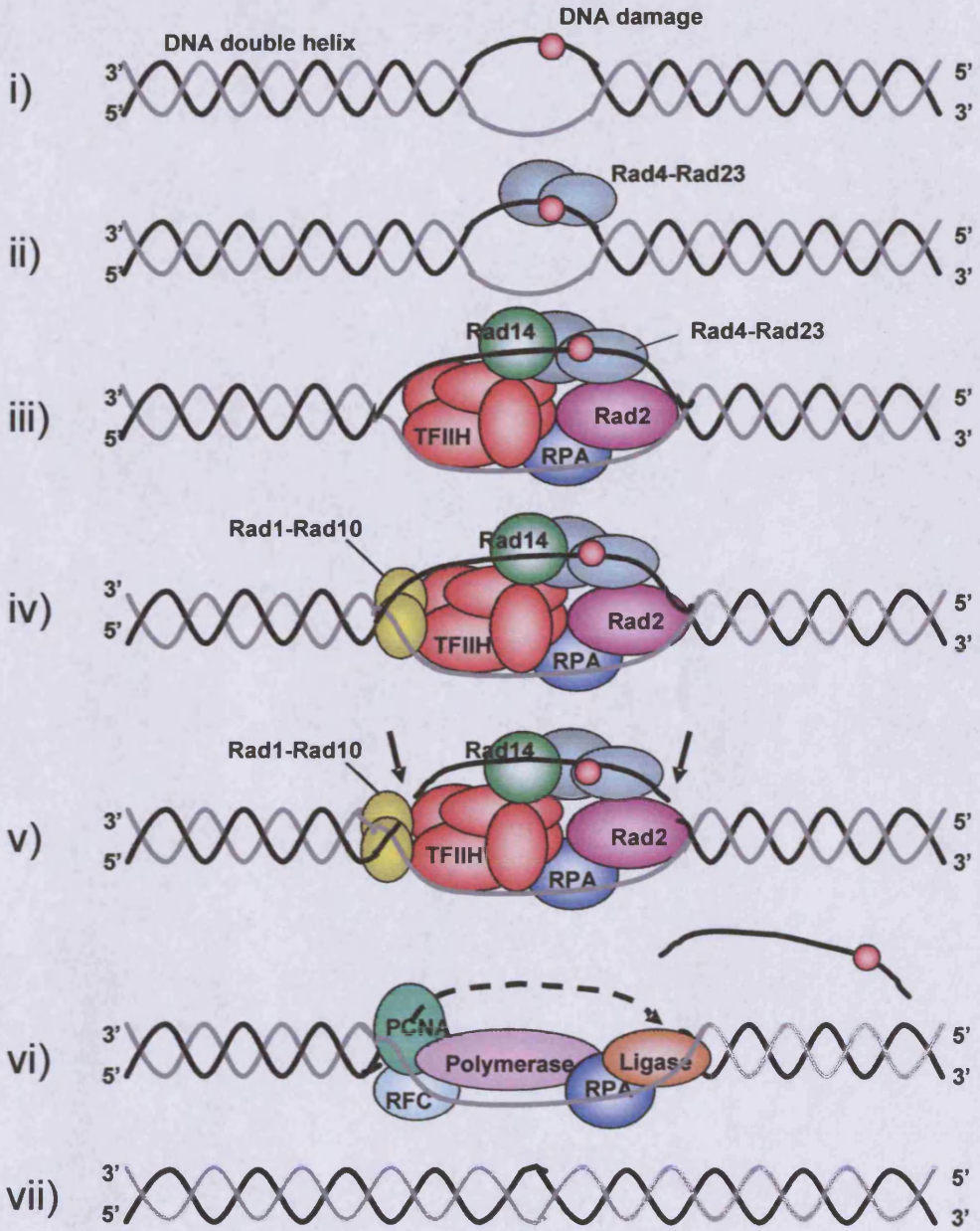

Figure 1.6. *Overview of NER in Yeast.* Helix-distorting DNA damage such as a pyrimidine dimer is induced, e.g. by UV light (i) and is recognised by the Rad4-Rad23 complex (ii). Further proteins are recruited including Rad14, RPA and TFIIH, which contains subunits Rad25 and Rad3 with helicase activity to unwind the DNA, forming a 'bubble' (iii). Rad1-Rad10 complex is recruited (iv). Bimodal incision occurs whereby Rad1-Rad10 cuts 5' to the damage and Rad2 cuts 3' to the damage (v). The oligonucleotide containing the damage is then excised before repair synthesis catalysed by polymerase fills in the gap (vi). The new DNA is finally sealed to the polynucleotide chain by DNA ligase to restore the DNA structure (vii).

regions of the genome, specifically the transcribed strand (TS) of active genes. The details of each pathway will be discussed further in Section 1.2.2.6.

Damage recognition during GGR is thought to involve the yeast Rad4-Rad23 complex (human XPC-HR23B), Rad14 (human XPA) and the single-stranded DNA binding protein RPA (replicating protein A) complex (Prakash and Prakash, 2000; Friedberg, 2001). Purified Rad4 (XPC) protein preferentially binds DNA inflicted with various types of DNA damage identified as NER substrates (Friedberg *et al.*, 2005; Wood, 1999; Sugasawa *et al.*, 1998; 2001; Friedberg, 2001) and is likely the initial and rate-limiting event in NER (Sugasawa *et al.*, 1998; Friedberg, 2001). The recognition of a specific subset of lesions, including UV-induced CPDs and 6-4 photoproducts, may be further enhanced by the DDB protein complex (XPE) (Keeney *et al.*, 1993; Tang *et al.*, 2000; Wittschieben *et al.*, 2005). The exact roles of DDB are yet to be clarified, but it appears the complex may be involved at a very early stage of NER, probably to recognise DNA damage in chromatin. The binding of the Rad4-Rad23 (XPC-HR23B) heterodimer is immediately followed by the recruitment of further proteins Rad14 (XPA), RPA, TFIIH complex and Rad2 (XPG).

TCR is generally thought to be initiated in RNA Pol II genes by the stalling of the polymerase complex at the site of DNA damage on the transcribed strand (TS) of an active gene (Mellon and Hanawalt, 1989). The arrested complex may then recruit further NER proteins to continue the repair process (Tsutakawa and Cooper, 2000; Friedberg, 2001). Although eukaryotic TCR has been best characterised for RNA Pol II transcribed genes, it has also been observed for rDNA transcribed by RNA Pol I in yeast (Verhage *et al.*, 1996; Conconi *et al.*, 2002; Meier *et al.*, 2002; Conconi, 2005). It is thought that potentially, most mechanisms involved in TCR of RNA Pol II genes

may also apply to Pol I transcribed rDNA if the rDNA is accessible to repair proteins (Conconi *et al.*, 2005; Conconi, 2005).

The molecular mechanisms of TCR are less well understood than GGR and in humans it is apparently independent of XPC damage recognition (Sugasawa *et al.*, 1998; Tsutakawa and Cooper, 2000). However, in yeast, the homologous protein Rad4 is required for both GGR and TCR in RNA Pol II transcribed genes (Guzder *et al.*, 1995; Prakash and Prakash, 2000), but is not required for TCR in RNA Pol I genes (Verhage *et al.*, 1996). Recently, it has been reported that the Rad4-independent repair of rDNA requires a protein showing homology to Rad4, newly termed Rad34 (den Dulk *et al.*, 2005; 2006). Rad4 and Rad34 may therefore play similar roles in different regions of the genome but are unable to replace each other as *rad34* mutants proficient in Rad4 cannot preferentially repair the transcribed strand of Pol I-transcribed genes (den Dulk *et al.*, 2005). Additionally, another protein, newly termed Rad33, has also been recently identified and implicated in both TCR and GGR of RNA Pol I transcribed rDNA (den Dulk *et al.*, 2006). In Pol II transcribed genes only GGR is completely defective in *rad33* mutants, although TCR shows reduced efficiency. Rad33 may stabilise Rad4/Rad23 but likely plays additional, as yet unknown roles in NER (den Dulk *et al.*, 2006).

Open complex formation

Following damage recognition and the initiation of NER, the DNA surrounding the lesion is unwound to form a 'bubble' structure, primarily through the activity of the general transcription factor TFIIH which is either recruited by Rad4-Rad23 (GGR) or as part of the stalled RNA pol II complex (TCR). TFIIH (or yeast transcription factor b) is a multiprotein complex which plays key roles in both NER

and transcription initiation (Wang *et al.*, 1994). Subunits Rad3 (XPD) and Rad25 (XPB) possess 5' to 3' and 3' to 5' DNA helicase activities respectively and cooperatively function to unwind the DNA and form the bubble structure of approximately 30 nucleotides in length (Sancar, 1996; Lindahl and Wood, 1999; Friedberg, 2001; Fuss and Cooper, 2006). The TFIIH helicases also perform this function of unwinding the DNA during transcription to facilitate initiation of transcription to generate new mRNA transcripts (Friedberg, 1996a), but in contrast, during NER, unwinding leads to discrete junctions between double- and single-stranded DNA at the bubble's edges, essential for the subsequent incision step (Friedberg, 2001). RPA and Rad14 (XPA) proteins recruited with TFIIH serve to stabilize the open complex, which is possibly further stabilized by Rad2 (XPG) (de Laat *et al.*, 1999; Friedberg, 2001).

Dual incision

In addition to stabilizing the DNA bubble, RPA and Rad14 (XPA) also help to position Rad1-Rad10 (XPF-ERCC1) complex and Rad2 (XPG) protein at the double-stranded/single-stranded DNA junctions at either edge of the DNA bubble. The binding of Rad1-Rad10 (XPF-ERCC1) consequently completes the assembly of the NER multiprotein complex. Rad1-Rad10 (XPF-ERCC1) and Rad2 (XPG) possess duplex/single-stranded DNA endonuclease activities to cut the DNA at each junction. The first incision is performed by Rad2 (XPG) 3' to the DNA lesion, which subsequently coordinates the second incision by Rad1-Rad10 (XPF-ERCC1) 5' to the damage (Wagasugi *et al.*, 1997; Constantinou *et al.*, 1999; de Laat *et al.*, 1999; Lindahl and Wood, 1999; Prakash and Prakash, 2000; Friedberg, 2001). The junction specificity of the Rad2 (3') and Rad1-Rad10 (5') endonucleases ensures that the

correct DNA strand of the bubble formation is cut during the incision step, thus preventing the formation of double strand breaks in the DNA. The damaged base is always located closer to the 3' incision than that at the 5' end but precise distances between the bimodal incisions may vary depending upon the nature of the lesion (Wood, 1997; Lindahl and Wood, 1999; Prakash and Prakash, 2000; Friedberg, 2001; Hoeijmakers, 2001) but generally, an oligonucleotide fragment of 25-32 nucleotides results, containing the DNA damage (Fuss and Cooper, 2006).

Excision of the damage-containing fragment

The oligonucleotide fragment containing the lesion is not passively removed from the DNA although the precise mechanism of excision remains unclear. However, in yeast, the Rad7-Rad16-Abf1 heterotrimeric protein complex, essential for the GGR subpathway of NER, may play a key role in excision by generating superhelical torsion in the DNA, mediated by the catalytic activity of Rad16, which enables displacement of the lesion-containing fragment (Reed *et al.*, 1998; Yu *et al.*, 2004).

Repair synthesis and DNA ligation

The excision of the damage-containing fragment renders the DNA with a large single-stranded gap which must be filled with newly-synthesised DNA. Such gaps may be susceptible to nuclease attack and so it may be possible that the excision step of NER is mechanistically linked to repair synthesis in order to avoid such attack (Friedberg, 2001). A second multi-protein complex is required for the repair synthesis and ligation steps to complete NER. DNA polymerases delta (Pol δ) and epsilon (Pol ε) are required for the repair synthesis step (Wu *et al.*, 2001) with

additionally required accessory replication proteins PCNA (proliferating cell nuclear antigen), RFC (replication factor C) and RPA (replication protein A) (Shivji *et al.*, 1995; Friedberg, 2001). The gap is filled using the intact opposite strand as a template and the final gap is sealed by DNA ligase to join the newly synthesised portion of DNA to the existing polynucleotide chain. In mammals, it is likely that DNA ligase I performs this function as gene mutations can lead to UV sensitivity (Barnes *et al.*, 1992). Ligation completes the NER process and the DNA helix is restored to its original, undamaged chemical structure.

1.2.2.6. Heterogeneity of NER in the genome

DNA damage is not repaired by NER uniformly throughout the genome but can follow one of two subpathways, dependent upon the transcriptional activity of the local DNA in which the damage occurs (Verhage *et al.*, 1998; Balajee and Bohr, 2000; Hanawalt, 2002). The major difference between the pathways lies in the damage recognition step of NER but either mechanism initiates the subsequent stepwise assembly of the core NER proteins common to both subpathways (Figure 1.7). Additionally, GGR and TCR also differ in the biological outcome of NER whereby GGR protects against cancers ultimately caused by mutations in the overall genome generated following replication of unrepaired lesions, whereas TCR ensures the accurate transcription of genes which helps protect against premature ageing (Mitchell *et al.*, 2003; Andressoo and Hoeijmakers, 2005; Fuss and Cooper, 2006)

(i) Global Genomic Repair.

GGR (or GG-NER) is the slower pathway of the two, which operates to remove DNA damage from the silent regions of the genome that are not transcribed,

including the non-transcribed strand (NTS) of active genes (de Laat *et al.*, 1999; Balajee and Bohr, 2000; Friedberg, 2001; Li and Smerdon, 2004). 6-4 photoproducts, which cause a higher degree of helical distortion to the DNA, are removed rapidly and predominantly by GGR, in comparison to CPDs which are repaired much more slowly by this pathway (Van Hoffen, 1995).

GGR in yeast requires the Rad7 and Rad16 proteins (Terleth *et al.*, 1989; Verhage *et al.*, 1994; Reed *et al.*, 1998) which function as a complex, along with Abf1 (autonomously replicating sequence binding factor 1) protein (Wang *et al.*, 1997; Yu *et al*, 2004). The heterotrimer complex is thought to generate superhelicity in DNA mediated by the catalytic activity of the Rad16 protein, and the torsion generated is necessary during the excision step of NER to release the damage-containing oligonucleotide (Yu *et al.*, 2004). Additionally, the Rad7-Rad16-Abf1 complex may also play a role in early DNA damage recognition during GGR (Guzder *et al.*, 1997; 1998; Prakash and Prakash, 2000).

(ii) Transcription-Coupled Repair.

TCR (or TC-NER) operates to preferentially repair transcribed genes faster than non-transcribed regions of the genome (Bohr *et al.*, 1985), specifically operating on the transcribed strand (TS) of transcriptionally active genes (Mellon *et al*, 1987; Mellon and Hanawalt, 1989; Smerdon and Thoma, 1990). TCR was initially observed, and has been best characterised, in the removal of CPDs, but it has also been demonstrated for other types of DNA damage in many diverse organisms (Mellon and Hanawalt, 1989; Friedberg, 1996a; Wood, 1997). TCR is thought to be initiated by a stalled RNA polymerase II complex at the site of the lesion which acts as the damage recognition signal and subsequently recruits the core NER machinery

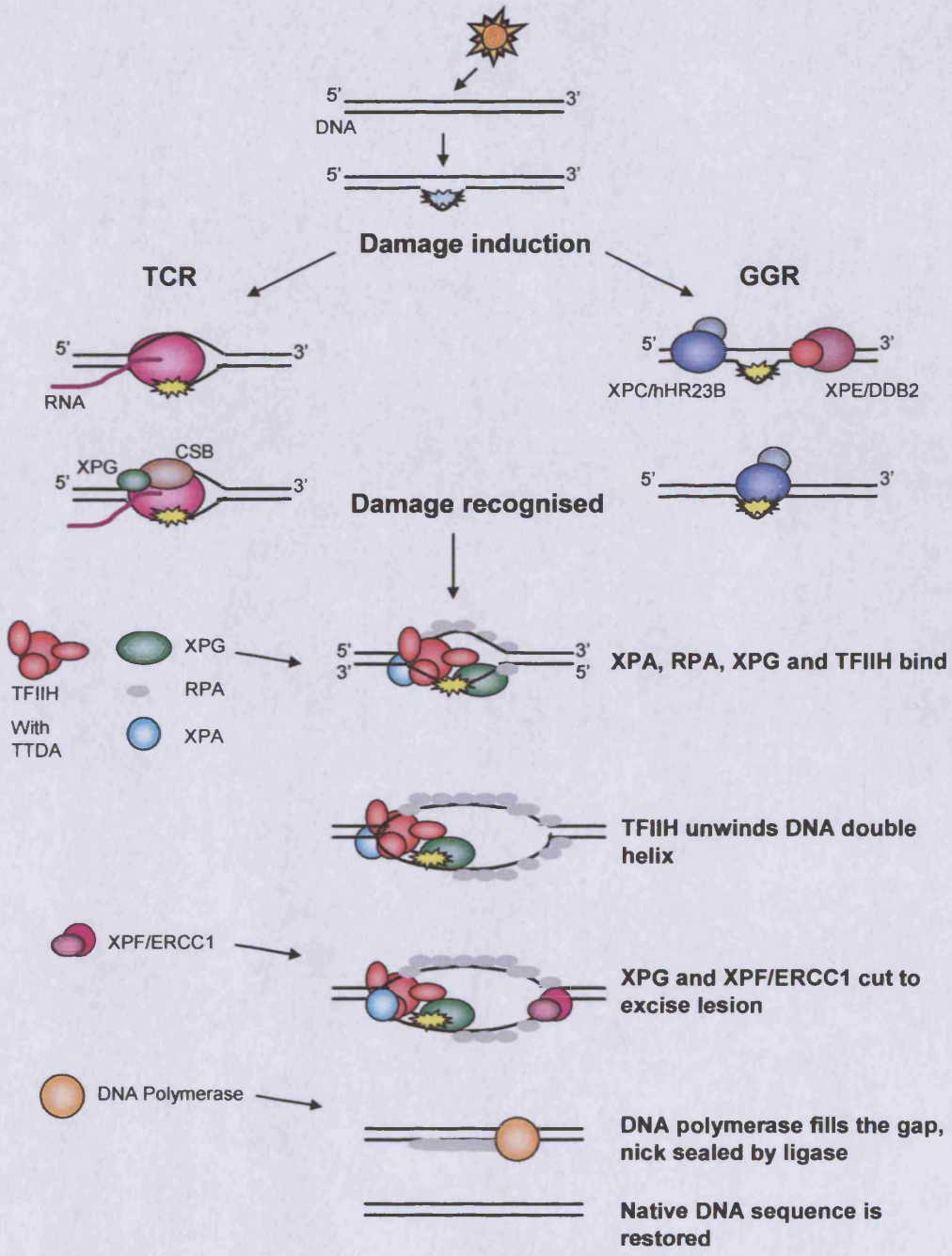

Figure 1.7. *Heterogeneity of NER in eukaryotes.* The GGR and TCR subpathways of NER differ in the recognition of DNA damage in transcriptionally silent or active regions of the genome respectively. GGR requires the XPC/hHR23B (yeast Rad4-Rad23) complex for damage recognition, facilitated by XPE/DDB complex for some types of damage including UV-induced photoproducts. TCR is initiated by the stalled RNA Pol II complex at the site of DNA damage on the transcribed strand of an active gene, which recruits further proteins such as XPG (Rad2) and CSB (Rad26). Both mechanism leads to a similar stepwise assembly of NER proteins and repair process to restore the native DNA structure, as previously detailed.

(Mellon and Hanawalt, 1989; Mu and Sancar, 1997; Tornaletti and Hanawalt, 1999; Citterio *et al.*, 2000).

Two important human proteins essential for TCR are CSA (Cockayne Syndrome A) and CSB (Cockayne Syndrome B). The nomenclature of these proteins reflects the human disorder resulting from the defective proteins, which confers UV sensitivity and renders the cell deficient in the TCR pathway (de Boer and Hoeijmakers, 2000; Bootsma *et al.*, 2001; Mitchell *et al.*, 2003). The yeast homologues of the *CSA* and *CSB* genes have been identified as *RAD28* (Bhatia *et al.*, 1996) and *RAD26* (van Gool *et al.*, 1994) respectively. The molecular function of Rad28 has yet to be clarified but *rad28* cells are not defective in TCR (Bhatia *et al.*, 1996). To date, the precise function of CSB/Rad26 in TCR remains to be clarified but Rad26 has been implicated in various roles. The Rad26 protein is a DNA-dependent ATPase (Guzder *et al.*, 1996a) and both CSB and Rad26 belong to the Swi2/Snf2 family of chromatin remodelling proteins, hence may be involved in altering protein-DNA interactions during DNA repair (Ura and Hayes, 2002; Green and Almouzni, 2002). In *rad26* cells the resultant defect in TCR is believed to be due to an inability to release stalled transcription complexes at sites of DNA damage (Tijsterman and Brouwer, 1999). Rad26 is also believed to be required for the recruitment of TFIIH (You Z, *et al.*, 1998) which is vital in the stepwise assembly of the NER machinery. *RAD26* and *CSB* have been reported to play a role in transcription elongation in yeast and humans respectively (Lee *et al.*, 2001; Selby and Sancar, 1997) and, interestingly, Rad26 appears to promote transcription through DNA bases suffering from certain forms of damage to advocate cell survival (Lee *et al.*, 2002). Furthermore, this function appears to be independent of any excision repair pathway (Lee *et al.*, 2002).

Unlike CSB cells, *rad26* yeast cells do not show increased UV sensitivity and TCR is not completely abolished (van Gool *et al.*, 1994; Verhage *et al.*, 1997), suggesting alternative subpathways of TCR may exist in eukaryotes. This has been reported to be the case by Li and Smerdon (2002), who identified an alternative, Rad26-independent TCR subpathway mediated by the Rpb9 subunit of the RNA Pol II complex itself. The Rpb9 TCR subpathway appears to be most effective in the coding regions of genes, in contrast to the Rad26 pathway which operates with equal efficiency in both the coding and transcribed regions. The study also suggests a role for Rpb4, another subunit of RNA pol II, in the regulation of both TCR pathways. The deletion of both *RAD26* and *RPB9* genes completely abolishes TCR, indicating there are no other TCR subpathways for RNA pol II genes in yeast (Li and Smerdon, 2002; 2004).

1.2.2.7. Human consequences of NER deficiencies

Cellular responses to DNA damage, whether attempts at repair or alternative signalling cascades to induce cell senescence (arrested growth) or apoptosis, are vital in the promotion of longevity and in the prevention of cancers in humans (Mitchell *et al.*, 2003; Andressoo and Hoeijmakers, 2005). The importance of damage responses to maintain genetic integrity is highlighted by the dramatic clinical consequences observed in several rare human disorders, whereby the causative genes are known to play key roles either directly in DNA repair or in signal transduction processes to initiate alternative cellular responses to persistent damage (Mitchell *et al.*, 2003). NER is a vital repair pathway and key NER proteins have been implicated in the human disorders xeroderma pigmentosum (XP), Cockayne syndrome (CS) and trichothiodystrophy (TTD) and other conditions conferring UV (solar) sensitivity (de

Boer and Hoeijmakers, 2000; Friedberg, 2001; Mitchell *et al.*, 2003; Fuss and Cooper, 2006). XP and CS are particularly important conditions as much of our current knowledge and understanding of NER has been elucidated from studies of patients suffering from these disorders. A summary of the implicated genes, clinical features and molecular defects associated with each disorder is given in Table 1.3.

Table 1.3 Summary of human disorders resulting from defects in NER.

Human Disease	Genes	Clinical Features	Molecular Defect
Xeroderma pigmentosum (XP)	XPA, XPB, XPC, XPD, XPE, XPF, XPG, XPV	Sun sensitivity, cancer Neurological defects	NER, translesion synthesis
Cockayne Syndrome (CS)	CSA, CSB	Sun sensitivity, post-natal developmental defects, Neurological defects, premature ageing	Transcription-coupled repair (TCR)
XP / CS	XPB, XPD, XPG	Both XP and CS	Both global and transcription-coupled NER
Trichothiodystrophy (TTD)	XPD	Premature aging, brittle hair, scaly skin	NER
UV-sensitive Syndrome	CSB, unknown gene(s)	sun sensitivity	Transcription-coupled repair (TCR)
Photosensitive	XPB, XPD, TTDA	Sun sensitivity, post-natal developmental defects	NER, transcription

(Adapted from Fuss and Cooper, 2006)

Xeroderma pigmentosum (XP)

XP was first described in the late nineteenth century (Hebra and Kaposi, 1874) and named in reference to the characteristic dry, pigmented skin characteristically observed in patients. It is a rare, recessive hereditary disease which has been well characterised and linked to defects in NER (Cleaver, 1968; Kraemer *et* al, 1987; Hoeijmakers, 1994; Bootsma *et al.*, 1998; de Boer and Hoeijmakers, 2000; Friedberg,

2001; Mullenders *et al.*, 2001; Magnaldo and Sarasin, 2004). The main symptoms of XP include increased UV sensitivity, pigmentary changes, premature skin ageing and a predisposition to the development of malignant tumours. Eye and neurological abnormalities are also common. XP can be detected at the age of 1-2 years, and the average age of onset of skin cancer is 8 years. Fewer than 40% of XP patients survive past the age of 20 years. Seven XP repair genes *XPA-XPG* have been identified which play key roles as part of the core NER machinery in both the TCR and GGR pathways (detailed previously in Section 1.2.2.5). Additionally, the XP-variant (*XPV*) gene has been identified, which encodes a DNA polymerase involved in DNA replication past UV lesions, termed 'translesion synthesis' (Fuss and Cooper, 2006). The seven complementation groups which correspond to defects in the *XPA-XPG* genes have been described and differ in their frequency of incidence (for example, XPA is relatively common compared to XPE which is rare) and disease severity (for example, XPG is severe whereas XPF is relatively mild). There is currently no cure for XP but clinical treatments and gene therapies are continually being researched and developed (Herouy *et al.*, 2003; Magnaldo and Sarasin, 2004; Khader *et al.*, 2005).

Cockayne syndrome (CS)

CS was first described in the 1930s (Cockayne, 1936) and is a developmental disease characterised by symptoms including dwarfism, profound mental retardation, premature ageing and increased sun sensitivity. Unlike XP, however, there is no predisposition to skin cancer (Bootsma *et al.*, 2001; Friedberg, 2001; Fuss and Cooper, 2006). There are two subtypes of CS: classic CS, or CS-I, which becomes apparent in childhood and typically causes death by 20-30 years of age, and severe

CS, or CS-II, which is apparent at birth and typically results in childhood death at 6-7 years.

In 90% of cases, CS arises from defects in either the *CSA* or *CSB* genes (Friedberg, 1996b; 2001; Rapin *et al.*, 2000). Both gene products are required for the TCR subpathway of NER, although the precise function of CSB remains to be determined. CSA and CSB, in conjunction with core NER proteins TFIIH (XPB and XPD) and XPG, are thought to function in the removal of a stalled polymerase at a DNA lesion and in recruiting further NER proteins (van den Boom *et al.*, 2002; Mitchell *et al.*, 2003). Interestingly, it has been reported that a complete deficiency in the CSB protein may cause UV-sensitive syndrome (UVsS), a very mild disorder characterised by sun sensitivity and mild freckling without the severe clinical features of XP and CS, but may not result in Cockayne syndrome (Horibata *et al.*, 2004).

In rare cases, specific mutations in *XPB, XPD* and *XPG* result in a disorder of XP combined with CS (XP/CS) in which patients are severely affected with clinical manifestations of both diseases (Rapin *et al.*, 2000; Lindenbaum *et al.*, 2001). Skin cancer at a young age is observed in some but not all cases (Lehmann, 2000).

Trichothiodystrophy (TTD)

TTD is characterised by sulphur-deficient brittle hair, icthyosis (fish-like scales on the skin), mental retardation, and photosensitivity in most cases (Pollitt *et al.*, 1968; Lehmann, 2000; Bootsma *et al.*, 2001; Friedberg, 2001). In most cases of TTD, NER of UV-induced lesions is defective but skin cancer has not been documented for TTD (Weeda *et al.*, 1997; Friedberg, 2001). The *XPB* and *XPD* genes have been implicated in photosensitive TTD but the severe skin and neurological features of XP and CS are not developed (Stefanini *et al.*, 1986;

Hoeijmakers, 1994; Weeda *et al.*, 1997; Lehmann, 2000; Bootsma *et al.*, 2001; Friedberg, 2001). Besides XPB and XPD, a third TTD complementation group, TTD-A has also been identified (Giglia-Mari *et* al, 2004) and the TTDA protein (also called Tfb5) was recently identified in yeast as a subunit of TFIIH (Ranish *et al.*, 2004). Thus, remarkably, TTDA, XPB and XPD defects are all associated with subunits of TFIIH, suggesting mutations in TFIIH components may cause transcriptional insufficiency in addition to NER effects, which may explain part of the non-XP clinical features of TTD (Giglia-Mari *et* al, 2004).

The genetic defects for XP, CS and TTD often involve common genes, such as *XPB* and *XPD* and yet different manifestations are apparent and only XP patients exhibit a predisposition to cancer. The precise mechanisms of how mutations in the same key genes can lead to different clinical disorders are yet to be fully understood (Friedberg, 2001).

1.3 DNA Repair and Transcription

NER and transcription are intimately linked processes in both prokaryotic and eukaryotic cells. This link is clearly apparent by the TCR phenomenon (see Section 1.2.2.6) whereby a stalled RNA polymerase activates repair of DNA lesions in the transcribed strand (TS) of active genes (Mellon *et al*, 1987; Mellon and Hanawalt, 1989; Smerdon and Thoma, 1990). In *E. coli*, NER is mediated by the Uvr protein system (see Section 1.2.2.4), which preferentially repairs lesions in the TS by TCR (Selby and Sancar, 1994; Mellon, 2005). TCR is abolished by mutations in the *MFD* (mutation frequency decline) gene (Selby and Sancar, 1991; Selby *et al.*, 1991; Selby and Sancar, 1994). The Mfd protein is a coupling factor with dual roles in the

dissociation of a stalled RNA polymerase complex at the site of a DNA lesion and the recruitment of NER proteins (Scicchitano and Mellon, 1997). Following repair, the next polymerase complex to traverse the gene is able to resume transcription. A similar mechanism exists in eukaryotes involving the general transcription factor TFIIH, known to have dual roles in transcription and repair.

1.3.1 TFIIH

Independently of TCR, TFIIH is a vital component of both the transcription and NER machineries (Feaver *et al.*, 1993; Drapkin *et al.*, 1994; Wang *et al.*, 1994). In transcription, the DNA helicase activity of TFIIH is required for unwinding the DNA helix at the transcription start site during transcription initiation (Dvir *et al.*, 1996; Holstege *et al.*, 1996). It also regulates the transition from initiation to elongation, presumably mediated by its CTD kinase activity (Dahmus, 1994; O'Brien *et al.*, 1994), and has additionally been shown to promote the transition from very early elongation complexes to stable elongation complexes, thus performing multiple functions prior to, during and following transcription initiation (Dvir *et al.*, 1997; Hampsey, 1998).

The roles of TFIIH in NER were detailed in Section 1.2.2.5, and the complex is particularly important in the formation of the open complex DNA structure whereby the helicase subunits XPD (yeast Rad3) and XPB (Rad25) unwind the local DNA. TFIIH is either recruited to the damage site by Rad4-Rad23 (GGR) or as part of the stalled RNA pol II complex (TCR).

TFIIH exists in alternative forms, consisting of a core-TFIIH component which can associate with other proteins to form the holo-TFIIH complex associated with transcription or the repairosome complex associated with NER (Svejstrup *et al.*,

1995). The yeast TFIIH form active in transcription is composed of a 5-subunit core, the Ssl2 protein and a complex of three additional polypeptides that possesses protein kinase activity (Svejstrup *et al.*, 1995; Hampsey, 1998). However, the TFIIH complex associated with NER does not contain the kinase complex and in addition to the core and Ssl2 components, interacts with all other proteins known to be required for NER in yeast: Rad1, Rad2, Rad4, Rad10, and Rad14 (Svejstrup *et al.*, 1995; Hampsey, 1998). Since the kinase and repair complexes can associate and dissociate reversibly from the core TFIIH, a model has been proposed whereby the kinase form is required for initiation but can be replaced by the repair form when DNA damage is encountered (Svejstrup *et al.*, 1995) but this model is challenged by the evidence for sequential assembly of NER proteins rather than a pre-existing repairosome (Friedberg *et al.*, 2005; Guzder *et al.*, 1996b; Araujo and Wood, 1999; Prakash and Prakash, 2000; Araujo *et al.*, 2001; Friedberg, 2001; Volker *et al.*, 2001; Politi *et al.*, 2005).

Overall, TFIIH is clearly a vital component of transcription and NER and provides a functional link between the two processes. Its importance is further highlighted by the clinical disorders resulting from defective NER which largely result from defects in TFIIH subunits. The precise mechanisms of TFIIH in transcription and NER remain elusive and our understanding will be greatly enhanced by innovative techniques such as live-cell imaging to monitor the dynamic movements of TFIIH *in vivo* (Volker *et al.*, 2001; Hoogstraten *et al.*, 2002; Fuss and Cooper, 2006; Giglia-Mari *et al.*, 2006) and help unravel the specific mechanisms involved in human NER disorders.

1.4 Chromatin Implications in Transcription and DNA Repair

1.4.1 Chromatin Structure

In order to fit into the nucleus of a cell, eukaryotic DNA is associated with histones and other proteins to be packaged compactly into chromatin (Kornberg, 1977; Wolffe, 1998; Lewin, 2000; Luger, 2006). The basic unit of chromatin is the nucleosome (Luger *et al.*, 1997), which comprises of 147bp of DNA wrapped around a histone octamer of two each of the core histone proteins H2A, H2B, H3 and H4. Histones H3 and H4 are extremely highly conserved, suggesting a significant overlap in function in all eukaryotes. H2A and H2B are also conserved but show a degree of species-specific variation (Lewin, 2000). Nucleosomes are connected in a 'beads on a string' manner by linker DNA, and are subsequently compacted into further higher order chromatin structures by sequential steps of folding and coiling, ultimately resulting in highly condensed chromatin and the metaphase chromosome structure visible under a light microscope (Figure 1.8).

The 'linker' histone protein H1 also plays an important role in DNA packaging in many eukaryotes, including humans. Located outside of the core nucleosome, the precise function of histone H1 remains elusive, but it is thought it may have a structural function in helping secure DNA to the core histone octamer (Lewin, 2000; Philippe and Hansen, 2001) and possibly roles in chromatin modification (Veron *et al.*, 2006). Previously, H1 was not thought to exist in yeast, but a possible homologue has been identified, encoded by the *HHO1* (Histone H One) gene. (Ushinsky *et al.*, 1997; Patterton *et al.*, 1998; Freidkin and Katcoff, 2001; Veron *et al.*, 2006).

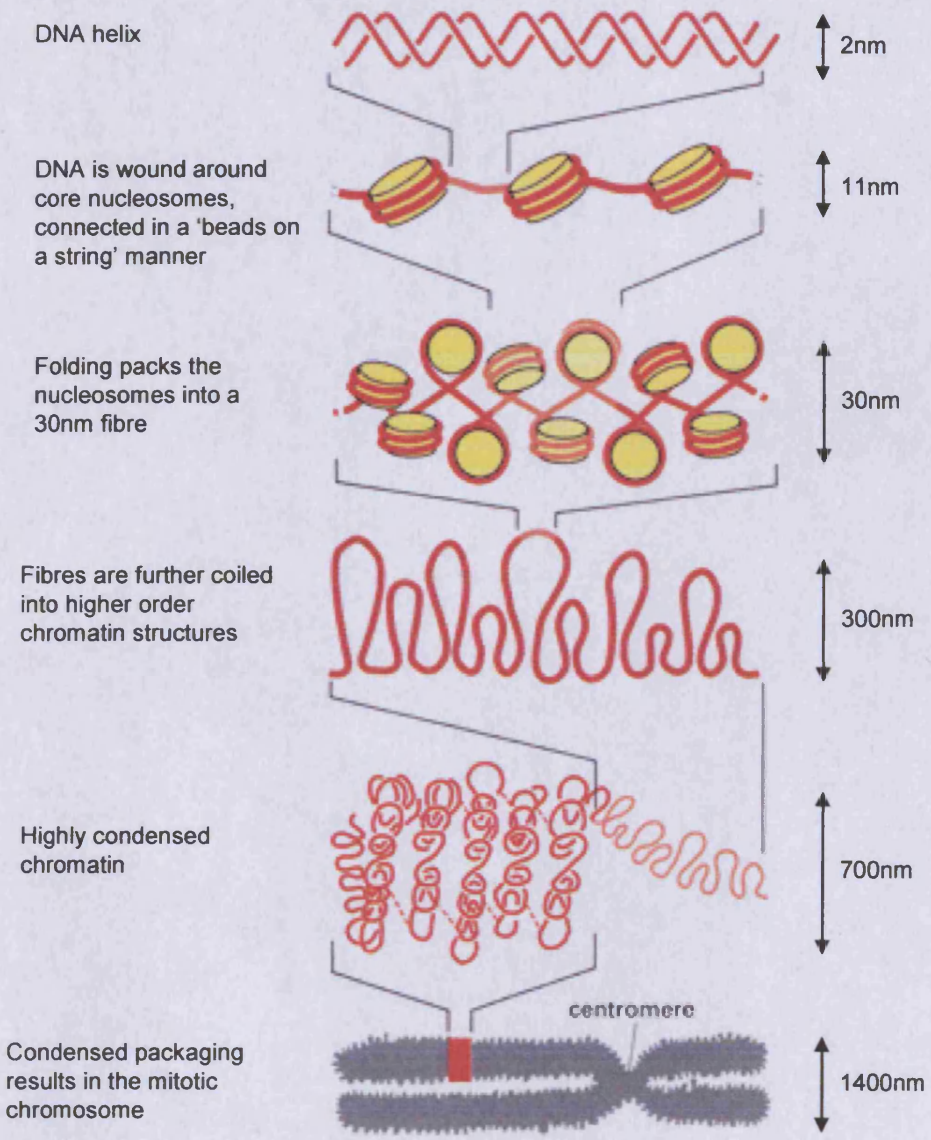

Figure 1.8. *Chromatin organisation to package DNA in eukaryotes.* The DNA double helix associates with histones to form nucleosomes, which are arranged in a 'beads on a string' configuration. This is folded and coiled into a solenoid to form a chromatin fibre, which is then further coiled and supercoiled to eventually package and condense the chromatin into chromosomes. *(Adapted from http://anatomy.iupui.edu/courses/histo_D502/D502f04/lecture.f04/cell.f04/cellf04.html.html)*

However, rather than roles in chromatin organisation, its gene product may instead be involved in recombination (Patterton *et al.*, 1998; Downs *et al.*, 2003).

Protruding from each of the core histone proteins is a flexible, amino-terminal 'tail' of 25-40 residues, which contains multiple sites for modification that are important in chromatin function. The tails of histones H3 and H4 are particularly highly conserved. Important modifications include acetylation, deacetylation, methylation and phosphorylation, which may change the overall charge of histone proteins and thereby alter the functional properties of the core histones, how they interact with other proteins and ultimately help modulate chromatin structure (Wu and Grunstein, 2000).

1.4.2 Implications of chromatin structure

1.4.2.1. Chromatin and the formation of UV-induced damage

UV-induced CPDs and 6-4 photoproducts are the best studied forms of DNA damage in chromatin. The two lesions are not distributed with equal incidence throughout the genome and this is partially dependent upon the local chromatin structure, in addition to DNA sequence and protein associations (Thoma, 1999; 2005; Ura and Hayes, 2002). CPDs are induced in core nucleosomal DNA of UV-treated chromatin with a periodicity of 10.3 bases, with the highest incidence at the sites where the minor groove of the helix faces away from the histone surface (Gale *et al.*, 1987; Pehrson, 1989; Gale and Smerdon, 1990). Such periodicity is not observed in the linker regions of DNA (Pehrson, 1995). In contrast, 6-4 photoproducts are distributed more randomly throughout nucleosomal DNA but preferentially form in linker and nucleosome-free regions of DNA (Gale and Smerdon, 1990). The

reasoning for the distinction between the formation of CPDs and 6-4 photoproducts remains unclear, but there appears to be no site within nucleosomal DNA that totally resists damage formation (Thoma, 2005).

1.4.2.2. Chromatin and DNA-mediated processes

The structure of chromatin clearly impedes essential DNA-mediated processes such as transcription, DNA repair and replication as the DNA is tightly compacted and access by the relevant proteins is severely restricted (Luger *et al.*, 1997; Moggs and Almouzni, 1999). Chromatin organisation is heterogeneous throughout the genome and exists as two main forms: euchromatin is the 'relaxed' or 'open' state whereby the DNA is less tightly compacted and thus more accessible, whereas heterochromatin is much more tightly compacted in a 'closed' state typically observed in silent regions of the genome. Chromatin, however, is dynamic and can undergo local conformational changes, involving the active repositioning of nucleosomes (Widom, 1998; Workman and Kingston, 1998), to exist in either repressive or more permissive states, a phenomenon central to the regulation of processes such as transcription and repair. Chromatin dynamics can be modulated by post-translational histone modifications, such as acetylation, and by ATP-dependent chromatin remodelling activities (Kingston and Narlikar, 1999; Wolffe and Hayes, 1999; Ura and Hayes, 2002; Saha *et al.*, 2006). Such activities to alter nucleosome positioning may be targeted to specific loci or may function globally to effect structural chromatin changes (Becker and Horz, 2002; Peterson and Cote, 2004; Thoma, 2005).

1.4.3. Histone Acetylation

Histone acetylation is a particularly important and well-characterised modification involved in gene regulation and nucleosome assembly (Wade *et al.*, 1997; Workman and Kingston, 1998), achieved via histone acetyltransferases (HATs). The process involves the transfer of an acetyl group from acetyl-CoA to the ε-amino group of specific lysine residues in the amino-termini of histone tails, neutralising the positive charge. This is a reversible reaction whereby histone deacetylases (HDACs) can remove the acetyl group and restore a positive charge, counteracting the effects of acetylation (Figure 1.9).

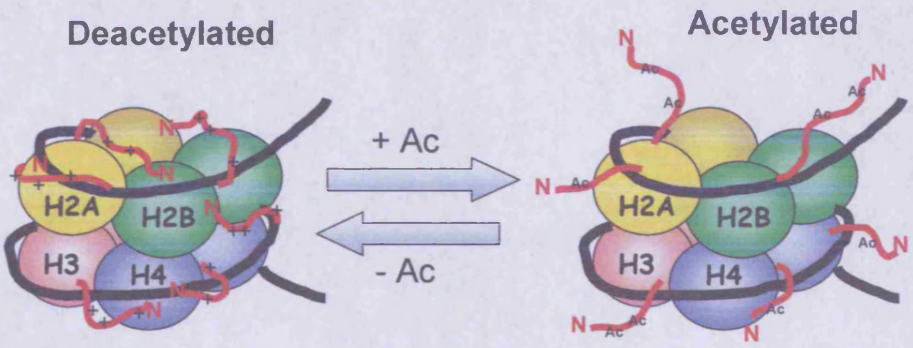

Figure 1.9. *Acetylation and deacetylation of histone tails.* Histone acetylation by histone acetyltransferases (HATs) involves the addition of an acetyl group (Ac) to the ε-amino group of the *N*-termini tails protruding from the core histones, neutralising the positive charge. Each histone has specific targets for acetylation. The functional properties of the histones and interactions with other proteins or DNA are altered, which helps modulate chromatin in the regulation of transcription and DNA repair. Acetylation is a reversible modification whereby histone deacetylases (HDACs) can remove the acetyl group and restore a positive charge, counteracting the effects of acetylation.

Each core histone has specific target sites for modification. Particularly important sites for acetylation include histone H3 lysines at amino acid positions 9, 14, 18 and

23, and histone H4 lysines 5, 8, 12 and 16 (Roth *et al.*, 2001). Acetylation is thought to affect histone interactions with other histones and non-histone proteins, and reduce their affinity for DNA, helping to modulate chromatin structure so that it is more permissive to transcription (Roth *et al.*, 2001; Grant, 2001), and other DNA mediated processes.

1.4.3.1. Histone acetyltransferases (HATs)

There are two broad classes of HATs which have been identified. Nuclear A-type HATs are those thought to be mainly involved in acetylation activity associated with gene regulation, such as Gcn5. Cytoplasmic type-B HATs such as Hat1 are thought to be involved in transportation of newly synthesised histones from the cytoplasm to the nucleus to be deposited onto newly replicated DNA (Brownell and Allis, 1996; Roth *et al.*, 2001). Gcn5 was first identified as an archetypal nuclear HAT (Brownell *et al.*, 1996; Kuo *et al.*, 1996) and since then, over 20 HATs have been identified, and grouped into several families (Chen *et al.*, 2001; Grant, 2001; Roth *et al.*, 2001). The main HAT families include:

1) The GNAT (Gcn5-related *N*-acetyltransferases) superfamily contains HATs associated with transcriptional initiation (Gcn5, PCAF), elongation (Elp3), histone deposition and telomeric silencing (Hat1).
2) The p300/CBP family are coactivators for multiple transcription factors which cooperate with other HATs in gene activation (Grant and Berger, 1999).
3) The MYST family include MOZ, Ybf2/Sas3, Sas2, Tip60 and Esa1. Members of this family are associated with the H3-specific NuA_3 complex and the H4-specific NuA_4 complex (Grant, 2001).

4) Further HATs have been grouped as basal transcription factors, such as $TAFII_{250}$ (of TFIID) and nuclear receptor cofactors such as ACTR and SRC1 (Grant and Berger, 1999; Roth *et al.*, 2001).

In addition to the acetylation of specific lysine residues of core histones, HATs may also interact with ATP-dependent chromatin remodelling complexes such as SWI/SNF to modulate chromatin structure during transcription regulation (Hassan *et al.*, 2001). For example, HAT activities have been reported to precede the recruitment of remodelling complexes during gene activation (Syntichaki *et al.*, 2000; Dilworth *et al.*, 2000; Mitra *et al.*, 2006). Additionally, histone deacetylation has also been shown to be coupled to chromatin remodelling, such as the human NRD (nucleosome remodelling and deacetylating) complex (Tong *et al.*, 1998) and HDACs have been shown to inhibit recruitment of chromatin-modifying activities in transcriptional repression (Deckert and Struhl, 2002), further demonstrating the link between acetylation and chromatin remodelling complexes in gene regulation.

1.4.3.2. Histone deacetylases (HDACs)

To date, ten HDACs have been identified in yeast: Rpd3, Hda1, Hos1, Hos2 and Hos3 (Rundlett *et al.*, 1996) and the NAD+-dependent Sir2 family of Sir2, Hst1, Hst2, Hst3 and Hst4 (Landry *et al.*, 2000). Over 19 homologues have been identified in humans and classified based on their similarity to the yeast HDACs (Verdin *et al.*, 2003). Class I are similar to Rpd3 (HDACs 1, 2, 3 and 8) and class II are more similar to Hda1 (HDACs 4, 5, 6, 7, 9 and 10). Class III HDACs include the seven human sirtuins and are similar to the yeast Sir2 (silent information regulator 2) family and, unlike the zinc-dependent activity of classes I and II, are NAD+-dependent

(Landry *et al.*, 2000; Tanny and Moazed, 2001; Denu, 2003; Yang and Grégoire, 2005). The specific roles and activities of HDACs are discussed in further detail in Chapter 3.

Many of the identified HDACs function as corepressors of transcription and can be recruited to promoters to promote localised deacetylation of chromatin (Wu and Grunstein, 2000; Deckert and Struhl, 2002). Additionally, HDAC activity has been linked to the formation and regulation of highly condensed heterochromatic regions of the genome (Ekwall *et al.*, 1997; Taddei, *et al.*, 2001; Robyr *et al.*, 2002).

1.4.3.3. Histone acetylation and transcription regulation

Precisely how transcription occurs in a chromatin environment has posed an intriguing and challenging question that has led to many further lines of study investigating how chromatin affects other cellular processes such as DNA repair. Links between acetylation and transcriptional regulation were initially proposed over 30 years ago (Allfrey, 1977) and have since been well characterised (Edmondson and Roth, 1996; Wade *et al.*, 1997; Kuo and Allis, 1998; Struhl, 1998; Workman and Kingston, 1998; Walia *et al.*, 1998; Meijer and Smerdon, 1999; Morales *et al.*, 2001; Horn and Peterson, 2002). Important discoveries identified known transcriptional activators to possess HAT activity, such as Gcn5 in yeast (Brownell *et al.*, 1996; Kuo *et al.*, 1996) and p300/CBP in mammals (Bannister and Kouzarides, 1996; Ogryzko *et al.*, 1996; Grunstein, 1997). Increased histone acetylation generally correlates with increased access of transcription factors to nucleosomal DNA (Lee *et al.*, 1993; Vettese-Dadey *et al.*, 1996), and thus the facilitation of transcription. Similarly, histone deacetylation is generally associated with the repression of transcription, first highlighted by the discovery that the repressor proteins Rpd3 in yeast and HDAC in

humans were histone deacetylases (Grozinger *et al.*, 1999; Wu and Grunstein, 2000). There are however exceptions, whereby histone acetylation has been linked to gene silencing in yeast (Braunstein *et al.*, 1996; Kelly *et al.*, 2000) and deacetylation has been linked to gene activation (Bernstein *et al.*, 2000; Wang *et al.*, 2002; Nusinzon and Horvath, 2005; 2006).

The heterogeneity of chromatin in the genome also reflects the transcriptional status of DNA, further highlighting the connection between the two (Thoma, 1999; Balajee and Bohr, 2000). Actively transcribed chromosomal regions often contain hyperacetylated histones whereas histones in silent, heterochromatic regions are hypoacetylated. A steady state level of histone acetylation is achieved in the cell by the balancing of the two opposing enzymic activities (Wade, 2001). Certain pairs of HATs and HDACs may even operate as 'functional pairs' to oppose each other's activity in gene regulation. For example, histone H3 acetylation by Gcn5 and histone H4 deacetylation by Rpd3 have distinct, opposing effects on transcription at the yeast *IME2* gene (Burgess *et al.*, 1999) and the HAT Esa1 and Rpd3 both target histone H4 lysine 12 at the *PHO5* promoter (Vogelauer *et al.*, 2000). The specific mechanisms of how HDACs and HATs are modulated in the creation of specific acetylation patterns to govern chromatin structure in transcription regulation remain unresolved and continue to pose a fascinating challenge. Modes of regulating chromatin structure in transcription however, may well apply to the regulation of other DNA-mediated processes such as DNA repair and recombination. The biological relevance of acetylation is further demonstrated by the implication of HAT and/or HDAC activities in diverse cellular processes such as cell cycle progression, DNA recombination, repair and apoptosis, and in cancer (Roth *et al.*, 2001).

1.4.4. NER in a chromatin environment

NER removes bulky lesions from the genome and is sub-divided into the TCR (transcription-coupled repair) and GGR (global genomic repair) pathways. Whilst TCR removes lesions from the transcribed strand of active genes only, GGR removes damage from the remaining, untranscribed regions, and hence is responsible for the repair of damage in nucleosomal DNA (Hoeijmakers, 2001; Hanawalt, 2002).

Chromatin remodelling following DNA repair was first demonstrated over 25 years ago (Smerdon and Lieberman, 1978; 1980) but the precise mechanisms of how chromatin is modulated during NER are still being unravelled. Pioneering studies showed that repair synthesis by NER is greatly reduced in UV-damaged nucleosomal DNA (Wang *et al.*, 1991) or simian virus 40 (SV40) mini-chromosomes (Sugasawa *et al.*, 1993) compared to naked DNA.

Generally, there are three main areas of consideration to decipher how NER occurs in chromatin: (*i*) how lesions are detected in chromatin, (*ii*) how the lesions are accessed and repaired, and (*iii*) how the chromatin is restored to its initial state upon the completion of repair, which have led to the 'access, repair, restore' (ARR) model of unfolding and refolding chromatin during NER (Lieberman *et al.*, 1979; Smerdon, 1991; Moggs and Almouzni, 1999; Smerdon and Conconi, 1999; Thoma, 1999; Green and Almouzni, 2002; Gontijo *et al.*, 2003; Gong *et al.*, 2005). Early recognition and repair steps in chromatin remain the least well characterised aspects of NER in chromatin but affinities for the recognition proteins required and efficiency of damage excision have been shown to be reduced in nucleosomal DNA (Hara *et al.*, 2000).

Accessing the DNA during NER is believed to involve the recruitment of histone modifying enzymes, such as HATs and HDACs, and chromatin remodelling factors (Meijer and Smerdon, 1999), such as the ATP-utilizing chromatin assembly

and remodelling factor (ACF) which can catalyse nucleosome movement (Ura *et al.*, 2001). The coupling of transcription and repair (TCR) provides further links between chromatin remodelling and NER as remodelling associated with transcription may play a role in affording access of NER proteins to damaged DNA on the transcribed strand of active genes (Kingston and Narlikar, 1999). Histone modifications have also been linked to altering the accessibility of damaged nucleosomal DNA during NER. For example, histone H3 acetylation activity can be directed to UV-induced damage *in vitro* by the TBP-free TAFII (TFTC) complex which contains both the HAT Gcn5 and the SAP130 subunit which specifically binds damaged DNA (Brand *et al.*, 2001). Finally, once NER has repaired DNA damage, the chromatin structure must be returned to its prior state to preserve the epigenetic information (Gong *et al.*, 2005). Hence nucleosomes are effectively reloaded onto DNA following repair synthesis (Smerdon and Lieberman, 1978). Repair-coupled nucleosome assembly is likely to aid the restoration of chromatin structure and is believed to involve chromatin assembly factors such as CAF1 (chromatin assembly factor 1), shown to play a role in repair-associated chromatin assembly *in vitro* (Gaillard *et al.*, 1996). Supportive of this notion, yeast mutant cells defective in CAF1 subunits CAC1, CAC2 and CAC3 (*cac* mutants) are UV sensitive and show defects in gene silencing (Kaufman *et al.*, 1997; Enomoto and Berman, 1998). Additionally, *in vivo* evidence has been presented by the immunolocalisation of CAF1 following UV damage and the biochemical indications that CAF1 is recruited to chromatin following such damage (Martini *et al.*, 1998). Further evidence for the role of CAF1 in repair synthesis during NER comes from the observation that it is recruited with PCNA (Martini *et al.*, 1998; Green and Almouzni, 2003) and may be part of a general surveillance mechanism that assembles a repressive chromatin structure during recombination and

repair processes (Ridgway and Almouzni, 2000). Recently, recruitment of CAF1 was found to be localized to the site of damage rather than part of a global response to UV (Green and Almouzni, 2003). Additionally, CAF1 appears to be dependent upon the incision steps of NER, supporting its proposed likely role in the restoration of chromatin structure during the late stages of NER (Green and Almouzni, 2003).

Repair of CPDs on the transcribed strand of active genes appears to be homogeneous due to transcription-coupled chromatin organisation facilitating repair but in non-transcribed regions, NER appears faster in linker DNA and towards the 5'end of positioned nucleosomes than in central nucleosomal DNA, a trend which has been observed in yeast at numerous genes including *MET16*, *URA3*, *MET17* and *GAL1-10* (Wellinger and Thoma, 1997; Tijsterman *et al.*, 1999; Li and Smerdon, 2002b; Powell *et al.*, 2003; Ferreiro *et al.*, 2004). This pattern has however not been observed in human cells (Jensen and Smerdon, 1990) which may be due to evolutionary subtleties between yeast and human chromatin structure and DNA repair (Thoma, 2005).

1.4.4.1. Histone acetylation and NER in chromatin

Despite recent advances in our understanding of NER in chromatin (Gong *et al.*, 2005; Reed, 2005; Teng *et al.*, 2005; Thoma, 2005), many aspects remain unresolved, such as the precise nature and mechanisms of histone modifications and interactions with other proteins that help govern chromatin structure both globally and at specified loci in the genome.

Histone acetylation has been well-studied and is an important modification in transcription regulation and NER. Although generally associated with chromatin accessibility, acetylation may primarily serve to destabilise higher order structures

(Wolffe and Hansen, 2001). Increased global acetylation correlates with increased repair (Smerdon *et al.*, 1982; Ramanathan and Smerdon, 1989) and effects of histone acetylation at specific loci have also been studied. At the transcriptionally active yeast *MFA2* gene, the HAT Gcn5 has been shown to play a role in both photoreactivation and NER, but appears to have little effect on global repair (Teng *et al.*, 2002). Gcn5 is also required for efficient NER at *MFA2* in the transcriptionally repressed state, associated with positioned nucleosomes (Yu *et al.*, 2005). Gcn5 plays a role in hyperacetylation following UV irradiation but at specific loci only, such as *MFA2*, as genome-wide histone hyperacetylation in response to the UV is largely unaffected (Yu *et al.*, 2005), similar to the effects observed in transcription activation (Holstege *et al.*, 1998). NER is able to operate in transcriptionally repressed regions without loss of repression (Verhage *et al.*, 1994; Teng *et al.*, 1997; Yu *et al.*, 2005). Hence the model of 'unfolding-access-refolding' of chromatin during NER has been proposed (Smerdon and Conconi, 1999; Meijer and Smerdon, 1999; Green and Almouzni, 2002). It remains unclear however, how histone modifications and chromatin remodelling complexes common to multiple processes can regulate such processes independently, for example how NER is regulated without disturbing transcriptional status.

Histone deacetylation has been less well studied in NER, but is likely to be important in maintaining the correct levels and patterns of acetylation governing chromatin structure, as during transcription regulation where many HDACs are implicated in repression and localised deacetylation of chromatin at specific promoters (Kingston and Workman, 1998; Wu and Grunstein, 2000; Deckert and Struhl, 2002). General inhibition of HDAC activity using known inhibitors such as sodium butyrate results in genome-wide hyperacetylation and this correlates with an

increased rate of repair (Smerdon *et al.*, 1982, Williams and Friedberg, 1982; Ramanathan and Smerdon, 1989). HDACs have also been shown to interact with chromatin remodelling complexes (Tong *et al.*, 1998; Deckert and Struhl, 2002) and chromatin assembly factors (Green and Almouzni, 2003) which also likely play important roles in chromatin changes during NER. HDACs have also been implicated in the repair of other types of DNA damage, such as the non-homologous end-joining (NHEJ) of DNA double-strand breaks (Pray-Grant *et al.*, 2002; Jazayeri *et al.*, 2004).

1.5 The *S. cerevisiae MFA2* Gene

This study has employed the yeast *MFA2* gene as a model gene to study the repair of CPDs by NER. It is a well characterised gene, its regulation is relatively well understood and the existence of five human sequence homologues suggests that molecules similar to the *MFA2* gene product may have biological relevance in higher organisms (Mallet *et al.*, 1995).

1.5.1. *MFA2* is an a-cell specific gene

Yeast cells exist as three different mating types: haploid mating types **a** and α, and the diploid **a**/α type (Herskowitz, 1989). *MFA2* encodes an **a**-factor precursor (Michaelis and Herskowitz, 1988), a mating pheromone that is produced by **a** cells only, required for mating with α cells. Accordingly, α cells have a cell surface receptor for the **a**-factor (Nasmyth, 1982). There are two forms of the pheromone, differing by a single amino acid, one encoded by *MFA2* and the other by *MFA1*. The deletion of both genes is required to render **a** cells defective in mating as both *mfa1*

and *mfa2* single mutants can still produce adequate **a**-factor (Michaelis and Herskowitz, 1988).

Haploid cells are determined as either **a** or α type by the presence of *MAT***a** or *MATα* alleles at the mating type MAT locus, located near the centromere of chromosome III. In **a** mating type cells, the *MAT***a** allele expresses the **a**1 and **a**2 genes, whereas in α cells, the α1 and α2 genes are expressed by the *MATα* allele. Mating types can be switched by replacing the central Y region of one *MAT* allele with an alternative copy carrying the opposite mating information in the storage loci *HMR* or *HML* (Haber, 1998).

MFA2 is expressed in **a** cells only. In α cells, the α1 protein activates transcription of α-specific genes (Emr *et al.*, 1983; Fields and Herskowitz, 1985) and α2 protein represses transcription of **a**-specific genes (Wilson and Herskowitz, 1984). Thus *MFA2* has an additional advantage as a model gene in that transcription can be controlled by the simple selection of mating type, enabling the study of DNA repair in both the presence and absence of transcription.

1.5.2. Regulation of *MFA2*

The expression of **a**-specific genes such as *MFA2* in **a** cells is believed to be dependent upon the binding of Mcm1 (minichromosome maintenance protein 1), a protein of the MADS box family, to the α2 operator in the upstream promoter region (Figure 1.10a). However, in α cells, transcription is repressed by the cooperative binding of both Mcm1 and α2 proteins at the α2 operator (Johnson, 1995). Additionally, the Tup1-Ssn6 general repressor complex is required for full repression of *MFA2* (Patterton and Simpson, 1994) (Figure 1.10b).

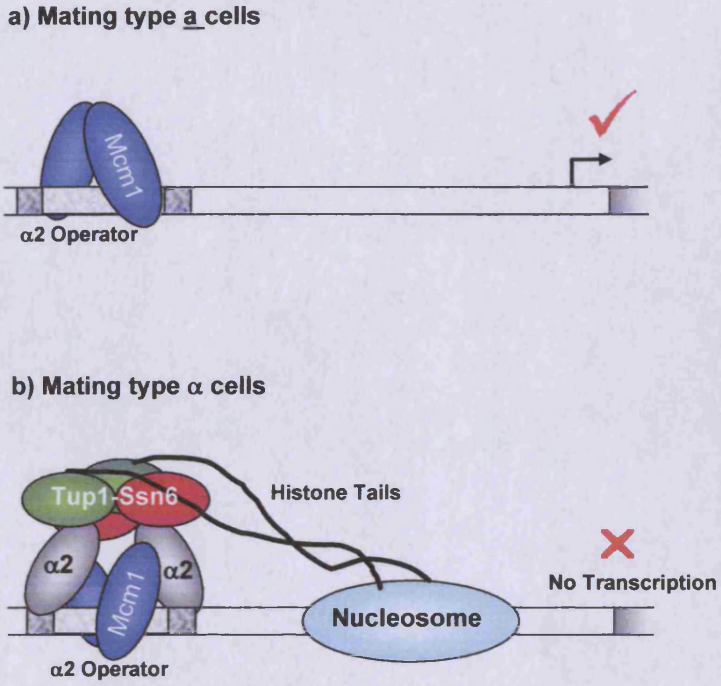

Figure 1.10. *Model MFA2 regulation in a and α cells.* In α cells **(a)**, Mcm1 binds to the α2 operator to enable transcription. However, in a cells **(b)**, the dimeric Mcm1 cooperatively binds to the operator with two α2 molecules binding to the flanking regions of the Mcm1 binding site (Tan and Richmond, 1998). For full repression, the Tup1-Ssn6 repressor complex is also required, thought to be involved in positioning nucleosomes next to the α2 operator via interactions with histone tails and histone deacetylases to prevent transcription factors accessing the TATA box region..

The Tup1-Ssn6 complex is well characterized as a general repressor of a diverse set of genes in yeast and Tup1 homologues have been identified in several other organisms, including the *Drosophila* Groucho and human TLE proteins (Fisher and Caudy, 1998; Levanon *et al.*, 1998). The complex does not directly bind DNA but is recruited by DNA-binding factors, including α2 (Komachi *et al.*, 1994; Smith *et al.*, 1995), but the full details of the mechanism of repression remain elusive. One aspect seems to involve Tup1 directly affecting general transcription as direct interactions of the complex with components of the general transcription machinery

have been observed (Guldener *et al.*, 1996; Redd *et al.*, 1997; Papamichos-Chronakis *et al.*, 2000; Zaman *et al.*, 2001). Repression however is also linked to changes in chromatin structure. Certain genes are associated with highly positioned nucleosomes when repressed by Tup1-Ssn6 (Roth *et al.*, 1990; Cooper *et al.*, 1994; Li *et al.*, 2001; Fleming and Pennings, 2001; Teng *et al.*, 2001). Tup1 has been shown to preferentially bind to underacetylated H3 and H4 histone tails *in vitro* and combined mutations in the H3 and H4 tails causes large derepression of Tup1-Ssn6 repression *in vivo* (Edmondson *et al.*, 1996; Huang *et al.*, 1997). Additionally, Tup1-Ssn6 has been shown to physically interact with at least three histone deacetylases (HDACs): Rpd3, Hos2 (Watson *et al.*, 2000; Davie *et al.*, 2003) and Hda1 (Wu *et al.*, 2001b), and a combined loss of Rpd3, Hos1 and Hos2 has been reported to abolish Tup1-Ssn6-mediated repression (Watson *et al.*, 2000). Tup1-Ssn6 repression may therefore involve chromatin modifications to position nucleosomes adjacent to the α2 operator through direct interactions with hypoacetylated histone tails and histone deacetylases, subsequently restricting access to the TATA box region (Smith and Johnson, 2000, Teng *et al.*, 2001).

Thus three mechanisms have been proposed to explain Tup1-Ssn6 repression: ***i***) direct interaction with the general transcription machinery or activators, ***ii***) nucleosome positioning by interacting with histone tails, and ***iii***) recruitment of histone deacetylases. It is likely that multiple redundant mechanisms are used in repression, which may be important in the role of Tup1-Ssn6 as a global corepressor (Smith and Johnson, 2000; Zhang and Reese, 2004).

1.5.3. *MFA2* as a model gene

MFA2 is a well-characterised gene with its sequence available (Mallet *et al.*, 1995). Figure 1.11 gives the sequence of the coding region and flanking regions of *MFA2* as obtained by the *RsaI-RsaI* restriction digest. The fact that it is an **a** cell-specific gene enables the control of transcription by simple mating type selection. Additionally, the local chromatin structure has been characterised using MNase mapping (Teng *et al.*, 2001). Four positioned nucleosomes are present in α cells where *MFA2* is repressed but these are not detected in **a** cells where it is transcribed. The *MFA2* gene therefore provides a good model for the study of links between transcription, DNA repair and chromatin structure.

MFA2 is located on chromosome XIV and is a relatively small gene, consisting of a coding region of 117bp and a transcribed region of 328bp, giving the advantage that it can be visualised on a single sequencing gel to study the repair of CPDs in the transcribed, upstream and downstream regions. Different restriction fragments can be obtained to focus on specific regions of interest and a restriction map of *MFA2* is shown in Figure 1.12.

This study employed the *RsaI-RsaI* fragment (869bp) containing the *MFA2* coding region plus flanking regions 337bp upstream and 415bp downstream. The *BstBI-BstBI* fragment was also used to obtain a larger fragment, encompassing the same regions but with larger flanking regions of 606bp upstream and 459bp downstream, generating a 1182bp fragment.

Figure 1.11 *MFA2 Sequence.* The upper sequence reads 5' to 3' of the Watson strand. The *MFA2* coding region (117bp) is shown in bold and base pairs are numbered taking the 'A' of the ATG start codon as +1. The upstream region (-1 to -337) and downstream region (+117 to +532) are also shown, as obtained by the *RsaI-RsaI* restriction fragment. The Mcm1 binding site (-221 to-251) and TATA box (-119 to -125) are indicated by shading.

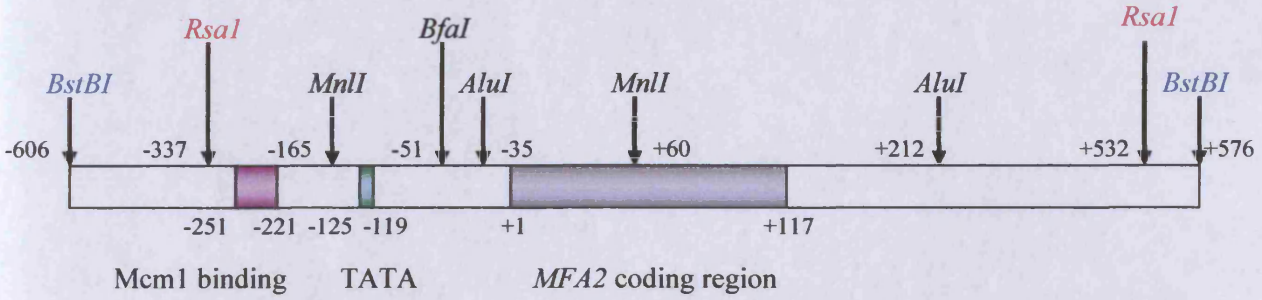

Figure 1.12 *Restriction map of the MFA2 gene and flanking regions.* Various restriction digestions can generate fragments generating different regions within and surrounding *MFA2*. The *RsaI-RsaI* and *BstBI-BstBI* fragments, 869bp and 1182bp respectively, both contain the coding and control regions of *MFA2* with flanking regions; the *RsaI-BfaI* fragment (286bp) encompasses the control region only; the *AluI-AluI* fragment (247bp) is entirely in the transcribed region and the *MnlI-MnlI* fragment (225bp) focuses on the transcription initiation region only.

1.6 The Present Study

Histone modifications clearly play vital roles in the regulation of DNA-mediated processes such as transcription and DNA repair by regulating chromatin structure. The roles of histone acetyltransferases (HATs) and deacetylases (HDACs) in transcription regulation have been relatively well studied and documented but far less is known about their roles in DNA repair. It is postulated that their effects upon chromatin during transcription regulation may also apply during repair to facilitate and restrict the accessibility to DNA in a chromatin environment as required during NER. Thus, increased acetylation due to general HDAC inhibition would be associated with increased repair, which has been observed (Smerdon *et al.*, 1982; Ramanathan and Smerdon, 1989).

The role of the HAT Gcn5 in NER in yeast has been studied at specific loci, including *MFA2* (Teng *et al.*, 2002). It is required for efficient NER at *MFA2*, in both the actively transcribed and repressed states but appears to have little effect on global repair (Teng *et al.*, 2002; Yu *et al.*, 2005). The present study aims to investigate the roles of yeast histone deacetylases in transcription (results presented in Chapter 3) and in NER, both globally and at a specific locus, the *MFA2* gene (results presented in Chapter 4). The effects of mutations in single HDAC genes (*RPD3* and *HAD1*) and multiple mutations (various combinations of *RPD3*, *HDA1*, *HOS1*, *HOS2* and *HOS3*) were examined in each case.

Clearly, histone acetylation is not the only important histone modification in the regulation of transcription and repair. ATP-dependent chromatin remodelling complexes such as the Swi/Snf family have also been linked to altering chromatin structure in both transcription (Kingston and Narlikar, 1999; Wolffe and Hayes, 1999; Ura and Hayes, 2002; Saha *et al.*, 2006) and NER (Bucheli and Sweder, 2004). It may also be likely that other types of post-translational histone modification such as phosphorylation, methylation and ubiquitination are also involved. Like acetylation, these activities also largely affect the histone tails and alter the functional properties of nucleosomes. Thus a 'histone code' of specific patterns of different modifications may exist to regulate the higher-order structure of chromatin and recruit proteins for various pathways (Strahl and Allis, 2000; Fischle *et al.*, 2003; Cosgrove *et al.*, 2004). Histone phosphorylation has been implicated in the repair of DNA double-strand breaks (Rogakou, 1998; Downs *et al.*, 2000) and the tolerance of DNA damage, suggestive of a possible damage-responsive histone code (Harvey *et al.*, 2005). Thus in chapter 5, this study begins to look at the possible roles of histone phosphorylation

in the repair of CPDs by NER at *MFA2*, using yeast strains carrying mutations in the histones H2A/H2B at serine positions known to be targets of phosphorylation.

Chapter 2

Materials and Methods

This chapter describes the experimental techniques and approaches that were routinely used during this study. A separate Materials and Methods section within each chapter describes those methods or additional details that are specific to that particular chapter.

2.1 Yeast strains used

Throughout this study, various haploid strains of the yeast *Saccharomyces cerevisiae* were used. The genotypes of these strains were as follows:

W303a *MATa ade2-1 trp1-1 can1-100 leu2-3 his3-11,15 ura3-5*

W303α *MATα ade2-1 trp1-1 can1-100 leu2-3 his3-11,15 ura3-5*

W303*Δrpd3* as W303α except *rpd3::URA3*

W303*Δhda1* as W303α except *hda1::URA3*

DY 5140 as W303α except *hda1::URA3, hos2::TRP1, rpd3::LEU2*

DY 6444 as W303α except *hda1::URA3 hos1::HIS3, hos2::TRP1, rpd3::LEU2*

DY 6445 as W303α except *hos1::HIS3, hos2::TRP1 rpd3::LEU2*

DY 6446 as W303α except *hda1::URA3, hos1::HIS3, rpd3::LEU2*

DY 6447 as W303α except *hda1::URA3, hos1::HIS3, hos2::LEU2*

JHY2 *MATa (hta1-htb1)::LEU2, (hta2-htb2)::TRP1 <pJHA$_2$> his3Δ200 trp1Δ63 lys2-128δ ura3-52 leu2Δ1* (as FY406 described by Hirschhorn *et al*, 1995)

JHY3 as JHY2 except pJHA$_2$ is replaced with pJHA$_3$ *(hta1-S$_{125}$*)*

JHY9 as JHY2 except $pJHA_2$ is replaced with $pJHA_9$ *(HTA1/htb1-S_{125}*)*

JDY22 as W303α except *hta1-S_{129}stop/hta2-S_{129}stop* (No markers as the genomic mutation was created using a *hisG-URA3-hisG* cassette, removed after integration)

The W303 strains were obtained from Y. Teng, University of Wales Cardiff School of Medicine, Heath Park, Cardiff, U.K.; the DY strains were from Dr. David Stillman, Dept. of Oncological Sciences, University of Utah Health Sciences Centre, Salt Lake City, UT 84132; and the JHY strains were from J. Downs, Wellcome/CRC Institute, Cambridge, U.K.

2.2 Growth and storage conditions

Throughout the study, all growth media, glassware and other equipment used were autoclaved to sterilise, and all manipulations were performed under aseptic conditions.

The yeast strains in frequent use were grown and stored in appropriate medium at 4°C. To archive strains, the yeast cells were grown to mid exponential phase and stored in medium containing 30% glycerol at -70°C. A fresh preculture of each strain was prepared before experimental use by inoculating 50ml of medium with the stock culture and incubating at 28°C, with agitation, until stationary phase growth was reached. This was then stored at 4°C.

For repair experiments, large volumes of cultures were required. These were obtained by inoculating fresh medium with a calculated amount of the preculture, depending on the growth rate of the strain and time allowance for cell growth. Generally, unless otherwise stated, the cells were grown overnight at 28°C with agitation, to achieve a density of $2\text{-}4\times10^7$ cells/ml the following morning.

2.3 Analysis of UV sensitivity - Cell survival

UV-induced DNA damage is normally repaired by various repair pathways in the cell. However, if a mutation is present which may affect such processes, a particular yeast strain may show higher, or lower, sensitivity to UV light. The UV sensitivity of the strains used throughout this study were tested and compared by exposing samples to various doses of UV light and monitoring the survival of cells by counting the number of colonies after 3 days growth. For ease and accuracy, the cultures were diluted appropriately, using existing survival curves as a guide, to achieve about 200 colonies per plate. The details of the procedure were as follows:

1) YPD agar plates were prepared (see Appendix I) and labelled in advance. 10ml of cell cultures were grown overnight to give a density of $2\text{-}4\times10^7$ cells/ml. Serial dilutions were prepared according to the strain and UV dose. For example, samples to be irradiated at the higher UV doses were diluted just 10- or 100-fold, whereas those exposed to lower UV doses were diluted up to 10000-fold.
2) The diluted cell suspensions were mixed well using a vortex before pipetting 100µl onto the agar plates. Triplicates of each sample were prepared. Glass beads (diameter 3mm) were added to the plates and shaken laterally to spread the cells evenly across the surface of the agar. The plates were then turned upside down.
3) The 245nm UV lamp (VL-215G, Vilber Lourmat, France) was switched on 30mins in advance and calibrated. One plate at a time was then placed centrally under the UV lamp and treated at a dose rate of $10J/m^2{\cdot}s$. Usually, doses of 0, 20, 40, 80, 120 and $160J/m^2$ were applied.

4) Following irradiation, the plates were immediately placed in darkness to avoid repair by photoreactivation and were incubated at 28°C for 3 days. The number of colonies on each plate was then counted and survival curves created to determine UV sensitivity.

2.4 UV irradiation of cells for repair analysis

The UV spectrum is divided into three parts, UV-A (400 – 320nm), UV-B (320-290nm) and UV-C (290-100nm). The shorter the wavelength, the greater the frequency and the greater the energy. Solar radiation consists mainly of UV-A and UV-B radiation since penetration of the ozone layer drops dramatically for wavelengths of radiation below 320nm. Yet UV-C radiation is usually used for experimental studies which emits radiation of wavelength 254nm, close to the absorption maximum of DNA at about 260nm, thus inducing damage such as CPDs more efficiently (Friedberg, *et al.*, 2005). However, when yeast cells are treated with UV, they exist as a suspension in PBS buffer. When UV radiation enters a liquid medium, its penetration diminishes rapidly with increasing depth and any particulate matter causes scattering of the radiation and shadowing of other matter below, further reducing the amount of radiation received. It is therefore vital that UV irradiations are performed using a shallow dish and using a constant swirling motion, to ensure that cells receive a constant, steady dose of UV rather than cells at the top receiving a higher dose than those in a suspension of greater depth. Standardising the dose received also helps prevent some cells receiving too high a dose of UV radiation as the short wavelengths which penetrate contain high energy photons that can break chemical bonds within the suspension, leading to water splitting. In addition, dissolved organic matter from living organisms can also be sources of photoproducts

when UV radiation is absorbed. Consequently, reactive products such as oxygen, free radicals and hydrogen peroxide may be formed (De Haan, 1993).

This section describes the UV irradiation procedure which was employed to induce damage formation in yeast DNA prior to DNA extraction. Cell cultures were grown to exponential phase as described in section 2.2 and chilled phosphate buffered saline (1×PBS, see Appendix 1) was used to adjust the concentration to 2×10^7 cells/ml. 50ml aliquots were then irradiated by exposure to 254nm UV light. The UV lamp was switched on 30 minutes prior to use to ensure stable emission of light. A sample of cells was taken before UV irradiation commenced, as an untreated control sample, and stored on ice in the dark to reduce exposure to visible light. Thereafter, at each repair time interval, cells were collected by centrifugation at 4°C using a Beckman Avanti J-25 centrifuge. The details of the irradiation procedure were as follows:

1) Yeast cells from an overnight culture at a density of $2\text{-}4\times10^7$ cells/ml were collected by centrifugation (Beckman Avanti J-25 centrifuge, JA-10 rotor) at 4000rpm for 5 min.
2) Cells were washed and resuspended in a small volume of chilled PBS. If the cells clumped together, brief sonication was applied to disperse them homogeneously. Chilled PBS was then added to adjust the cell concentration to 2×10^7 cells/ml and give a final volume of approximately 1400ml
3) A 200ml sample was taken from the cell suspension as an untreated control (U). This was kept on ice in the dark.
4) A 50ml batch of the cell suspension was placed in a Pyrex dish (diameter 14cm) giving a depth of approximately 3mm. The cell suspension was then irradiated under a VL-215G lamp (Vilber Lourmat, France) for 15 seconds at a

dose rate of 10 J/m^2·s, previously calibrated with a UVX radiometer (UVP Inc., CA, USA). During irradiation, the dish was gently swirled to ensure a uniform dose of UV was received by all cells. This irradiation step was repeated for further 50ml batches of the cells until all cells had been treated. Each batch was pooled into a sterile, foil-wrapped flask on ice.

5) After irradiation, 200ml of cells were taken immediately to serve as a sample (0) with zero repair time.

6) 800ml of the remaining UV-treated cells were collected by centrifugation and resuspended in 1000ml of fresh medium which had been pre-warmed to 28°C. The cells were then incubated in the dark at 28°C with agitation to enable DNA repair. At each repair time (after 1, 2, 3 and 4 hours) a 250ml sample was taken.

7) All samples were collected by centrifugation as previously, resuspended in 40ml chilled PBS 50mM EDTA and kept on ice in the dark.

2.5 Extraction of yeast DNA

To isolate DNA from the yeast cells, zymolyase was used to produce spheroplasts which were then lysed with sodium dodecyl sulphate (SDS). RNAse A and proteinase K treatments were used to digest RNA and protein respectively, followed by phenol/chloroform extractions and precipitation with ethanol. This method is suitable for extraction of genomic DNA from up to 1×10^{10} cells. A 250ml cell suspension of density 2×107 cells/ml could normally yield 500-600μg of DNA. The details of the DNA extraction procedure are as follows:

1) Cells were collected by centrifugation as previously and resuspended in 5ml sorbitol-TE solution (see Appendix I).

2) 0.5ml of zymolyase 20T (10mg/ml in sorbitol-TE solution, ICN Biochemicals, Inc.) and 0.5ml of 0.28M β-mercaptoethanol (Sigma) was added to each sample and mixed well by shaking. Cells were incubated overnight at 4°C in the dark.
3) The following morning, the cells were shaken gently and incubated at 37°C for 1hour. The production of spheroplasts was checked using a light microscope. For an additional check, small tester samples were added to sorbitol-TE solution, which resulted in a cloudy solution. If SDS was also added, the solution turned clear.
4) Spheroplasts were gently centrifuged at 3000rpm for 5min (Beckman JA20 rotor), washed with 5ml of SEC buffer (see Appendix I) and resuspended in 5ml of 1:1 (v/v) lysis buffer/1×PBS solution (see Appendix I). 200µl of RNAse A (Sigma) was then added (10mg/ml in H_2O) and mixed well. Samples were incubated for 1 hour at 37°C with occasional shaking.
5) Following RNAse A treatment, 0.5ml proteinase K (Sigma, 5mg/ml in TE buffer) was added and the samples were incubated firstly at 37°C for 1 hour and then at 65°C for a further 1-2 hours with regular mixing.
6) An equal volume (approximately 6ml) of phenol:chloroform:isoamyl alcohol (25:24:1in volume, Sigma) was added and the samples shaken to mix well. They were then centrifuged at 10000rpm for 10mins (Beckman JA20 rotor). The aqueous top layer containing the DNA was carefully removed from each sample and transferred to a fresh disposable polypropylene tube using a 3ml plastic Pasteur pipette. This extraction was repeated, followed by a third extraction in the same manner with chloroform:isoamyl alcohol (24:1 in volume, Sigma). Complete deproteinization was observed when no protein

layer could be seen at the interface of the aqueous upper layer and the lower layer.

7) The DNA was precipitated by adding 2 volumes (12ml) of cold 100% ethanol (stored at -20°C), mixing gently and storing overnight at -20°C.
8) DNA pellets were collected by centrifugation at 3000rpm for 20mins and allowed to air-dry. They were then resuspended in 0.5-1ml TE buffer, depending on the size of the pellet. 1 volume of cold isopropanol (-20°C) was added for a second DNA precipitation. The samples were incubated at room temperature for 20-30mins, regularly mixed by gentle inversion. The pellets were then carefully removed with a pipette tip and transferred to fresh eppendorf tubes. When thoroughly dried, the pellets were resuspended in 600-800µl of TE buffer.
9) The quality of DNA obtained was checked using non-denaturing agarose gel electrophoresis (see section 2.6). Clean DNA samples gave a sharp bright band on an ethidium bromide (EtBr) stained agarose gel when viewed under a UV transilluminator.
10) The DNA samples were stored at 4°C if they were to be used immediately, or at -20°C

2.6 Non-denaturing agarose gel electrophoresis

The quality of yeast DNA obtained from extraction was determined by electrophoresis on a non-denaturing 1% agarose gel which was subsequently viewed under a UV transilluminator. The presence of sharp, bright bands indicated clean genomic DNA samples.

1) 5µl of each DNA sample was mixed with 5µl of H_2O and 5µl of non-denaturing loading buffer (see Appendix I).
2) Samples were loaded onto a 1% (gram/ml) agarose gel which was prepared in 1×TAE buffer (see Appendix I) and contained EtBr (0.1µl/ml, Sigma). Gels were electrophoresed under 1×TAE at 70-90V for 30-60mins.
3) Gels were viewed under a UV transilluminator. Genomic DNA runs as a discrete high molecular weight band, hence sharp bright bands are visible.

2.7 Detection of repair in the overall yeast genome

An immunological slot-blot assay was used to detect *in vivo* removal of UV-induced DNA damage. A specific monoclonal antibody raised against cyclobutane pyrimidine dimers (CPDs) was used to detect the presence of CPDs in the yeast genome. Untreated (U) samples were blotted as controls, along with samples taken immediately after UV treatment (0h repair) and at regular intervals during repair (1h, 2h, 3h and 4h after irradiation). The DNA content in each sample was quantified using Molecular Analysis software (BioRad) and the loading adjusted accordingly to ensure equal amounts in each sample. The slot-blot procedure was as follows:

1) The slot-blot transfer kit (Bio-Dot SF Microfiltration Apparatus, Bio-Rad) was cleaned with water and 70% ethanol, dried and assembled. A Vacugene pump (Pharmacia Biotech, UK) was attached to the outlet valve. Two pieces of dry Whatman paper (Whatman International Ltd., UK) were placed onto the base of the blotting apparatus, followed by a third piece soaked in 0.4N NaOH solution. A piece of GeneScreenPlus nylon membrane (NEN Life Sciences Products, Inc., USA) was then cut to size, soaked in 0.4N NaOH and placed on top, before tightly securing the apparatus lid.

2) A pressure of 50mbar was applied using the vacuum pump and 200µl of 0.4N NaOH was loaded into each well as a rinse.

3) The samples (DNA dissolved in TE buffer) were prepared by adding calculated amounts to 0.4N NaOH to give a concentration of 100ng of DNA and a final volume of 200µl. The samples were loaded carefully into the wells and left for 15-20 minutes to pass through the membrane. The wells were finally rinsed with a further 200µl of 0.4N NaOH before the blotting was complete.

4) The membrane was carefully removed from the apparatus, washed with 1×TBST (see Appendix I) and then left overnight at 4°C, immersed in blocking solution (3% milk powder in 1×TBST) to saturate non-specific binding.

5) The membrane was sealed in plastic to form a 'bag'. 2µg of monoclonal mouse H3 CPD-specific antibody (AFFITECH AS, Oslo, Norway) in 10ml of 3% milk powder / 1×TBST solution was added to the bag and any air bubbles were carefully removed. The bag was sealed and left to incubate at room temperature for 1 hour on a shaking platform. The membrane was then removed from the bag and washed three times with 1×TBST.

6) 5µl of an alkaline phosphatase-linked anti-mouse antibody (ECF Western Blotting Reagent Pack, Amersham) was diluted in 10ml of 3% milk powder / 1×TBST solution and then incubated with the membrane for another hour. Washes with 1×TBST were again performed to remove excess antibody.

7) 2ml of ECF detection solution (36 mg of ECF substrate in 60ml of ECF dilution buffer, ECF Western Blotting Reagent Pack, Amersham) was pipetted onto a piece of Clingfilm on a smooth surface. The membrane was

placed face down on top of the solution, with care taken to avoid air bubbles and to ensure the entire surface of the membrane was exposed to the solution. This was left for 2 minutes incubation at room temperature.

8) The membrane was removed and the edge blotted onto filter paper to remove excess ECF solution. The fluorescent emission from the samples on the membrane was then scanned using a phosphorimager scanner (STORM 860, Molecular Dynamics, Inc.).
9) Finally, quantification was carried out using ImageQuant software (Molecular Dynamics, Inc.).

2.8 Studying DNA repair at gene resolution

In order to study the repair of UV-induced CPDs at a specific gene, a Southern Blotting technique was used, originally devised by Bohr *et al.* (1985). This involved five main steps:

1) Genomic yeast DNA was firstly digested using an appropriate restriction endonuclease to obtain a fragment containing the DNA sequence of interest.
2) The fragment was then cut at the sites of CPDs by a CPD-specific endonuclease.
3) These cut fragments were separated by electrophoresis on a denaturing agarose gel, resulting in single strand DNA fragments being positioned on the gel according to their size.
4) A Southern Blotting technique was employed to transfer the fragments to a GeneScreenPlus nylon membrane (NEN Life Sciences Products, Inc., USA)

and the sequence of interest could then be detected using a specific [^{32}P]-labelled DNA probe.

5) Finally, the amount of probe bound at the position of the undamaged, full-length restriction fragment was quantified. An overview of the procedure is illustrated in Figure 2.1.

UV irradiated and untreated DNA samples were treated with a restriction endonuclease to obtain the fragment of interest. Each sample was then equally divided into two, one of which was subsequently treated with *Micrococcus luteus* (ML), a CPD-specific endonuclease which cuts the DNA at the sites of a CPD. The other portion was mock-treated with TE buffer. Any restriction fragments free of CPDs (undamaged) would remain intact whereas damaged fragments would be cut into varying sizes. Intact fragments would therefore resolve at a different position when run on an agarose gel. Both the ML-treated and TE-treated samples were electrophoresed and the DNA transferred to a membrane by Southern blotting. The membrane was then hybridised with a specific probe to detect undamaged, full-length fragments. Following exposure to a phosphorimaging screen and scanning, the amount of probe bound at the position of intact fragments was quantified. The ratio of band densities of the ML-treated and TE-treated samples was used to calculate the proportion of undamaged fragments at each repair time point. As repair time was increased, the bands of the ML-treated samples intensified, which was indicative of fewer CPDs present, hence DNA repair progression.

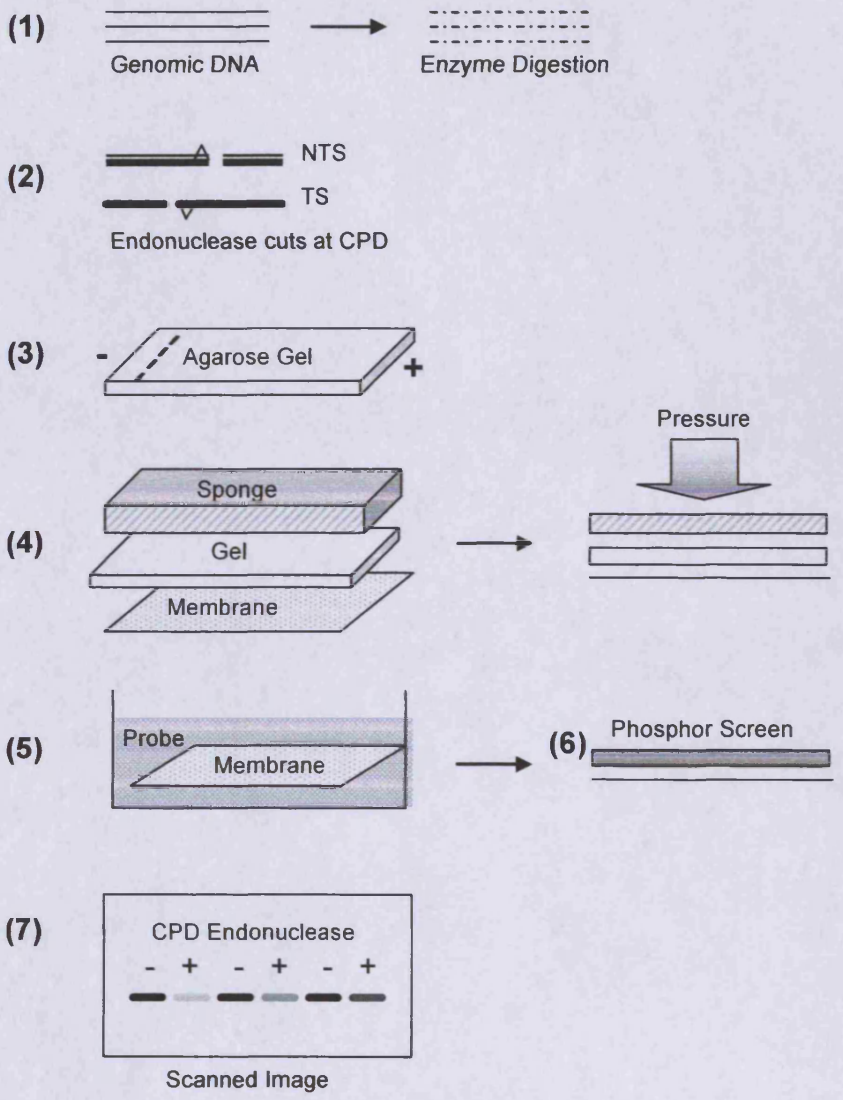

Figure 2.1 *Examining CPD repair at gene resolution.* **(1)** Genomic DNA is digested by a restriction endonuclease to obtain the fragment of interest. **(2)** DNA fragments are cut by a CPD-specific enzyme. **(3)** Fragments are separated by gel electrophoresis. **(4)** Southern Blotting is used to transfer the DNA to a membrane. **(5)** The membrane is hybridised with a strand-specific probe which anneals to the complementary fragments on the membrane. **(6)** The membrane is then exposed to a phosphorimaging screen which is then scanned to visualise the positioning of the ^{32}P label **(7)**. The intensity of the pixels on the image correlates to how much intact fragment is present. *(Adapted from Y. Teng PhD Thesis, 2000)*

During repair experiments, the presence of any replicated DNA, which would normally be damage-free, may mask true repair effects. Previous studies (Teng, PhD thesis, 2000; Reed, PhD thesis, 1996) have deduced that exposure of the yeast cells to UV as performed in this study results in a delay in cell cycle progression, and hence replication, for several hours. Therefore, DNA repair effects studied over 4 hours during this study would be unaffected.

The details of the techniques used to study DNA repair at the level of the gene follow.

2.8.1 DNA digestion with restriction endonuclease

In this study, DNA repair was examined at the *MFA2* gene. Restriction endonucleases were used to obtain a fragment containing a particular sequence of interest. Initially, *RsaI* was used, which cuts at the positions -337 and +532 (where +1 denotes the start codon ATG of *MFA2*), yielding an 869bp fragment containing the whole *MFA2* transcribed sequence. However, the enzyme *BstBI* yielded a larger fragment of 1182bp which still encompassed the *RsaI* fragment, cutting at positions -606 and +576. This resulted in a larger quantity of bound probe and thus a stronger signal when the membrane was finally scanned for quantification. This enzyme was therefore used in preference. All restriction enzyme digestions were carried out according to the manufacturer's guidelines. Briefly, the procedure was as follows:

1) 2µl (10 units/µl) of restriction endonuclease was used to digest 10µg of genomic DNA in a total mixture volume of 100µl. The reaction conditions were as specified by the manufacturer (65°C, 2 hours for *BstBI*). All reactions were carried out in 1.5ml Eppendorf tubes, and all manipulations were performed using Gilson P20, P100, P200 and P1000 pipettes.

2) Following digestion, 5µl of each sample was loaded onto a 1% agarose gel to check the quality of digestion (see section 2.6). Successful DNA digestion results in a smear when viewed under a transilluminator.
3) Phenol/chloroform extraction was used to remove the enzyme from the mixture, followed by a chloroform extraction which removed traces of phenol. 1 volume (100µl) was used for each extraction. When removing the aqueous layer containing the DNA, care was taken not to disturb the precipitate.
4) To precipitate the DNA, 1 volume (100µl) of pre-chilled (-20C) isopropanol and 1/10 volume (10µl) of 3M sodium acetate (pH 5.3) were added. The samples were mixed by inversion and kept at -20°C for at least 30 minutes. The DNA pellets were collected by centrifugation in a microfuge at maximum speed for 15 minutes. Suction was used to remove all traces of supernatant and the pellets were left to dry for a few minutes. The pellets were resuspended in 42µl of TE buffer.

2.8.2 Incision of DNA at the sites of CPDs

To cut the DNA at the sites of CPDs *Micrococcus luteus* (ML) endonuclease was used. The above DNA samples were divided into two aliquots of 20µl and transferred to new Eppendorf tubes. 5µl of ML was added to one sample, and 5µl of TE buffer was added to the other. Both ML-treated and untreated samples were incubated at 37°C for 1 hour.

2.8.3 Denaturing gel electrophoresis and Southern blotting

ML treatment results in single strand nicks at CPD sites. To resolve these single

stranded DNA fragments, gel electrophoresis was used under denaturing conditions:

1) Two gels at a time were prepared by melting 4.5g agarose in 200ml H_2O before adding a solution of 100µl H_2O + 3ml of 5M NaCl + 600µl of 0.5M EDTA, pH8.0). The solution was cooled to about 50°C and poured, taking care to remove any bubbles.

2) A comb with 20 teeth was quickly placed into each gel to create the wells into which the samples were to be loaded. The gel was allowed to set for 1 hour and then submerged in 1 litre of running buffer (986ml of H_2O + 12ml of 3M NaOH + 2ml of 0.5M EDTA, pH 8.0). This was left for at least 30 minutes to equilibrate before loading the samples.

3) To stop the ML incubation and prepare for loading, 15µl of denaturing loading buffer (See Appendix I) was added to each sample.

4) After removing the comb, the DNA samples were carefully loaded onto the gel. The gel was run overnight, for 16 hours at 18V.

5) The following morning, the gel was neutralised by immersion in 1M Tris-HCl, pH 7.5, 1.5M NaCl for 30 minutes. A nylon-based membrane (GeneScreenPlus, NEN) and two pieces of Watman paper were cut to size and soaked in 10×SSC (See Appendix I) for 10 mins.

6) The fractioned DNA fragments on the gel were then transferred to the membrane using a Pressure Blotter (Stratagene Ltd., UK) with a pressure of 80 psi for 2 hours. The transferring buffer was 10×SSC.

2.8.4 Hybridisation of the membrane with a radioactive probe

1) The membrane carrying the transferred DNA was rinsed with distilled water and rolled inside a glass tube containing pre-hybridisation solution (1ml of 10% SDS, 1ml of 50% dextran sulphate, 0.6g of NaCl, 8ml of H_2O) at 65°C for 1 hour on the rotating spindle in a Hybaid oven.

2) 100µl of radioactive strand specific probe (see section 2.9) was added to the tube before placing it back into the Hybaid oven for incubation at 65°C overnight under constant rotation.

3) The membrane was then washed twice with 200ml of 2×SSC followed by two further washes with 200ml of washing buffer (1% SDS, 2×SSC) to remove excess unbound and non-specifically bound probe. Each wash was performed in a tray on the shaking platform of the Hybaid oven at 65°C for 15 mins. The radioactive signal was checked with a Geiger counter to ensure there was a 'band' of strong signal on the membrane where the probe had bound.

4) The membrane was wrapped in Clingfilm and placed into a cassette against a phosphorimager screen (Molecular Dynamics, Inc.). Exposure was allowed overnight at room temperature. The image was then generated by scanning the screen using a phosphorimager scanner (Storm 860, Molecular Dynamics, Inc.).

All manipulations involving radioactive isotopes were performed according to the relative safety code.

2.8.5 Analysis of the radiolabelling results

The images obtained above were quantified and analysed using ImageQuant software (Molecular Dynamics, Inc.). The intensity of each selected band was measured as a volume (V), which is the sum of the intensity of every pixel in the selected area. The ratio of DNA which is not sensitive to the CPD specific endonuclease can be calculated using the following equation:

(I= intact fragments; D= damaged fragments; R= repaired fragments)

$$\%\,(I)_t = \frac{V_{t+ML\,Endo}}{V_{t-ML\,Endo}} \times 100$$

t = repair time (0, 1, 2, 3, 4 hours)

The ratio of DNA which is sensitive to the CPD specific endonuclease, i.e. the percentage of damaged fragments remaining at a given time point, was calculated as:

$$\%\,(D)_t = 100 - \%\,(I)_t$$

$$= (1 - \frac{V_{t+ML\,Endo}}{V_{t-ML\,Endo}}) \times 100$$

Hence the percentage of repaired fragments was deduced by:

$$\%\,(R)_t = \frac{\%\,(D)_0 - \%\,(D)_t}{\%\,(D)_0} \times 100$$

2.9 Preparation of strand-specific radiolabelled probes

The probes used in this study were designed to detect the transcribed strand (TS) and non-transcribed strand (NTS) of the *MFA2* fragment of interest separately.

The technique basically uses 5' biotinylated primers and Dynabeads to fish out single strand DNA. Dynabeads are coated with streptavidin which binds tightly to biotin. In turn, the Dynabead-biotin complex can be isolated from the remainder of a mixture using a magnetic particle concentrator (MPC) which collects the beads against the side of an Eppendorf by creating a magnetic field. The main steps of the probe synthesis procedure are outlined below and illustrated in Figure 2.2.

1) The DNA sequence of interest was downloaded from the *Saccharomyces cerevisiae* Genome Database (SGD™). Primers were designed using Oligo software (Version 3.4 MedProbe, Normay), one of which was biotinylated, the other unbiotinylated (Oswel, UK).

2) The DNA sequence was amplified by PCR, the conditions of which were optimized to obtain the best quality PCR product. Genomic DNA was used as a template.

3) The PCR products were then checked on a 1% agarose gel to ensure good quality.

4) The double-stranded PCR products were isolated using Dynabeads and a MPC, then denatured by incubation with 0.1M NaOH.

5) The biotinylated and unbiotinylated strands were separated by collecting the Dynabeads (bound to the biotinylated strand) using the MPC and using a pipette to remove the supernatant containing the unbiotinylated strand).

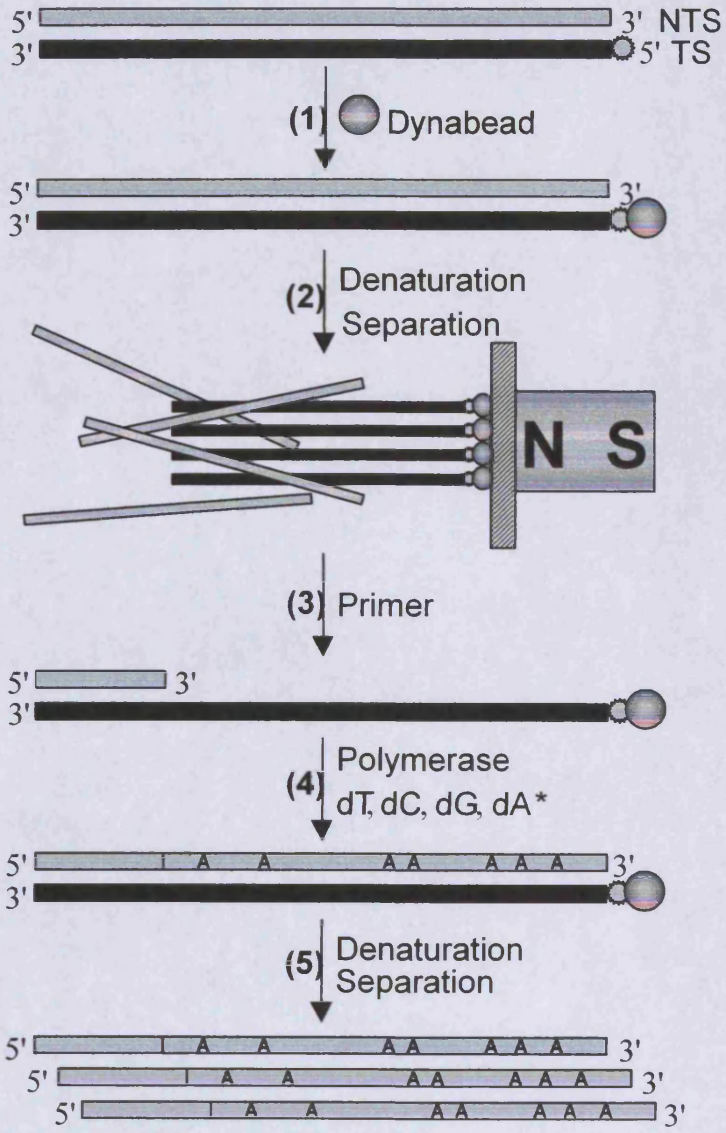

Figure 2.2 *Schematic representation of the technique for probe synthesis.* **(1)** Dynabeads bind to the biotin ( ) end to enrich appropriate PCR products **(2)** Double stranded DNA is denatured in 0.1 M NaOH. The beads with associated single stranded DNA are kept on the Eppendorf wall in a MPC. The supernatant is removed. **(3)** Second primer anneals to the 3' end of the single stranded DNA. **(4)** [α^{32}P]dATP (dA*) and the other three dNTPs are recruited for the primer extension reaction by DNA polymerase. **(5)** The newly synthesized probe is separated from the template in a MPC. *(Adapted form Teng, PhD thesis, 2000 with permission)*

6) The probe was synthesised upon the biotinylated single stranded DNA template by primer extension using Sequenase Version 2.0 T7 DNA Polymerase (Amersham Pharmacia Biotech) and a α-[^{32}P] dATP (6000 Ci/mmol, Amersham) spiked dNTP mixture. The mixture was heated at a denaturing temperature and immediately placed in the MPC so that the [^{32}P] incorporated probe could be collected with a pipette as a supernatant.

2.9.1 PCR amplification of the sequence of interest

A pair of primers, one biotinylated and one unbiotinylated, was used to amplify the DNA sequence of interest using standard PCR reactions.

1) The following PCR reagents were mixed together and made up to a total reaction volume of 50µl with H_2O.

   1µl of each primer (20µM, for sequence see individual chapters)
   1µmol of dNTPs
   5µl of 10×Taq buffer (Promega)
   3µl of $MgCl_2$ (25 mM)
   1ng of DNA template
   1.25 units of Taq polymerase (Promega)

2) PCR was then carried out in an OmniGene thermal cycler (Hybaid) to amplify the sequence. The parameters were programmed as:

   First denaturation: 2 min at 95°C
   Denaturation: 30 cycles of 30 seconds at 95°C
   Annealing: 30 seconds at 57°C
   Extension: 20-30 seconds at 72°C
   Samples left for 4mins at 72°C to complete the DNA synthesis

The quality of the PCR products obtained was then checked by loading 3µl onto a 1% agarose gel (as described in section 2.6).

2.9.2 Preparation of the radiolabelled probe

1) 20µl of Dynabeads were washed twice with 1×BW (binding and washing) buffer (see Appendix I) and resuspended in 20µl 2×BW buffer.
2) 10µl of PCR product (see Section 2.9.1) and 10µl TE buffer were added to bind to the biotin end of the PCR products. This was incubated at room temperature for 15 minutes, using a pipette to mix occasionally. During incubation, the Dynabeads bound to the PCR product. A MPC was used to collect the beads and the supernatant was discarded.
3) The beads were washed twice with 60µl of H_2O, resuspended in 20µl of 0.1M NaOH and incubated for 15 minutes at room temperature to denature the dsDNA. The biotinylated strand associated with the beads was kept on the Eppendorf wall using a MPC, and the supernatant containing the other strand was abandoned.
4) The beads were washed three times with 60µl of H_2O and resuspended in 16.4µl of H_2O. 0.6µl of the appropriate non-biotinylated primer (10µM) and 4µl sequenase reaction buffer (Amersham) were added. After mixing the solution thoroughly using a pipette, the tube was incubated at 65°C for 2 min, and then allowed to cool slowly to room temperature for 30 minutes. The tube was then put on ice.
5) 4µl of 5×dATP buffer (0.1 mM dTTP, dGTP and dCTP), 2.8µl of 0.1M DTT, 2µl of α-[^{32}P] dATP (6000 Ci/mmol, Amersham), 6µl of Sequenase (30 times dilution in sequenase dilution buffer, Amersham), were added and mixed well.
6) The solution was incubated at 37°C for 10 minutes. The beads and associated dsDNA fragment were collected using the MPC and the supernatant was discarded.

7) Following two washes with 60µl of TE buffer, the beads were resuspended in 100µl TE buffer. This was incubated at 95°C for 3 minutes to denature the DNA fragments. The beads and the biotinylated ssDNA were localised on the Eppendorf wall by the MPC and the supernatant containing the newly synthesised radioactive probe was immediately transferred to a fresh tube on ice.
8) The probe was then used for hybridisation with the membrane as described in section 2.8.4. Often, the TS and NTS probes were prepared simultaneously, and one was stored at -20°C until required.

2.10 Studying DNA repair at nucleotide resolution

To study the induction and repair of UV-induced CPDs at a specific nucleotide position an end-labelling technique was used as described by Teng *et al.* (1997). This again involved the application of specifically designed probes and Dynabeads. The main steps are outlined below and an overview is illustrated in figure 2.3.

1) Genomic DNA was digested with appropriate restriction endonucleases.
2) The obtained fragment of interest was then cut at the sites of CPDs by a CPD-specific endonuclease and the DNA was denatured to obtain the resulting ssDNA fragments of varying lengths.
3) A specifically designed probe was used to isolate the ssDNA fragments and also provide a template for end-labelling. The probe was complementary to the 3' end of the DNA sequence of interest and biotinylated at its 5' end. A

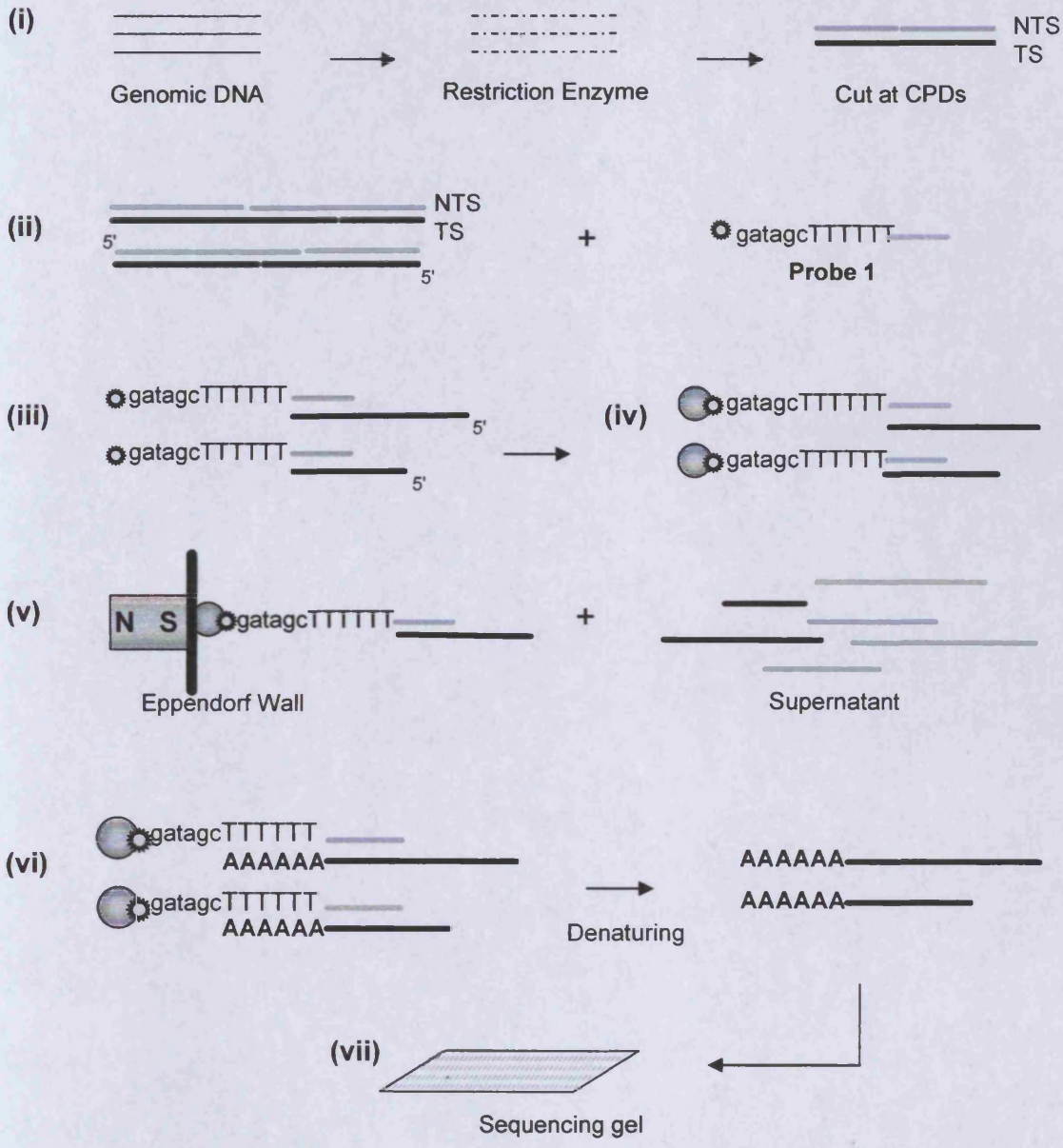

Figure 2.3 *Purification and end-labelling DNA fragments.* **(i)** Genomic DNA is treated firstly with restriction enzyme, followed by CPD-specific endonuclease. **(ii)** Probe 1 is added to the dsDNA which has been cut at CPDs. **(iii)** Probes anneal to the complementary sequences at the 3' end. **(iv)** Dynabeads are added to bind to the biotin at the 5' end of the probe. **(v)** The Dynabeads and associated DNA fragments are isolated with a MPC, and the supernatant is kept for purification of the opposite strand. **(vi)** The purified DNA is radioactively labelled at the 3' end and **(vii)** loaded onto a sequencing gel (Adapted from Yu, PhD thesis, 2003).

short oligonucleotide was inserted between the complementary sequence and the 5' biotinylated end. This consisted of a six dT overhang adjacent to the complementary sequence, to provide a template to incorporate radioactive dATPs into the isolated ssDNA fragments, and six random nucleotides between the dTs and the 5' biotinylated end which eliminated any steric hindrance from the Dynabeads while radioactive dATPs were incorporated.

4) The radioactively labelled ssDNA fragments were then separated using denaturing polyacrylamide gel electrophoresis.

Finally, the gel was scanned and the resulting image quantified using ImageQuant software (Molecular Dynamics, Inc.).

2.10.1 Digestions with restriction and CPD-specific enzymes

1) The following reagents were mixed together and made up to a total reaction volume of 300µl with H_2O.

   100µl DNA (50-60µg)
   6µl restriction endonuclease
   30µl appropriate buffer (10× concentration)
   3µl BSA (if indicated by manufacturer guidelines)

2) The samples were incubated at 37°C for at least 1 hour.

3) The quality of DNA digestion was checked on a 1% agarose gel, as described in section 2.8.1.

4) Phenol and phenol/chloroform extractions were performed, as described in section 2.8.1.

5) The DNA was precipitated by adding 1/10 volume of 3M sodium acetate and 1 volume of isopropanol, and storing at -20°C for at least 30 mins. The pellet was dried thoroughly and resuspended in 110µl of TE buffer.

6) 10µl of CPD-specific *ML* endonuclease was added and the samples were incubated at 37°C for 1 hour. Phenol and phenol/chloroform extractions were performed as previously and the samples were transferred to 0.5ml Eppendorfs.

2.10.2 Purification of CPD-incised single stranded DNA fragments

1) 30µl of 5M NaCl was added to the above 120µl DNA solution, resulting in a final sodium concentration of 1M (for optimal Dynabead-biotin binding).

2) 1µl of biotinylated probe complementary to the 3' end of the TS was added and the samples were incubated at 95°c for 5 mins to denature the DNA. This was followed by incubation at the annealing temperature 55°C for 15 mins to enable the primer to anneal to the DNA fragments.

3) 10µl of Dynabeads were washed twice with 1×PBS 0.1% BSA, twice with 1×BW buffer and resuspended in 1 volume of 1×BW buffer. 10µl of beads was added to each sample and incubated at r.t. for 15 mins with occasional mixing with a pipette.

4) The beads were isolated with a MPC and the supernatant was transferred to a fresh tube for isolation of the NTS.

5) 50µl of 1×BW buffer was added to the beads and they were incubated at 55°C (annealing temperature) for 5 mins, to decrease non-specific binding. The

supernatant was immediately removed and discarded.

6) The beads were washed twice with H_2O. Care was taken to remove all of the liquid before resuspending the beads in 6µl of H_2O.

7) For NTS isolation, steps 2-6 were repeated but using a different probe, complementary to the 3' end of the NTS; and incubations at 55°C, 5 mins and annealing temperature 57°C, 15 mins (step 2).

2.10.3 End labelling the DNA fragments with α-[^{32}P] dATP

1) 1µl of Sequenase buffer, 0.7µl of 0.1M DDT, 1µl (5µCi) of α-[^{32}P] dATP (6000Ci/mmol. Amersham) and 2µl of Sequenase (diluted 1:30 in dilution buffer, Amersham) were added to the beads and mixed well.

2) The solution was incubated at r.t. for 10 min to enable labeling. The beads were collected using the MPC and washed twice with TE buffer.

3) Finally, the labelled DNA fragments were eluted from the beads by adding 3µl of formamide loading buffer (95% formamide, 20mM EDTA, 0.05% Bromophenol Blue) and resolved by electrophoresis on a 6% denaturing polyacrylamide gel as described below.

2.10.4 Denaturing polyacrylamide gel electrophoresis

A 0.4 mm thick denaturing polyacrylamide gel was used in this study to resolve the single stranded DNA fragments.

1) To create the gel, two glass plates measuring 20cm × 60cm and 20cm × 62cm were used to construct a mould. The plates were washed thoroughly with

detergent and water and then washed using absolute ethanol. Dimethyldichlorosilane solution (2% in 1,1,1-trichloroethane, BDH Chemicals) was applied to the inner surface of the shorter plate to later enable easy separation of the gel from the glass plates following electrophoresis. The plates were separated at the edges with 0.4 mm thick spacers and firmly sealed with vinyl insulation tape.

2) 80ml of 6% acrylamide EASI gel (acrylamide:bis-acrylamide = 19:1, 7M urea, 1×TBE, ScottLab) was mixed with 650µl of 10% APS and 35µl of TEMED in a small conical flask. This was degassed using a vacuum for 10 minutes.

3) The solution was slowly poured into the gel mould, taking care to avoid or remove any bubbles that formed in the gel. A comb was immediately inserted into the top of the gel to create the loading wells, and the gel was left to set for at least 1 hour.

4) A GIBCO electrophoresis system (Model SA) and a Pharmacia power pack (EPS 3500) were used to run each sequencing gel. To achieve the optimum temperature of the gel for electrophoresis to separate the ssDNA, 50°C, it was pre-run in 1×TBE buffer for 30 minutes at an output of 70W.

5) 2.5µl of loading buffer (see Appendix I) was added to the DNA samples and they were carefully loaded into the gel. Electrophoresis was carried out for 2.5 hours at an output of 70W.

6) The glass plates were then separated carefully so that the gel was only stuck to one plate and a piece of Whatman filter paper, previously cut to size, was placed on top of the gel to allow a close attachment to it. The supporting paper and gel were cautiously peeled from the glass plate and a piece of

Clingfilm carefully placed on top of the gel. The gel was dried using a BioRad gel dryer for two hours under vacuum at 80 °C.

7) Once dried, the gel was exposed to a phosphorimager screen in a cassette and left overnight. The screen was then scanned with a phosphorimager screen scanner (Storm 860, Molecular Dynamics, Inc.) to obtain the resulting image, which was then quantified as described below.

2.10.5 Quantification and repair analysis

Quantification and analysis of the gel image was undertaken using ImageQuant software version 5.0 ((Molecular Dynamics, Inc.).

1) The intensity of each band reflected the frequency of DNA damage at a specific site and was measured as collective pixel values. To account for any slight variation in the loading of DNA samples in each lane, which may have clouded true repair effects, an adjustment was made as the total signal from individual lanes was multiplied by a factor to give equal values, and then the signal of each band was accordingly multiplied.

2) The value from the non-irradiated DNA sample was subtracted as non-specific background. The damage remaining after particular repair times was presented as a percentile with respect to the initial damage (0 lane, 100% damage).

$$\% \text{ Damage} = \frac{[\text{Damage}]_t}{[\text{Damage}]_0} \times 100$$

(where t = a given repair time, 0 = the starting time point of repair)

3) To generate repair curves, data points representing the percentage of damage at defined sites at each repair time were applied to an exponential curve.

4) Finally the time point where 50% of the damage was removed ($T_{50\%}$ value), was calculated to compare repair rates of individual CPDs.

2.11 Analysis of gene expression

A Northern blotting technique was routinely used to analyse the relative transcription levels of a set of genes in different genetic backgrounds. This method allowed detection and quantification of the amounts of mRNA from a preparation of total yeast RNA.

Quantitative PCR was also employed to detect and quantify gene expression levels when a more sensitive and precise method was required. The same samples obtained from total yeast RNA extraction could be used for either or both methods.

When working with RNA, standard advised precautions were taken and all glassware and equipment was autoclaved twice to eliminate RNAse degradation.

2.11.1 Extraction of total yeast RNA

Total RNA was isolated from yeast cells using a hot phenol method (Schmitt *et al.*, 1990). The details were as follows:

1) 10ml of YPD medium was inoculated and grown overnight at 30°C on a shaking platform, to a density of 2-4×10^7cells/ml. The following morning, 1ml of this culture was used to inoculate 10ml of fresh YPD and left to grow

for 4-5 hours, again to a density of 2-4×10^7cells/ml. The cells were collected by centrifugation at 3500rpm, 5 mins and washed with 0.5ml of sterile H_2O.

2) The cells were transferred to a 1.5ml Eppendorf. 0.5 ml of RNA lysis buffer (10 mM Tris, pH 7.5; 10mM EDTA, pH 8.0; 0.5% SDS) and 1 volume (0.5ml) of phenol (pH 4.3±0.2, Sigma) were added and mixed well by vortex. The tube was incubated at 65°C for 30 mins, using a vortex to mix frequently, and was then immediately placed on ice for 10 mins.

3) Centrifugation was applied at 13000rpm for 5 mins and the top aqueous layer was carefully transferred to a fresh tube. 1/10 volume (50µl) of 3M sodium acetate was added to maintain the correct pH conditions. Phenol/chloroform and chloroform extractions were then performed as previously described.

4) 2 volumes of absolute ethanol were added and the tube was left at -20°C overnight to precipitate the RNA. The pellets were collected by centrifugation, washed with 80% ethanol and resuspended in 100µl of sterile H_2O.

2.11.2 Northern blotting technique

The Northern blotting technique is in essence similar to Southern blotting as described previously, but involving the transfer of RNA rather than DNA. The extracted RNA was firstly separated using formaldehyde-agarose (FA) gel electrophoresis, and then transferred to a nylon membrane. This was subsequently hybridised with a radioactively labelled probe and was finally scanned and analysed.

2.11.2.1 Formaldehyde-agarose (FA) gel electrophoresis

1) To prepare the gel, 2.4g agarose was melted in 20ml of 10×FA buffer (see Appendix I) and 180ml of H_2O. This was cooled to about 65°C before adding 2µl of EtBr and 3.6ml of 37% formaldehyde (Sigma) immediately prior to pouring.

2) A gel mould was prepared in an electrophoresis tank (Bio-Rad) and a plastic comb was inserted to create the wells for loading. The gel was poured into the mould and left to set for 45mins before adding 1 litre of 1×FA running buffer to equilibrate for a further 45mins.

3) 10µl of 5×RNA loading buffer (see Appendix I) was added to each RNA sample before carefully loading into the wells. (For subsequent gels, the loading was adjusted based on quantification of the initial gel, to equalise the amount of RNA in each sample). The gel was then run at 50-60V for 3-4 hours, or until the dye visibly reached the centre of the gel.

4) The gel was rinsed three times in distilled H_2O and viewed under a UV transilluminator to visualise the characteristic bands of RNA.

2.11.2.2 Northern blotting, detection and analysis of RNA

1) 2 pieces of Whatman paper and the membrane ((GeneScreenPlus, NEN) were cut to size and soaked in 20× 1M phosphate buffer (see Appendix I) for 15 mins. The fractioned RNA in the gel was then transferred to the membrane using a Stratagene pressure blotter, using 20× diluted 1M phosphate buffer for transfer. Due to the buffer's low salt concentration, the transfer took 4-5 hours to complete.

2) The membrane was placed under a UV transilluminator for 2mins to fix the RNA, and then baked for 1 hour at 80°C to remove the formaldehyde.

3) Radioactively labelled probes were prepared as described in section 2.8, using the appropriate PCR products and primers. Two probes were created, one to bind to transcribed fragments (thus detecting mRNA levels) of the gene of interest (*MFA2)* and another to detect mRNA levels of a known control gene (*ACT1)*.

4) RNA was hybridised with the first probe as described in section 2.8, with the exception that phosphate hybridisation buffer (0.5M phosphate buffer, 7% SDS, 1% BSA, 1mM EDTA) was used during the hybridisation process, and phosphate washing buffer (40mM phosphate buffer, 4% SDS, 1mM EDTA) was used to wash the membrane when hybridisation was complete.

5) After hybridisation with one probe, the membrane was boiled twice with stripping solution (0.1×SSC, 1% SDS) for 20mins to strip the probe from the membrane. The hybridisation process was then repeated with the second probe. Thus mRNA levels of both the gene of interest and the control gene were detected and compared using the same membrane.

6) The membrane was wrapped in Clingfilm and placed into a cassette against a phosphorimager screen (Molecular Dynamics, Inc.). Exposure was allowed overnight at room temperature. The image was then generated by scanning the screen using a phosphorimager scanner (Storm 860, Molecular Dynamics, Inc.). Finally, mRNA levels were quantified using ImageQuant software (Molecular Dynamics, Inc.).

2.11.3 Quantitative PCR (qPCR)

Quantitative PCR (qPCR) enables fast, sensitive and precise measurement of gene expression (mRNA levels) using RNA samples extracted as described in section 2.11.1. The technique consisted of two stages. Firstly, a reverse transcription PCR (RT-PCR) reaction was performed using the TaqMan®Gold RT-PCR Kit (PE/Applied Biosystems) to create cDNA, using the RNA as a template. In the second stage, the cDNA was prepared for PCR using the iQTM SYBR®Green Supermix (Bio-Rad) and was then amplified and analysed using the iCycler iQ real-time PCR detection system (Bio-Rad).

The direct detection of PCR product was enabled by measurement of fluorescence, emitted proportionally during the PCR reaction, due to the binding of the SYBR®Green dye to dsDNA. The fluorescence data was collected by a camera, then processed and analysed using the iCycler software (Bio-Rad). Real-time detection enables fluorescence to be monitored during each PCR cycle, allowing data to be collected during the most exponential phase of PCR amplification, the threshold cycle (C_t), which is more sensitive than the collection of data from the end-point accumulation of PCR product alone. The C_t is inversely proportional to the copy number of the target template. The initial amounts of cDNA and hence mRNA can be calculated accurately to measure gene expression.

2.11.3.1 Reverse Transcription (RT) to create cDNA

RNA was used as a template to create cDNA using the TaqMan®Gold RT-PCR Kit (PE/Applied Biosystems) according to the manufacturer's instructions. All reactions were performed in 0.5ml thin-walled eppendorf tubes and all manipulations

were performed as recommended when handling RNA.

The following components were mixed together to give a total reaction volume of 20µl:

RNA	1µl
RNAse-free H_2O	6.7µl
10×TaqMan RT buffer	2µl
25mM $MgCl_2$	4.4µl
DeoxyNTPs mix	4µl
Oligo $d(T)_{16}$ primer	1µl
RNAse inhibitor	0.4µl
Multiscribe Reverse Transcriptase (50U/µl)	0.5µl

The thermal cycling parameters for two-step PCR were as follows: Primer incubation step at 25°C for 10mins, to maximise primer-RNA template binding; reverse transcription at 48°C for 30mins; and finally, reverse transcriptase inactivation at 95°C for 5mins. All cDNA samples were diluted 100× and a series dilution of 10×, 100×, 1000× and 10000× of an arbitrary sample was prepared in order to create a set of standard samples. The inclusion of standards enabled a standard curve to be produced for analysis. The cDNA could then be stored at -20°C until further use.

2.11.3.2 Quantitative real-time PCR analysis

1) The iCycler iQ real-time PCR detection system (Bio-Rad) apparatus was set up and switched on according to the manufacturer's instructions.

2) The following components were mixed to prepare the PCR reaction mixture to a total volume of 20µl:

iQTM SYBR®Green Supermix (Bio-Rad)	10µl
cDNA	1µl
Forward Primer (20mM)	0.5µl
Reverse Primer (20mM)	0.5µl
H_2O	8µl

For each cDNA sample, including the set of standards, the above PCR mix was prepared in triplicate, and two sets were made, one using primers for the gene of interest (*MFA2*) and the second using primers for the control gene (*ACT1*).

3) The samples were carefully loaded into the wells of a 96-well plate (Bio-Rad) and a sheet of sealing plastic (Bio-Rad) was secured on top, taking care not to touch the surface of the plastic. A vortex was used to mix the samples and the plate was placed into the iCycler.

4) The parameters for the qPCR reaction were as follows:

    1. 95°C for 3min
    2. 95°C for 30sec
    3. 52°C for 30sec*
    4. 72°C for 10sec
    5. Steps 2-4 repeated 40 times
    6. 95°C for 30sec
    7. 55°C for 30sec*
    8. Step 7 repeated 40 times, increased by 1°C with each repeat

*Fluorescence data was collected during step 3 and after step 7.

5) When the reaction was complete, the plate was removed and analysis could be undertaken immediately. The iCycler software (Bio-Rad) deduced the

threshold cycle (C_t), an arbitrary number of PCR cycles in which all of the amplification graphs in the comparison are in the linear range, although this could be overridden and selected manually. As the C_t is inversely proportional to the copy number of the target template, a low C_t value represents a high template concentration and *vice versa*. The software also calculated the mean value (of the triplicate reactions) and standard deviation for each sample. The inclusion of a standard curve in addition enabled eventual calculation of the amount of mRNA originally present in each sample. The overall turnover time for the experimental and analytical acquisition of data was just a few hours.

Chapter 3

Histone Deacetylases and Transcription at Yeast *MFA2*

3.1 Introduction

Eukaryotic DNA is packaged into chromatin which has implications for DNA-mediated cellular processes such as transcription, recombination and DNA repair. The basic unit of chromatin, the nucleosome, comprises of 147bp of DNA wrapped around a histone octamer of the core histone proteins H2A, H2B, H3 and H4. Nucleosomes are subsequently compacted into further higher order chromatin structures (Luger *et al.*, 1997 Lewin, 2000; Luger, 2006). Chromatin organization plays a vital role in affording access to the target DNA sequences by proteins such as transcription factors and repair proteins. Chromatin structure can be altered by two main types of modification. ATP-dependent remodelling complexes such as the Swi/Snf family can affect the positioning of nucleosomes upon the DNA, whereas post translational modifications of the core histones, such as acetylation and deacetylation, can alter their properties and hence the nature of interactions with each other, with DNA and with other proteins (Wang *et al.*, 2003). Histone modifications primarily affect the amino-terminal tails which protrude from the core nucleosome structure when chromatin is in a relaxed state.

Histone acetylation is achieved via histone acetyltransferases (HATs) and involves the addition of an acetyl group to the ε-amino group of specific lysine residues in the amino-termini of histone tails. This is a reversible reaction whereby histone deacetylases (HDACs) can remove the acetyl group and counteract the effects of acetylation. Increased acetylation (increased HAT activity) generally correlates

with increased gene expression and similarly, decreased acetylation (increased HDAC activity) usually correlates with repression of gene activity. Hence actively transcribed chromosomal regions often contain hyperacetylated histones whereas histones in silent, heterochromatic regions are hypoacetylated (Grunstein, 1990; Turner, 1993). A steady state level of histone acetylation is achieved in the cell by the balancing of the two opposing enzymic activities (Wade, 2001). HAT and HDAC activities may be targeted to a specific gene promoter, more generally targeted or untargeted to exert genome-wide effects (Verdin *et al*, 2003).

Histone deacetylases (HDACs) were first identified a decade ago (Taunton *et al.*, 1996; Carmen *et al.*, 1996; Rundlett *et al.*, 1996). To date, ten HDACs have been identified in yeast, namely Rpd3, Hda1, Hos1, Hos2 and Hos3 (Rundlett *et al.*, 1996) and the NAD+-dependent Sir2 family of Sir2, Hst1, Hst2, Hst3 and Hst4 (Landry *et al.*, 2000). At least 19 homologous HDACs have also been identified in human cells (Taunton *et al.*, 1996; Gray and Ekström, 2001; Yang and Seto, 2003). The HDACs have been classified into four classes, based on sequence similarity and function (see Table 3.1). Class I HDACs are similar to yeast Rpd3, consisting of Hos1, Hos2 and human HDACs HDAC1, 2, 3, and 8. Class II HDACs are more similar to Hda1 and include human HDACs 4, 5, 6, 7, 9 and 10 which have been sub-classified further to classes IIa (HDACs 4, 5, 7 and 9) and IIb (HDACs 6 and 10) based on sequence homology and domain organisation (Verdin *et al.*, 2003). The human HDAC11 has been more difficult to classify and was initially considered most similar to class I HDACs. However, recently HDAC11 has been considered in its own right as a new class IV HDAC (Yang and Grégoire, 2005; Voelter-Mahlknecht *et al.*, 2005). Class III HDACs include the seven human sirtuins and are similar to the yeast Sir2 (silent information regulator 2) family. These are functionally distinct from the zinc-

dependent HDACs of classes I and II, and are NAD+-dependent in their activity (Landry *et al.*, 2000; Tanny and Moazed, 2001; Denu, 2003; Yang and Grégoire, 2005). In yeast, Sir2 plays a major role in regulating genomic stability by chromatin silencing (Kyrylenko *et al.*, 2003) but the roles of the sirtuins in humans remain less clear. Table 3.1 summarises the proposed and possible functions of each class of HDAC, with their cellular localization and sensitivity to common HDAC inhibitors (Rundlett *et al.*, 1996; Bernstein *et al.*, 2000; Gao *et al.*, 2002; Robyr *et al.*, 2002; Wang *et al.*, 2002; Verdin *et al.*, 2003; Yang and Grégoire, 2005; Voelter-Mahlknecht *et al.*, 2005)

Table 3.1. Classification of yeast and human deacetylases (HDACs)

	Yeast	Human	Function	Localisation & Tissue Distribution	Sensitivity to HDAC Inhibitors
Class I	RPD3 HOS1 HOS2	HDAC1 HDAC2 HDAC3 HDAC8	Roles in global & specific gene repression Also, Hos2 possible role in gene activation	Found in most cell types Almost exclusively nuclear	Trichostatin A (TSA) sensitive
Class II	HDA1 HOS3	Class IIa HDAC4 HDAC5 HDAC7 HDAC9 Class IIb HDAC6 HDAC10	Likely to have roles in cellular proliferation and differentiation	Able to shuttle between nucleus and cytoplasm hHDACs expressed in most tissues HDACs 9 & 4 - higher expression in tumour tissue than healthy tissue	Highly TSA sensitive
Class III	SIR2	SIRT1-7 (Sirtuins)	NAD+ dependent for deacetylase activity Roles in yeast gene silencing, heterochromatin Functions in human cells still largely unknown	Found in the nucleus, cytoplasm and mitochondria	TSA-resistant
Class IV		HDAC 11	May have distinct physiological roles from other HDACs	High expression in kidney, heart, brain, skeletal muscle & testis Localised predominantly in nucleus	Trapoxin-sensitive

The present study focuses on the class I and class II HDACs. The functions of class I Rpd3-like deacetylases and the complexes in which they exist have been relatively well characterised, whereas less is known about those involving the class II Hda1-like enzymes (Rundlett *et al.*, 1996; Wu *et al.*, 2001b).

Functions of Rpd3

Rpd3 (reduced potassium dependency 3) has been implicated in both global repression (Robyr *et al.*, 2002; Bernstein *et al.*, 2000; Vogelauer *et al.*, 2000; Braunstein *et al.*, 1993) and targeted, promoter-specific repression of gene activity (Deckert and Struhl, 2002) in yeast. Rpd3 preferentially deacetylates histone H4, particularly lysines 5, 8 and 12, and commonly functions as part of a protein HDAC complex with the corepressor Sin3, which was first identified as a negative regulator of HO expression in yeast (Sternberg et al, 1987; Nasmyth *et al.*, 1987). Sin3 is a Swi/Snf suppressor and is required for the regulation of various yeast genes (Vidal et al, 1991). The Rpd3-Sin3 complex is recruited by Ume6 (Kadosh and Struhl, 1997; Zhang *et al.*, 1998) to targeted promoters of early meiotic genes in yeast. Ume6 binds to the URS1 (Upstream Repression Sequence 1) site in the 5' region of these promoters and Rpd3 deacetylates local histones H3 and H4 over a range of 1-2 nucleosomes (Kadosh and Struhl, 1998; Rundlett *et al.*, 1998) to exert repression. Genome-wide studies, however, have revealed that although Ume6 plays a key role in repression by Rpd3, 57% of intergenomic regions affected by Rpd3 use other recruiting mechanisms (Robyr *et al.*, 2002; Kurdistani *et al.*, 2002). Although Rpd3 acetylates a wide range of genes, there appears to be a significant over-representation of genes regulating cell cycle progression (Bernstein *et al.*, 2000; Fazzio *et al.*, 2001; Robert *et al.*, 2004). Interestingly, Rpd3 appears to counteract heterochromatic silencing at typically Sir2-repressed loci (Rundlett *et al.*, 1996; De Rubertis *et al.*, 1996) and has also been implicated in the activation of certain genes (Bernstein *et al.*, 2000), some of which are repressed by Sir2 (Bernstein *et al.*, 2000). Rpd3 may also play a role in chromatin assembly as it deacetylates lysine residues 5 and 12 of

histone H4, associated with the deposition of newly synthesised histone H4 (Sobel *et al.*, 1995).

Functions of Hda1

The class II HDAC Hda1 also exerts both global and targeted repression in yeast (Robyr *et al.*, 2002; Bernstein *et al*, 2000) and primarily deacetylates histones H3 lysine residues 9 and 18 and H2B lysine 16 (Wu *et al.*, 2001b). Globally, there is a degree of redundancy between Hda1 and Rpd3 but most targeted promoters are affected by one or the other (Robyr *et al.*, 2002). Hda1 functions as part of a different repressor complex to that including Rpd3 (Rundlett *et al.*, 1996; Wu *et al.*, 2001b). Similarly to Rpd3, most Hda1 activity appears to be recruited by other novel mechanisms (Robyr *et al.*, 2002) but it can be recruited to specific promoters by the Tup1-Ssn6 corepressor complex, which mediates repression of diverse classes of genes including those controlled by mating type, DNA damage and anaerobic stress (Edmondson *et al.*, 1998). However, some studies have questioned the involvement of Hda1 in Tup1-mediated repression and suggest that the class I HDACs have a more predominant role (Watson *et al.*, 2000; Davie *et al.*, 2003). Hda1 also functions at distinct subtelomeric chromosomal domains which resemble heterochromatin but are distinct from Sir2-regulated regions. These Hda1-Affected SubTelomeric (HAST) domains contain genes which are activated in conditions of environmental stress, and are likely repressed by Tup1-Ssn6 mediated Hda1 deacetylation (Robyr *et al.*, 2002).

Functions of Hos1, Hos2 and Hos3

The Hos (HDA One Similar) HDACs Hos1, Hos2 and Hos3 are less well characterised but genome-wide studies have suggested that Hos1 and Hos3

preferentially deacetylate ribosomal DNA, and Hos2 affects ribosomal protein (RP) genes (Robyr *et al.*, 2002) where it deacetylates both the promoter and coding regions. Rpd3 also affects the RP genes (Kurdistani *et al.*, 2002) and the two HDACs show a degree of redundancy. In contrast to other class I HDACs, Hos2 has been implicated in the direct activation of such genes of high activity genome wide, possibly playing a role in reverting chromatin disrupted by RNA polymerase to its original state, permissive for efficient transcription (Wang *et al.*, 2002). At certain promoters, Rpd3 and Hos2 actually exert opposing effects, despite similar histone specificities, but the mechanisms involved remain unclear (Wang *et al.*, 2002).

In many instances, multiple HDACs work alongside each other (Robyr et al., 2002; Wang *et al.*, 2002;) or are paired with HATs to exert opposing effects upon the acetylation at a particular promoter. For example, Gcn5 and Rpd3 exert opposing effects on *IME1* transcription (Burgess *et al.*, 1999); Esa1 and Rpd3 acetylate and deacetylate, respectively, lysine 12 of histone H4 at the *PHO5* promoter (Vogelauer *et al.*, 2000).

Deacetylation by various single or combinations of HDACs is important in determining the precise acetylation state of histones and organisation of chromatin both globally and at specific promoters within the genome, hence may play roles in processes intimately linked to chromatin structure such as transcription, DNA replication and DNA repair.

HDACs and Transcription at MFA2

The experiments presented in this chapter examined the roles of class I and class II deacetylases in regulating transcription at the yeast *MFA2* gene, an **a** cell-specific gene which is regulated by chromatin-mediated repression (Patterton and

Simpson, 1994). *MFA2* is repressed in α cells by the co-operative binding of Mcm1 and α2 proteins to the P-box region of the *MFA2* promoter along with the recruitment of the Tup1-Ssn6 complex, a global repressor in yeast. In repressed α mating type cells, four nucleosomes are positioned at the control and coding regions of *MFA2* (Teng *et al.*, 2001) but this positioning is lost in **a** cells where *MFA2* is actively transcribed.

HATs such as Gcn5 are known to facilitate gene expression by hyperacetylation of core histones resulting in an open chromatin structure to enable various transcription factors and regulatory proteins to access DNA and promote transcription. With respect to *MFA2*, Gcn5p is needed for optimal transcription; without it only 20% of the normal mRNA level is present in **a** mating type cells (Teng *et al.*, 2002). It therefore follows that HDACs may also play major roles in determining precise acetylation states of histones, governing gene expression by altering the local chromatin architecture. This chapter looks at the possible effects of class I HDAC Rpd3, class II HDAC Hda1 and five different combinations of class I and/or class II HDACs upon transcription of *MFA2*.

3.2 Materials and Methods

Yeast Strains

W303a *MATa ade2-1 trp1-1 can1-100 leu2-3 his3-11,15 ura3-5*

W303α *MATα ade2-1 trp1-1 can1-100 leu2-3 his3-11,15 ura3-5*

W303*Δrpd3* as W303α except *rpd3::URA3* (Created in this study)

W303*Δhda1* as W303α except *hda1::URA3* (Created in this study)

DY 5140 as W303α except *hda1::URA3, hos2::TRP1, rpd3::LEU2*

DY 6444 as W303α except *hda1::URA3 hos1::HIS3, hos2::TRP1, rpd3::LEU2*

DY 6445 as W303α except *hos1::HIS3, hos2::TRP1 rpd3::LEU2*

DY 6446 as W303α except *hda1::URA3, hos1::HIS3, rpd3::LEU2*

DY 6447 as W303α except *hda1::URA3, hos1::HIS3, rpd3::LEU2*

Construction of the rpd3Δ and hda1Δ strains

Primer Design

The *URA3* gene was used to disrupt firstly *RPD3* and then *HDA1* in a W303 background. Both genes are located on chromosome XIV. *RPD3* is 1302bp, found at position 19302 to 18001, and *HDA1* is 2120bp, at coordinates 593223-595343. The yeast genome database (SGD™, www.stanford.edu/saccharomyces/) and Microsoft Oligo software were used to design forward (F) and reverse (R) primers for each gene. Each forward primer was designed to start approximately 300bp upstream of the gene start site and each reverse primer designed to start approximately 300bp downstream of the end of the gene (see Figures 3.1 and 3.2). The *URA3* primer sequences (obtained from Y. Teng) were then added on to complete the final primer sequences, which were as follows (*URA3* sequences underlined):

RPD3

F: 5'-TCACCCCAAGTGTGTCGCGGGCCCGTGGAATTCTCATGTTTGACAGC-3'

R: 5'-TCAACAGCGGTGGGACGAGACGCGGTGCCTGACTGCGTTAGCA-3'

HDA1

F: 5'-GCCATTTTCCCGCACCGTTTGGCCGTGGAATTCTCATGTTTGACAGC-3'

R: 5'-CCACTGCTCCTCGCGGGACGAACGGTGCCTGACTGCGTTAGCA-3'

CAAAAGGCGAGAGAGGCTAAACCTTGTGTCATATTTTTCGATGAAATCGATTCAGTAGCA
CCCAAACGTGGTAATCAAGGTGATTCGGGTGGTGTTATGGATCGTATCGTTTCACAGTTA
CTAGCAGAGTTAGATGGTATGAGTACCGACGCTGACGGTGTATTTGTTATCGGAGCAACA
AACAGACCAGACTTATTGGACGAAGCACTACTAAGACCAGGACGATTCGATAAATTGTTA
TATTTAGGCATTCCGGATACGGATACCAAACAATTGAATATTTTAGAGGCTCTGACTCGC
AAATTCGTGCTCGACAACGACGTAAAGCTTATTGAGTTGGCAAAGCTATGTCCATTTAAT
TACACCGGGGCAGATTTTTATGCTCTCTGCTCAGATGCAATGCTTAACGCCATGTCAAGA
ATTGCACGCATGGTAGAAAAAAAAGTTTCTCAGCATAACGAATTGACGGGAGAGAATATT
TCTACA**CGTCGCTGGTTTGATAAGATTGCGA**CAAAAGAGGATACTAAGGTTGTCGTAAAA
ATGGAAGACTTCTTGAAAGCACAAGAGCAGC**TCACCCCAAGTGTGTCGCGGGC**TGAACTG
AATCATTATGAAGCGGTGAGAGCTAATTTTGAAGGTGCTTAAGTAATATCAACTCAGAGC
GTATAGGTAAATTTGTAAATATATGTCCCATATTTTGCCTTGAAATTTATCTTTTTATTT
ACTTACCCTCCCCGGCTCATAGTATCTATCGAAAGGGAAAAACAGAAAAGATACTAGTAG
TTGATTATACATAATAAAAATTTGAAGTAATAACCATAAAGGTTCATAAAACAATTGCGC
CATACAAAACATTCGTGGCTACAACTCGATATCCGTGCAG**ATGGTATATGAAGCAACACC**
TTTTGATCCGATCACGGTCAAGCCAAGCGATAAAAGACGCGTTGCATATTTTTACGATGC
AGACGTTGGGAACTATGCATATGGAGCAGGTCACCCGATGAAGCCGCATAGAATAAGAAT
GGCACATTCCCTTATTATGAATTATGGCTTGTACAAGAAGATGGAAATTTACAGAGCTAA
GCCGGCAACGAAACAAGAAATGTGTCAGTTCCATACTGATGAATACATTGATTTTTTATC
GAGGGTTACTCCAGATAATTTAGAAATGTTTAAAAGAGAAAGTGTCAAGTTTAATGTCGG
AGATGATTGTCCTGTCTTTGATGGGCTCTATGAGTACTGTAGCATATCTGGTGGTGGCTC
TATGGAAGGAGCTGCTCGTCTGAATAGAGGCAAATGTGATGTTGCTGTCAACTATGCGGG
TGGTTTGCATCATGCAAAAAAATCGGAAGCTTCTGGGTTTTGTTATTTAAATGACATAGT
ACTGGGCATTATTGAGCTACTACGATACCACCCCAGAGTTCTGTATATTGATATTGATGT
GCACCATGGTGATGGTGTAGAGGAAGCGTTTTATACAACGGATCGTGTCATGACATGTTC
TTTCCACAAATATGGTGAGTTTTTCCCTGGCACAGGTGAACTGAGAGATATAGGGGTGGG
TGCAGGAAAAAACTACGCGGTCAATGTGCCATTAAGAGACGGTATTGACGATGCTACGTA
TAGATCTGTGTTTGAACCTGTGATAAAAAAAATTATGGAATGGTATCAACCTTCTGCTGT
CGTGTTACAGTGTGGTGGGGACTCCTTGTCCGGCGATCGTCTTGGTTGCTTTAATCTTTC
CATGGAAGGCCATGCTAATTGTGTAAACTATGTGAAATCCTTTGGGATCCCAATGATGGT
TGTTGGTGGAGGAGGCTATACTATGAGAAATGTTGCAAGGACATGGTGCTTTGAAACAGG
TCTACTAAATAACGTTGTCTTGGATAAAGATTTACCGTACAATGAATATTACGAATATTA
CGGTCCAGATTATAAGTTAAGTGTTAGACCTTCGAATATGTTCAATGTAAATACTCCCGA
ATATCTTGACAAGGTAATGACCAATATATTTGCTAATTTGGAAAACACAAAGTATGCCCC
TAGTGTTCAGTTGAATCACACACCTAGGGATGCCGAAGATTTGGGTGATGTTGAAGAAGA
TTCTGCCGAGGCTAAAGATACGAAGGGTGGTTCGCAATATGCGAGGGACCTACATGTTGA
GCATGACAATGAATTCTATTGAAAAAAAGAGTTGGAAGTATATACGAATATAAATAATGT
GAAACAAAAGAAGAAAAGTGAATAAAAGGCACTTAAGACGCTATCCAATTGTGTATGAGA
AGTGCAAACTCAATTTTTTTGCAAAAGACTTTTCTCAAACCTTTAATTGATGCGTTCCGT
TCATACATCAACCGCGTCCCATACGTTTCGAAGAAAATTGCCTATATGTGTTATTTACAT
ACTAGAGATATTTTAATATTGAAACAGTTGTATTTCTATTGTAATTACTATCTAAA**CGTC**
TCGTCCCACCGCTGTTGATAAAGCGGTGCCAATATAATTTAT**AATCACGCCTGGGTAAAT**
GACTTTTAATTTCTTAAATCATCGAAGTATGCGAAAACAAGAAGTCTTTATTCATAATAA
AAAACAAATTCGGTTACTACGACTTTTATATGTCATTCAATATTTGGTAATAATTTTACA
GTATTAACCCTATCCTCATCTGATTCACTCTCTTCTAATTGCATATATTTTCAAATTCGC
TTTCAGCGCTGTACAAAACCAGTAAGCAGATCTCGTACGAAGACTCAAATAAGTTGCATT
GTTCGTATTCAAGGAAACCGGGGGGCAAAATTTCCAACCATATTTAAGTATGACAATATT
TCCAAGTCAAGGATGCATGCTGTTCTTCTCTTCATTAACTAGCTAACCAATTAGCTGAAC
GGCTTTGTATTTTACTTAACATATTGTCTATTGCATAAAAAACCACTATTCAGCATGACT
GACTTGTTTAAACCTCTACCTGAACCACCTACCGAATTGGGACGTCTCAGGGTTCTTTCT
AAAACTGCCGGCATAAGGGTTTCACCGCTAATTCTGGGAGGAGCTTCAATCGGCGACGCA

Figure 3.1 Partial sequence of yeast chromosome IV, reading 5' to 3', encompassing the *RPD3* gene (indicated in bold). The shaded areas indicate the sequences used in designing the forward and reverse primers, and the underlined areas mark the sequences used in designing the second set of primers.

TGTAGAAATTCATGCTTTTTCGTAGCTAACTTCTCAGTGAAACACTTGGTGAAGAACCAG
CTCTTCTCTTAA**CCTCATCGAATATTTTAGGCCAGTTTTT**TTTTTCCTCACTT**GCCATTT**
TCCCGCACCGTTTGGAAATCTCGAGGAAAATGCTTCTTTCCAAAAGTTTAATCAGGTCAC
TAATTAGGTAAATAGAGCTGGGAGGAAGCATATACAGTGTTTCGTCTGTGGAAGGAACTT
TTATTTTTCTTAAATGTTTTAATTTTTAGTGACCTAATTCACATAACAAAATATTGAGAA
AGGGAAAGTTGAGCACTGTAATACGCCGAACAGATTAAGC**ATGGATTCTGTAATGGTTAA**
GAAAGAAGTACTGGAAAATCCAGACCATGATTTAAAAAGAAAGCTAGAAGAGAACAAAGA
AGAAGAGAATAGCCTCTCTACTACTTCTAAAAGTAAAAGGCAGGTTATTGTTCCCGTTTG
CATGCCAAAAATCCATTATTCACCGCTGAAAACTGGTCTTTGCTATGACGTTAGAATGAG
GTATCATGCAAAGATTTTCACATCGTACTTCGAGTACATTGATCCACATCCAGAGGACCC
AAGAAGAATATATCGTATTTATAAAATACTAGCAGAGAATGGTCTGATTAACGACCCCAC
TTTAAGCGGCGTGGATGACCTTGGTGATTTAATGCTGAAGATACCTGTAAGAGCCGCAAC
CTCCGAAGAAATCTTGGAAGTTCATACAAAGGAACATTTAGAGTTTATTGAAAGCACAGA
AAAAATGAGCCGAGAAGAGTTATTAAAAGAGACTGAAAAAGGTGATTCCGTATATTTCAA
TAATGATTCTTACGCGAGTGCTAGGCTGCCTTGTGGTGGCGCCATTGAAGCATGCAAGGC
GGTTGTCGAGGGGCGTGTAAAAAACTCTCTAGCTGTCGTAAGACCACCTGGCCATCATGC
AGAGCCTCAAGCTGCGGGTGGTTTTTGTCTCTTCAGTAATGTTGCTGTTGCTGCCAAGAA
TATCTTAAAGAACTACCCAGAAAGTGTAAGAAGGATAATGATTTTAGATTGGGATATTCA
TCATGGTAATGGCACACAAAAGTCATTCTATCAAGACGATCAGGTGCTATATGTGTCATT
ACACAGATTTGAAATGGGTAAATACTATCCTGGGACCATCCAAGGACAATATGATCAAAC
TGGTGAGGGTAAGGGTGAAGGATTCAATTGTAATATTACTTGGCCGGTCGGCGGTGTTGG
TGATGCAGAATATATGTGGGCATTTGAACAGGTAGTTATGCCTATGGGGAGAGAATTCAA
GCCTGACTTGGTGATTATTTCTTCAGGGTTTGATGCCGCGGATGGTGATACTATCGGACA
ATGTCATGTCACCCCAAGTTGTTATGGACACATGACACATATGTTAAAATCTCTAGCTAG
AGGTAATCTTTGTGTAGTTTTGGAAGGTGGATATAACTTGGATGCGATTGCAAGAAGCGC
TTTGAGTGTAGCAAAAGTACTAATAGGGGAGCCTCCTGATGAACTACCTGATCCATTAAG
TGATCCCAAGCCTGAGGTCATAGAAATGATAGACAAAGTAATTCGGTTACAGTCCAAGTA
TTGGAACTGTTTTAGAAGGAGACATGCTAACTCCGGTTGTAATTTTAACGAACCTATTAA
CGACTCGATAATATCTAAAAATTTTCCTCTGCAGAAGGCTATTCGTCAACAACAGCAACA
CTATTTAAGCGACGAATTTAATTTCGTTACTTTACCGTTAGTAAGCATGGATTTACCAGA
TAATACAGTGCTATGTACTCCAAACATTTCCGAATCTAACACTATAATTATAGTCGTTCA
TGATACTTCTGATATCTGGGCAAAGAGAAATGTTATTTCAGGTACAATTGACTTATCCTC
ATCAGTTATCATTGATAATTCTCTAGACTTTATCAAATGGGGACTTGACAGGAAATACGG
CATCATTGATGTAAATATACCTCTAACTCTGTTTGAACCTGACAATTACTCAGGAATGAT
TACATCCCAAGAAGTTCTAATATATTTATGGGATAACTACATCAAGTATTTTCCTTCTGT
TGCCAAAATTGCTTTTATTGGAATAGGAGACTCATACTCAGGTATCGTACATCTGCTTGG
TCACAGGGATACTAGGGCTGTTACTAAAACGGTAATTAATTTCTTGGGAGACAAGCAGTT
AAAGCCACTAGTTCCTCTAGTAGATGAAACATTGAGTGAATGGTACTTCAAAAACTCACT
TATATTTTCAAACAATAGCCACCAATGCTGGAAAGAAAATGAAAGCAGAAAACCAAGAAA
AAAATTCGGTAGAGTTTTGAGATGTGATACGGACGGGTTAAACAATATAATTGAAGAAAG
ATTTGAAGAGGCTACAGACTTTATACTGGATTCGTTTGAAGAATGGAGTGATGAAGAATG
AGGAAAAACTGGCCATTAATAATTTTTTTTCGGCAACCTTCATGCCTTATGAAAGTTGAA
TAATAATAAAGTTGTTACAATGTTCATTGTATAATCCAATATATCTAAAATAGGAAAAAG
AAATGAACAAATGCATTAAGCTGTGTTTTACTAAGTATTATGGGAAAACGTATACATTAA
AGTGGATGCTTACATATATAACACATTGTAATAAAGGTTCTTTGAACATGTTACCAGCCT
CTTCAGAGATCGATCCGGTTCTGTTGAGCCAAATACTCACTTATCCAAGGATAACT**TTCG**
TCCCGCGAGGAGCAGTGGTTTTGGAGGAGGTTTAGGCTTTAAA**TGTGAAGGCTTAGGTGG**
TGGGGTAGGTTTTGTTTTTTTGTCTTTTGAAATCGGGCCACTTGATTTCAGCATTGTTGG
CTTATCTATCTCCCCTTTCTCATGCAGCTTGACCTTGGACATTTTCCTAGCGTTGAATGA

Figure 3.2 Partial sequence of yeast chromosome IV, reading 5' to 3', encompassing the *HDA1* gene (indicated in bold). The shaded areas indicate the sequences used in designing the forward and reverse primers, and the underlined areas mark the sequences used in designing the second set of primers.

The oligonucleotide primers were obtained from MWG (mwg-biotech.com). The SGD was used to check for repeats of the primer sequences in the genome and the Oligo software was used to check for self-annealing and false primer sites.

The primers were obtained from MWG (mwg-biotech.com) and adjusted by appropriate dilution for use at a concentration of 100pmol/µl. A second set of primers was also designed for each gene, outside of the regions covered by the first se to check for successful disruption of the genes following transformation (See Figures 3.1 and 3.2). PCR was performed to create fragments containing the *URA3* gene plus the flanking sequences from the target gene, using wild type yeast cells and each set of forward and reverse primers.

The PCR products were then electrophoresed on a 1% agarose gel to confirm the correct size bands were achieved. The PCR mixture (total volume 50µl) and parameters were as follows:

PCR reagents:

DNA	10µl
Taq Buffer	5µl
$MgCl_2$	4.5µl
F Primer (100µM)	0.2µl
R Primer (100µM)	0.2µl
dNTP mix (10mM)	1.75µl
Taq Polymerase	0.5µl
H_2O	27.85µl

PCR parameters:

1. 94°C, 4 min
2. 94°C, 20 sec
3. 55°C, 30 sec
4. 68°C, 1 min

5. Go to 2, 10 times
6. 94°C, 20 sec
7. 55°C, 30 sec
8. 68°C, 1 min & 30 sec
9. Go to 6, 25 times
10. 72°C, 10 min
11. End

Transformation using lithium acetate

Wild type W303α cells were transformed with the PCR products to disrupt the genomic copies of *RPD3* and then *HDA1* to create *rpd3Δ* and *hda1Δ* strains. A lithium acetate method was used as described by Gietz *et al.*, 1992. Following transformation, the cells were grown on YNBD minimal media plates (see Appendix I) lacking uracil in order to identify successfully transformed cells with the target gene disrupted. The transformation procedure was as follows:

1) Yeast cells were grown in 10ml of YPD overnight at 28°C to a density of 1×10^7 cells/ml. These cultures were then used to inoculate 10ml of fresh YPD at a density of 2×10^6 cells/ml and incubated at 28°C for a further 4-5 hours, to reach a final density of 1×10^7 cells/ml.
2) The cells were collected by centrifugation at 10000rpm for 30s and washed with 1ml of H_2O. A second wash was performed using 1ml of solution A (see Appendix I) before resuspending the cells in 100µl of solution A.
3) 50µl of these cells was transferred to a fresh tube. 5µl of carrier DNA (salmon sperm DNA, 10µg/µl in H_2O, denatured at 100°C for 20mins), 300µl of solution B (see Appendix I) and 5µl of the PCR product were added to the tube and mixed well by vortexing. The tubes were incubated at 28°C with

agitation for 30mins. A control sample was also created lacking the PCR product.

4) The tubes were then incubated at 42°C for a 15 minute heat-shock, before being collected by centrifugation and resuspended in 1ml of YPD.
5) The cells were incubated at 28°C with agitation for one hour, collected by centrifugation and washed with 1ml of TE buffer.
6) After resuspension in 1ml of TE buffer, 100µl were spread onto a glucose minimal medium plate lacking uracil. The plates were grown at 28°C for 3 days. Transformant colonies could then be identified. Cells from these colonies successfully integrated the PCR product and hence the target gene (*RPD3* or *HDA1*) was disrupted.

Rapid DNA extraction using glass beads

A rapid method using glass beads for extracting DNA (Hoffman and Winston, 1987) was used to obtain DNA from the transformed cells. The DNA was then used in a PCR reaction to check for successful transformation. Briefly, the procedure was as follows:

1) 10ml of the transformed yeast cells was grown overnight at 28°C.
2) Cells were collected by centrifugation, resuspended in 0.5ml of H_2O and transferred to 1.5ml Eppendorf tubes. The tubes were spun down and the supernatant carefully discarded, resuspending the cells in the residual liquid.
3) 0.2ml of lysis solution (2% Triton X-100, 1% SDS, 100mM NaCl, 10mM Tris pH 8.0, 1mM EDTA), 0.2ml of phenol-chloroform and 0.3g of glass beads (Sigma) were added and mixed well by vortexing for 3-4mins.

4) 0.2ml of TE buffer was added and mixed. The tubes were then spun for 5mins and the aqueous top layer was transferred carefully to a new tube. 1ml of ethanol was added and mixed, before spinning for 10mins in a microfuge.
5) The pellets were resuspended in 0.4ml of TE buffer containing 1µl RNAse A (10µg/ml) and incubated at 37°C for 15mins.
6) 40µl of 3M NaAc and 1ml of isopropanol were added and mixed well. The tubes were spun for 10mins and the pellets dried thoroughly before resuspending in 0.5ml of TE buffer.
7) PCR was performed as previously except using the newly extracted DNA and the second set of primers for each target gene. DNA from W303α cells was used as a control. The PCR products were then electrophoresed on a 1% agarose gel to observe larger size bands for successful transformants compared to wild type DNA.
8) The PCR products were finally checked by digestion with a restriction enzyme that cuts either the target gene or *URA3* but not both. *BsaAI* cuts at *RPD3* but not *URA3* so was used to confirm *rpd3Δ* cells; *BstBI* cuts *URA3* but not *HDA1* so was used to confirm *hda1Δ* cells.

MFA2 transcription levels

Expression of the *MFA2* gene was analysed using both Northern blotting and real-time quantitative PCR (qPCR) techniques as described in Chapter 2.

Primers

For the detection of MFA2 mRNA in Northern blotting experiments:

M1: 5'-biotin-CTATCATCTTCATACAACAATAACTACCA-3', T_a = 60°C

M2: 5'-CTAATGATGAGAGAATTGGAATAAATTAGT-3', T_a = 60°C

For the detection of ACT1 mRNA in Northern blotting experiments:

A1: 5'-biotin-GCCGGTTTTGCCGGTGACG-3', T_a = 52°C

A2: 5'-CCGGCAGATTCCAAACCCAAAA-3', T_a = 52°C

For the detection of MFA2 mRNA in qPCR experiments:

M RT1: 5'-ACAACAATAACTACCAACCTTAAT-3'

M RT2: 5'-TTGTCTTTCTTTTCAGAGGATTTA-3'

For the detection of ACT1 mRNA in qPCR experiments:

A RT1: 5'-GTATGCTCTGCTAAGACTATCG-3'

A RT2: 5'-GCCAGCGGAGTTAGTACC-3'

3.3 Results

3.3.1 Construction of the *rpd3Δ* and *hda1Δ* strains

The target genes *RPD3* and *HDA1* were disrupted by the insertion of *URA3*. The successful disruptions, and thus creation of *rpd3Δ* and *hda1Δ* strains in a W303α isogenic background was confirmed by PCR and digestion with restriction enzymes *BsaAI* and *BstBI* (Figure 3.3). The restriction enzyme *BsaAI* cuts at a site present in the *RPD3* gene but not in *URA3*. Digestion therefore indicates the presence of the intact *RPD3* gene and hence no integration of the *URA3* gene (Figure 3.3B). Restriction enzyme *BstBI* cuts at a site within *URA3* but not *HDA1* hence digestion indicates the successful integration of *URA3* (Figure 3.3D). The single HDAC mutant strains *rpd3Δ* and *hda1Δ* could then be used in the *MFA2* transcription experiments

(and later repair studies) to examine the effect of deleting a single class I (*RPD3*) or class II (*HDA1*) histone deacetylase gene.

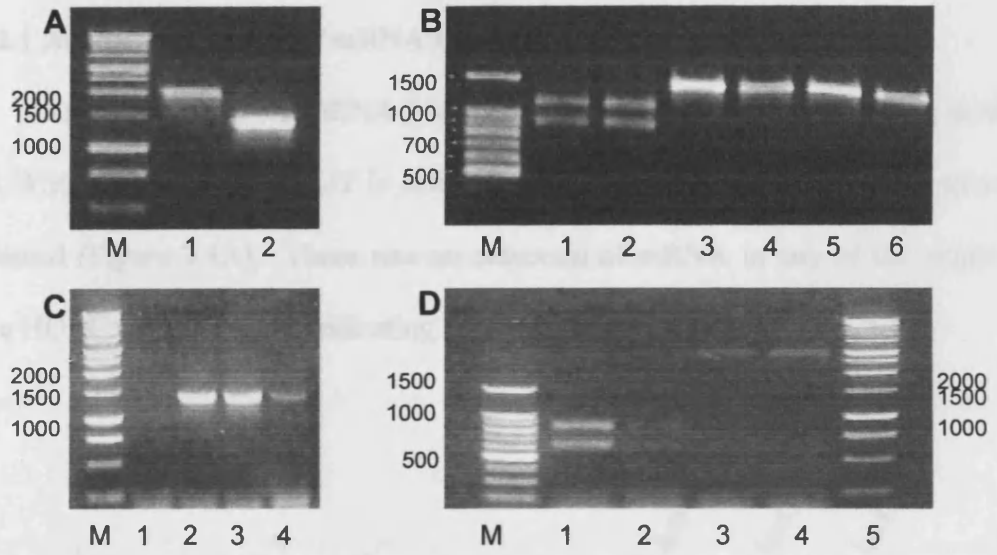

Figure 3.3 *Confirmation of rpd3Δ and hda1Δ strains.* Lanes marked M: DNA ladders, 100bp or 1kb as indicated. **A:** Lane 1: wild type PCR product of the *RPD3* gene of approx. 1900bp compared to the *rpd3Δ* PCR product of approx.1500bp in lane 2. **B:** Lanes 1 & 2: PCR products digested by *BsaAI* indicative of intact *RPD3*, lanes 3 to 6: no digestion, i.e. *RPD3* is disrupted. **C:** Lanes 2-4 show PCR products of approx. 1500bp, indicative of *HDA1* being replaced by the smaller *URA3* gene, PCR of wild type DNA (lane 1) unsuccessful, but would produce a band of over 2.5kb. **D:** Lanes 1&2: *BstBI* digestion of PCR product, i.e. the presence of *URA3*, lanes 3&4: no digestion, hence intact *HDA1*.

3.3.2 Effects of HDAC deletions upon *MFA2* transcription

MFA2 is actively transcribed by RNA polymerase II in mating type **a** cells but is repressed in mating type α cells. Northern blotting and real-time quantitative PCR (qPCR) techniques were used to detect mRNA levels to examine the transcription of *MFA2* in wild type (mating type **a** and α) cells and in histone deacetylase mutant strains *rpd3α, hda1α, rpd3hos1hos2α, rpd3hos1hda1α* and *hda1hos1hos2α* strains.

ACT1 mRNA levels were used as an internal control during each method as *ACT1* is transcribed in both **a** and α mating type cells.

3.3.2.1 Northern Analysis of mRNA Levels

As expected, *MFA2* mRNA levels were detected by Northern blotting in wild type W303**a** cells where *MFA2* is active but not in W303α cells where the gene is repressed (Figure 3.5A). There was no detection of mRNA in any of the single or triple HDAC mutant strains, indicating gene repression was maintained.

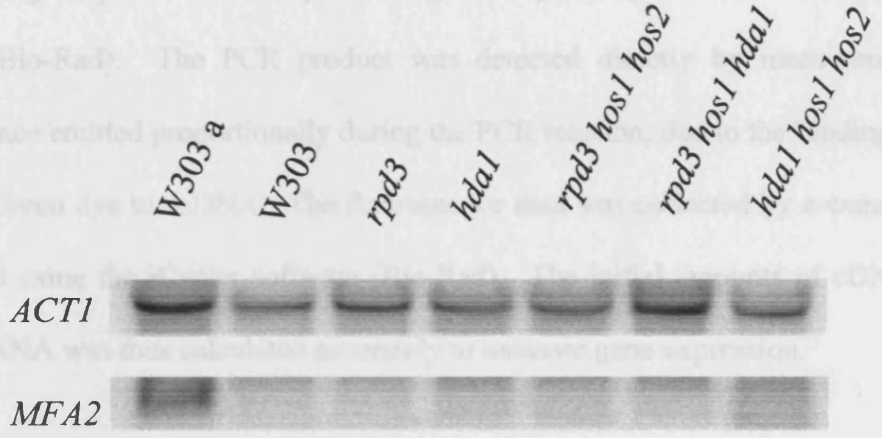

Figure 3.5 *Northern Analysis of ACT1 and MFA2 mRNA expression levels.* *ACT1* and *MFA2* mRNA levels were detected by Northern blotting in W303 **a** and α cells, rpd3α and hda1α single mutant strains and triple mutant strains *hos1hos2rpd3α*, *hda1hos1rpd3α* and *hda1hos1hos2α*. *ACT1* (top lane) was detected in all samples and used to normalise loading quantities. *MFA2* mRNA (bottom lane) was detected in W303 **a** cells only. No derepression was detectable for any of the HDAC mutations tested.

However, it has previously been reported that the *rpd3hos1hos2* strain does in fact cause four-fold derepression of *MFA2* in α cells and results in transcription levels similar to those observed in the mating type **a** cells carrying the same combination of mutations (Watson *et al.*, 2000). As a result of this confliction, a second method with

increased sensitivity in the detection of mRNA was employed, involving real-time quantitative PCR (qPCR).

3.3.2.2 qPCR Analysis of mRNA levels

The technique consisted of two stages: (1) a reverse transcriptase PCR (RT-PCR) reaction was performed using the TaqMan®Gold RT-PCR Kit (PE/Applied Biosystems) to create cDNA, using extracted mRNA as a template, and (2) the cDNA was prepared for PCR using the iQTM SYBR®Green Supermix (Bio-Rad) and was subsequently amplified and analysed using the iCycler iQ real-time PCR detection system (Bio-Rad). The PCR product was detected directly by measurement of fluorescence emitted proportionally during the PCR reaction, due to the binding of the SYBR®Green dye to dsDNA. The fluorescence data was collected by a camera and processed using the iCycler software (Bio-Rad). The initial amounts of cDNA and hence mRNA was thus calculated accurately to measure gene expression.

3.3.2.3 Quantification of qPCR data

The iCycler software (Bio-Rad) was used to quantify and analyse the data obtained during the real-time qPCR experiment described in section 2.11.3. Typical graphical images obtained are shown in Figure 3.6. A melt curve (Figure 3.6A) was viewed for each primer set to verify the production of a single PCR product. To quantify the PCR products, the threshold cycle (C_t) was first deduced by the software, which is an arbitrary number of PCR cycles in which all of the amplification graphs in the comparison are in the linear range. The C_t (indicated by the solid horizontal line in the graphs of Figures 3.6C and 3.6D) could also be manually selected if any adjustment was required. The C_t value is an exponent (2^{Ct}), hence a low C_t value

represents a high amount of transcript and a high C_t value indicates a low amount of transcript. A standard curve was also obtained (Figure 3.6B) to enable the initial quantities of mRNA in each sample to be calculated.

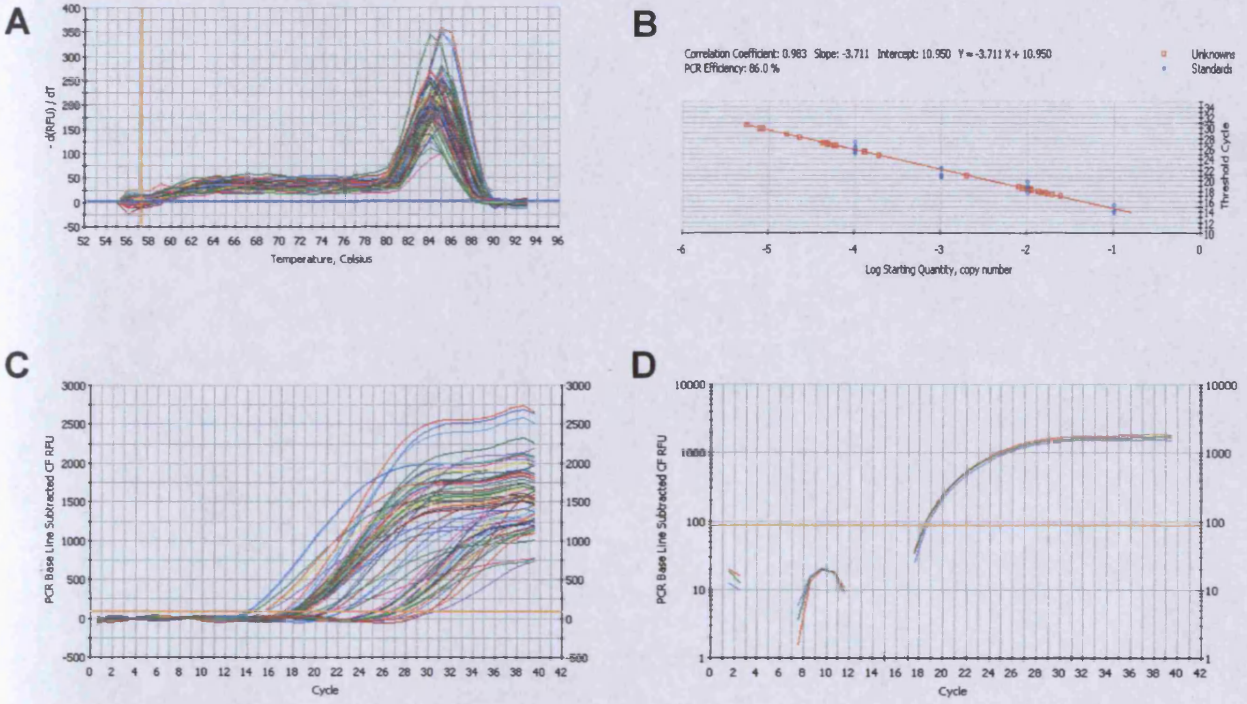

Figure 3.3 *Analysis of mRNA levels using qPCR.* Quantification data is generated using the iCycler software (Bio-Rad). A melt curve (A) is obtained for each sample run in the iCycler. The single peak verifies the formation of a single PCR product. A standard curve (B) enables initial mRNA quantities to be calculated from the resultant PCR products. A PCR quantification curve (C) is used to calculate the cycle threshold (Ct), a number of PCR cycles where each graph is in the linear range, depicted by the solid horizontal line through the graphs. The curves can be rearranged and selected individually, enabling each triplicate set to be viewed independently to assess the validity of each data set (D). The Ct value is again indicated by the horizontal line.

The iCycler software additionally generated the corresponding numerical data, from which values for (i) the quantity of initial mRNA, (ii) the mean quantities for each

triplicate data set and (iii) the standard deviations were extracted. Microsoft Excel was then utilized to generate comparative ratios of mRNA initially present in each sample (see Appendix II). The overall results are displayed graphically in Figure 3.7 and are supportive of the results obtained by Northern blotting as discussed above.

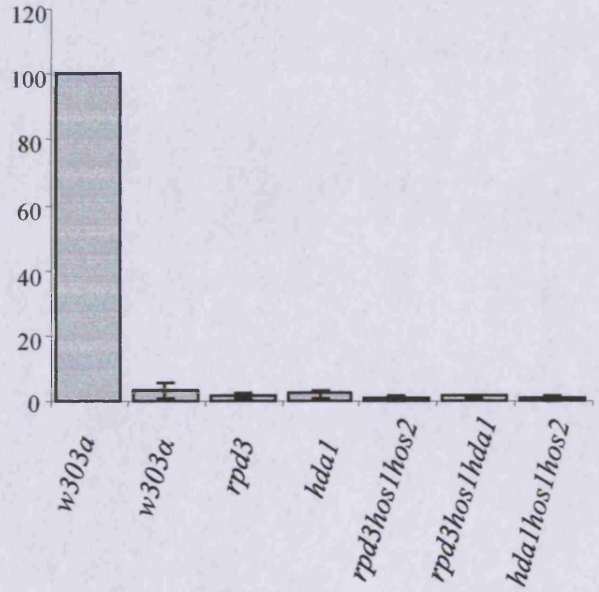

Figure 3.7 *Relative MFA2 mRNA expression levels from qPCR analysis.* *MFA2* mRNA levels detected by quantitative PCR, shown relative to expression in W303**a** cells, taken as 100%. Data are the average of triplicate samples of multiple independent experiments. None of the tested HDAC mutations appear to result in significant derepression of *MFA2*, supporting trends suggested by Northern analysis.

As with the Northern blotting, mRNA was detected in W303**a** cells and this was taken as 100% for comparison to the W303 and HDAC mutant α strains. No single or triple mutant strain showed any significant increase in mRNA levels compared to W303α. Thus two independent experimental techniques indicated that the deletion of one or more of the HDACs examined did not result in derepression of *MFA2*, conflicting with reports by Watson *et al.* (2000) where the *rpd3hos1hos2* deletion was reported to cause significant derepression. This particular mutation is

however clearly interesting and so was also investigated in terms of the effect upon DNA repair which, like transcription, is a DNA-mediated process in which chromatin plays a crucial role and so may likely be affected by deletion of one or more histone deacetylase genes. These results are presented Chapter 4.

3.4 Discussion

The activities of histone acetyltransferases (HATs) and histone deacetylases (HDACs) during transcriptional regulation and their involvement in modulating chromatin structure have been topics of major interest over recent years. HATs and HDACs are important cofactors for specific activator and repressor proteins (Brownell and Allis, 1996; Kadosh and Struhl, 1998) and it remains unclear as to how their opposing activities are precisely balanced to create specific chromatin structures at target promoters. At *MFA2*, repression is mediated by the Tup1-Ssn6 repressor complex which does not bind DNA directly but is recruited by the α2 DNA-binding factor (Komachi *et al.*, 1994; Wahi and Johnson, 1995). Previous studies have reported that full repression by Tup1-Ssn6 appears to require interactions with histone tails and components of the general transcription machinery (Watson *et al*, 2000). Tup1 interacts directly with the N-terminal tails of histones H3 and H4 and preferentially binds to underacetylated isoforms *in vitro* (Edmondson *et al.*, 1996). Combined mutations in the H3 and H4 tails have been shown to cause large derepression of Tup1-Ssn6 mediated repression *in vivo* (Edmondson *et al.*, 1996; Huang *et al.*, 1997). Thus increased acetylation may negatively influence repression *in vivo*, suggesting a possible role for HDACs in Tup1-mediated repression to help regulate acetylation levels (Watson *et al.*, 2000). Additionally, Tup1 has been shown

to interact directly with at least three of the HDACs: class I HDACs Rpd3 and Hos2 (Watson *et al.*, 2000) and class II HDAC Hda1 (Wu *et al.*, 2001b).

The involvement of multiple HDACs in transcriptional repression of *MFA2* was examined here using Northern hybridisation and real-time qPCR techniques, and the results are presented. When either *RPD3* or *HDA1* was disrupted, there was no detectable increase in mRNA levels observed with either the Northern blotting or qPCR method. This suggests that the alteration of acetylation pattern caused by deleting one HDAC alone does not cause sufficient acetylation levels to lead to the derepression of *MFA2*. It also supports previous reports that there is likely a degree of overlap between the functions of the different HDACs (Robyr *et al.*, 2002; Kurdistani *et al.*, 2002; Wang *et al.*, 2002). It was speculated that the combined deletions of HDAC genes may have a greater, summative effect and possibly result in acetylation levels and patterns to be altered so as to hyperacetylate histones H3 and H4 sufficiently to diminish Tup1 binding and result in derepression of *MFA2*. Previous studies by Edmondson *et al.* (1996) have shown that high levels of acetylation are needed to prevent Tup1 binding, and additionally, that histones H3 and H4 serve redundant functions in Tup1-Ssn6 mediated repression. Three combinations of different HDAC mutations were tested in the present study - *rpd3hos1hos2, rpd3hos1hda1* and *hda1hos1hos2*. In agreement with the previous study by Watson *et al.* (2000), the *rpd3hos1hda1* and *hda1hos1hos2* strains showed no significant increase in *MFA2* mRNA levels, indicating that any essential functions in gene expression control affected by the mutations can be compensated for by other activities or mechanisms in the cell. However, in contrast to the same study, the results here also detected no derepression of *MFA2* for the *rpd3hos1hos2* strain using either of the two methods. This may possibly be due to different treatments during

techniques used as Watson *et al.* used an S1 nuclease protection assay (as described by Iyer and Struhl, 1996) which was not performed in this study. Another possibility is that the strains used were constructed differently, possibly with non-identical isogenic backgrounds. The strains however, were originally from the same source, so this is unlikely, but they may not have been constructed simultaneously, or may have incurred contamination or mutation over time and use. Also, the wild type strain used for comparisons during this study, although isogenic, was not from the same source as the triple HDAC mutant strains.

Watson *et al.* (2000) detected a four-fold increase in *MFA2* mRNA levels in the *hos1hos2rpd3* α strain, comparable to levels detected in **a** cells carrying the same mutations. The same study also detected derepression in the same mutant strain at *SUC2*, another Tup1-Ssn6 regulated gene, when cells were grown under repressive conditions of high glucose levels. Additionally, an earlier study by the same group also observed loss of repression of an **a** cell specific reporter gene in the *hos1hos2rpd3* strain (Edmondson *et al.*, 1998). The *rpd3hos1hos2* mutation is clearly interesting and it has been shown that Rpd3 and Hos2 both interact with the Tup1-Ssn6 complex, although it is not yet clear whether this interaction occurs via Tup1, Ssn6 or both proteins (Watson *et al.*, 2000).

Considering the results of the present study and previous reports (Edmondson *et al.*, 1998; Watson *et al.*, 2000), it appears that other combinations of HDAC mutations do not have an effect on Tup1-Ssn6 mediated repression at *MFA2*, but it must be noted that not all combinations of HDAC mutations have been tested. Double mutant strains *rpd3hos1* and *rpd3hos2* have been shown to have no effect on repression of *MFA2* or *SUC2* (Watson *et al.*, 2000). It is therefore the specific simultaneous mutation of all three *RPD3, HOS1* and *HOS2* genes which may cause

the unique acetylation levels and patterns required to affect repression of *MFA2*. All three HDACs have been reported to play roles in deacetylation of ribosomal DNA and ribosomal protein (RP) genes (Robyr *et al.*, 2002; Kurdistani *et al.*, 2002) which may suggest functional relationships between them. It remains unclear as to exactly how these HDACs operate during repression at *MFA2*, but there is clearly evidence to support a model of repression by Tup1-Ssn6 involving the recruitment of HDACs.

While the aforementioned studies indicate the likely major roles of Rpd3, Hos2 and Hos1, other studies have identified Hda1 as the more likely major player acting with Tup1 (Wu, *et al.*, 2001; Robyr *et al.*, 2002) although a definite correlation between loss of transcriptional repression and loss of deacetylation by Hda1 has yet to be clearly established. A recent study employing genome-wide expression microarrays reported that Hda1 may primarily function with Tup1 to exert transcriptional repression but partially represses only about 30% of Tup1-repressed genes (Green and Johnson, 2004). The present study has identified no evidence of a major role for Hda1 in the repression of *MFA2* as strains where *HDA1* was deleted, either singly or in combination with other HDACs, showed no detectable increase in mRNA expression levels. Green and Johnson (2004) also reported that upon deletion of *HDA1*, many Tup1-repressed genes are hyperacetylated at H3 lysine 18, but not derepressed, suggesting that repression is not caused by deacetylation alone but rather by multiple, partially overlapping mechanisms. Recent studies have begun to identify and characterise specific and genome-wide roles and targets for HDACs but little is understood about the precise mechanisms and roles of HDACs during transcriptional repression. The importance of further investigation and usefulness of yeast as a model organism is highlighted by the existence of proteins homologous to Tup1 in other organisms, such as Groucho in *Drosophila,* which shares some

sequence similarity to Tup1 and also recruits Rpd3 to enable repression (Guoqing *et al.*, 1999). The mammalian TLE proteins, similar to both Tup1 and Groucho, also act as repressors and interact with histones and a mammalian homologue of yeast Ssn6 (Grbavec *et al.*, 1999). Hence, the conserved nature of Tup1-like proteins and their vital roles in transcriptional regulation is clear. The roles of HDACs are emerging as far more complex than originally anticipated and further advances in technologies such as expression microarrays and ChIP variations are currently working towards unravelling the intriguing web of activities in the cell governing the regulation of gene expression, both at specific promoters and genome-wide.

Chapter 4

The roles of histone deacetylases in nucleotide excision repair at the yeast *MFA2* gene

4.1 Introduction

Cells of living organisms are constantly exposed to solar UV radiation which induces damage in the DNA, the main forms of which are cyclobutane pyrimidines dimers (CPDs) and 6-4 photoproducts (6-4 PPs). Both are bulky, helix-distorting lesions and, if not removed from the genome, have implications in causing mutations which can ultimately lead to a predisposition to skin cancer in humans (Friedberg, 2001). Cells have therefore evolved an array of repair mechanisms to contend with such damage. Both CPDs and 6-4 PPs are repaired by the nucleotide excision repair (NER) pathway, a vital repair mechanism which has been highly conserved in eukaryotes from yeast to human cells. NER is a complex process and involves the interactions of over 30 proteins to repair naked DNA. These are recruited in a sequential and stepwise fashion (Guzder *et al.*, 1996b; Araujo and Wood, 1999; Friedberg, 2001; Friedberg *et al.*, 2005). Briefly, NER involves the recognition of helix-distorting DNA damage, dual incisions on the damaged strand either side of the lesion, followed by excision of the oligonucleotide containing the lesion. Gap repair synthesis then uses the opposite intact strand to synthesise new DNA which is finally ligated to complete the repair process and restore the original, undamaged chemical structure of the double helix. In humans, defective NER has been implicated in rare hereditary disorders such as xeroderma pigmentosum (XP), Cockayne syndrome (CS) and trichothiodystrophy (TTD), which characteristically cause severe symptoms including sensitivity to sunlight, neurological defects, premature ageing (CS and

TTD), and in the case of XP, a predisposition to skin cancer (de Boer and Hoeijmakers, 2000; Bootsma *et al.*, 2001; Friedberg, 2001; Mitchell *et al.*, 2003).

Within the genome, the rate of NER is heterogeneous in part due to two distinct subpathways of NER (Thoma, 1999; Balajee and Bohr, 2000). Transcription-coupled repair (TCR) preferentially repairs CPDs in the transcribed strand (TS) of actively transcribed genes at a faster rate than those found in the non-transcribed strand (NTS) of active genes and in either strand of inactive genes (Mellon *et al.*, 1987; Mellon and Hanawalt, 1989; Smerdon and Thoma, 1990). The transcriptionally inactive regions of the genome are repaired by global genomic repair (GGR) (de Laat *et al.*, 1999; Balajee and Bohr, 2000; Friedberg, 2001; Li and Smerdon, 2004).

A further complexity for NER in eukaryotes is the packaging of DNA into nucleosomes and higher order chromatin structures, limiting the access of the DNA to proteins such as NER proteins and transcription factors. During TCR, chromatin is 'opened up' to become more accessible apparently due to the passage of RNA pol II along the DNA (Friedberg, 2001), whereas during GGR, global relaxation of chromatin is required to enable the detection of lesions throughout the genome (Friedberg, 2001; Green and Almouzni, 2002; Rubbi and Milner, 2003). Thus NER is intimately linked to both transcription and chromatin structure. The heterogeneity of NER correlates not only with transcriptionally active and inactive regions but also with the functional division of chromatin within the genome into highly condensed heterochromatic regions where genes are inactive, and euchromatic chromatin which is more open and accessible, facilitating DNA-mediated processes (Thoma, 1999; Balajee and Bohr, 2000). The implication of a chromatin environment upon transcription has been well studied (Edmondson and Roth, 1996; Wade *et al.*, 1997; Kuo and Allis, 1998; Struhl, 1998; Workman and Kingston, 1998; Walia *et al.*, 1998;

Meijer and Smerdon, 1999; Pérez-Martin, 1999; Morales *et al.*, 2001; Horn and Peterson, 2002) but much less is known about chromatin-related events during NER.

DNA packaged into chromatin is repaired by NER less efficiently than naked DNA (Wang *et al.*, 1991; Sugasawa *et al.*, 1993). The precise mechanisms by which NER operates in chromatin are still unclear but links have been observed between nucleosome positioning and the accessibility of chromatin (Green and Almouzni, 2002; Ura and Hayes, 2002; Thoma, 2005). Slower NER has been observed in core nucleosomal DNA compared to NER of lesions in linker DNA regions between nucleosomes (Wellinger and Thoma, 1997; Tijsterman, *et al.*, 1999; Teng *et al.*, 2005; Thoma, 2005).

Chromatin reorganisation and the specific positioning of nucleosomes have been implicated in the regulation of gene expression. Nucleosomes have been mapped at precise positions in the control and coding regions of the yeast **a** cell-specific genes *STE6, BAR1* (Shimizu *et al.*, 1991) and *MFA2* (Teng *et al.*, 2001) in α cells where the genes are repressed, but this specific local chromatin structure is lost in mating type **a** cells where the gene is active. Chromatin reorganisation involves both ATP-dependent nucleosome remodelling activities such as the Swi/Snf family complexes, to physically reposition nucleosomes, and post-translational histone modifications such as acetylation of the N-terminal tails of the core histones, which alter the interactions between histones and DNA or other proteins (Widom, 1998; Workman and Kingston, 1998; Kingston and Narlikar, 1999; Wolffe and Hayes, 1999; Hassan *et al.*, 2001; Ura and Hayes, 2002; Mitra *et al.*, 2006; Saha *et al.*, 2006). Such activities are likely required to modulate nucleosome positioning or assembly during NER to facilitate access of repair proteins in a similar fashion to that observed in affording access of the transcription machinery during regulation of gene

expression. However, subtle differences must exist between the two processes as NER can still operate despite transcriptional repression, for example, at a cell-specific genes in yeast, such as *MFA2*, in mating type α cells (Yu *et al.*, 2005).

MFA2 transcription in yeast can be controlled by the simple selection of mating type, enabling NER to be studied in the presence or absence of transcription. Thus it offers an ideal model system to study the links between chromatin structure, transcription and repair (Teng *et al.*, 1997; 1998; 2000; 2002; Yu *et al.*, 2005). At *MFA2*, CPDs are repaired faster by NER on the TS of the active gene than the NTS and this enhanced repair begins before the transcription start site, likely due to changes in local chromatin structure during *MFA2* activation, making the DNA more accessible (Teng *et al.*, 1997). Four nucleosomes have been mapped at the control and coding regions of the repressed *MFA2* gene in α cells (Teng *et al.*, 2001). These are termed nucleosomes -1, -2, +1 and +2, in reference to their position relative to the start site of *MFA2* transcription. Nucleosome -2 is positioned in the control region, upstream of the α2 operator at approximate nucleotide positions -412 to -272. Nucleosome -1 is also in the coding region, between the Mcm1 binding site and the start of transcription at positions -207 to -62. Nucleosomes +1 and +2 are positioned in the transcribed region at positions -58 to +88, and +122 to +245, respectively (See Figure 4.1). This precise positioning of nucleosomes however is not seen in the active *MFA2* gene and thus may be disrupted during activation of the gene (Teng *et al.*, 2001).

The mechanisms of histone acetylation and deacetylation by histone acetyltransferases (HATs) and histone deacetylases (HDACs) respectively have been implicated in modulating chromatin structure and transcription regulation (Wade *et*

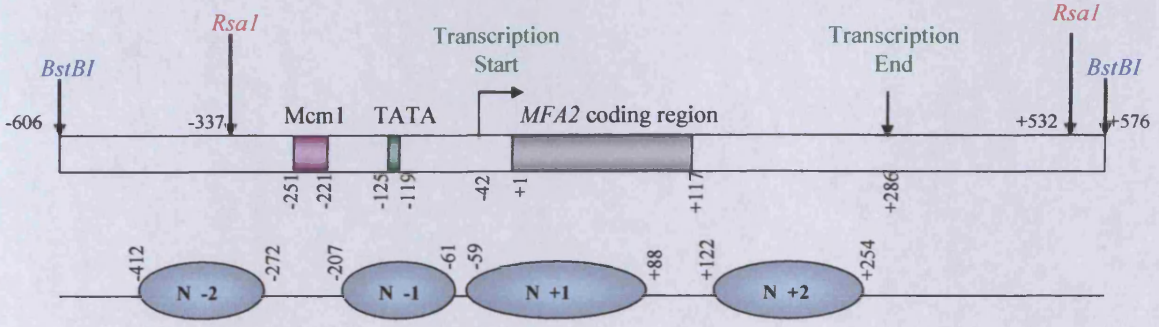

Figure 4.1. *Nucleosomes mapped at the MFA2 gene in mating type α cells.* The nucleotide positions of the TATA box, Mcm1 binding site and *MFA2* coding regions are indicated, denoted numerically taking the start point of the *MFA* coding region as +1. Also indicated are the start and end points of transcription and the restriction fragments *RsaI-RsaI* and *BstBI-BstBI*, which were both used during this study. The positions of the four mapped nucleosomes in the *MFA2* region are indicated and denoted N-2, N-1, N+1 and N+2. These are observed in mating type α cells only, where *MFA2* transcription is repressed, and not in **a** cells where *MFA2* is transcribed.

al., 1997; Kuo and Allis, 1998; Struhl, 1998; Workman and Kingston, 1998; Walia *et al.*, 1998; Meijer and Smerdon, 1999; Wu and Grunstein, 2000; Morales *et al.*, 2001; Horn and Peterson, 2002; Deckert and Struhl, 2002). At the specific *MFA2* locus, the role of the yeast HAT Gcn5 has previously been studied. Gcn5 acts as a catalytic subunit of the H3/H2B-specific nucleosomal HAT complexes ADA and SAGA (Grant *et al.*, 1997), and a third, more recently identified complex SLIK (Pray-Grant *et al.*, 2002). Gcn5p is required for optimal *MFA2* transcription; without it only 20% of the normal mRNA level is present in mating type **a** cells (Teng *et al.*, 2002). Yeast HDACs have also been implicated during transcriptional repression of **a** cell specific genes. Repression is mediated by the general repressor Tup1-Ssn6 complex. The precise mechanisms of repression remain unclear but it has been linked to interactions with the general transcriptional machinery (Guldener *et al.*, 1996; Redd *et al.*, 1997; Papamichos-Chronakis *et al.*, 2000; Zaman *et al.*, 2001), and linked to changes in

chromatin structure as certain Tup1-Ssn6 repressed genes are associated with highly positioned nucleosomes (Roth *et al.*, 1990; Cooper *et al.*, 1994; Li *et al.*, 2001; Fleming and Pennings, 2001; Teng *et al.*, 2001). Tup1 preferentially binds to underacetylated H3 and H4 histones *in vitro* (Edmondson *et al.*, 1996) and interacts directly with at least three HDACs (Watson *et al.*, 2000; Wu *et al.*, 2001b; Davie *et al.*, 2003), suggesting roles for HDACs in Tup1-Ssn6 mediated repression. A combination of mutations in the HDAC genes *RPD3*, *HOS1* and *HOS2* has been reported to completely abolish Tup1-Ssn6 mediated repression at the *MFA2* and *SUC2* genes (Watson *et al.*, 2000), although this effect was not observed at *MFA2* during the present study (Chapter 3).

The importance of histone acetylation and deacetylation during NER is less well understood but mechanisms of chromatin modulation in transcription may be similar during NER to regulate access to DNA by the effector proteins. Indeed, similar to the general effects of acetylation upon transcription, increased acetylation (due to HDAC inhibition) has been correlated with increased rates of NER (Smerdon *et al.*, 1982; Ramanathan and Smerdon, 1989). The effects of specific HATs and local implications at specific loci have also been studied. At *MFA2*, Gcn5 HAT activity is important for the efficient repair of UV-induced CPDs in both the transcriptionally active and repressed state, but appears to have little effect upon genome-wide global repair (Teng *et al.*, 2002; Yu *et al.*, 2005). This mirrors the effects of Gcn5 observed in transcription activation (Holstege *et al.*, 1998).

The roles of specific HDACs in NER however have been less well studied, although HDACs have been implicated in other repair pathways such as the requirement of the Sin3-Rpd3 complex and possible roles of Sir2 in the non-homologous end-joining (NHEJ) repair of DNA double-strand breaks (Lewis and

Resnick, 2000; Pray-Grant *et al.*, 2002; Fernandez-Capetillo and Nussenzweig, 2004; Jazayeri *et al.*, 2004; Kruszewski and Szumiel, 2005).

The experiments described in this chapter examined the effects of specific HDACs upon the repair of CPDs during NER, globally and at the *MFA2* gene. Firstly, the single and triple HDAC mutant strains used in Chapter 3 were all analysed to deduce their effects on UV-sensitivity as an indicator of possible roles in the general repair of UV-induced damage. Secondly, single mutant strains *rpd3Δ* and *hda1Δ,* and triple mutant strains *rpd3hos1hos2Δ* and *rpd3hos1hda1Δ* were studied to observe their effects upon global NER of CPDs and NER at the *MFA2* gene. Global NER was analysed using an Immuno Slot-Blot assay, and repair at *MFA2* was studied both at the level of the gene, using a Southern blotting method, and at nucleotide resolution using the 3' end-labelling technique previously developed in our laboratory (Teng *et al.*, 1997).

4.2 Materials and Methods

The UV irradiation of cells, DNA extractions, analysis of UV sensitivity, analysis of NER of CPDs in the overall genome, at the level of the gene and at nucleotide resolution, were all performed as described in Chapter 2.

Yeast Strains

The following *Saccharomyces cerevisiae* strains were grown in YPD medium (see Appendix I).

W303a *MATa ade2-1 trp1-1 can1-100 leu2-3 his3-11,15 ura3-5*

W303α *MATα ade2-1 trp1-1 can1-100 leu2-3 his3-11,15 ura3-5*

W303*Δrpd3* as W303α except *rpd3::URA3*

W303*Δhda1* as W303α except *hda1::URA3*

DY 6445 as W303α except *hos1::HIS3, hos2::TRP1 rpd3::LEU2*

DY 6446 as W303α except *hda1::URA3, hos1::HIS3, rpd3::LEU2*

Primers

The same primers were used for both the *BstBI-BstBI* fragment (-606 to +576) used in Southern blotting experiments and the *RsaI-RsaI* fragment (-337 to +532) used in 3' end labelling experiments. Both fragments contain the same *MFA2* gene regions but the *BstBI* fragment encompasses larger flanking regions thus giving a larger fragment to generate better signals during the Southern blotting experiments.

Primer 1a: 5'-biotin-gatagctttttACACCATCTACTACATAATTAATTGATAGTTTCCT-3'

(T_a=55°C)

Primer 2a: 5'-biotin-gatagctttttACGGACTTGATGCAGCTGAAAAACCATTATTTAAA-3'

(T_a=57°C)

Primer 1b: 5'-gatagcACACCATCTACTACATAATTAATTGATAGTTTCCT-3' (T_a=55°C)

Primer 2b: 5'-gatagcACGGACTTGATGCACGTGAAAAACCATTATTTAAA-3' (T_a=57°C)

4.3 Results

4.3.1 Analysis of UV sensitivity

The sensitivity of cells to UV radiation reflects the ability of cells to repair UV-induced DNA damage in the overall genome. UV sensitivity of the single HDAC

mutant strains *rpd3* and *hda1* and triple mutant strains *rpd3hos1hos2, rpd3hos1hda1* and *hda1hos1hos2* were examined, as UV sensitivity of a mutant strain can be indicative of a role of the gene(s) in DNA repair.

Briefly, yeast cells from each strain were exposed to increasing doses of UV radiation and then left to grow on YPD plates for three days, after which the resulting colonies were counted. The percentage of colonies surviving, compared to colonies on the untreated plates, taken as 100% survival, was calculated for each strain. Survival curves were plotted to compare the sensitivity of each strain relative to the wild type W303 strain and are shown in Figure 4.2. These data were compared to previous studies of the survival of PSY316 wildtype, *gcn5, rad2* and *rad16* strains at similar doses, used as benchmark data to determine the degree of UV sensitivity (data obtained from Y. Teng). Deletion of *RAD2* causes extreme UV sensitivity and is lethal at small doses of UV, 5-10J/m^2. Deletion of *GCN5* causes mild UV sensitivity and deletion of *RAD16* causes high UV sensitivity (Teng *et al.*, 2002). It should be noted that different sets of isogenic backgrounds were used, and the *gcn5, rad2* and *rad16* strains were not tested in the same study as the HDAC mutants, thus only general trends of the curves were considered.

The single mutant strains *rpd3* and *hda1* showed similar trends to each other. Up to doses of 80J/m^2 the percentage of colonies surviving was very similar to that observed in the wild type W303α strain, with approximately 65-70% survival at 20J/m^2, 25-30% at 40 J/m^2 and 3-5% at 80J/m^2. The triple mutant strains showed a more marked increase in sensitivity to UV. At 20J/m^2 and 40J/m^2, the triple mutant strains showed slight increases in sensitivity compared to the wild type cells, with approximately 50% and 20-30% survival respectively.

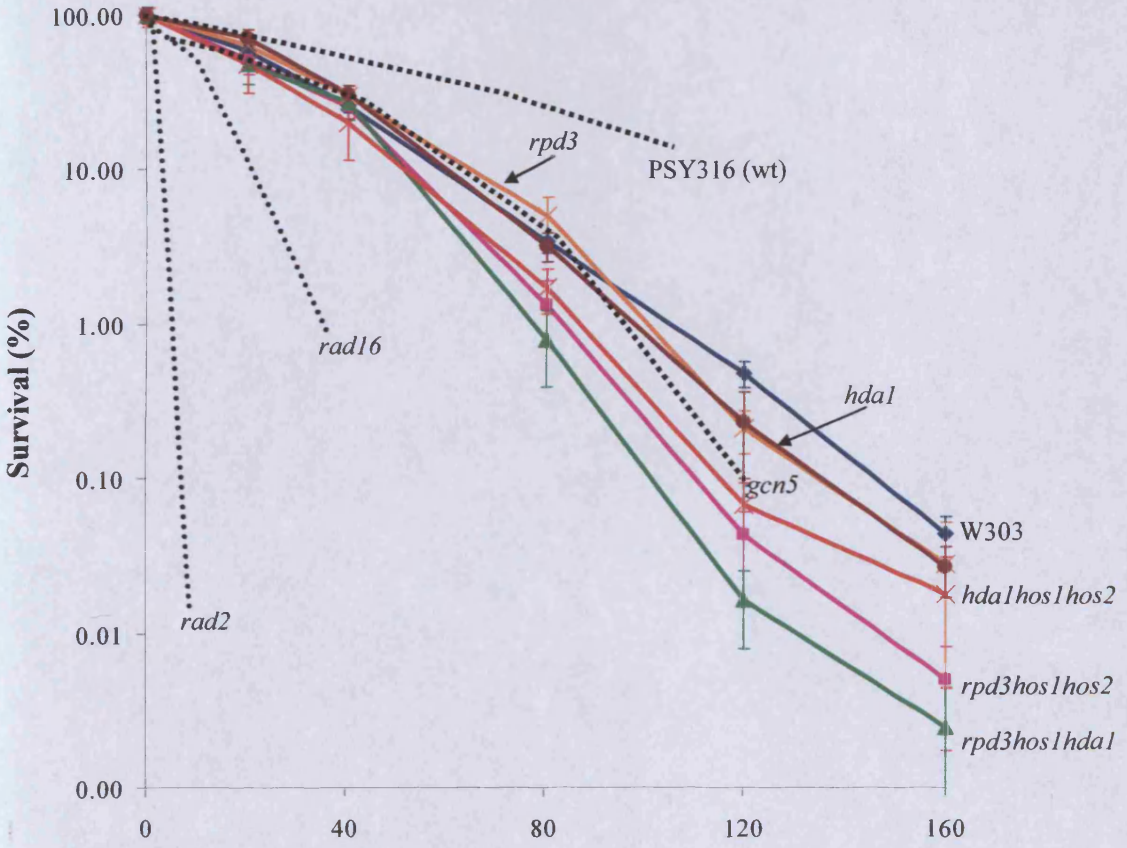

Figure 4.2 *Survival curves to measure sensitivity of strains to UV irradiation.* α cells of each strain were treated with doses of UV radiation ranging from 20 to 160 J/m^2. The percentage of colony survival represents the proportion of cells that survived irradiation and grew to form colonies over 3 days, taking wildtype survival at 0 J/m^2 as 100%. These data represent the averages of at least 3 independent experiments and standard deviations are depicted by error bars. The dotted curves represent superimposed data from a previous study (obtained from Y. Teng), showing survival of PSY316 wt, *gcn5*, *rad16* and *rad2* strains as a benchmark comparison. *rad2Δ* is lethal at very small UV doses, *rad16Δ* causes high UV sensitivity and *gcn5Δ* causes mild sensitivity.

At doses of 80J/m^2 and higher, however, the increased UV sensitivity of the three triple mutant strains was noticeably higher than the wild type and single mutant cells. The most sensitive strain was that carrying combined mutations in the *RPD3, HOS1* and *HDA1* genes with 0.8% and 0.07% colony survival at 80J/m^2 and 120J/m^2 respectively, compared to 3% and 0.5% survival of the wild type cells. The

rpd3hos1hos2 and *hda1hos1hos2* strains were slightly less sensitive to UV, but still markedly more sensitive than the wild type and single mutant strains.

These data suggest that the deletion of either the class I HDAC *RPD3* or class II *HDA1* gene has a very slight effect upon general repair of UV-induced lesions in the cell whereas combined mutations in three different HDAC genes has a greater effect rendering the cell less able to repair lesions efficiently and thus moderately sensitive to the detrimental effects of UV radiation. The triple mutant strains *rpd3hos1hos2* and *rpd3hos1hda1* were found to have the most profound effects on UV sensitivity and so were selected to further investigate the effects of these HDAC mutations upon the repair of CPDs by NER, both globally and at *MFA2*.

4.3.2 Global repair of CPDs in genomic DNA is enhanced by the deletion of multiple histone deacetylase genes

The removal of CPDs by NER was firstly examined in the overall genome, using an immunological slot-blot assay as described in Chapter 2. Briefly, cells were irradiated with UV to induce CPDs and sampled immediately and then after 1, 2, 3 and 4 hours allowed for repair. Care was taken to keep the cells in darkness at all times to prevent the repair of CPDs by photoreactivation, which occurs in minutes, from masking effects of NER, which occurs over hours. DNA was extracted and quantified using Molecular Analysis software (Bio-Rad) to equalise the samples for loading (Figure 4.3). Equal amounts from untreated cells and irradiated cells sampled at different repair times were blotted onto a membrane which was incubated with a CPD-specific monoclonal antibody and visualised with fluorescence.

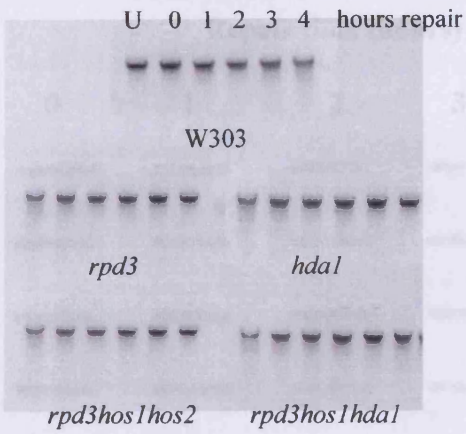

Figure 4.3 *DNA quantification.* Samples were quantified using Molecular Analysis software (Bio-Rad) and loading amounts adjusted accordingly to equalise loading of the samples for the CPD antibody assay.

A typical image obtained is shown in Figure 4.4A. The intensity of each band on the image correlates with the quantity of CPDs present in the overall genome of cells within that sample, i.e. the darker the band, the more CPDs are present. The decrease in intensity over time is therefore indicative of repair of CPDs, and was quantified using ImageQuant software (Molecular Dynamics, CA, USA), enabling the calculation of the percentage of CPDs repaired at each time point (Appendix AIII.2). The averages of at least four experiments were used and a quantitative graph produced, shown in Figure 4.4B. In the *hda1* single mutant strain, CPDs were removed from the overall genome at a rate similar to that of the wild type strain, taking about 1.6 hours to remove 50% of CPDs. The *rpd3* strain appeared to take slightly longer at about 2 hours, although a larger standard deviation for the *rpd3* data was observed. The triple mutant strains however showed a faster rate of NER, with the *rpd3hos1hda1* strain removing 50% of CPDs in about 1.2 hours and the *rpd3hos1hos2* strain even faster at just over 1 hour.

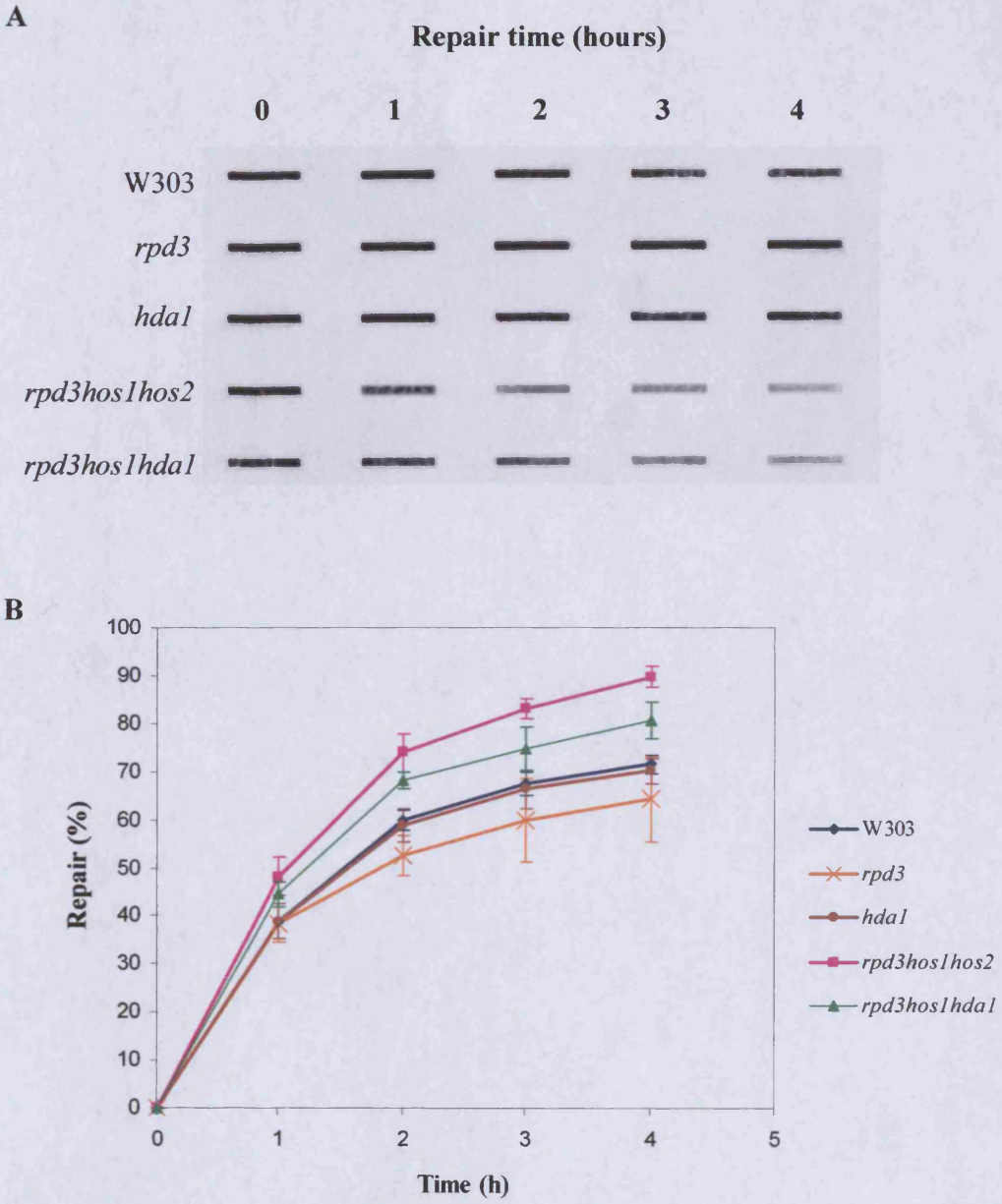

Figure 4.4 *The removal of CPDs by NER from the total genomic DNA.* (**A**) A typical gel image obtained from the immunological slot-blot assay showing the removal of CPDs from the genomic DNA following UV irradiation at a dose of 150J/m^2. Monoclonal CPD antibody was used as a probe to detect CPDs in the genome following CPD induction by UV irradiation and incubations of 0, 1, 2, 3 and 4 hours to enable DNA repair. The intensity of each band represents the quantity of CPDs present. (**B**) Quantitative graph using the average data from four gels. The standard deviation at each point is depicted by error bars

The gel images and graphical trends in Figure 4.2 clearly show that the faster NER in these strains continues over the 4 hour duration of the experiment. It therefore appears that the combinatorial effect of deleting multiple HDAC genes enhances the removal of CPDs by NER on a global level, and that the specific combinations of deacetylases have different effects, with the *rpd3hos1hos2* strain exhibiting the largest impact.

4.3.3 Multiple HDAC deletions result in an increased rate of repair at the *MFA2* gene

The repair of CPDs at the *MFA2* gene was next examined using a Southern blotting method originally devised by Bohr *et al.* (1985). Briefly, cells were exposed to UV to induce CPD formation in the DNA and sampled immediately and then after hourly repair times as previously described. The DNA was extracted and digested with the *BstBI* endonuclease (Figure 4.5). *BstBI* yields a fragment of 1182bp, cutting at nucleotide positions -606 and +576.

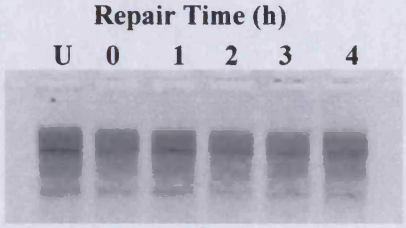

Figure 4.5 *BstBI restriction digestion.* A typical gel image obtained in checking the quality of restriction endonuclease digestion by *BstBI.* The smear for each sample rather than a sharp band indicates successful digestion.

Following *BstBI* digestion, DNA was cut with a CPD-specific endonuclease before being fractionated by electrophoresis and transferred to a membrane by Southern

blotting. A radioactive strand-specific probe was used to detect intact *MFA2* fragments which were then visualised using a phosphorimager. A typical image obtained is shown in Figure 4.6A.

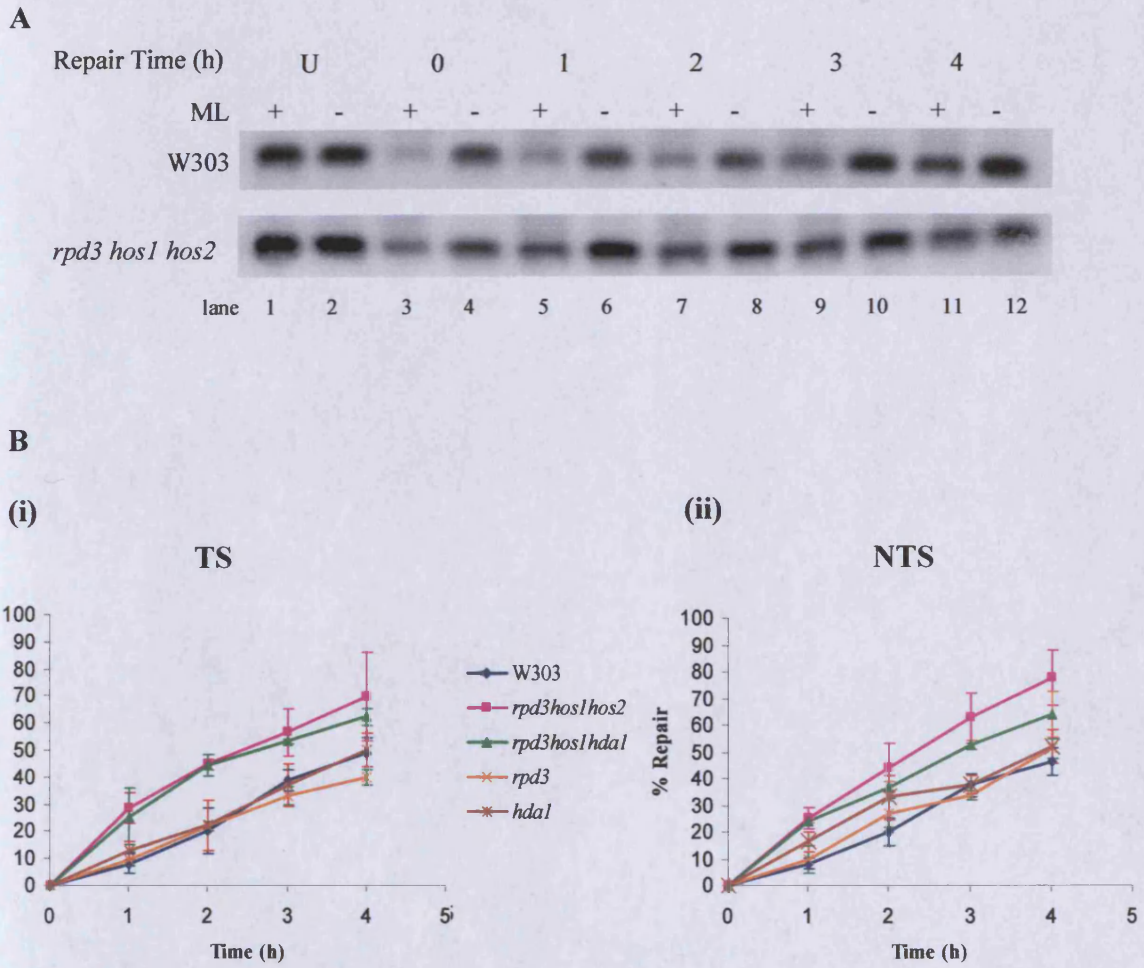

Figure 4.6 *Southern blotting detection of NER of CPDs at the MFA2 gene.* **A:** A typical image obtained, shown here for the wild type W303 and *rpd3hos1hos2* α strains only. Samples were collected either before UV treatment (U) or at designated repair times (0-4 hours as indicated above the bands). *ML*-treated samples (+) were cut at CPDs and were compared to uncut (-) controls. **B:** Graphical representation of repair over 4 hours. Data are the average of at least 3 experiments and standard deviations are depicted by error bars. The repair in the transcribed strand TS (i) and non-transcribed strand NTS (ii) of *MFA2* were analysed separately.

The intensity of the bands (Figure 4.6A) correlates with the amount of full-length, undamaged, *MFA2* fragments; hence darker bands are observed for non-irradiated samples (U) and control samples not cut with the CPD-specific endonuclease *ML* (-). In samples where CPDs are detected (+), the intensity of the bands reflects repair, with faint bands indicating the presence of many CPDs, few intact fragments and thus little repair; and increasingly darker bands indicating fewer CPDs and more intact fragments. Therefore, the increasing intensity of bands in lanes 3, 5, 7, 9 and 11 is indicative of repair.

The bands were quantified using ImageQuant software (Molecular Dynamics, CA, USA) and the ratio of band densities of the ML-treated to TE-treated samples was used to calculate the proportion of undamaged fragments at each repair time point (see Appendix III.3). This was plotted graphically (Figure 4.6B) and due to the strand specificity of the probes, repair of the transcribed strand (TS) and non-transcribed strand (NTS) of *MFA2* could be analysed individually. For repair of the TS (Figure 4.3B(i)), the *rpd3* and *hda1* single mutant strains showed similar rates of CPD repair as the wild type W303 strain over the four hours observed, repairing approximately 20% of CPDs in 2 hours and requiring 4 hours or more to repair 50% of CPDs. . The two triple mutant strains however, had a more marked effect on repair and appeared to repair CPDs at a significantly faster rate compared to the wild type and single mutant cells. The rates for both *rpd3hos1hos2* and *rpd3hos1hda1* were similar throughout the repair time, repairing 45% of CPDs at 2 hours, and repairing 50% of CPDs in approximately 2.5 hours. For the repair of the NTS, the *rpd3* strain showed similar repair to the wild type strain. *Hda1* cells showed slightly faster repair during the first three hours of repair compared to W303, having repaired 33% of CPDs compared to 20%, by 2 hours, but at later repair times, CPD repair was similar to wild type at

approximately 35% in 3 hours, and 50% in 4 hours. The two triple mutant strains again showed a greater effect on repair rates. The *rpd3hos1hos2* strain showed a slightly greater effect, with the repair of 50% of CPDs achieved by 2.5 hours, compared to just under 3 hours in the *rpd3hos1hda1* strain and approximately 4 hours in the single mutant and wild type strains.

Resembling the trends observed in the removal of CPDs from the overall genome, the deletion of either *RPD3* or *HDA1* does not appear to greatly affect the repair of CPDs at the *MFA2* gene but the combinatorial effects of deleting *RPD3, HOS1* and *HOS2*, or *RPD3, HOS1 and HDA1* results in an increased rate of repair, and the former mutation showing a slightly greater effect on repair of the NTS.

4.3.4 HDACs in repair of CPDs at nucleotide resolution

A direct 3' end-labelling method has previously been developed in our lab to compare the repair of CPDs at individual bases (Teng *et al.*, 1997; 2002; 2005). This technique was employed to study the effects of the *rpd3*, *hda1*, *rpd3hos1hos2* and *rpd3hos1hda1* strains compared to wild type cells upon the repair of CPDs at nucleotide resolution at the *MFA2* gene.

Briefly, cells were irradiated with UV and allowed 0-4 hours for repair, before extracting DNA. The DNA was then restricted with *RsaI* endonuclease to obtain the fragment of interest containing the coding and control regions of *MFA2* A CPD-specific endonuclease (ML) was then used to incise the fragment at the sites of CPDs. Specific 5' biotinylated probes with overhang modifications were created and used to enrich for the fragments of varying lengths cut at CPDs, isolated using Dynabeads and a magnetic particle concentrator (MPC). The overhang in the probe was used as a template to incorporate radioactivity to the 3' end of the fragments, which were

subsequently eluted and loaded onto a denaturing sequencing gel. The gel was then scanned using a Storm phosphorimager and typical images obtained are given in Figure 4.7.

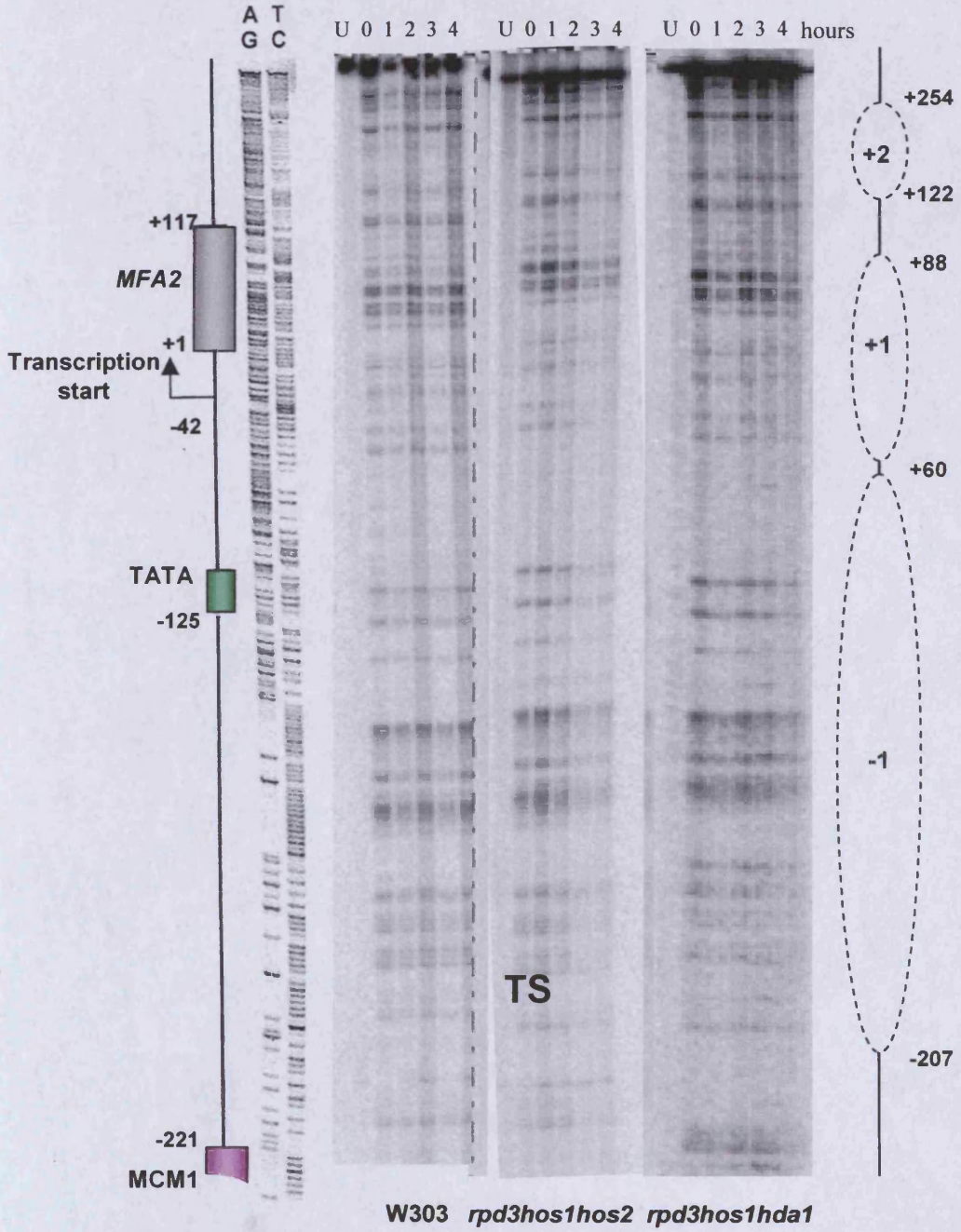

Figure 4.7 (A)

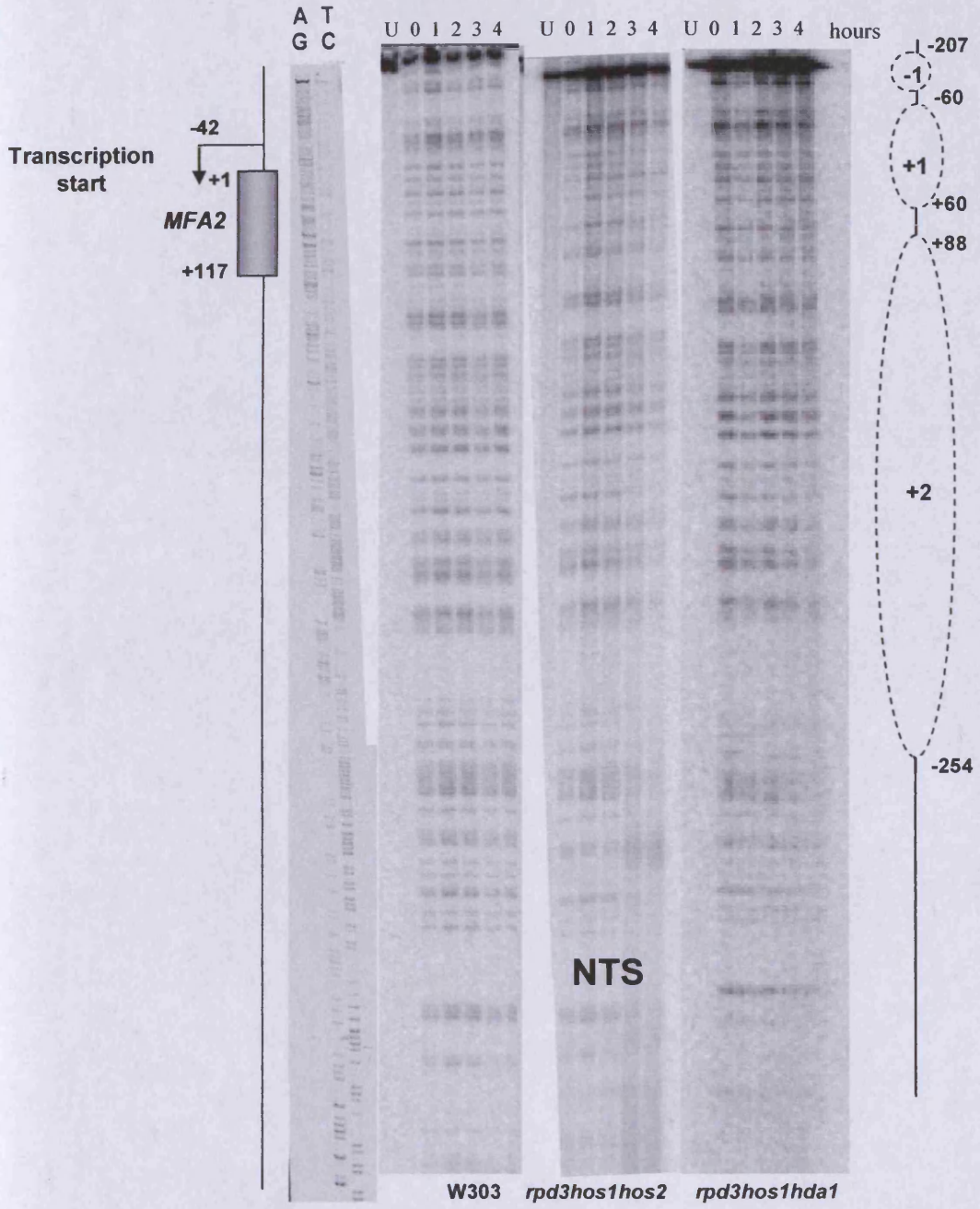

Figure 4.7 (B)

Figure 4.7 *Typical images of CPD repair at nucleotide resolution for the RsaI fragment in wild type and HDAC triple mutant strains.* (**A**) shows data for the TS of the *RsaI* fragment, (B) shows data for the NTS of the same fragment. The top of each lane is labelled with the repair time allowed following UV treatment at a dose of 150J/m^2. Lanes marked U represent the untreated control samples. Lanes AG and TC are the DNA sequence ladder for *MFA2*. Bands down the gels indicate the positions of single CPDs. The nucleotide positions of *MFA2* and its upstream regions are indicated on the left and the approximate nucleosome positions on the right. Numbering takes the start of the *MFA2* coding region as +1.

The approximate positions of mapped nucleosomes at *MFA2* (Teng *et al.*, 2001) are also indicated alongside the gels in Figure 4.7, enabling chromatin implications to be considered in the repair of CPDs at specific positions, as NER at *MFA2* is modulated by local chromatin structure (Teng *et al.*, 2005). The top band of each gel represents intact restriction fragments containing no CPDs, and the remaining bands down the gel in each lane represent CPDs at specific nucleotide positions, referenced by the adjacent DNA sequence ladder. Each lane represents a sample from cells not treated with UV (U) and cells allowed 0, 1, 2, 3 and 4 hours for repair post UV, as indicated at the top of each gel. The untreated samples contain no CPDs hence no bands down the gel. The intensity of each band reflects the quantity of lesions at that position, thus a decrease in intensity over time is indicative of repair, and the signals were quantified using ImageQuant software (Molecular Dynamics, CA, USA). Uneven loading in the lanes was accounted for where necessary in the calculations.

At each lesion site, damage was calculated by dividing the proportion of signal at that point by the total signal for the lane as a whole. The time taken to remove 50% of CPDs ($T_{50\%}$) was calculated at each site and plotted graphically (Figure 4.8). Where bands were in close proximity on the gel in clusters and showed similar repair effects, they were sometimes quantified as groups of bands rather than individuals. For ease of comparison, both the TS and NTS data are shown on the same graph. The closer to the mid-line a given point is, the faster the repair of that particular single CPD or CPD cluster. The data show the results of at least two independent gels but error bars are not shown in order to avoid cluttering the graph. Standard deviations at each point are given in Appendix III.4.

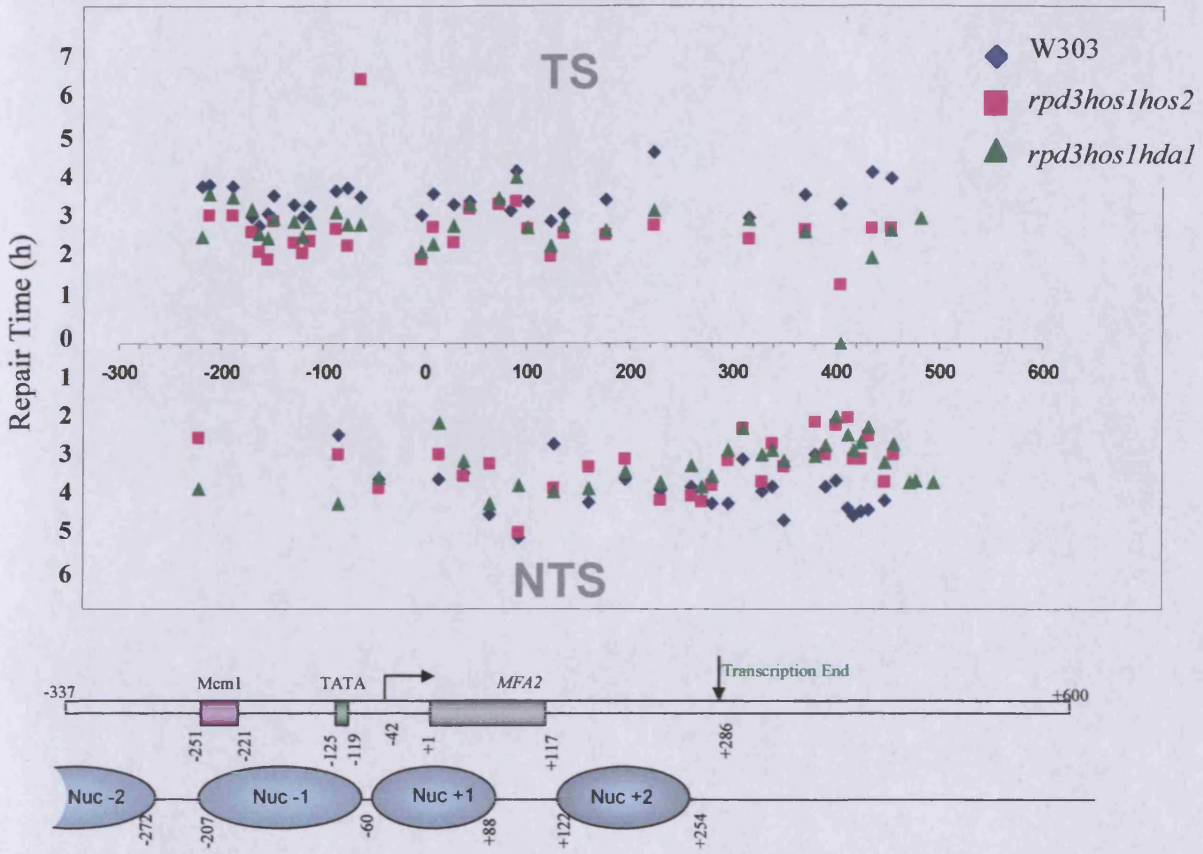

Figure 4.8 *Typical images of CPD repair at nucleotide resolution for single or clusters of CPDs.* Each graphical point represents the time taken to repair 50% of the initial CPDs ($T_{50\%}$) at each lesion site detected. This was calculated or extrapolated from ImageQuant data using Excel software. The averages of at least two independent experiments were used. Standard deviations were calculated but are not displayed to avoid cluttering the graph. Both the data sets for the TS (upper half of graph) and NTS (lower half) are displayed, with the points closest to the mid line indicating the fastest repair rates. For reference, the *MFA2* gene and upstream regulatory region, and approximate nucleotide positions at *MFA2* are indicated below the graph, numerically referenced taking the start of the *MFA2* coding region as +1.

The overall general trends of the data sets resemble those observed by Southern blotting: the *rpd3hos1hos2* and *rpd3hos1hda1* mutant strains show faster repair of CPDs than wild type cells at the majority of sites analysed, particularly evident in the data for the TS, and the NTS data for the region of nucleotide positions

+300 to +450. At nucleotide position -213 on the TS, close to the Mcm1 binding site, all strains showed relatively slower repair, possibly due to Mcm1 and α2 proteins binding. The wild type strain repaired 50% of CPDs ($T_{50\%}$) in 4.4±0.4 hours and both mutant strains showed faster repair with *rpd3hos1hda1* cells taking 4.2±0.6 hours and *rpd3hos1hos2* cells showing the fastest repair at 3.6±0.6 hours. There was insufficient data for this region of the NTS to make repair comparisons. For the TS region -207 to +59 where nucleosome -1 is positioned, all three strains show a similar pattern of faster repair than at the Mcm1 binding site. Slower repair was observed at the nucleotide position -150, fairly central in the nucleosomal region, where the $T_{50\%}$ for wild type cells was 4.1±0.5 hours, *rpd3hos1hos2* was 2.4±0.8 hours and *rpd3hos1hda1* was 3.5±1.0 hours. Faster repair was seen at positions either side of this in all three strains, with $T_{50\%}$ values of 3.6±0.6 hours, 2.4±0.8 hours and 3.0±0.3 hours for W303, *rpd3hos1hos2* and *rpd3hos1hda1*, respectively, at position -156; and $T_{50\%}$ values of 3.9±0.7 hours, 2.8±0.8 hours and 3.4±0.6 hours at nucleotide position -130. At positions -122 to -77, which are closer to the nucleosome edge and coincide with the TATA box region (-125 to -119), repair remained at a similar rate in each strain with *rpd3hos1hos2* cells showing the fastest rate of repair at each site. At the TS positions -65 to +88, relating to the position of nucleosome +1, there were no clear trends of repair rates observed with respect to chromatin structure, i.e. faster repair towards the edges or in linker DNA, but again both mutants showed faster repair than wild type cells. For repair within nucleosome +2 in the *MFA2* coding region, position +122 to +254, faster repair was observed at position +122 in all strains, with $T_{50\%}$ values of 3.4±1.0 hours, 2.4±0.9 hours and 2.7±0.7 hours for wild type, *rpd3hos1hos2* and *rpd3hos1hda1*, respectively, compared to positions closer to the centre of the nucleosome such as at +177 and +224. For TS positions +316 to +481, limited data

was obtained to identify any clear effects, but the trend of faster repair in the HDAC mutants appeared to continue.

For repair on the NTS, at many positions repair of 50% of CPDs apparently took longer than 4 hours so $T_{50\%}$ values were determined by extrapolation of repair curves. There was limited data for the control region due to the bands obtained with the *RsaI* restriction fragment. Again at most positions, the HDAC mutant strains appeared to repair CPDs faster than the wild type strain. In terms of chromatin effects, at the positions of nucleosomes +1 and +2, the repair rates actually appeared to increase towards the centre but due to the inconsistent quality of gels and lack of data at positions +270 to +230, +126, +63, -45 and -122 for the wild type cells, valid repair effects could not be identified. From nucleotide position +296 where *MFA2* transcription terminates to +432, the HDAC mutant strains show faster repair than the wild type, which took longer than the 4 hour duration to repair 50% of CPDs at most sites in this region. At most sites, the two HDAC mutant strains appeared to show similar $T_{50\%}$ values, but the standard deviations were large at many positions within the region, for example at position +412, the $T_{50\%}$ for *rpd3hos1hos2* was 3.2±1.2 hours and the $T_{50\%}$ for *rpd3hos1hda1* was 3.0±1.8 hours, so it was difficult to accurately compare the strains.

Due to inconsistent gel quality overall, incomplete data in parts and large variations in results between experiments for some regions, the 3' end-labelling results were not used to form confident observations of repair effects at specific nucleotide positions. Due to time constraints of this study, further modifications to enhance experimental technique and improve the quality of the gels and quantification could not be completed. However, overall trends of faster repair of CPDs in the

HDAC mutant strains compared to wild type were apparent at the majority of sites analysed.

4.4 Discussion

The packaging of eukaryotic DNA into chromatin poses a multitude of complexities for DNA-mediated processes including transcription and DNA repair. Cells have evolved an array of mechanisms to enable these processes to occur, involving the modulation of chromatin such that target DNA sequences can be accessed by effector proteins when required. Chromatin structure can be altered by ATP-dependent remodelling activities, such as Swi/Snf proteins, which can move or reposition nucleosomes, and also by post-translational modifications of the core histone tails which alter the interactions of histones with other proteins and DNA, thus affecting the properties of the nucleosome and the resultant chromatin structure. Acetylation of the N-terminal tails of core histones is widely accepted as a conserved mechanism for regulating chromatin functional states. The key roles of histone acetyltransferase (HAT) enzymes in gene activation have been well documented. There is also an increasing level of understanding of the roles played by histone deacetylases (HDACs), which reverse the acetylation reaction, generally in gene repression and silencing. HATs and HDACs serve to create a steady state of acetylation in the cell which can be altered by the increase or decrease of these activities to regulate transcription of genes, both globally and at specific loci.

Less is understood about the roles of HATs in DNA repair, and even less about the roles of HDACs. A previous study by Teng *et al.* (2002) identified a role for the HAT Gcn5 in two repair pathways, photoreactivation (PR) and NER; both

were reduced at the transcriptionally active *MFA2* in the regulatory region and in the transcribed and non-transcribed strands of the gene. However, no detectable effect was observed for repair in the genome overall, thus an effect of the absence of Gcn5 on the transcription of NER genes and a concomitant reduction in NER overall did not occur. These data were substantiated for the repressed *MFA2* where repair is also reduced in the *gcn5* deletion mutant, and this correlated with a marked reduction in UV-induced histone acetylation at both the nucleosomes in the *MFA2* control region, but not in the genome overall (Yu *et al* 2005). The results presented in this Chapter help address the roles of yeast HDACs in nucleotide excision repair (NER), both globally and at the specific *MFA2* locus, using a similar systematic approach to Teng *et al.*, 2002. Repair rates of NER in the wild type strain were compared to those for *rpd3* and *hda1* single mutant strains, and *rpd3hos1hos2* and *rpd3hos1hda1* triple mutant strains. Repair was studied by exploring the removal of CPDs from the genome overall and at the *MFA2* gene. Differences in repair outcomes may reflect variations in the chromatin environment of the region(s) being repaired, and also the functionality of the repair machinery in each strain. A literature search did not find any evidence of any of the NER genes being up-regulated in response to the HDAC single or triple mutations used.

Global Repair

The UV survival experiments demonstrated that the deletion of either the class I HDAC *RPD3* or class II HDAC *HDA1* alone has little effect on the sensitivity of cells to UV irradiation at a dose of $150J/m^2$ as the survival curves were similar to that of wild type cells. The three triple mutants tested however did show an increase in sensitivity to UV compared to the isogenic wild type strain. This is suggestive of a

degree of redundancy between different HDACS in the cell, supported by recent microarray studies exploring genome-wide transcription effects of HDAC deletions (Bernstein *et al.*, 2000; Robyr *et al.*, 2002) and studies relating to effects of HDACs upon transcription at specific loci (Watson *et al.*, 2000; Davie *et al.*, 2003). The sensitivity was mild to moderate in each HDAC triple mutant strain, with the *rpd3hos1hos2* and *rpd3hos1hda1* strains showing slightly greater effects. An increase in UV sensitivity is indicative of possible roles of the mutated genes in pathways in the cell that are responsible for the repair of UV-induced damage. Photoreactivation and NER are the two pathways responsible for the removal of UV-induced lesions 6-4 photoproducts and CPDs. By performing survival experiments in dark conditions, photoreactivation was avoided as the photolyase enzyme requires light for the direct reversal of UV-induced damage (Sancar, 1990, 2000; Schleider *et al.*, 2005; Friedberg *et al.*, 2005). Thus changes in UV sensitivity in this study may reflect possible involvement in the NER pathway, although equally it could involve other pathways, such as recombination, lesion bypass, cell cycle arrest etc.

NER genes can be grouped into two categories, those that are essential for NER throughout the genome, including *RAD1, RAD2, RAD3, RAD4, RAD10, RAD14, SSL1, SSL2, TFB1, TFB2* and *TFB3*; and those that are not absolutely required for NER, including *RAD7, RAD16* and *RAD23*. Mutants defective in an essential gene exhibit hypersensitivity to UV whereas those defective in non-essential NER genes exhibit moderate to high sensitivity. In comparison to both *rad2* and *rad16* mutant cells, the combinations of gene disruptions in the HDAC triple mutants tested did not confer a high sensitivity to UV but did confer a slightly higher sensitivity than a *gcn5* mutant which affects NER at the *MFA2* locus but shows little effect on overall genomic repair (Teng et al., *2002*).

In order to study the specific removal of CPDs by NER from the overall genome following UV irradiation, an immuno slot-blot assay was used. The single HDAC mutations in *RPD3* and *HDA1* alone were found to have little change in global CPD removal but interestingly, when mutations of three different HDAC genes are combined, repair is affected, and is actually significantly faster than in the isogenic wild type cells; a surprising but consistent and intriguing result. The *rpd3hos1hos2* mutant showed the most striking increase, but the *rpd3hos1hda1* mutant also showed an increased rate of repair. Disruption of multiple HDACs therefore actually improves the ability of the cells to repair such damage, but it is likely that other processes may be detrimentally affected, for example transcriptional regulation of many genes appears to involve targeted recruitment of HDACs, and some genes are known to be targets for more than one HDAC, such as *ENA1* which is deacetylated by Rpd3 in its coding region and by Hda1 in its promoter region (Wu *et al.*, 2001b). Thus by deleting multiple HDACs, transcriptional regulation may be more severely affected at certain genes but not NER genes. Literature searches did not find evidence of NER genes being up- or down-regulated as a result of the HDAC mutations, so any global effects on the repair of CPDs were likely reflective of effects upon the NER pathway. Although there is some redundancy between the functions of HDACs, genome-wide microarray studies have revealed that they each exhibit a preference in targets for particular pathways or processes in the cell: Rpd3 appears to play distinct roles in cell cycle progression, Hda1 in carbohydrate transport and utilisation, Hos1 and Hos3 preferentially deacetylate ribosomal DNA, and Hos2 affects ribosomal protein (RP) genes (Bernstein *et al.*, 2000; Robyr *et al.*, 2002; Robert *et al.*, 2004). Thus multiple HDAC deletions may have a more profound effect on the cell

following UV as more cellular processes may be impaired, reducing the ability to recover.

An increased rate of global repair in the triple HDAC mutants appears to contrast the trends observed for cell survival following UV irradiation and raised questions of how cells may exhibit enhanced repair and yet also demonstrate an increased sensitivity to UV. Firstly, an increased rate of repair does not necessarily lead to increased survival rates as other essential processes in the cell such as replication, transcription and cell cycle progression may also be affected in response to the damage incurred. UV sensitivity measured by cell survival is therefore used as a suggestive guide only to possible or likely roles in repair for the mutated gene(s). Secondly, although the rate of repair is increased in the mutant strains, this repair may not necessarily be accurate and may lead to mutation and cell death at a later time point following UV. UV sensitivity merely measures the survival of cells and not the level of mutation that may be incurred as a result of UV-induced damage. It would be interesting to determine the mutation frequencies of the HDAC strains in coordination with survival rates following UV. Thirdly, the HDAC mutations may affect the regulation of genes involved in vital cellular processes, which may affect the viability of cells due to secondary effects following UV. For example the length and type of cell cycle arrests that operate. It would certainly be worth introducing mutations for various events related to cell survival with these HDAC mutants exhibiting UV sensitivity to determine if any of these events are influenced by such changes.

NER at MFA2

The Southern blotting experiments indicate that the triple HDAC mutant strains also exhibit a faster rate of repair at the *MFA2* gene compared to wild type and

single mutant strains *rpd3* and *hda1*. No major differences were observed between the transcribed strand (TS) and non-transcribed strand (NTS) of the gene, but this is to be expected as *MFA2* is repressed in mating type α cells so would not show preferential repair of the TS as detected in mating type **a** cells (Teng *et al.*, 1997; Teng and Waters, 2000).

MFA2 is regulated by the Tup1-Ssn6 global repressor complex (Patterton and Simpson, 1994) which is recruited by DNA-binding factors (Komachi *et al.*, 1994; Smith *et al.*, 1995). The precise mechanism of Tup1-Ssn6 mediated repression remains unclear but appears to involve both interactions with the general transcription machinery (Guldener *et al.*, 1996; Redd *et al.*, 1997; Papamichos-Chronakis *et al.*, 2000; Zaman *et al.*, 2001) and changes in chromatin structure as certain genes, including *MFA2*, are associated with highly positioned nucleosomes when repressed by the complex (Roth *et al.*, 1990; Cooper *et al.*, 1994; Li *et al.*, 2001; Fleming and Pennings, 2001; Teng *et al.*, 2001). Tup1 interacts with the N-terminal tails of histones H3 and H4 (Edmondson *et al.*, 1996), which contain residues that are deacetylated by HDACs Rpd3 and Hda1 respectively. Tup1-Ssn6 has also been shown to interact directly with HDACs Rpd3, Hos2 and Hda1 (Watson *et al.*, 2000; Wu *et al.*, 2001b; Davie *et al.*, 2003), suggesting likely involvement of these enzymes in repression by deacetylation of the histone tails thereby altering the local chromatin structure. I have postulated that similar roles may be involved in the mechanisms facilitating NER.

The observation that single mutations in *RPD3* or *HDA1* alone did not cause a large difference in repair at *MFA2* suggests that either the roles of the HDACs show a degree of redundancy, or that Hos2 has a more prominent role. Also, the *rpd3hos1hos2* mutant showed a slightly faster rate of repair in the NTS than the

rpd3hos1hda1 mutant. It has also been reported that Rpd3 and Hos2 may interact with the Tup1-Ssn6 complex simultaneously during repression (Davie *et al.*, 2003) and so may possibly work together during repair. Clearly, examining the effect upon repair of solely deleting *HOS2* and deleting both *HOS2* and *RPD3* is an important further step to be taken; this was not assessed here due to time constraints of the study. The similarity between the rates of the triple mutants in the TS however may suggest that the combined deletions of *RPD3* and *HOS1* are important, perhaps creating a specific acetylation pattern to alter interactions of histone proteins that sufficiently alters local chromatin structure at *MFA2*, affording better access of repair proteins to the target DNA containing CPDs. Hos1 may weakly interact with Tup1-Ssn6 (Davie *et al.*, 2003) but interaction of Rpd3 and Hos2 is far stronger (Watson *et al.*, 2000), suggesting Hos1 is unlikely to play a major role alone in repression of *MFA2*, and examining the *HOS1* single mutant would shed light on a possible role in repair.

Interestingly, the *rpd3hos1hos2* strain, which caused faster repair both globally and at *MFA2* compared to wild type cells, has been reported to cause 4-fold derepression of *MFA2* transcription (Watson, *et al.*, 2000). This observation may further support the notion that the triple mutation results in the alteration of local chromatin in such a fashion to increase accessibility of the nucleosomal target DNA. However, this effect on transcription was not observed in this study (Chapter 3).

Although Hda1 also interacts with the corepressor complex, its role in repression of some Tup1-Ssn6 regulated genes, including *MFA2,* appears to be of lesser magnitude than the class I HDACs Rpd3, Hos1 and Hos2 (Edmondson *et al.*, 1998; Watson *et al.*, 2000; Davie *et al.*, 2003). Major effects on repair were not observed for the *hda1* strain for global or local repair at *MFA2*, and the triple mutation

rpd3hos1hda1 produced a slightly lesser effect on global repair than *rpd3hos1hos2*, further supporting the hypothesis that class I HDACs play a more prominent role.

The higher resolution 3' end-labelling experiments demonstrated similar trends as observed by Southern analysis in that the two triple mutants exhibited faster rates of removal of CPDs from the *MFA2* region by NER, in both strands. The technique is useful for analysing NER at specific sites of CPD formation and for comparing different regions, such as the promoter and coding regions of the gene and has previously been employed to investigate repair effects at *MFA2*, including the Rad26-dependent preferential repair of the TS in *RADa* cells which begins near the start of the transcribed region and slows down again when transcription ceases (Teng *et al.*, 1997; 2002; 2005; Teng and Waters, 2002)). However, in this study, the quality of the individual gels was inconsistent and further experiments resulting in confident, reproducible trends are needed in order to make valid observations on the effects of the HDAC mutations on the repair of specific regions or sites within *MFA2*.

Possible roles for HDACs in NER

The results presented in this chapter indicate roles for HDACs in NER, both globally and at *MFA2*, although effects are largely not observed unless multiple deletions are made. This suggests probable redundancy in their function in repair, and indicates the importance of deacetylation in modulating chromatin structure during NER. A systematic analysis of all single, double and triple combinations of HDAC mutations would be useful in determining the most influential genes or combinations.

During the repair process, chromatin may exist in three possible states, a state prior to NER, during NER and following NER completion. It is not yet known at which stage(s) of NER the HDACs may be important. Repair of CPDs globally and at *MFA2* is more efficient than in wild type cells. The deacetylases may be involved

in the later stages of NER, when CPDs have actually been repaired, and HDACs may act in the restoration of chromatin to its pre-UV state following the completion of NER. Chromatin structure must be returned to its prior state to preserve the epigenetic information (Gong *et al.*, 2005) and nucleosomes are effectively reloaded onto DNA following repair synthesis (Smerdon and Lieberman, 1978). Chromatin assembly factors such as CAF1 (chromatin assembly factor 1) play a role in repair-associated chromatin assembly *in vitro* (Gaillard *et al.*, 1996) and CAF1 mutants (*cac1, cac2, cac3*) are also UV sensitive (Kaufman *et al.*, 1997; Enomoto and Berman, 1998). Biochemical evidence suggests CAF1 is recruited to chromatin following DNA damage (Martini *et al.*, 1998) and is recruited with PCNA (Martini *et al.*, 1998; Green and Almouzni, 2003). Recently, recruitment of CAF1 was found to be localized to the site of damage rather than part of a global response to UV (Green and Almouzni, 2003). Clearly, chromatin immunoprecipitation (ChIP) experiments to determine where and at what stage the HDACs localise, and with what other proteins if any, would be beneficial to investigate their roles in NER further. It is possible that HDACs may act to deacetylate chromatin, globally and locally, to aid the restoration of repressive chromatin following NER. Generally, HDAC activity correlates with transcriptional repression and silencing of genes so a similar role in creating repressive chromatin states may also apply to repair. If this is the case, one can argue that if HDACs function after the removal of CPDs, why should I see enhanced NER? It may be that there is an equilibrium between the activity of HATs and HDACs to give a level of acetylation that enables NER. Once this is upset by the absence of HDACs so as to give more acetylation, then more efficient NER can occur. This has not been selected for in evolutionary terms because increased acetylation due to HDAC absence is detrimental for some other processes that optimise UV survival.

During this study, attempts were made using Western blotting to explore effects upon global histone acetylation levels as a result of the HDAC mutations. This was not completed during the time course of the study, although the *rpd3hos1hos2* strain was examined in our lab, and found to exhibit a slight increase in acetylation levels of histone H3 (Y.Yu, personal communication). Additional experiments are needed to investigate this aspect in more detail. As mentioned earlier, Yu *et al.*, 2005, examined acetylation levels at two nucleosomes in the *MFA2* promoter region prior to and following UV irradiation by using ChIP with antibodies against acetylated histones H3 (lysine sites K9, K14) and H4 (K5, K8, K12, K16). In wild type cells, a dramatic increase in H3 acetylation was observed which gradually reduces to pre-UV levels as repair occurs. This was found to be primarily Gcn5-dependent. No such effects were observed for H4 acetylation. Total histone acetylation was also analysed and the UV-stimulated increase followed by restoration to pre-UV levels was found to be a genome-wide response to UV-induced damage (Yu *et al.*, 2005). In the same study, accessibility of chromatin was also tested by comparing the access of a restriction enzyme to a unique restriction site within the nucleosomal DNA, as histone acetylation and chromatin remodelling appear to be linked (Hassan *et al.*, 2001b; Neely and Workman, 2002; Mitra *et al.*, 2006). Following UV, chromatin appeared to gradually become more accessible, before returning to pre-UV levels. This is partially dependent on Swi2, although a *swi2Δ* mutant is not UV sensitive and repair at *MFA2* is not impaired, indicating there are other Swi/Snf factors that may compensate. Similar assays could be carried out for the HDAC mutant strains in mating type α cells, to assess the possible roles in determining precise acetylation levels and chromatin structures during and following repair, independently to any remodelling to facilitate transcription.

Overall, the results indicate roles for HDACs in NER. Enhanced repair but increased UV sensitivity suggests these roles may involve multiple pathways. Given the data of Yu *et al*, I propose that HDACs are involved in the later stages of NER and the restoration of chromatin to a repressive state, but that the balance of activity between HATs and HDACs is crucial for cell survival. The requirement of multiple mutations to produce significant repair effects suggests a degree of redundancy in HDAC function and possibly the importance of very specific levels and patterns of histone acetylation. This supports the idea of a 'histone code' constituting epigenetic information to determine precise biochemical activities in the cell, and which has been suggested for the regulation of transcription. The histone code consists of precise patterns of acetylation and other post-translational histone modifications including methylation, phosphorylation and ubiquitination, which together form a layer of specific biochemical 'instructions' to execute the genetic information encoded by DNA. Thus the modulation of chromatin structure in eukaryotic cells, important for transcription regulation and repair, is a complex and multi-faceted process, yet to be fully understood. The following chapter begins to look at possible roles of histone phosphorylation in NER in yeast.

Chapter 5

Possible roles of histone phosphorylation in nucleotide excision repair at the yeast *MFA2* gene

5.1 Introduction

As mentioned in the main introduction, histone proteins H2A, H2B, H3 and H4 are highly conserved proteins forming the basic unit of chromatin, the core nucleosome (Luger *et al.*, 1997). Each nucleosome contains 147bp DNA and is separated by 10-60bp of linker DNA in a 'beads on a string' manner, packaged as a fibre of an approximate 10nm diameter. Further stages of condensation into fibres of approximately 30nm diameter and finally highly condensed fibres of 400+ nm in diameter occur *in vivo* to enable large eukaryotic genomes to be packaged into a nucleus. However, when packaged in this state, the DNA is clearly inaccessible to proteins and protein complexes during vital cellular processes such as transcription, DNA repair and replication. Thus chromatin structure is dynamic and can undergo conformational changes through regulated folding/unfolding to become more accessible when required, thus more permissive to DNA-mediated processes. Core histones therefore contain a regulated globular domain that mediates interactions within the nucleosome and amino-terminal tails which extend from the nucleosome surface and are rich in basic amino acids (Peterson and Laniel, 2004). Both regions can be subjected to post-translational modifications, but the majority appear to occur on the histone tails. Modifications, including acetylation, methylation, phosphorylation, ubiquitylation, sumoylation and ribosylation of the histone tails are of great recent interest and new target sites are continually being identified (Peterson and Laniel, 2004; Millar and Grunstein, 2006).

Additionally, through technological advances in chromatin immunoprecipitation (ChIP) and genome-wide microarray analyses ('ChIP on chip') an increasing number of enzymatic activities have be attributed to preferential target sites of histone modifications, the best characterised of which are HATs and HDACs involved in transcription regulation (Bernstein *et al.*, 2000; Robyr *et al.*, 2002; Kurdistani *et al.*, 2004; Robert *et al.*, 2004; Pokholok *et al.*, 2005; Millar and Grunstein, 2006). Precise combinations of histone modifications have been linked to specific biological functions (Peterson and Laniel, 2004), for example, the combination of acetylation of H4 K8 and H3 K14 with phosphorylation of H3 S10 often correlates with transcriptional activation (Edmondson *et al.*, 2002), whereas hypoacetylation of H3 and H4 coupled with the tri-methylation of H3 K9 correlates with repression of transcription (Peterson and Laniel, 2004). Such patterns of specific modifications have been attributed to both global and local chromatin effects, and have collectively led to the notion of a 'histone code' or 'pattern' which forms a biochemical epigenome, analogous to a set of instructions to operate the DNA encoded genome. The main effects of such a code appear to be to regulate higher order chromatin structures and create a binding platform to help recruit effector molecules in cellular processes (Strahl and Allis, 2000; Fischle *et al.*, 2003; Cosgrove *et al.*, 2004). The currently known sites of histone modifications are shown in Figure 5.1. Recruitment of various histone modifying enzymes to sites of target modifications has been increasingly well understood over the past decade since the first HAT, a Gcn5 homologue, was identified in 1996 (Brownell *et al.*, 1996). Histone modification enzymes include HATs, HDACs, histone methyltransferases (HMTs) and histone kinases (Spencer and Davie, 1999; Peterson and Laniel, 2004;

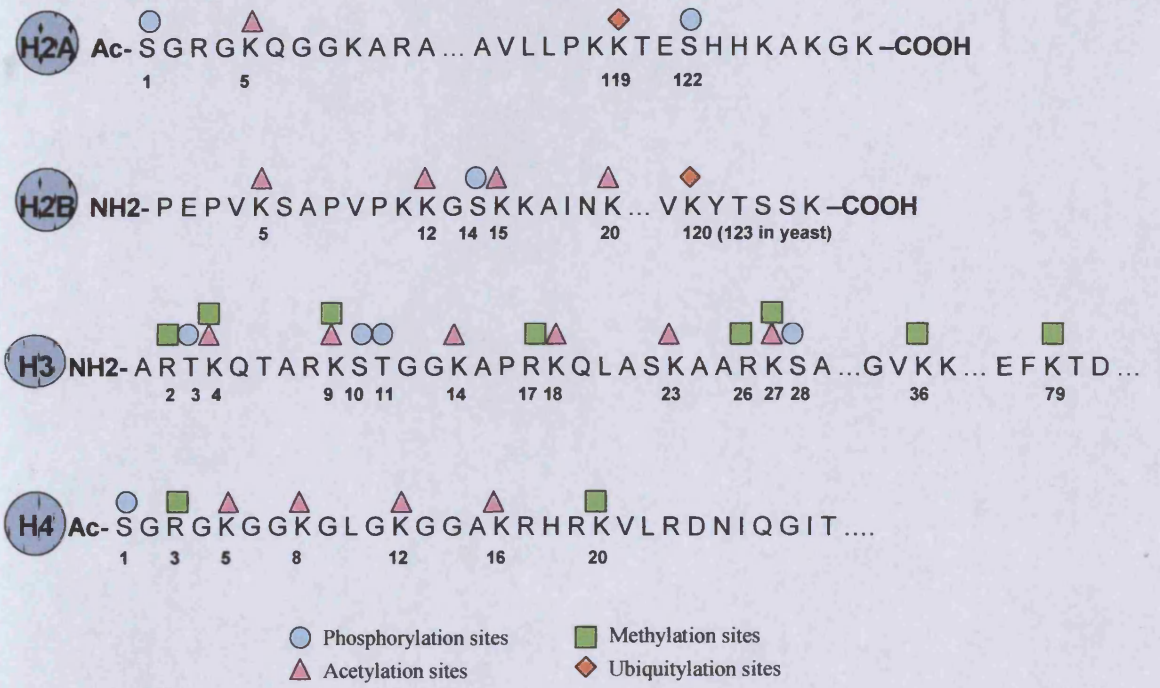

Figure 5.1 *Known sites of post-translational histone modifications.* Histone tails can be modified at multiple sites. Sites of acetylation at lysine residues (K) are indicated by pink triangles, sites of phosphorylation at serine (S) and threonine (T) residues indicated by blue circles, sites of methylation at lysines and arginine (R) residues by green squares and ubiquitylation of lysines by orange diamonds. *(Adapted from Peterson and Laniel, 2004)*

Millar and Grunstein, 2006) and have been implicated in many cellular processes including transcription, DNA repair, replication and centromeric heterochromatin formation (Ehrenhofer-Murray, 2004; Peterson and Laniel, 2004).

The importance of acetylation and deacetylation of histones during regulation of transcription has been well documented. The results presented in Chapter 4 show how histone deacetylases (HDACs) in *S. cerevisiae* also play roles during DNA repair via the NER pathway in a chromatin environment, independently of transcriptional influence. I postulated that other types of histone modifications may also play a role in NER.

Histone methylation and phosphorylation

Histone methylation in yeast is exerted via three known histone methyltransferases which can modify specific lysines in histone H3 tails with up to three methyl groups (Peterson and Laniel, 2004). It is apparently a relatively stable modification as there have been no true demethylases identified to date (Jaskelioff and Peterson, 2003; Ehrenhofer-Murray, 2004). Phosphorylation of serine or threonine residues in close proximity to a methylation site may be involved in the regulation of methylation-induced binding, for example phosphorylation of H3 S10 blocks heterochromatin protein 1 (HP1) binding to its substrate di-methylated H3-K9 site (Jaskelioff and Peterson, 2003) . Methylation is often observed alongside acetylation changes in transcriptional regulation (Jaskelioff and Peterson, 2003). Multiple modifications are possible at a single site, for example, histone H3 lysines K4, K9 and K27 are targets for both acetylation and methylation (Figure 5.1).

Histone phosphorylation targets serine (S) and threonine (T) residues of histone tails. Phosphorylation of the serine residue position 129 (S129) of the histone H2A tail occurs in response to DNA damage in yeast and has been identified as important in the repair of double strand breaks (DSBs) (Downs *et al.*, 2000; 2004; Redon *et al.*, 2003; Foster and Downs, 2005). H2A S129 is a target site for the phosphatidylinositol 3-kinase-like kinases (PIKKs), and members of this family such as Mec1 in *S. cerevisiae*, have been implicated in DNA-damage responses throughout the eukaryotes (Durocher and Jackson, 2001). Two other sites in close proximity to S129, namely H2A S122 and T126, have also been identified as sites of phosphorylation involved in DNA-damage responses in *S. cerevisiae* (Wyatt *et al.*, 2003; Harvey *et al.*, 2005). There is also evidence for interactions between acetylation and phosphorylation, for example, Gcn5, PCAF and p300 HATs

preferentially acetylate histone H3 *in vitro* when the histone is phosphorylated at S10 (Cheung *et al.*, 2000; Lo *et al.*, 2000; Chen *et al.*, 2001). Increasing evidence of cross-talk between the different histone modifications hints at the complexity and sophistication of chromatin regulation in DNA-mediated cellular processes. The experiments described in this chapter began to examine a possible role for phosphorylation of specific residues in NER in *S. cerevisiae*. Histone H2A S122 and S129 mutants, and histone H2B S125 mutants were initially analysed for UV sensitivity but only the H2B S125 truncation mutant was investigated further, alongside the isogenic wild type, using Immuno slot-blot and Southern blotting techniques to assess the removal of CPDs by NER from the overall genome and at *MFA2*, respectively.

5.2 Materials and Methods

The UV irradiation of cells, RNA extractions, Northern blotting and DNA extractions were performed as described in Chapter 2. Analysis of UV sensitivity, NER of CPDs in the overall genome and NER at *MFA2* were all performed as described in Chapters 2 and 4.

Yeast Strains

The following *Saccharomyces cerevisiae* strains were grown in YPD medium (see Appendix I), stored at 4°C whilst in use and at -70°C longer term.

JHY2 *MAT***a** *(hta1-htb1)Δ::LEU2, (hta2-htb2)Δ::TRP1 <pJHA$_2$>* (wild type)

JHY3 as JHY2 except plasmid pJHA$_2$ replaced with pJHA$_3$ *(hta$_1$-S$_{129}$A/HTB$_1$)*

JHY9 as JHY2 except plasmid pJHA$_2$ replaced with pJHA$_9$ *(HTA$_1$/htb$_1$-S$_{125}$stop)*

W303α *MATα ade2-1 trp1-1 can1-100 leu2-3 his3-11,15 ura3-5* (wild type)

JDY22 as W303α except *(hta$_1$-S$_{129}$stop/hta$_2$-S$_{129}$stop).* No markers as genomic mutations were generated using a hisG-URA3-hisG cassette.

FHY10 as JHY2 except *MAT**a**^{1}* (wild type)

FHY14 as JHY2 except *MAT**a**^{1} and (htb$_1$-S$_{125}$ stop)* (as JHY9 but *MATα*^{1})

(^{1} Initially, these strains were believed to be *MATα* but when later checked by Northern blotting, were found to express *MFA2* mRNA, indicative of mating type **a** cells).

FHY47 as JHY2 except *(hta$_1$-S$_{122}$A)*

FHY25 as JHY2 except plasmid pJHA$_2$ is replaced with pHTA$_1$ *(htb$_1$-K$_{123}$R-S$_{125}$A-S$_{126}$A).* This strain is phenotypically indistinguishable from JHY9.

The above strains were kindly donated by J. Downs, Lister Fellow, Biochemistry Department, Cambridge, U.K. The JHY/FHY strains originated from strain FY406 (Hirschhorn *et al.*, 1995). The wild type JHY2 strain has both genomic copies of histones H2A and H2B disrupted and is kept alive by the plasmid pJHA2 which has wild type *HTA1* and *HTB1* under the control of their own promoter (*HIS3* marker, CEN/ARS plasmid). The JHY9 mutant strain (*htb1-S125**) shows strong sensitivity to various DNA damaging agents but exhibits no detectable effect on checkpoints or transcriptional responses to DNA damage, thus may be a good candidate for affecting NER at the site of a lesion (J. Downs, personal communication). The triple point mutation in the FHY25 strain (*htb$_1$-K$_{123}$R-S$_{125}$A-S$_{126}$A*) is phenotypically indistinguishable from the truncation of the tail in strain JHY9 (and FHY14).

The plasmid pGAL-HO was also received from J. Downs (originally from S. Buratowski, Harvard Medical School, Boston, Massachusetts) for use in mating type switching experiments to convert *MAT***a** strains to *MAT*α as required. This was amplified using a QIAprep Spin Miniprep kit (QIAGEN Ltd, UK) as follows:

1. The plasmid sample was mixed with heat-shocked *E. coli* and heated at 50°C for 10 seconds. Cells were grown overnight at 37°C on Luria Bertani (LB) medium plates (see Appendix I).
2. Five colonies from the plates were inoculated in liquid LB medium to which 100μg/ml (1/500 dilution) of ampicillin was added (20μl of 50mg/ml stock). The cells were grown overnight at 37°C, 225rpm.

The protocol in the QIAGEN Miniprep handbook was then followed using the included solutions and buffers:

1. Overnight cultures were resuspended in 250μl P1 buffer with RNAse added and transferred to Eppendorf tubes.
2. 250ml of buffer P2 was added and mixed by gentle inversion of tubes until viscous, for up to 5 mins.
3. 350μl of buffer N3 was added and immediately mixed by gentle inversion to avoid localised precipitation.
4. Samples were centrifuges at 13000rpm for 10 mins and the supernatant was transferred with a pipette to a QIAprep spin column.
5. The column was washed using 500μl buffer PB and centrifuged for 30-60 seconds, discarding the flow-through, then washed with 750μl buffer PE. Residual washing buffer was removed by centrifugation for 1 min.

6. The column was placed in a clean Eppendorf and 2.5µl of buffer EB was added to the centre of the column. After 1 min, the column was centrifuged for a further 1 min.
7. The products of amplification were visualised on a 1% agarose gel (Figure 5.2). Samples 2-5 were collated and diluted with 100µl H_2O.

Figure 5.2 *Amplification of plasmid pGAL-HO.* The plasmid was amplified using a QIAGEN miniprep kit and visualised on an agarose gel as shown. Samples 2-5 were of the best quality and were subsequently collated and diluted for use in mating-type switching of the histone mutant strains..

Primers

The following primers were used to obtain the *BstBI-BstBI* fragment containing *MFA2* during Southern blotting experiments:

Primer 1a: 5'-biotin-gatagctttttACACCATCTACTACATAATTAATTGATAGTTTCCT-3'

(T_a=55°C)

Primer 2a: 5'-biotin-gatagctttttACGGACTTGATGCAGCTGAAAAACCATTATTTAAA-3'

(T_a=57°C)

Primer 1b: 5'-gatagcACACCATCTACTACATAATTAATTGATAGTTTCCT-3' (T_a=55°C)

Primer 2b: 5'-gatagcACGGACTTGATGCACGTGAAAAACCATTATTTAAA-3' (T_a=57°C)

Mating-type Switching

S. cerevisiae exists as two haploid forms of mating types **a** and α which can mate to form **a**/α diploid cells. Both mating types are employed in repair studies at *MFA2* as it enables effects to be studied in the presence and absence of transcription, in **a** and α cells respectively. The haploid mating type depends on the genotype at the mating type (*MAT*) locus on chromosome III. A haploid cell is able to switch from *MAT***a** to *MAT*α, or vice versa, by a cassette model switching process (Hicks *et al.*, 1977; Strathern *et al.*, 1982; Haber, 1998). Switching depends on the *HO* gene which encodes the Ho endonuclease that produces a double-strand break (DSB) at its target sequence. Three gene target sequences exist, one near the locus from which **a** or α information is transcribed and two at the silent storage loci containing copies of this information, *HML*α and *HMR***a**. In cells of each mating type, a portion (the Y sequence) is unique to that mating type and during switching it is this Y cassette that is replaced with the information for the opposite mating type, initiated by the Ho DSB. Most laboratory yeast strains carry the *ho* allele and have a stable mating type, but by introducing *HO* on a plasmid by transformation, mating-type switching can be induced.

Attempts were made to switch the *MAT***a** strains FHY10 and FHY14 to *MAT*α by transformation with the pGAL-HO plasmid, using the lithium acetate method as described in Chapter 3 (Gietz *et al.*, 1992). However, this was not completed successfully within the duration of this study.

5.3 Results

5.3.1 Mutations at certain sites of histone phosphorylation result in mild UV sensitivity

UV sensitivity of mutated strains can be an indication of roles in DNA repair for the mutated gene(s), and can be tested by irradiating cells and measuring their survival. As with the HDAC mutant strains in Chapter 4, the JHY/FHY histone mutant strains were exposed to increasing doses of UV radiation and grown on YPD plates for three days before counting the surviving colonies. The percentage of colonies surviving, compared to 100% survival on the untreated plates, was calculated for each strain. Survival curves were plotted to compare the UV sensitivity of each strain relative to the wild type strains and are shown in Figure 5.3. Survival curves for the *rad16* mutant strain (highly UV sensitive) and the *gcn5* mutant (mild sensitivity) are also indicated, with their wild type strain PSY316, as benchmark comparisons (see section 4.3.1).

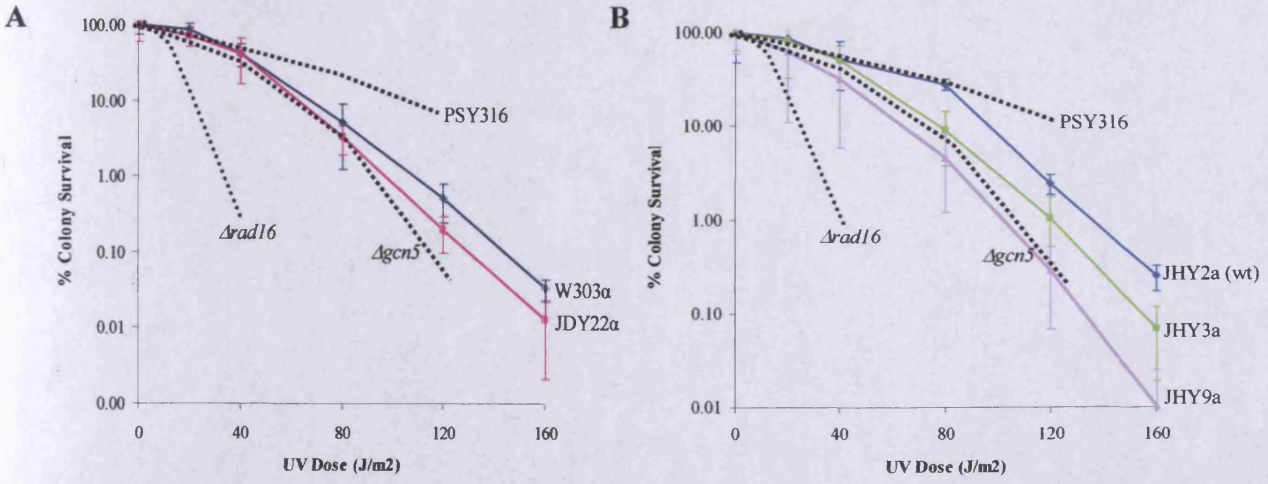

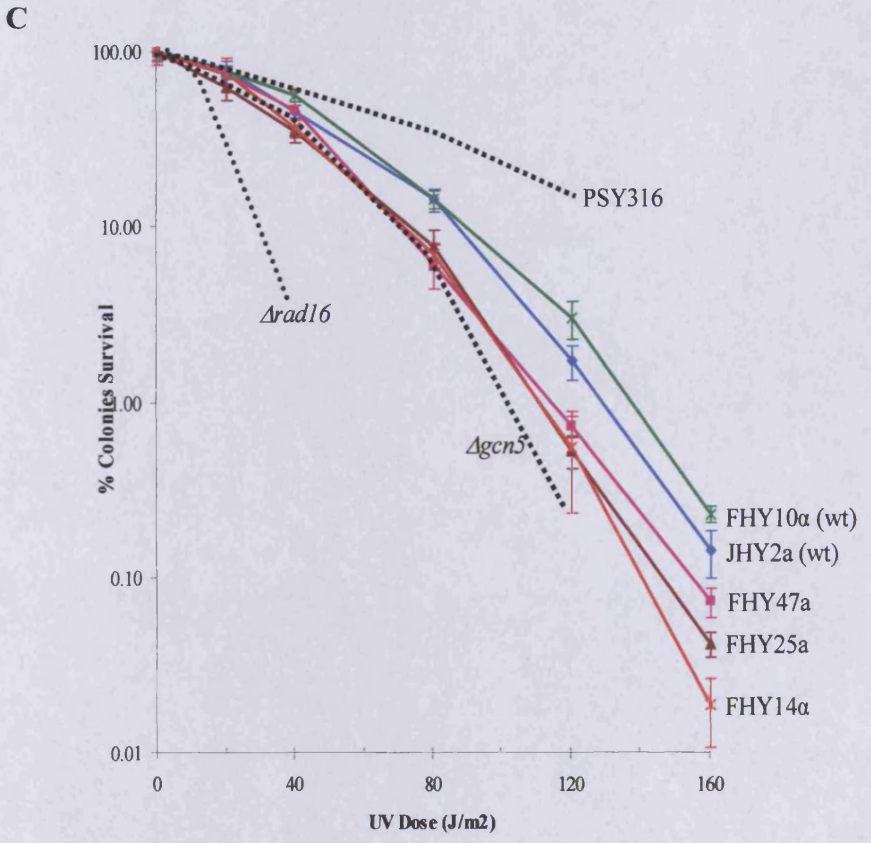

Figure 5.3. *Survival curves to measure sensitivity of histone mutant strains to UV irradiation.* Cells of each strain were treated with doses of UV radiation ranging from 20 to 160 J/m^2 and grown alongside an untreated sample. Each sample was performed in triplicate in each experiment. The percentage of colony survival represents the proportion of cells that survived irradiation and grew to form colonies over 3 days, taking wild type survival at 0 J/m^2 as 100%. These data represent the averages of at least 3 independent experiments and standard deviations are depicted by error bars. The dotted curves represent superimposed data from a previous study (obtained from Y. Teng), showing survival of PSY316 wt, *gcn5* and *rad16* strains as a benchmark comparison. *rad16Δ* causes high UV sensitivity and *gcn5Δ* causes mild sensitivity. **(A)** shows the survival curves for the JDY22 strain and its wild type W303 strain. **(B)** shows the curves for the *MAT***a** JHY strains, and **(C)** shows the curves for the FHY strains.

The JDY22α strain (*hta1* mutant) showed a very slight increase in UV sensitivity compared to W303α wild type cells (Figure 5.3A), indicating this mutation did not appear to have a significant effect on the overall DNA repair following UV in

the cell. The JDY22 strain was not investigated further during this study. The JHY strains were received in advance of the FHY strains so UV sensitivity was tested separately and the survival curves are shown in Figures 5.3B and 5.3C, respectively. The JHY3 mutant strain (*hta1-S129A*) showed mild sensitivity to UV compared to wild type cells and similar sensitivity to *gcn5* mutant cells. The deletion of *GCN5* has little effect on global DNA repair (Teng *et al.*, 2002), and the survival curve for JHY3 suggests that the *hta1-S129A* mutation also has little effect. Strains carrying the *htb1-S125** mutation however, showed slightly higher UV sensitivity compared to JHY3 and wild type cells. At 20 J/m^2, survival was similar with an average of 77% wild type cells and 75% *htb1-S125** cells. At 40J/m^2, however, Survival of the mutant cells dropped to an average of 36% compared to 56% wild type cells, and at 80J/m^2, 7% of mutant cells survived compared to 14% wild type.

These data suggest that the truncation of the histone H2B tail at the serine residue position 125 does induce mild UV sensitivity and hence phosphorylation at this site or further along the tail, such as S129, may play a role in DNA repair. The wild type (FHY10) and S125 truncated mutant strains (FHY14) were thus explored further to examine the removal of CPDs by nucleotide excision repair (NER) from the overall genome and at the *MFA2* gene. Similar survival rates were also observed for the FHY47 (*hta1-S122A*) strain and FHY25 (*htb1-K123R-S125A-S126A*), the latter being phenotypically indistinguishable from the S125 truncation mutant. However, these mutants were not investigated further during this study.

5.3.2 Northern blotting to detect transcription of *MFA2* to verify mating type

MFA2 is actively transcribed by RNA polymerase II in mating type **a** cells but is repressed in mating type α cells. RNA was extracted from the histone mutant strains and Northern blotting was used to detect the presence or absence of *MFA2* transcription, and hence verify the mating type of each strain. The *ACT1* gene, transcribed in both mating types was used as a control. A typical image obtained is shown in Figure 5.4.

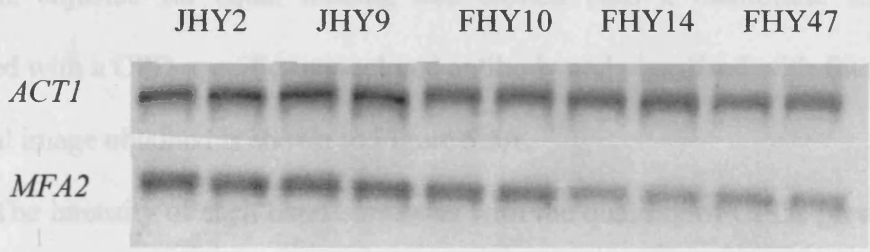

Figure 5.4 *The detection of mRNA by Northern blotting.* Total RNA was extracted from cells and Northern blotting was used to detect mRNA of *MFA2* and *ACT1*. The presence of a band indicates mRNA and hence transcription of the gene. Duplicates of each sample were used

As expected, JHY2, JHY9 and FHY47 cells all showed strong bands in the detection of mRNA for both the *ACT1* and *MFA2* genes. FH10 and FHY14 cells however were also found to transcribe *MFA2*, indicating that they were also mating type **a** cells rather than mating type α as initially thought. Therefore, strains JHY2 and FHY10 were genotypically identical, and similarly for S125 truncation mutant strains JHY9 and FHY14. In light of this, mating type switching experiments were performed using the FHY cells but they were not successfully switched during the course of this study.

5.3.3 Global repair of CPDs in genomic DNA is not affected by the mutation of serine position 125 of the histone H2B tail

The wild type and H2B truncation mutant strains were next examined for effects upon the removal of CPDs from the overall genome using an immunological slot-blot assay as described in Chapters 2 and 4. Briefly, cells were irradiated with UV to induce CPDs and sampled immediately and then after 1, 2, 3 and 4 hours allowed for repair. Experiments were performed in darkness to explore effects due to repair by NER and not photoreactivation. Following repair, DNA was extracted from the cells, adjusted for equal loading and blotted onto a membrane which was incubated with a CPD-specific monoclonal antibody and visualised with fluorescence. A typical image obtained is shown in Figure 5.5A.

The intensity of each band correlates with the quantity of CPDs present in the overall genome of cells within that sample, i.e. darker bands indicate higher quantities of CPDs. The decrease in intensity over time is therefore indicative of repair of CPDs, and was quantified using ImageQuant software (Molecular Dynamics, CA, USA). The percentage of CPDs repaired at each time point was calculated (see Appendix A IV.2). The averages of three experiments were used and a quantitative graph produced (Figure 5.5B). No significant difference was observed between the wild type and the H2B mutant strains in the repair of CPDs in the overall genome, suggesting that phosphorylation at position S125 or further of the histone H2B tail is unlikely to play a role in global NER.

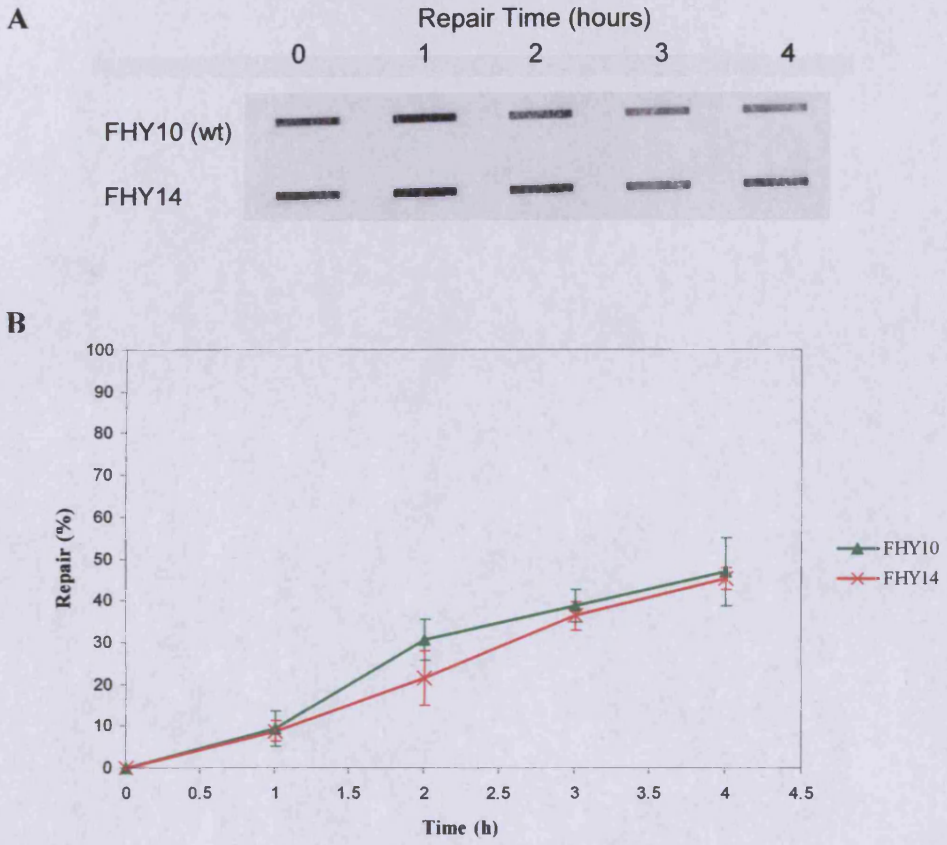

Figure 5.5 *The removal of CPDs from the total genomic DNA.* (**A**) A typical gel image obtained from the immunological slot-blot assay. Monoclonal CPD antibody was used to detect CPDs in the genome following UV irradiation at 150J/m^2 and incubations for 0, 1, 2, 3 and 4 hours (repair time). The intensity of each band represents the quantity of CPDs present. (**B**) Quantitative graph using the average data from three gels. The standard deviation at each point is depicted by error bars

5.3.4 Mutation of the serine residue at position 125 of the H2B tail does not cause a change in the rate of NER at *MFA2* in mating type a cells

The repair of CPDs at the *MFA2* gene was next examined using the Southern blotting method described in Chapter 4. Following UV irradiation of cells to induce CPDs, each strain was sampled at hourly intervals up to 4 hours, during which NER was able to operate but photoreactivation was prevented by keeping cells in the dark.

DNA was extracted and digested with the *BstBI* endonuclease, and subsequently cut with a CPD-specific endonuclease. Electrophoresis was used to fractionate the samples before Southern blotting onto a membrane. A radioactive strand-specific probe was used to detect intact *MFA2* fragments which were then visualised using a phosphorimager. A typical image obtained is shown in Figure 5.6A.

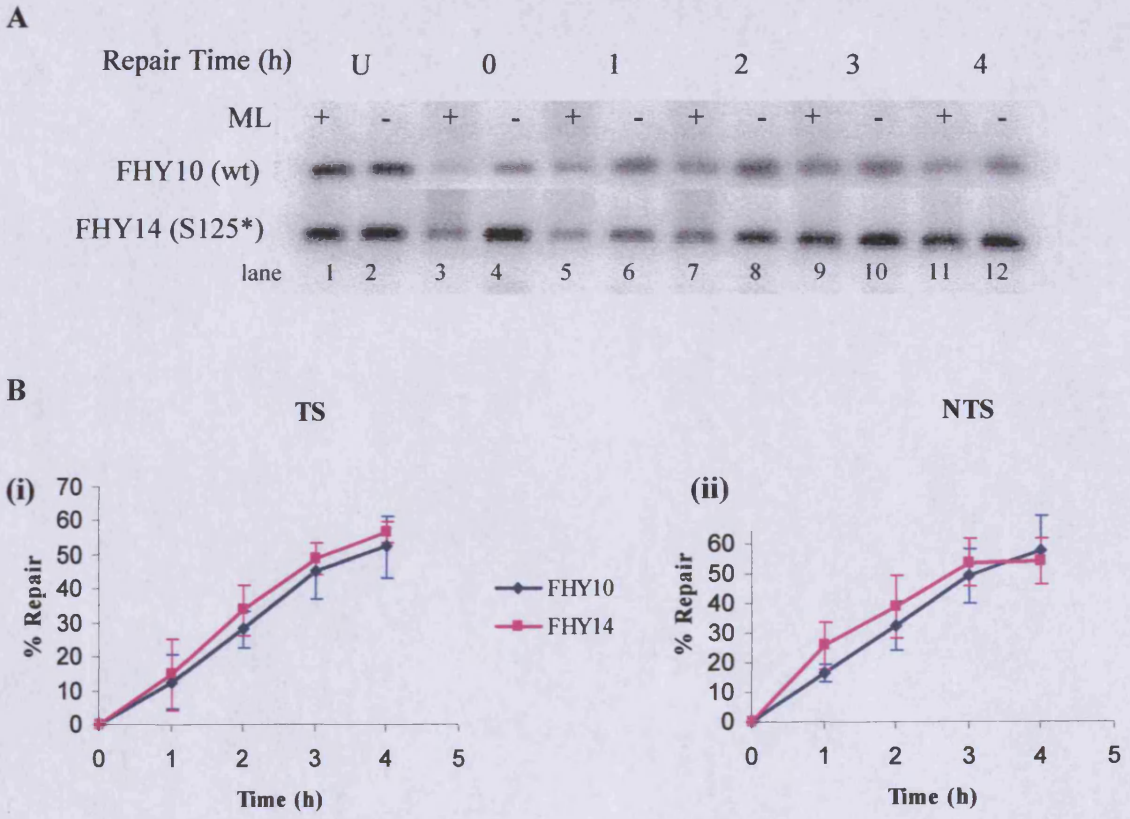

Figure 5.6 *Southern blotting detection of NER of CPDs at the MFA2 gene.* **(A)** shows a typical image obtained, shown here for the NTS of the wild type (top band) and S125 truncated histone H2B mutant (lower band). Samples were collected before UV treatment (U) and at designated repair times (0-4 hours as indicated above the bands). *ML*-treated samples (+) were cut at CPDs and were compared to uncut (-) controls. **(B)** Graphical representation of repair over 4 hours. Data are the average of at least 3 experiments and standard deviations are depicted by error bars. The repair in the transcribed strand TS (i) and non-transcribed strand NTS (ii) of *MFA2* were analysed separately.

The intensity of each band (Figure 5.6A) correlates with the amount of full-length, undamaged, *MFA2* fragments within that sample; hence darker bands are observed for non-irradiated samples (U) and control samples not cut with the CPD-specific endonuclease *ML* (-). In *ML* (+) samples where CPDs are detected, the band intensity reflects repair: fainter bands indicative of many CPDs, fewer intact fragments and thus lower levels of repair. The increasing intensity of bands in lanes 3, 5, 7, 9 and 11 over time therefore signifies repair. The bands were quantified using ImageQuant software (Molecular Dynamics, CA, USA) as described in Chapters 2 and 4, and the proportion of undamaged fragments at each repair time point was calculated (see Appendix AIV.3). This was plotted graphically, shown independently for the TS and NTS (Figure 5.6B).

For the repair of CPDs in both the transcribed and non-transcribed strands (TS and NTS respectively), there was little difference between the rates observed in the wild type strain compared to those of the histone mutant strain. For each strain, the rate of repair in the TS was slightly higher than that of the NTS, but due to the resolution limits of the assay and resultant relatively large standard deviations, a significant difference could not be confirmed. The high resolution approach described in Chapter 4, exploring NER at the level of the nucleotide, would be useful to examine this aspect more closely at different regions of *MFA2*.

5.4 Discussion

Post-translational histone modifications are important factors in the regulation of chromatin structure which is essential for effector proteins to gain access to DNA during vital cellular processes such as transcription, DNA repair and recombination.

Whilst acetylation has received most attention in recent years, other modifications have also been implicated in chromatin regulation, mainly focussed on transcriptional control, and the importance of interplay between the different classes of modifications is becoming increasingly apparent (Edmondson *et al.*, 2002; Sun and Allis, 2002; Jaskelioff and Peterson, 2003; Daniel *et al.*, 2004; Ehrenhofer-Murray, 2004). Phosphorylation of yeast histone H2A at serine residues 122 and 129 have previously been implicated in DNA repair (Downs *et al.*, 2000; Harvey *et al.*, 2005).

Experiments measuring cell survival following UV irradiation indicated that truncating the histone H2B tail at the serine residue position 125, a target site for phosphorylation, results in mild UV sensitivity. Cells mutated at three positions, lysine (K) 123, S125 and S126, which confers a similar phenotype to the S125 truncation, resulted in a similar level of UV sensitivity. This may be indicative of a role in DNA repair for phosphorylation of this site, or of histone modifications targeting sites further along the histone H2B tail. However, UV sensitivity may also reflect possible involvement in other cellular pathways, such as recombination, lesion bypass or cell cycle regulation. Cells mutated at S129 of the histone H2A tail also showed a slight increase in UV sensitivity compared to wild type cells, but to a lesser extent than the H2B S125 truncation. The H2A S129 residue is phosphorylated in response to DNA damage and has previously been implicated in the repair of DNA double strand breaks (Downs *et al.*, 2000; 2004; Redon *et al.*, 2003; Foster and Downs, 2005). Histone H2A S122 and threonine (T) 126 have also been identified as sites of phosphorylation involved in DNA-damage responses in *S. cerevisiae* (Wyatt *et al.*, 2003; Harvey *et al.*, 2005). In support of these studies, cells mutated at histone H2A S122 also demonstrated mild UV sensitivity in this study, suggestive of a role in DNA repair.

The H2B S125 truncation mutant was further examined for effects on removal of CPDs from the overall genome by NER. Little difference was observed between the mutant and wild type cells, which suggests that any putative roles in NER for phosphorylation of S125 are at best likely to be specific to certain genes or regions of the genome. The S125 mutant exhibits strong sensitivity to various DNA damaging agents but has no detectable effect on cell cycle checkpoints or damage-induced transcriptional responses (J. Downs, personal communication), further supporting a possible role in some aspect of DNA repair.

The H2B S125 mutant was thus examined for repair at the *MFA2* gene. Ideally, the wild type and mutant cells would be compared as mating type α, where *MFA2* transcription is repressed, allowing for clarity of true repair effects without the possibility of chromatin modifications in response to transcription events facilitating or hindering repair. However, during this study, mating type α cells could not be obtained. Southern blotting experiments did not detect a significant difference between the wild type and mutant **a** cells in the repair of CPDs at the active *MFA2* gene. Experiments using mating type α cells will be vital in determining whether transcription events and associated chromatin structure has facilitated repair in the mutant cells and whether NER at *MFA2* in this strain is in fact impaired in the absence of transcription. Additionally, Southern blotting has limited resolution and detects NER at the level of the gene. The nucleotide-resolution 3' end-labelling approach described in chapter 4 would be informative in assessing repair of CPDs at specific sites of the *MFA2* gene in mutant cells, to detect subtle repair effects in the promoter or transcribed regions compared to wild type cells.

The experiments in this study have merely touched the surface of examining histone phosphorylation involvement in NER, and without further analysis using α

cells, it is not clear whether there is a role in NER at *MFA2* for any of the histone phosphorylation sites studied here. The evidence of the genome-wide experiments suggests that any roles in NER are likely to be specific to certain regions or genes rather than in global repair. The increasing evidence for an epigenetic histone code and the interplay between different modifications and the enzymes they recruit suggests that histone phosphorylation may play important roles in regulating chromatin structure during transcription, DNA repair and other processes, in coordination with other histone modifications and other mechanisms for altering chromatin structure such as ATP-dependent remodelling activities. Observations that the phosphorylation of H3 S10 enhances histone H3 acetylation by Gcn5, a HAT required for efficient NER at *MFA2* in yeast, and also the mammalian HATs PCAF and p300, may suggest that phosphorylation may be needed for enhancing or regulating the effects of histone acetylation in determining chromatin structure rather than a more direct role in repair. Here it would be worth examining if this mutant has normal amounts of mainly Gcn5 mediated histone H3 acetylation after UV at the repressed *MFA2*, as reported by Yu *et al* (2005). Chromatin immunoprecipitation (ChIP) experiments and genome-wide microarray experiments prior to and following UV irradiation also would help determine where kinases are recruited to and which genes may be affected, in response to UV-induced DNA damage, in the mutant strains compared to wild type. An original aim of this study was in fact to determine the transcriptome of the histone mutants using Affymetrix chips in this manner but this was not achieved due to time constraints of the study. Additionally, the overall levels of phosphorylation in the cell can be examined before and after UV using Western blotting techniques. It is apparent that overall phosphorylation levels do show an increase in wild type cells following UV, and this increase is faster than increases

observed for acetylation levels (Y. Yu, personal communication). To take this a step further and examine local effects of phosphorylation following UV, antibodies of very high quality are required for pulling down specific sites of histone phosphorylation. To date, no such antibodies are available, hence this aspect has not yet been pursued.

Chapter 6

General Discussion and Further Experiments

The precise nature of DNA repair remains a fascinating and unresolved challenge. The simple eukaryote *Saccharomyces cerevisiae* provides an invaluable model in which to investigate many aspects of repair and its interplay with transcription and chromatin structure, especially because many of these aspects have been highly conserved throughout evolution; its use has enabled key pioneering discoveries.

The experiments presented within this study aimed to explore the roles of yeast histone deacetylases (HDACs) in transcription and nucleotide excision repair (NER), using the *MFA2* gene as a model gene as NER effects can be studied independently of transcription. Much previous research has explored the roles of histone acetylation by histone acetyltransferases (HATs) in transcription and, to a lesser extent, DNA repair, but less is known about the roles of HDACs, particularly with regards to repair. The first part of this study (presented in Chapter 3) investigated the effect of various single and combinatorial HDAC mutations on transcription of the yeast *MFA2* gene. The second part (presented in Chapter 4) then focussed on the roles of HDACs in NER, firstly exploring the repair of CPDs in global DNA and secondly the repair of CPDs at the *MFA2* gene. Finally, yeast strains harbouring mutations at sites of histone phosphorylation were also studied (Chapter 5) to ascertain possible roles in NER, both globally and at *MFA2*. This was undertaken in light of the increasing evidence for important roles of an epigenetic histone code and interplay between different post-translational histone modifications in chromatin regulation. As each aspect was discussed in detail within the relevant chapters, this

chapter will focus on the requirements and possible routes of further investigation to enhance our understanding of the roles of the histone modifications in NER.

HDACs and UV sensitivity

The first aspect of the study which requires further exploration is the observation that triple HDAC mutant cells show an increase in UV sensitivity but such effects are not observed with the single mutants *rpd3* or *hda1*. Changes in UV sensitivity compared to wild type cells may reflect possible involvement in the NER pathway, although equally it could involve other pathways, such as recombination, lesion bypass or cell cycle arrest, as DNA damage initiates a wide range of coordinated cellular responses (Zhou and Elledge, 2000). A logical and systematic approach is required to deduce which cellular pathway(s) the triple HDAC mutants affect. Pathways which may be affected could be studied using Affymetrix chips to analyse the effects of the HDAC mutations on genes involved in these pathways. Are certain genes up- or down-regulated following UV in comparison to wild type? Similarly, other mutations in various response pathways to UV can be examined.

Possible pathways affected by the HDAC mutants can also be determined using a genetic approach of combining different mutations and observing the resultant phenotypes. For example, observing the phenotypes of mutants defective in other pathways such as the cell cycle arrest in combination with HDAC mutations could also help identify their roles – do such multiple mutant cells still arrest the cell cycle where they should and do they show an even greater increased UV sensitivity?

Here, one could begin with examining effects in combination with a *rad9* mutation. The Rad9 protein in yeast is a DNA damage checkpoint protein, part of a surveillance mechanism in the cell to detect damage and initiate and coordinate the

cellular responses via signal transduction pathways, believed to operate by activating the Rad53 checkpoint signalling kinase (Weinert and Hartwell, 1990; Toh and Lowndes, 2003; Sweeney *et al.*, 2005). Combining *rad9* mutants or other cell cycle mutants with HDAC mutants and systematically testing each for increased UV sensitivity will help determine the precise pathways involved.

Second, UV sensitivity assays using survival rates as indicators merely test the ability of cells to initially survive exposure to different doses of UV radiation. Although repair may occur to facilitate survival, this repair is not necessarily accurate and may be error-prone. We cannot tell from these experiments whether non-lethal mutations have been incurred and to what extent. Unexcised pyrimidine dimers in yeast DNA can initiate mutagenesis following several DNA replications (Kilbey and James, 1979). UV-induced mutation levels may be sufficient that cell death will eventually result following attempts to repair or bypass the damage, but this may not be an immediate effect. Thus mutation frequency experiments would be useful to gain a greater insight into how the HDAC mutations may affect the incidence of UV-induced damage and non-lethal mutations in addition to immediate lethal damage.

The fact that UV sensitivity effects of triple HDAC mutations were observed but no such effects for the single mutations may imply that the HDACs play a vital role in responses to UV and thus functional redundancy exists between them. Systematically testing the UV sensitivity and mutation frequencies of all single, double and triple HDAC mutants would give a wider view of which HDACs may be more important than others in the cellular response pathways to UV damage.

HDAC mutations enhance NER

Interestingly, the results presented in Chapter 4 showed that the triple mutants *rpd3hos1hos2* and *rpd3hos1hda1* consistently demonstrated enhanced removal of CPDs by NER compared to wild type cells, both in global repair and at the *MFA2* gene. Such effects were not observed for the single *rpd3* and *hda1* mutants. To determine precisely which HDACs play the most important roles in NER, all single mutants and combinations of all possible double and triple mutants should be examined for repair effects both globally and at *MFA2* using the techniques described in this study.

Why should the HDAC mutations enhance NER despite an increase in UV sensitivity? A further step to be taken in order to address this aspect is the analysis of histone acetylation levels in the mutants using chromatin immunoprecipitation (ChIP) techniques. During this study, a Western blotting technique was employed to determine genome-wide histone acetylation levels before and after UV. It was initially attempted using wild type cells but the experiments were not successfully completed. This should be continued, and employed using the HDAC mutant strains showing enhanced NER so that overall histone acetylation levels can be compared to wild type in response to UV. It is hypothesised that a deletion of HDACs would increase acetylation levels and that this may consequently alter chromatin structure sufficiently to facilitate NER. In our laboratory, a preliminary examination of acetylation levels post-UV in the *rpd3hos1hos2* mutant has indicated an increase in histone H3 acetylation levels (Y. Yu, personal communication), but this needs to be followed up with further experiments and analysis.

However, if increased acetylation enhances repair, why should UV sensitivity increase in these mutants? HDACs play vital roles in the cell in establishing and

maintaining precise acetylation levels and patterns to govern chromatin which influences essential processes such as transcription and repair. Even though deletion of HDACs causing an increase in acetylation levels increases the efficiency of NER, the effect upon the equilibrium between HAT and HDAC activities in the cell may detrimentally affect other processes such as transcription or cell cycle regulation, thus resulting in an overall decreased survival rate following UV exposure.

In addition to overall histone acetylation levels, it would also be informative to examine local effects of the HDAC mutations at specific nucleosomes, as the repressed *MFA2* gene is associated with positioned nucleosomes. Similar techniques could be applied as described by Yu *et al.*, 2005, as previously mentioned, examining acetylation levels at the two nucleosomes positioned in the *MFA2* promoter region before and after UV irradiation, using ChIP with antibodies against acetylated histones H3. Little effect was observed for H4 acetylation by Yu *et al.*, 2005, but in wild type cells, a dramatic increase in H3 acetylation following UV was observed which gradually reduced to pre-UV levels during repair. This was found to be primarily Gcn5-dependent. Alterations in local acetylation levels due to the HDAC mutations could be determined in a similar manner to assess whether HDACs are also involved in establishing the precise acetylation levels required for optimal NER at *MFA2*. Indeed, experiments in our group by Teng (personal communication) have shown that deletion of the gene for the *MFA2* repressor Tup1, even in the absence of functional transcription (via TATA box mutation), still gives a chromatin state associated with transcriptional activation. Importantly, this is considered to prevent recruitment of HDACs. It results in high levels of histone acetylation and, just like in the HDAC mutants, enhanced NER - faster even than when the gene is transcriptionally active. Intriguingly, his studies have shown a *TUP1* deletion, even

in the absence of functional transcription, abolishes the requisite for Rad16 in GGR, and a *rad16* mutant has reduced histone acetylation at the 2 nucleosomes in the *MFA2* control region. These results further emphasise a central role for the levels of histone acetylation in governing the rate of NER, albeit directly or indirectly.

The effects of the HDAC mutations observed during this study do not completely reflect changes seen in NER for *gcn5*. Gcn5 HAT activity is required for efficient NER at *MFA2* but deletion of *GCN5* does not result in total abolishment of repair or any major effect on global NER (Teng *et al.*, 2002). However, there is a residual enhancement of histone aceylation after UV in the absence of gcn5 (Yu *et al* 2005). Is this implicative of roles for multiple HATs? Experiments investigating NER have not yet been performed with mutations in multiple HATs, and if this were done, perhaps a role for multiple HATs in global NER would become apparent, which may help explain why only local NER effects are seen in *gcn5* cells. The essential role of histone acetylation in governing chromatin structure during NER may also suggest a likelihood of multiple HAT involvement, perhaps providing a degree of redundancy as suggested for the HDACs, yet specific enzymes operating predominantly at specific genes.

Chromatin rearrangement is thought to occur during NER (Smerdon and Conconi, 1999; Meijer and Smerdon, 1999; Green and Almouzni, 2002). This is considered to be mediated by ATP dependant Swi/Snf factors, of which there are numerous examples in the cell (Kingston and Narlikar, 1999; Wolffe and Hayes, 1999; Ura and Hayes, 2002; Wang, 2003; Allard *et al.*, 2004; Johnson *et al.*, 2005; Saha *et al.*, 2006). In addition to acetylation levels, changes in the accessibility of chromatin mediated by these chromatin remodelling factors can be explored in the

HDAC mutants compared to wild type cells, using techniques described by Yu, *et al.*, 2005. Chromatin may be digested with a specific restriction enzyme such as *RsaI*, which cuts at a unique DNA sequence (nucleotide position -337 in relation to the *MFA2* start codon) within the nucleosome -2 positioned at the repressed *MFA2* promoter. By measuring the proportion of total chromatin cut by the endonuclease before and after UV, a comparison of the accessibility to the target DNA can be made. Similarly, this can be done using the restriction endonuclease *BsaAI* with a unique target site within nucleosome -1, also positioned at the repressed *MFA2* promoter (Yu, *et al.*, 2005). Gcn5 was found to have little effect on chromatin accessibility using this technique but a possible role for Swi2 was identified (Yu *et al.*, 2005), thus strengthening the evidence for chromatin remodelling at *MFA2* during NER. Possible roles for HDACs in such remodelling during NER could thus be determined.

It would also be interesting to look at microarray studies of HAT/HDAC targets and using ChIP technology to explore whether there are functional pairs of HATs and HDACs operating in NER to oppose each other and finely regulate the acetylation levels and patterns in the cell. Pairs of HATs and HDACs exerting opposing effects at certain promoters have been identified in transcription regulation, for example Gcn5 and Rpd3 exert opposing effects on *IME1* transcription (Burgess *et al.*, 1999); Esa1 and Rpd3 acetylate and deacetylate, respectively, lysine 12 of histone H4 at the *PHO5* promoter (Vogelauer *et al.*, 2000). Are there specific pairs of opposing activities involved in NER at *MFA2*? This approach should be feasible once the technology to examine repair throughout different regions of the genome via ChIP on chip has been developed; this is currently underway in the group.

Histone phosphorylation and NER

The experiments in this study exploring histone phosphorylation mutants could not clearly indicate whether there is a role in NER at *MFA2* for any of the histone phosphorylation sites studied here. The evidence of the genome-wide CPD repair experiments suggests that any roles in NER are likely to be specific to certain regions or genes rather than in global repair. The next step to be taken with these mutants is to repeat the described experiments using mating type α cells where *MFA2* is not transcribed as this is vital to determine any effects upon NER independently of transcription.

We may next examine phosphorylation levels before and after UV in wild type and mutant cells. Early indications from Western blotting approaches in our lab suggest that global phosphorylation levels do increase in wild type cells in response to UV and that a faster increase is observed than for that of acetylation levels (Y. Yu, personal communication). Logically, phosphorylation levels at individual nucleosomes to identify any local effects would next be examined, using a similar approach as described by Yu *et al.*, 2005. However, for this to be successful, antibodies of exceptional quality are required for pulling down specific sites of histone phosphorylation. Currently, no such antibodies are available, hence this aspect has not yet been pursued.

Roles for histone H2A phosphorylation have been implicated in another repair pathway in yeast - the non-homologous end-joining (NHEJ) repair of DNA double-strand breaks (Downs *et al.*, 2000; 2004; Redon *et al.*, 2003; Foster and Downs, 2005; Harvey *et al.*, 2005). This repair pathway also involves HDAC activities (Lewis and Resnick, 2000; Pray-Grant *et al.*, 2002; Fernandez-Capetillo and Nussenzweig, 2004; Jazayeri *et al.*, 2004; Kruszewski and Szumiel, 2005), emphasising the possibility of

interplay between different histone modifications and supporting the notion of a histone code which can modulate chromatin structure and also create specific patterns of histone modifications which may play important roles in recruiting proteins during cellular processes including transcription and repair pathways (Strahl and Allis, 2000; Fischle *et al.*, 2003; Cosgrove *et al.*, 2004; Cosgrove and Wolberger, 2005).

Roles for the various histone phosphorylation sites may be suggested by performing a transcriptome analysis of the mutant strains using combined ChIP and microarray chip techniques (ChIP-on-chip) and identifying which genes (and hence possible pathways) are affected by these mutants, and also comparisons between phosphorylation levels in different regions of the genome in response to UV between the wild type and mutant cells. The transcriptome analysis was an original aim of this study but was prevented due to time constraints. Clearly there are many further avenues to be explored with the histone mutants and this study serves as a preliminary investigation to be continued.

Remaining questions to be addressed

The results of this study regarding enhanced NER in HDAC mutants both globally and locally to *MFA2* have raised intriguing new questions in addition to identifying roles for these activities in NER. Previous studies with the HAT Gcn5 revealed a local requirement for efficient NER at *MFA2* but little effect on global NER (Teng *et al.*, 2002). To date, only the *gcn5* single mutant has been investigated, and in light of the results for the HDAC mutants here, it would be interesting to investigate mutations in multiple HATs. Would we then see a global effect on NER? Are there multiple HATs involved which may show some redundancy as it seems with the HDACs? What effect would knocking out all the HATs have – if some

levels of NER remain, as with *gcn5*, are there other factors involved and could these involve different types of histone modifications?

Histone modifications are important in determining chromatin structure and have been shown to play a role in modifying chromatin in response to UV at the repressed *MFA2* promoter (Yu *et al.*, 2005). However, these chromatin changes do not trigger transcriptional activation of *MFA2* (Yu, *et al.*, 2005). Therefore, although the chromatin is modified sufficiently to afford access to the restriction site employed in the assay described by Yu *et al.*, 2005, the modification does not promote TBP (TATA box binding protein) recruitment and thus transcription initiation. In this study, the HDAC mutants showed increased NER but no effects on transcription were observed, i.e. *MFA2* retained its repressive state. The chromatin changes required for NER may therefore differ from those required for transcription. How might this be achieved? It is possible that HDACs may play a role in this aspect to exclude TBP binding as histone modifications have been suggested to form a histone code which may determine binding substrates, or occlude binding sites, for effector proteins in addition to roles in modulating higher order chromatin structures. It is an intriguing and ongoing challenge to unravel the mechanisms by which the cell can link cellular processes such as transcription and multiple repair pathways, which rely on numerous common factors for chromatin regulation, yet retain the ability for each process to function independently when required.

New evolving technologies will help approach the many remaining questions regarding the regulation and interplay between transcription, DNA repair and chromatin structure. Developments in antibodies will help to identify precise sites of histone modifications in response to UV and help decipher the nature of the coordinated cellular response to damage. Tagging gene products is an extremely

useful technique – here, tagging the HDAC products, perhaps with GFP and related molecules, would enable us to track them in the cell to clarify which genes or regions they are recruited to, the timescale of their deacetylation activity, which proteins function cooperatively and so on. This technique may prove easier than relying on highly specific antibodies and could complement their use. Equally triple tagging the gene products should enable IP without the use of antibodies, for biochemical analyses

Overall, the complex intimate relationship between NER, transcription and chromatin structure is slowly being unravelled, but as one aspect is apparently resolved, a multitude of new questions are raised. The understanding of DNA repair mechanisms in the cell continues to lag behind that of transcription but it continues to pose a fascinating challenge.

Finally, one should not forget that HDAC inhibitors have an increasing role in tumour therapy (La Thangue, 2004; Mai *et al.*, 2005; Marks and Dokmanovic, 2005; Mork *et al.*, 2005; Carey and La Thangue, 2006; Lin *et al.*, 2006). Here, their precise mode of action is still very unclear, and I will not discuss their use further. However, by resolving which chromatin modifying/remodelling enzymes operate in what domains to enable repair it may be possible to reduce the repair of DNA damage by anticancer agents such as cisplatin (processed in part by NER) in specific regions of the genome, and where protooncogenes have been activated. This could selectively impair the function of these genes at less toxic doses of cispaltin so providing an exciting avenue for exploring the effectiveness of specific combinations of drugs for specific cancers.

Appendix I

Growth Media, Solutions and Buffers

Growth Media

All media listed require sterilisation using an autoclave for 20-30 minutes at 15psi.

YNBD minimal medium	***200ml***
Yeast nitrogen base w/o amino acids	1.4g
Glucose	4g
Agar (to make YNBD plates)	4g
H_2O	200ml

Cool media to 50°C after sterilisation before the addition of any required amino acids.

YPD medium	**1000ml**
1% Yeast extract	10g
2% Bacto peptone	20g
2% Glucose	100ml of 20% solution
H_2O to final volume	900ml

YPD plates	**400ml**
1% Yeast extract	4g
2% Bacto peptone	8g
2% Glucose	40ml of 20% solution
2% Bacto agar	8ml
H_2O to final volume	360ml

LB Medium (plates)	**1 litre**
0.5% Yeast extract	5g
1% Bacto tryptone	10g
1% NaCl	10g
(2% Bacto agar	8ml)
Deionised H_2O to 1 litre	360ml

Adjust the pH to 7.0 using 5M NaOH.

Stock Solutions and Buffers

Stock solutions are prepared in quantities of 1 litre unless otherwise specified. All solutions are sterilised by autoclaving as above unless otherwise stated.

1 M DTT (Dithiothreitol)

DTT	3.09 g

Dissolved in 20 ml of 0.01 M sodium acetate (pH 5.2).

Sterilise by filtration. Do not autoclave DTT or solutions containing DTT.

0.5M EDTA (pH 8.0)

$EDTA{\cdot}Na_2{\cdot}2H_2O$	186.1g
H_2O	800 ml

Stir vigorously on a magnetic stirrer. Adjust the pH to 8.0 with ~ 20 g of NaOH pellets.

Add H_2O to make up to 1 litre.

5 M NaCl

NaCl	292.2g
H_2O	up to 1 litre

Phosphate Buffered Saline (PBS)

NaCl	8g
KCl	0.2g
$Na_2HPO_4{\cdot}2\ H_2O$	1.44g
KH_2PO_4	0.24 g
H_2O	800 ml

Adjust the pH to 7.4 with 5 M NaOH. Add H_2O to 1 litre.

1M Phosphate solution

$Na_2HPO_4{\cdot}12\ H_2O$	179g
H_3PO_4 (85%)	4 ml
H_2O	up to 1 litre

10% SDS (Sodium dodecyl sulfate)

SDS (electrophoresis grade)	100g
H_2O	900 ml

SDS is not autoclaved but H_2O is sterilised before preparation. Heat to 65°C to aid dissolution. Adjust the pH to 7.2 by adding a few drops of concentrated HCl. Add H_2O to make 1 litre.

3M Sodium acetate (pH 5.2)

Sodium acetate·$3H_2O$	408.1g
H_2O	800 ml

Adjust the pH to 5.2 with glacial acetic acid. Add H_2O to make 1 litre.

20× SSC

NaCl	175.3g
Sodium citrate dehydrate	88.2g
H_2O	800 ml

Adjust the pH to 7.0 with NaOH. Add H_2O to make 1 litre.

1×TE Buffer

10mM Tris-HCl (pH 7.5)	10ml
1mM EDTA (pH 8.0)	2ml

Add H_2O to make up to 1 litre.

1M Tris

Tris base	121.1g
H_2O	800 ml

Adjust the pH accordingly by adding concentrated HCl. Add H_2O to make up to 1 litre.

pH	HCl
7.4	70 ml
7.6	60 ml
8.0	42 ml

DNA and RNA Extraction Solutions

DNA Lysis Buffer

Urea	4 M
NaCl	200 mM
Tris-HCl (pH 8.0)	100 mM
CDTA	10 mM
n-Lauroyl Sarcosine	0.5% (w/v)

RNA Lysis Buffer

Tris-HCl (pH 7.5)	10 mM
EDTA (pH 8.0)	10mM
SDS	0.5%

SEC Buffer

Sorbitol	1.0 M
EDTA	100 mM
Citrate Phosphate buffer (pH 5.8)	10 mM

Sorbitol-TE solution

Sorbitol	0.9 M
Tris-HCl (pH 8.0)	100 mM
EDTA	100 mM

Enzyme digestion buffers

Micrococcus luteus enzyme (ML) stock buffer

Tris (pH 7.5)	10 mM
Ethylene glycol	10%
β-Mercaptoethanol	1 mM

Solutions for Gel Electrophoresis

Prepared in quantities of 1 litre unless otherwise specified.

50× TAE

2 M Tris base	242 g
1 M Sodium Acetate·$3H_2O$	136 g
50 mM EDTA·Na_2·$2H_2O$	19 g

Adjust to pH7.2 with glacial acetic acid. Add H_2O to make 1 litre.

Diluted 50× for use in the preparation of gels and running buffers.

10×TBE

Tris base	108 g
Boric acid	55 g
$Na_2EDTA·2H_2O$	9.3 g

Add H_2O to make 1 litre.

Denaturing running buffer

NaOH	36 mM
EDTA	1 mM.

Non-denaturing loading buffer		**10ml**
Ficoll	10%	1g
SDS	0.5%	0.5ml of 10% solution
Bromophenol Blue	0.06%	6mg

Made up in 1×TAE.

Denaturing loading buffer		**10ml**
NaOH	50 mM	166µl of 3M stock
EDTA	1 mM	20µl of 0.5M stock
Ficoll	2.5%	0.25g
Bromophenol blue	0.025%	2.5mg

Sequencing gel-loading buffer

Deionized formamide	95%
EDTA (pH 8.0)	20 mM
Xylene cyanol FF	0.05%
Bromophenol blue	0.05%

Neutralising gel washing buffer

Tris-HCl (pH7.5)	1 M
NaCl	1.5 M

Fixative solution for sequencing gel

Methanol (15%)	600 ml
Acetic acid (5%)	200 ml

Add H_2O to make 4 litres.

Solutions for Southern, Northern and Western Blotting

10×FA gel buffer

3-[N-Morpholino]propanesulfonic acid (MOPS) (free acid)	200 mM
Sodium acetate	50 mM
EDTA	10 mM

Adjust pH to 7.0 with NaOH.

1×FA gel running buffer

10×FA gel buffer	100 ml
37% (12.3) Formaldehyde	20 ml
RNase-free water	880 ml

5×RNA loading buffer	**10ml**
Saturated aqueous bromophenol blue	16 µl
0.5 M EDTA, pH 8.0	80 µl

37% (12.3) formaldehyde	720 µl
Formamide	3 ml
10×FA gel buffer	4 ml

Add RNase-free water to make 10 ml.

10×MOPS buffer

Morpholinopropanesulphonic acid (0.4 M)	83.7 g
Sodium Acetate·H_2O (0.1 M)	13.6 g
EDTA·Na_2·$2H_2O$ (10 mM)	1.87 g

Adjust pH to 7.2 with NaOH. Add H_2O to make 1 litre.

(Pre)hybridisation solution for DNA	**10ml**
SDS (1%)	1 ml (10%)
Dextran Sulphate (10%)	1 g
NaCl (1M)	0.58 g

Add H_2O to make 10 ml. Heat to 65°C for 10mins before adding the NaCl and heating again at 65°C before use.

(Pre)hybridisation solution for RNA	**10ml**
Phosphate solution (1M)	5 ml
SDS (20%)	3.5 ml
BSA	0.25 mg
EDTA (0.5M, pH 8.0)	20 µl

Add H_2O to make 10 ml. Heat to 65°C before use.

Probe stripping solution	**500ml**
SSC (20x)	2.5 ml
SDS (10%)	50 ml
H_2O	to 500 ml

10×TBST

Tris-Base (1M, pH 8.0)	100 ml

NaCl (5M)	300 ml
Tween 20	5 ml
H_2O	to 1 litre

2×Dynabead Washing and Binding Buffer (2×BW)

NaCl	2 M
Tris-HCl (pH 8.0)	10 mM
EDTA	1 mM

Solutions for Transformation

Each solution to be filter sterilised

Solution A	**10ml**
10×LiAc (100mM)	1 ml
10×TE buffer (10, 1mM)	1 ml
H_2O	8ml

Solution B	**10ml**
10×LiAc (100mM)	1 ml
10×TE buffer (10, 1mM)	1 ml
PEG 50% (40%)	**8ml**

Appendix II

Data from experiments presented in Chapter 3

A II.1 mRNA levels analysis from qPCR.

The data represent the mRNA levels of *MFA2* as a percentage, taking *MFA2* transcription in a cells as 100%.

Experiment 1a

ACT1	1	2	3	mean	st dev	ratio	
w303a	1.57E-02	1.55E-02	1.99E-02	1.70E-02	2.48E-03	1.00	
w303alpha	8.37E-03	1.22E-02	1.34E-02	1.13E-02	2.63E-03	0.66	
rpd3	2.51E-03	9.10E-03	8.92E-03	6.84E-03	3.75E-03	0.40	
hda1	1.14E-02	1.35E-02	1.57E-02	1.36E-02	2.16E-03	0.80	
rpd3hos1hos2	8.35E-03	9.05E-03	1.23E-02	9.90E-03	2.11E-03	0.58	
rpd3hos1hda1	6.28E-03	9.89E-03	1.59E-02	1.07E-02	4.85E-03	0.63	
hos1hos2hda1	8.41E-03	7.56E-03	1.43E-02	1.01E-02	3.66E-03	0.59	
MFA2	**1**	**2**	**3**	**mean**	**st dev**	**ratio**	**adjusted**
w303a	1.17E-02	1.11E-02	1.28E-02	1.19E-02	8.62E-04	1.00	100.00
w303alpha	2.04E-04	2.36E-04	2.28E-04	2.22E-04	1.67E-05	0.02	2.81
rpd3	6.21E-05	9.26E-05	1.09E-04	8.78E-05	2.37E-05	0.01	1.83
hda1	8.30E-05	7.30E-05	8.03E-05	7.88E-05	5.15E-06	0.01	0.83
rpd3hos1hos2	2.40E-05	1.97E-05	2.65E-05	2.34E-05	3.45E-06	0.00	0.34
rpd3hos1hda1	6.30E-05	9.94E-05	7.34E-05	7.86E-05	1.88E-05	0.01	1.05
hos1hos2hda1	1.26E-05	2.45E-05	2.95E-05	2.22E-05	8.68E-06	0.00	0.31
PCR efficiency mfa2 =89.3%							
Correlation coefficient = 0.992							

Experiment 1b

ACT1	1	2	3	mean	st dev	ratio	
w303a	1.59E-02	1.57E-02	2.05E-02	1.74E-02	2.69E-03	1.00	
w303alpha	8.38E-03	1.25E-02	1.36E-02	1.15E-02	2.73E-03	0.66	
rpd3		9.24E-03	9.02E-03	9.13E-03	1.56E-04	0.52	
hda1	1.15E-02	1.37E-02	1.60E-02	1.38E-02	2.25E-03	0.79	
rpd3hos1hos2	8.45E-03	9.21E-03	1.27E-02	1.01E-02	2.24E-03	0.58	
rpd3hos1hda1	6.40E-03	1.01E-02	1.61E-02	1.09E-02	4.88E-03	0.63	
hos1hos2hda1	8.46E-03	7.66E-03	1.44E-02	1.02E-02	3.69E-03	0.59	
MFA2	**1**	**2**	**3**	**mean**	**st dev**	**ratio**	**adjusted**
w303a	1.28E-02	1.14E-02	1.33E-02	1.25E-02	1.01E-03	1.00	100.00
w303alpha	2.09E-04	2.50E-04	2.37E-04	2.32E-04	2.10E-05	0.02	2.81
rpd3	6.45E-05	9.49E-05	1.15E-04	9.13E-05	2.53E-05	0.01	1.39
hda1	9.04E-05	7.87E-05	8.38E-05	8.43E-05	5.87E-06	0.01	0.85
rpd3hos1hos2	2.57E-05	2.07E-05	2.73E-05	2.46E-05	3.44E-06	0.00	0.34
rpd3hos1hda1	6.39E-05	1.01E-04	7.47E-05	7.98E-05	1.90E-05	0.01	1.02
hos1hos2hda1	1.19E-05	2.40E-05	2.95E-05	2.18E-05	9.03E-06	0.00	0.30
PCR efficiency mfa2 =88.5%							
Correlation coefficient = 0.990							

Experiment 1c

ACT1	1	2	3	mean	st dev	ratio	
w303a	0.0145	1.37E-02	1.50E-02	0.0144	0.000618	1	
w303alpha	0.00985	9.88E-03	1.11E-02	0.0103	0.000728	0.715278	
rpd3	0.00516	7.34E-03	6.23E-03	0.00624	0.00109	0.433333	
hda1	9.43E-03	1.13E-02	1.11E-02	0.0106	0.00105	0.736111	
rpd3hos1hos2	7.21E-03	6.39E-03	8.97E-03	0.00752	0.00132	0.522222	
rpd3hos1hda1	5.65E-03	7.11E-03	5.48E-03	0.00608	0.000894	0.422222	
hos1hos2hda1	7.18E-03	7.17E-03	9.41E-03	0.00792	0.00129	0.55	
MFA2	1	2	3	mean	st dev	ratio	adjusted
w303a		0.00843	0.00907	0.00875	0.000457	1	100
w303alpha	0.000196	0.000204	0.000217	0.000206	1.09E-05	0.023543	3.291429
rpd3	8.15E-05	8.64E-05	0.000106	9.13E-05	0.000013	0.010434	2.407912
hda1	9.03E-05	7.64E-05	0.00014	0.000102	3.33E-05	0.011657	1.583612
rpd3hos1hos2	6.36E-05	5.47E-05	8.62E-05	6.82E-05	1.63E-05	0.007794	1.492523
rpd3hos1hda1	6.64E-05	2.18E-05	1.56E-05	3.46E-05	2.77E-05	0.003954	0.936541
hos1hos2hda1	3.75E-05		4.56E-05	4.16E-05	5.72E-06	0.004754	0.864416

Experiment 2a

ACT1	1	2	3	mean	st dev	ratio	
w303a	1.16E-02	1.48E-02	2.14E-02	1.59E-02	4.98E-03	1.00	
w303alpha	2.15E-03	1.90E-03	2.06E-03	2.04E-03	1.31E-04	0.13	
rpd3	2.97E-03	2.64E-03	2.95E-03	2.85E-03	1.83E-04	0.18	
hda1	9.52E-03	1.28E-02	1.17E-02	1.14E-02	1.68E-03	0.72	
rpd3hos1hos2	6.94E-03	7.90E-03	1.09E-02	8.59E-03	2.08E-03	0.54	
rpd3hos1hda1	6.39E-03	5.95E-03	6.62E-03	6.32E-03	3.41E-04	0.40	
hos1hos2hda1	1.22E-02	1.03E-02	4.85E-03	9.11E-03	3.81E-03	0.57	
MFA2	1	2	3	mean	st dev	ratio	adjusted
w303a	1.88E-02	1.53E-02	2.78E-02	2.06E-02	6.48E-03	1.00	100.00
w303alpha	1.28E-04	1.15E-04	1.03E-04	1.15E-04	1.21E-05	0.01	4.35
rpd3	1.31E-05	2.57E-05	2.62E-05	2.17E-05	7.45E-06	0.00	0.59
hda1	2.59E-04	3.22E-04	2.41E-04	2.74E-04	4.23E-05	0.01	1.86
rpd3hos1hos2	8.93E-06	5.62E-05	1.34E-04	6.62E-05	6.29E-05	0.00	0.59
rpd3hos1hda1	6.26E-05	8.23E-05	5.74E-05	6.74E-05	1.32E-05	0.00	0.82
hos1hos2hda1	2.28E-05	5.59E-05	1.08E-05	2.98E-05	2.33E-05	0.00	0.25

Experiment 2b

ACT1	1	2	3	mean	st dev	ratio	
w303a	1.14E-02	1.07E-02	1.42E-02	1.21E-02	1.86E-03	1.00	
w303alpha	2.14E-03	2.09E-03	2.46E-03	2.23E-03	1.99E-04	0.18	
rpd3	2.01E-03	2.81E-03	2.59E-03	2.47E-03	4.16E-04	0.20	
hda1	7.67E-03	8.23E-03	1.11E-02	9.02E-03	1.87E-03	0.75	
rpd3hos1hos2	6.62E-03	6.73E-03	8.56E-03	7.30E-03	1.09E-03	0.60	
rpd3hos1hda1	6.61E-03	7.00E-03	7.63E-03	7.08E-03	5.19E-04	0.59	
hos1hos2hda1	1.12E-02	1.54E-02	1.39E-02	1.35E-02	2.14E-03	1.12	
MFA2	1	2	3	mean	st dev	ratio	adjusted
w303a	1.02E-02	7.32E-03	9.09E-03	8.88E-03	1.47E-03	1.00	100.00
w303alpha	9.09E-05	1.08E-04	2.47E-04	1.49E-04	8.59E-05	0.02	9.10
rpd3	2.25E-05	1.95E-04	7.98E-04	3.38E-04	4.07E-04	0.04	18.65
hda1	1.34E-04	3.21E-04	3.51E-04	2.69E-04	1.18E-04	0.03	4.06
rpd3hos1hos2	1.54E-05	1.47E-04	1.65E-04	1.09E-04	8.16E-05	0.01	2.03
rpd3hos1hda1	3.13E-05	1.30E-04	1.84E-04	1.15E-04	7.74E-05	0.01	2.21
hos1hos2hda1	2.09E-04	2.32E-04	2.33E-04	2.24E-04	1.37E-05	0.03	2.26

Experiment 2c

ACT1	1	2.00E+00	3.00E+00	mean	st dev	ratio	
w303a	1.19E-02	1.53E-02	2.21E-02	1.65E-02	5.22E-03	1.00	
w303alpha	2.69E-03	2.39E-03	2.28E-03	2.46E-03	2.11E-04	0.15	
rpd3	4.07E-03	3.86E-03	2.98E-03	3.64E-03	5.76E-04	0.22	
hda1	6.94E-03	9.92E-03	1.29E-02	9.92E-03	2.98E-03	0.60	
rpd3hos1hos2	6.89E-03	7.48E-03	8.41E-03	7.59E-03	7.65E-04	0.46	
rpd3hos1hda1	1.00E-02	9.75E-03	9.69E-03	9.82E-03	1.73E-04	0.60	
hos1hos2hda1	1.28E-02	1.35E-02	1.05E-02	1.23E-02	1.56E-03	0.75	
MFA2	1	2	3	mean	st dev	ratio	adjusted
w303a	1.25E-02	9.44E-03	9.46E-03	1.05E-02	1.77E-03	1.00	100.00
w303alpha	8.23E-05	7.43E-05	4.70E-05	6.78E-05	1.85E-05	0.01	4.33
rpd3	3.31E-05	1.66E-05	1.81E-05	2.26E-05	9.15E-06	0.00	0.98
hda1	2.56E-04	1.78E-04	2.33E-04	2.22E-04	4.01E-05	0.02	3.52
rpd3hos1hos2	3.71E-05	5.80E-05	8.56E-05	6.02E-05	2.43E-05	0.01	1.25
rpd3hos1hda1	5.46E-05	6.60E-05	1.42E-04	8.74E-05	4.73E-05	0.01	1.40
hos1hos2hda1	3.61E-05	2.57E-05	1.56E-05	2.58E-05	1.03E-05	0.00	0.33

Experiment 3a

ACT1	1	2	3	mean	st dev	ratio	
w303a	1.24E-02	1.30E-02	1.77E-02	1.44E-02	2.93E-03	1	
w303alpha	1.08E-02	1.20E-02	1.18E-02	1.15E-02	5.98E-04	0.798611	
rpd3	4.27E-03	4.23E-03	4.32E-03	4.27E-03	4.46E-05	0.296528	
hda1	6.76E-03	7.28E-03	8.91E-03	7.65E-03	1.12E-03	0.53125	
rpd3hos1hos2	5.65E-03	6.04E-03	6.17E-03	5.95E-03	2.68E-04	0.413194	
rpd3hos1hda1	6.35E-03	5.56E-03	4.09E-03	5.33E-03	1.15E-03	3.70E-01	
hos1hos2hda1	1.71E-03	1.19E-03	1.54E-03	1.48E-03	2.64E-04	1.03E-01	
MFA2	1	2	3	mean	st dev	ratio	adjusted
w303a	1.78E-02	1.04E-02	1.30E-02	1.37E-02	3.74E-03	1.00E+00	100
w303alpha	1.10E-04	1.94E-04	1.48E-04	1.51E-04	4.18E-05	0.011022	1.380133
rpd3		3.03E-05	2.92E-05	2.98E-05	7.71E-07	0.002175	0.733551
hda1	1.72E-04	7.26E-05	9.48E-05	1.13E-04	5.22E-05	0.008248	1.552598
rpd3hos1hos2	2.73E-04	8.65E-06	3.87E-05	1.07E-04	1.45E-04	0.00781	1.890204
rpd3hos1hda1	6.23E-05	3.26E-05	6.56E-05	5.35E-05	1.82E-05	0.003905	1.055039
hos1hos2hda1	1.56E-05	1.61E-05	8.82E-06	1.35E-05	4.06E-06	0.000985	0.958769

Experiment 3b

ACT1	1	2	3	mean	st dev	ratio	
w303a	1.17E-02	1.32E-02	1.51E-02	1.34E-02	1.68E-03	1.00	
w303alpha	1.05E-02	1.16E-02	1.14E-02	1.12E-02	5.80E-04	0.84	
rpd3	4.20E-03	5.16E-03	4.72E-03	4.69E-03	4.80E-04	0.35	
hda1	6.73E-03	6.65E-03	8.05E-03	7.14E-03	7.86E-04	0.53	
rpd3hos1hos2	4.56E-03	5.44E-03	6.68E-03	5.56E-03	1.06E-03	0.41	
rpd3hos1hda1	3.89E-03	4.01E-03		3.95E-03	8.31E-05	0.29	
hos1hos2hda1	1.60E-03	1.68E-03	1.41E-03	1.57E-03	1.40E-04	0.12	
MFA2	1	2	3	mean	st dev	ratio	adjusted
w303a	1.04E-02	1.34E-02	1.21E-02	1.19E-02	1.48E-03	1.00	100.00
w303alpha	1.27E-04	1.49E-04	1.41E-04	1.39E-04	1.11E-05	0.01	1.40
rpd3	1.04E-05	1.95E-05	1.91E-05	1.64E-05	5.14E-06	0.00	0.39
hda1	8.12E-05	9.36E-05	1.08E-04	9.42E-05	1.32E-05	0.01	1.49
rpd3hos1hos2	8.97E-06	1.49E-05	2.21E-05	1.53E-05	6.57E-06	0.00	0.31
rpd3hos1hda1	3.13E-05	4.56E-05	4.08E-05	3.92E-05	7.25E-06	0.00	1.12
hos1hos2hda1	1.17E-05	1.42E-05		1.30E-05	1.81E-06	0.00	0.93

Experiment 3c

ACT1	1	2	3	mean	st dev	ratio
w303a	1.20E-02	1.15E-02	1.57E-02	1.31E-02	2.31E-03	1.00
w303alpha	9.76E-03	1.09E-02	1.06E-02	1.04E-02	6.06E-04	0.79
rpd3	2.97E-03	3.67E-03	2.96E-03	3.20E-03	4.08E-04	0.24
hda1	5.67E-03	6.98E-03	6.65E-03	6.44E-03	6.84E-04	0.49
d3hos1hos	4.41E-03	4.86E-03	5.40E-03	4.89E-03	4.93E-04	0.37
d3hos1hda	3.63E-03	4.64E-03	4.48E-03	4.25E-03	5.42E-04	0.32
s1hos2hda	1.45E-03	1.34E-03	1.90E-03	1.57E-03	2.94E-04	0.12

MFA2	1	2	3	mean	st dev	ratio	adjusted
w303a	1.24E-02	9.85E-03	1.00E-02	1.08E-02	1.41E-03	1.00	100.00
w303alpha	1.11E-04	1.21E-04	1.63E-04	1.32E-04	2.79E-05	0.01	1.54
rpd3	5.60E-05	4.87E-05	6.24E-05	5.57E-05	6.87E-06	0.01	2.11
hda1	1.48E-04	1.17E-04	1.42E-04	1.36E-04	1.64E-05	0.01	2.56
d3hos1hos	3.93E-05	9.10E-05	7.19E-05	6.74E-05	2.61E-05	0.01	1.67
d3hos1hda	6.28E-05		8.37E-05	7.32E-05	1.48E-05	0.01	2.09
s1hos2hda	2.35E-05	2.93E-05		2.64E-05	4.15E-06	0.00	2.04

Summary:

Strain	Experiment 1			Experiment 2			Experiment 3			Mean % Transcription	Standard Deviation
w303a	100.00	100.00	100.00	100.00	100.00	100.00	100.00	100.00	100.00	100.00	0.00
w303alpha	2.81	2.81	3.29	4.35	9.10	4.33	1.38	1.40	1.54	3.45	2.41
rpd3	1.83	1.39	2.41	0.59		0.98	0.73	0.39	2.11	1.30	0.75
hda1	0.83	0.85	1.58	1.86	4.06	3.52	1.55	1.49	2.56	2.03	1.13
hos1hos2rpd3	0.34	0.34	1.49	0.59	2.03	1.25	1.89	0.31	1.67	1.10	0.71
hda1hos1rpd3	1.05	1.02	0.94	0.82	2.21	1.40	1.06	1.12	2.09	1.30	0.51
hda1hos1hos2	0.31	0.30	0.86	0.25	2.26	0.33	0.96	0.93	2.04	0.92	0.76

Appendix III

Data from experiments presented in Chapter 4

A III.1 Cell survival following UV treatment.

W303 (wild type), 10^{-4} dilution

Experiment 1

UV Dose (J/m²)	Colonies/Plate Plate 1	Plate 2	Plate 3	Average	% S.D.	% Survival
0	600	804	820	741.3333	16.55	100.00
20	291	129	416	278.6667	19.41	37.59
40	66	67	130	87.66667	4.95	11.83
80	1.3	3.1	2.3	2.233333	0.12	0.30
120	0.18	0.17	0.04	0.13	0.01	0.02
160	0.006	0.012	0.008	0.008667	0.00	0.00

Summary

UV Dose (J/m²)	Mean % Survival	Mean % St Dev
0	100.00	12.58
20	58.21	9.71
40	26.01	2.92
80	3.34	0.52
120	0.47	0.09
160	0.04	0.01

Experiment 2

UV Dose (J/m²)	Colonies/Plate Plate 1	Plate 2	Plate 3	Average	% S.D.	% Survival
0	342	340	363	348.3333	3.66	100.00
20	271	269	291	277	3.49	79.52
40	187	178	184	183	1.32	52.54
80	29.6	33.4	30.3	31.1	0.58	8.93
120	5.46	6.68	7.36	6.5	0.28	1.87
160		0.524	0.724	0.624	0.04	0.18

Experiment 3

UV Dose (J/m²)	Colonies/Plate Plate 1	Plate 2	Plate 3	Average	% S.D.	% Survival
0	245	305	316	288.6667	13.24	100.00
20	115	174	137	142	10.33	49.19
40	63	69	55	62.33333	2.43	21.59
80	3.3	8.1	7.8	6.4	0.93	2.22
120	0.31	0.19	0.29	0.263333	0.02	0.09
160	0.016	0.033	0.033	0.027333	0.00	0.01

Experiment 4

UV Dose (J/m²)	Colonies/Plate Plate 1	Plate 2	Plate 3	Average	% S.D.	% Survival
0	278	487	439	401.3333	27.28	100.00
20	220	221	265	235.3333	6.40	58.64
40	112	99	115	108.6667	2.12	27.08
80	12	11.4	11.1	11.5	0.11	2.87
120	0.05	0.7	0.65	0.466667	0.09	0.12
160	0.05	0.077	0.025	0.050667	0.01	0.01

Experiment 5

UV Dose (J/m²)	Colonies/Plate Plate 1	Plate 2	Plate 3	Average	% S.D.	% Survival
0		864	838	851	2.16	100.00
20		509	616	562.5	8.89	66.10
40	154	171	109	144.6667	3.76	17.00
80	29	16.2	16.3	20.5	0.87	2.41
120	2.54	1.66	2.07	2.09	0.05	0.25
160	0.244	0.0246	0.141	0.136533	0.01	0.02

rpd3 mutant, 10^{-4} dilution

Experiment 1

UV Dose (J/m²)	Colonies/Plate Plate 1	Plate 2	Plate 3	Average	% S.D.	% Survival
0	158	126	169	151	14.79	100
20	85	88	73	82	5.26	54.30464
40	56	54	58	56	1.32	37.08609
80	11.2	5.1	12.3	9.533333	2.57	6.313466
120	0.34	0.18	0.27	0.263333	0.05	0.174393
160	0.017	0.022	0.046	0.028333	0.01	0.018764

Experiment 2

UV Dose (J/m²)	Colonies/Plate Plate 1	Plate 2	Plate 3	Average	% S.D.	% Survival
0	66	65	80	70.33333	11.92	100
20	59	52	52	54.33333	5.75	77.25118
40	37	27	25	29.66667	9.14	42.18009
80	4.1	6.4	6.5	5.666667	1.93	8.056872
120	0.35	0.3	0.16	0.27	0.14	0.383886
160	0.085	0.023	0.011	0.039667	0.06	0.056398

Experiment 3

UV Dose (J/m²)	Colonies/Plate Plate 1	Plate 2	Plate 3	Average	% S.D.	% Survival
0	289	277	269	278.3333	3.62	100
20	180	163	146	163	6.11	58.56287
40	44	25	30	33	3.54	11.85629
80	2.4	2.1	1.1	1.866667	0.24	0.670659
120	0.17	0.16	0.18	0.17	0.00	0.061078
160	0.023	0.035	0.015	0.024333	0.00	0.008743

Summary

UV Dose (J/m²)	Mean % Survival	Mean % St Dev
0	100.00	10.11
20	63.37	5.70
40	30.37	4.67
80	5.01	1.58
120	0.21	0.07
160	0.03	0.02

hda1 mutant, 10^{-4} dilution

Experiment 1

UV Dose (J/m²)	Colonies/Plate Plate 1	Plate 2	Plate 3	Average	% S.D.	% Survival
0	446	456	438	446.6667	2.02	100.00
20	369	384	322	358.3333	7.24	80.22
40	174	180	134	162.6667	5.60	36.42
80	16.6	14.8	18.6	16.66667	0.43	3.73
120	0.89	1.07	0.51	0.823333	0.06	0.18
160	0.194	0.132	0.213	0.179667	0.01	0.04

Experiment 2

UV Dose (J/m²)	Colonies/Plate Plate 1	Plate 2	Plate 3	Average	% S.D.	% Survival
0	234	295	383	304	24.64	100.00
20	289	260	267	272	4.98	89.47
40	104	98	131	111	5.78	36.51
80	11.8	19.8	13.1	14.9	1.41	4.90
120	0.58	0.87	2.11	1.186667	0.27	0.39
160	0.067	0.064	0.142	0.091	0.01	0.03

Experiment 3

UV Dose (J/m²)	Colonies/Plate Plate 1	Plate 2	Plate 3	Average	% S.D.	% Survival
0	293	314	274	293.6667	6.81	100.00
20	148	89	159	132	12.82	44.95
40	56	62		59	1.44	20.09
80	2.6	2	3.1	2.566667	0.19	0.87
120	0.19	0.49	0.25	0.31	0.05	0.11
160	0.018	0.02	0.041	0.026333	0.00	0.01

Summary

UV Dose (J/m²)	Mean % Survival	Mean % St Dev
0	100.00	11.16
20	71.55	8.35
40	31.01	4.28
80	3.17	0.68
120	0.23	0.13
160	0.03	0.01

DY 6445 (*rpd3hos1hos2* mutant), 10^{-4} dilution

Experiment 1

UV Dose (J/m²)	Colonies/Plate			Average	% S.D.	% Survival
	Plate 1	Plate 2	Plate 3			
0	300	329	342	323.67	6.64	100.00
20	137	198	174	169.67	9.49	52.42
40	87	101		94.00	3.06	29.04
80	2.6	5.5	4.2	4.10	0.45	1.27
120	0.1	0.17	0.09	0.12	0.01	0.04
160	0.009	0.002	0.009	0.01	0.00	0.00

Summary

UV Dose (J/m²)	Mean % Survival	Mean % St Dev
0.00	100.00	12.28
20.00	51.86	10.42
40.00	25.48	4.19
80.00	1.32	0.58
120.00	0.04	0.02
160.00	0.00	0.00

Experiment 2

UV Dose (J/m²)	Colonies/Plate			Average	% S.D.	% Survival
	Plate 1	Plate 2	Plate 3			
0	432	298	291	340.33	23.35	100.00
20	195	137	175	169.00	8.66	49.66
40	76	97	132	101.67	8.31	29.87
80	9	2.4	4.9	5.43	0.98	1.60
120	0.25	0.13	0.19	0.19	0.02	0.06
160	0.01	0.001	0.008	0.01	0.00	0.00

Experiment 3

UV Dose (J/m²)	Colonies/Plate			Average	% S.D.	% Survival
	Plate 1	Plate 2	Plate 3			
0	98	111	65	91.33	25.96	100.00
20	25	48	31	34.67	13.06	37.96
40	19	15		17.00	3.10	18.61
80	0.2	0.1	0.1	0.13	0.06	0.15
120	0.05	0.01	0.06	0.04	0.03	0.04
160	0.011	0.026	0.006	0.01	0.01	0.02

Experiment 4

UV Dose (J/m²)	Colonies/Plate			Average	% S.D.	% Survival
	Plate 1	Plate 2	Plate 3			
0	260	282	281	274.33	4.53	100.00
20	166	176	259	200.33	18.61	73.03
40	88	65	69	74.00	4.48	26.97
80	10.1	3.9	4	6.00	1.29	2.19
120	0.15	0.15	0.21	0.17	0.01	0.06
160	0.016	0.007	0.013	0.01	0.00	0.00

Experiment 5

UV Dose (J/m²)	Colonies/Plate			Average	% S.D.	% Survival
	Plate 1	Plate 2	Plate 3			
0	381	376		378.50	0.93	100.00
20	170	170	185	175.00	2.29	46.24
40	95	85	80	86.67	2.02	22.90
80	5	5.7		5.35	0.13	1.41
120	0.02	0.11	0.02	0.05	0.01	0.01
160	0.003	0.002	0.005	0.00	0.00	0.00

DY 6446 (*rpd3hos1hda1* mutant), 10^{-4} dilution

Experiment 1

UV Dose (J/m²)	Colonies/Plate Plate 1	Plate 2	Plate 3	Average	% S.D.	% Survival
0	338	200	198	245.33	32.71	100.00
20	184	72	29	95.00	32.62	38.72
40	91	86		88.50	1.44	36.07
80	0.4	0	0	0.13	0.09	0.05
120	0	0.02	0.01	0.01	0.00	0.00
160	0.003	0.032	0.004	0.01	0.01	0.01

Experiment 2

UV Dose (J/m²)	Colonies/Plate Plate 1	Plate 2	Plate 3	Average	% S.D.	% Survival
0	448	437	415	433.33	3.88	100.00
20	234	229	284	249.00	7.02	57.46
40	168	110	101	126.33	8.39	29.15
80	1.9	9.6	4.1	5.20	0.92	1.20
120	0.08	0.02	0.11	0.07	0.01	0.02
160	0.005	0.002	0.003	0.00	0.00	0.00

Experiment 3

UV Dose (J/m²)	Colonies/Plate Plate 1	Plate 2	Plate 3	Average	% S.D.	% Survival
0	568	564	600	577.33	3.42	100.00
20	370	218	306	298.00	13.22	51.62
40	157	95		126.00	7.59	21.82
80	4.4	3.5	0.7	2.87	0.33	0.50
120	0.1	0.11	0.18	0.13	0.01	0.02
160	0.005	0.007	0.009	0.01	0.00	0.00

Experiment 4

UV Dose (J/m²)	Colonies/Plate Plate 1	Plate 2	Plate 3	Average	% S.D.	% Survival
0	467	544	446	485.67	10.62	100.00
20	231	233	214	226.00	2.15	46.53
40	156	104	88	116.00	7.32	23.88
80	4.5	5.9	5.2	5.20	0.14	1.07
120	0.12	0.09	0.07	0.09	0.01	0.02
160	0.009	0.009	0.003	0.01	0.00	0.00

Experiment 5

UV Dose (J/m²)	Colonies/Plate Plate 1	Plate 2	Plate 3	Average	% S.D.	% Survival
0	515	453	481	483.00	6.43	100.00
20	198	278	231	235.67	8.32	48.79
40	126	82	125	111.00	5.20	22.98
80	4.8	8.4	3.4	5.53	0.53	1.15
120	0.13	0.15	0.01	0.10	0.02	0.02
160	0.016	0.025	0.009	0.02	0.00	0.00

Summary

UV Dose (J/m²)	Mean % Survival	Mean % St Dev
0.00	100.00	11.41
20.00	48.63	12.67
40.00	26.78	5.99
80.00	0.79	0.40
120.00	0.02	0.01
160.00	0.00	0.00

DY 6447 (*hos1hos2hda1* mutant), 10^{-4} dilution

Experiment 1

UV Dose (J/m²)	Colonies/Plate Plate 1	Plate 2	Plate 3	Average	% S.D.	% Survival
0						
20						
40	CELLS NOT GROWN WELL AND CONTAMINATED					
80						
120						
160						

Experiment 2

UV Dose (J/m²)	Colonies/Plate Plate 1	Plate 2	Plate 3	Average	% S.D.	% Survival
0	58	114	69	80.33	36.93	100.00
20	26	14	72	37.33	38.11	46.47
40	6	12	18	12.00	7.47	14.94
80	1	0.9	0.8	0.90	0.12	1.12
120	0.01	0.01	0.02	0.01	0.01	0.02
160	0.002	0	0	0.00	0.00	0.00

Experiment 3

UV Dose (J/m²)	Colonies/Plate Plate 1	Plate 2	Plate 3	Average	% S.D.	% Survival
0	233	238	214	228.33	5.55	100.00
20	157	172	139	156.00	7.24	68.32
40	84	60	43	62.33	9.02	27.30
80	6.4	5.5	6.1	6.00	0.20	2.63
120	0.2	0.31	0.19	0.23	0.03	0.10
160	0.01	0.021	0.017	0.02	0.00	0.01

Experiment 4

UV Dose (J/m²)	Colonies/Plate Plate 1	Plate 2	Plate 3	Average	% S.D.	% Survival
0	157	132	145	144.67	8.64	100.00
20	53	49	84	62.00	13.24	42.86
40	17	38	21	25.33	7.71	17.51
80	1.9	1.3	3.1	2.10	0.63	1.45
120	0.14	0.05	0.16	0.12	0.04	0.08
160	0.007	0.009	0.009	0.01	0.00	0.01

Experiment 5

UV Dose (J/m²)	Colonies/Plate Plate 1	Plate 2	Plate 3	Average	% S.D.	% Survival
0	162	200	201	187.67	11.85	100.00
20	76	84	49	69.67	9.77	37.12
40	60	25	29	38.00	10.21	20.25
80	1.8	1.6	5.7	3.03	1.23	1.62
120	0.1	0.18	0.09	0.12	0.03	0.07
160	0.008	0.127	0.188	0.11	0.05	0.06

Summary

UV Dose (J/m²)	Mean % Survival	Mean % St Dev
0	100.00	15.74
20	17.09	21.16
40	8.60	14.23
80	0.55	0.95
120	0.03	0.05
160	0.01	0.02

Data for Psy316a (wild type), Δgcn5, Δrad2 and Δrad16 strains, obtained from Y. Teng.

	UV Dose (J/m^2)	Dilution	Mean % Survival		UV Dose (J/m^2)	Dilution	Mean % Survival
Psy319a (wild type)	0	10^{4}	100	***gcn5a***	0	10^{4}	100
	10	10^{4}	92		10	10^{4}	84
	20	10^{4}	79		20	10^{4}	71
	40	10^{4}	64		40	10^{4}	38
	80	10^{4}	40		80	10^{4}	4.6
	120	10^{3}	15		120	10^{3}	0.19
	UV Dose (J/m^2)	Dilution	Mean % Survival		UV Dose (J/m^2)	Dilution	Mean % Survival
rad2a	0	10^{4}	100	***rad16a***	0	10^{4}	100
	5	10^{2}	0.78		5	10^{4}	90
	10	1	0.012		10	10^{4}	57
					20	10^{4}	18
					30	10^{3}	5.1
					40	10^{3}	0.90

A III.2 Genome-wide NER analysis – Immuno Slot-blot assay

W303 (wild type)

	Repair time (hours)	U	0	1	2	3	4
Exp 1	Volume	15907.03	433522.42	256599.98	175756.07	144652.55	125909.89
	Adjusted Volume	0.00	417615.39	240692.95	159849.04	128745.52	110002.86
	% Vol (damage)		100.00	57.64	38.28	30.83	26.34
	% Repair		0.00	42.36	61.72	69.17	73.66
Exp 2	Volume	1345960.94	20622523.86	13951082.22	9238288.13	7972349.56	7277484.28
	Adjusted Volume	0.00	19276562.92	12605121.28	7892327.19	6626388.62	5931523.34
	% Vol (damage)		100.00	65.39	40.94	34.38	30.77
	% Repair		0.00	34.61	59.06	65.62	69.23
Exp 3	Volume	145623.79	506355.00	356851.33	299118.01	272137.33	250803.10
	Adjusted Volume	0.00	360731.21	211227.54	153494.22	126513.54	105179.31
	% Vol (damage)		100.00	58.56	42.55	35.07	29.16
	% Repair		0.00	41.44	57.45	64.93	70.84
Exp 4	Volume	228806.78	2739111.64	1810271.42	1205974.45	991938.48	921314.07
	Adjusted Volume	0.00	2510304.86	1581464.64	977167.67	763131.70	692507.29
	% Vol (damage)		100.00	63.00	38.93	30.40	27.59
	% Repair		0.00	37.00	61.07	69.60	72.41
		Mean	0.00	38.85	59.83	67.33	71.54
		St Dev	0.00	3.67	1.95	2.40	1.92

rpd3 mutant

	Repair time (hours)	U	0	1	2	3	4
Exp 1	Volume	13393.80	217343.98	148444.67	101119.29	84465.25	79793.72
	Adjusted Volume	0.00	203950.18	135050.87	87725.49	71071.45	66399.92
	% Vol (damage)		100.00	66.22	43.01	34.85	32.56
	% Repair		0.00	33.78	56.99	65.15	67.44
Exp 2	Volume	1527410.74	15184290.10	9621483.45	8454114.08	6040017.29	5411980.83
	Adjusted Volume	0.00	13656879.36	8094072.71	6926703.34	4512606.55	3884570.09
	% Vol (damage)		100.00	59.27	50.72	33.04	28.44
	% Repair		0.00	40.73	49.28	66.96	71.56
Exp 3	Volume	47018.29	222662.86	149369.80	125136.24	117325.29	111524.57
	Adjusted Volume	0.00	175644.57	102351.51	78117.95	70307.00	64506.28
	% Vol (damage)		100.00	58.27	44.48	40.03	36.73
	% Repair		0.00	41.73	55.52	59.97	63.27
Exp 4	Volume	177856.06	2889137.76	1890527.05	1565789.22	1599158.31	1462025.06
	Adjusted Volume	0.00	2711281.70	1712670.99	1387933.16	1421302.25	1284169.00
	% Vol (damage)		100.00	63.17	51.19	52.42	47.36
	% Repair		0.00	36.83	48.81	47.58	52.64
		Mean	0.00	38.27	52.65	59.92	64.28
		St Dev	0.00	3.66	4.21	8.74	8.88

hda1 mutant

	Repair time (hours)	U	0	1	2	3	4
Exp 1	Volume	34089.35	364675.16	252386.75	163744.19	139660.61	130514.64
	Adjusted Volume	0.00	330585.81	218297.40	129654.84	105571.26	96425.29
	% Vol (damage)		100.00	66.03	39.22	31.93	29.17
	% Repair		0.00	33.97	60.78	68.07	70.83
Exp 2	Volume	1250771.54	16567084.04	10708197.13	8047071.30	6840860.33	5856195.69
	Adjusted Volume	0.00	15316312.50	9457425.59	6796299.76	5590088.79	4605424.15
	% Vol (damage)		100.00	61.75	44.37	36.50	30.07
	% Repair		0.00	38.25	55.63	63.50	69.93
Exp 3	Volume	20339.68	495619.65	298729.04	229310.78	199090.49	178704.13
	Adjusted Volume	0.00	475279.97	278389.36	208971.10	178750.81	158364.45
	% Vol (damage)		100.00	58.57	43.97	37.61	33.32
	% Repair		0.00	41.43	56.03	62.39	66.68
Exp 4	Volume	160766.48	2966987.57	1796389.67	1212733.95	970026.24	921243.49
	Adjusted Volume	0.00	2806221.09	1635623.19	1051967.47	809259.76	760477.01
	% Vol (damage)		100.00	58.29	37.49	28.84	27.10
	% Repair		0.00	41.71	62.51	71.16	72.90
		Mean	0.00	38.84	58.74	66.28	70.09
		St Dev	0.00	3.61	3.44	4.08	2.59

DY 6445 (*rpd3hos1hos2* mutant)

	Repair time (hours)	U	0	1	2	3	4
Exp 1	Volume	25274.59	213608.44	119919.27	71583.90	52948.10	46388.19
	Adjusted Volume	0.00	188333.85	94644.68	46309.31	27673.51	21113.60
	% Vol (damage)		100.00	50.25	24.59	14.69	11.21
	% Repair		0.00	49.75	75.41	85.31	88.79
Exp 2	Volume	1018366.92	7849992.04	4952456.27	3150952.28	2338808.94	1535555.97
	Adjusted Volume	0.00	6831625.12	3934089.35	2132585.36	1320442.02	517189.05
	% Vol (damage)		100.00	57.59	31.22	19.33	7.57
	% Repair		0.00	42.41	68.78	80.67	92.43
Exp 3	Volume	16397.26	214368.03	112016.52	59632.30	51290.61	41182.25
	Adjusted Volume	0.00	197970.77	95619.26	43235.04	34893.35	24784.99
	% Vol (damage)		100.00	48.30	21.84	17.63	12.52
	% Repair		0.00	51.70	78.16	82.37	87.48
Exp 4	Volume	192644.56	1346626.29	784452.38	501321.79	376379.72	304377.83
	Adjusted Volume	0.00	1153981.73	591807.82	308677.23	183735.16	111733.27
	% Vol (damage)		100.00	51.28	26.75	15.92	9.68
	% Repair		0.00	48.72	73.25	84.08	90.32
		Mean	0.00	48.14	73.90	83.11	89.75
		St Dev	0.00	4.02	3.96	2.02	2.13

DY 6446 (*rpd3hos1hda1* mutant)

	Repair time (hours)	U	0	1	2	3	4
Exp 1	Volume	31780.56	368352.52	209075.92	135347.29	109121.86	87563.96
	Adjusted Volume	0.00	336571.96	177295.36	103566.73	77341.30	55783.40
	% Vol (damage)		100.00	52.68	30.77	22.98	16.57
	% Repair		0.00	47.32	69.23	77.02	83.43
Exp 2	Volume	502562.93	7626248.26	4694895.82	2951953.93	2688081.58	2270722.26
	Adjusted Volume	0.00	7123685.33	4192332.89	2449391.00	2185518.65	1768159.33
	% Vol (damage)		100.00	58.85	34.38	30.68	24.82
	% Repair		0.00	41.15	65.62	69.32	75.18
Exp 3	Volume	16934.10	235834.16	139216.31	87052.53	75310.24	60284.57
	Adjusted Volume	0.00	218900.06	122282.21	70118.43	58376.14	43350.47
	% Vol (damage)		100.00	55.86	32.03	26.67	19.80
	% Repair		0.00	44.14	67.97	73.33	80.20
Exp 4	Volume	98419.59	1184823.85	689375.51	429389.73	322433.68	280235.44
	Adjusted Volume	0.00	1086404.26	590955.92	330970.14	224014.09	181815.85
	% Vol (damage)		100.00	54.40	30.46	20.62	16.74
	% Repair		0.00	45.60	69.54	79.38	83.26
		Mean	0.00	44.55	68.09	74.76	80.52
		St Dev	0.00	2.62	1.78	4.40	3.86

A III.3 NER at the level of the gene – Southern blotting analysis of removal of CPDs following UV irradiation

W303 (wild type), TS

Expt 1	U		0		1		2		3		4	
ML (+ or -)	+	-	+	-	+	-	+	-	+	-	+	-
Band Intensity	24930.58	27243.42	7114.38	37582.90	4298.89	15556.61	5770.53	17138.51	8883.52	18530.19	9463.38	17599.95
Intact fragment (%)		91.51		18.93		27.63		33.67		47.94		53.77
Damage (%)		8.49		81.07		72.37		66.33		52.06		46.23
Repair (%)				0.00		10.74		18.18		35.79		42.97

Expt 2	U		0		1		2		3		4	
ML (+ or -)	+	-	+	-	+	-	+	-	+	-	+	-
Band Intensity	114488.75	135075.73	9560.88	32576.43	49123.05	135274.56	69926.43	127344.95	74932.66	127598.79	61871.25	101316.40
Intact fragment (%)		84.76		29.35		36.31		54.91		58.73		61.07
Damage (%)		15.24		70.65		63.69		45.09		41.27		38.93
Repair (%)				0.00		9.86		36.18		41.58		44.89

Expt 3	U		0		1		2		3		4	
ML (+ or -)	+	-	+	-	+	-	+	-	+	-	+	-
Band Intensity	2626.62	3253.45	1575.98	3488.97	1224.58	2334.55	1373.23	2289.94	1388.48	2135.32	1260.40	1680.13
Intact fragment (%)		80.73		45.17		52.45		59.97		65.02		75.02
Damage (%)		19.27		54.83		47.55		40.03		34.98		24.98
Repair (%)				0.00		13.29		26.99		36.21		54.44

Expt 4	U		0		1		2		3		4	
ML (+ or -)	+	-	+	-	+	-	+	-	+	-	+	-
Band Intensity	6509.60	7437.27	2104.89	6362.54	1259.94	3243.56	1721.64	3998.98	1494.74	2686.79	3109.73	4572.55
Intact fragment (%)		87.53		33.08		38.84		43.05		55.63		68.01
Damage (%)		12.47		66.92		61.16		56.95		44.37		31.99
Repair (%)				0.00		8.61		14.90		33.70		52.19

Expt 5	U		0		1		2		3		4	
ML (+ or -)	+	-	+	-	+	-	+	-	+	-	+	-
Band Intensity	14470.62	16777.55	4049.78	15588.95	2816.56	9530.16	4078.77	10331.93	3504.16	6024.20	9456.51	15118.59
Intact fragment (%)		86.25		25.98		29.55		39.48		58.17		62.55
Damage (%)		13.75		74.02		70.45		60.52		41.83		37.45
Repair (%)				0.00		4.83		18.24		43.49		49.41

Expt 6	U		0		1		2		3		4	
ML (+ or -)	+	-	+	-	+	-	+	-	+	-	+	-
Band Intensity	98126.90	97383.88	15655.71	47271.77	19422.34	53134.60	27722.84	62538.48	16311.09	26429.13	32757.32	46087.70
Intact fragment (%)		100.76		33.12		36.55		44.33		61.72		71.08
Damage (%)		-0.76		66.88		63.45		55.67		38.28		28.92
Repair (%)				0.00		5.14		16.76		42.76		56.75

Expt 7	U		0		1		2		3		4	
ML (+ or -)	+	-	+	-	+	-	+	-	+	-	+	-
Band Intensity	17842.80	21335.77	3681.75	12830.55	3315.23	10654.84	4373.92	11823.41	7288.74	13019.15	9202.64	15455.49
Intact fragment (%)		83.63		28.70		31.11		36.99		55.98		59.54
Damage (%)		16.37		71.30		68.89		63.01		44.02		40.46
Repair (%)				0.00		3.39		11.64		38.27		43.26

Summary	0	1	2	3	4
Mean Repair (%)	0.00	7.98	20.42	38.83	49.13
Standard Deviation	0.00	3.62	8.39	3.82	5.57

W303 (wild type), NTS

Expt 1	U		0		1		2		3		4	
ML (+ or -)	+	-	+	-	+	-	+	-	+	-	+	-
Band Intensity	42275.84	50628.63	16720.76	44995.94	9825.71	23296.44	9898.25	18212.04	16067.45	28203.88	26816.34	41163.17
Intact fragment (%)		83.50		37.16		42.18		54.35		56.97		65.15
Damage (%)		16.50		62.84		57.82		45.65		43.03		34.85
Repair (%)				0.00		7.98		27.35		31.52		44.54

Expt 2	U		0		1		2		3		4	
ML (+ or -)	+	-	+	-	+	-	+	-	+	-	+	-
Band Intensity	30512.96	31694.07	6812.43	16248.88	9824.82	21727.29	11988.48	22548.77	7218.30	10777.82	13534.81	18822.10
Intact fragment (%)		96.27		41.93		45.22		53.17		66.97		71.91
Damage (%)		3.73		58.07		54.78		46.83		33.03		28.09
Repair (%)				0.00		5.67		19.36		43.13		51.63

Expt 3	U		0		1		2		3		4	
ML (+ or -)	+	-	+	-	+	-	+	-	+	-	+	-
Band Intensity	7375.07	8693.26	1427.73	4923.50	1266.72	3723.05	1645.40	4276.17	2841.57	4983.98	3099.51	5149.44
Intact fragment (%)		84.84		29.00		34.02		38.48		57.01		60.19
Damage (%)		15.16		71.00		65.98		61.52		42.99		39.81
Repair (%)				0.00		7.08		13.35		39.46		43.93

Expt 4	U		0		1		2		3		4	
ML (+ or -)	+	-	+	-	+	-	+	-	+	-	+	-
Band Intensity	9768.41	10213.09	2787.86	14587.83	2022.47	7298.56	2710.40	7416.03	3730.26	7676.69	3166.66	6145.04
Intact fragment (%)		95.65		19.11		27.71		36.55		48.59		51.53
Damage (%)		4.35		80.89		72.29		63.45		51.41		48.47
Repair (%)				0.00		10.63		21.56		36.45		40.08

Expt 5	U		0		1		2		3		4	
ML (+ or -)	+	-	+	-	+	-	+	-	+	-	+	-
Band Intensity	26452.21	31393.96	12399.13	27432.65	10610.97	21103.55	11670.81	20998.21	18777.90	28649.08	23248.04	31513.06
Intact fragment (%)		84.26		45.20		50.28		55.58		65.54		73.77
Damage (%)		15.74		54.80		49.72		44.42		34.46		26.23
Repair (%)				0.00		9.27		18.94		37.13		52.14

Summary	0	1	2	3	4
Mean Repair (%)	0.00	8.13	20.11	37.54	46.46
Standard Deviation	0.00	1.92	5.05	4.26	5.24

rpd3 mutant, TS

Expt 1	U		0		1		2		3		4	
ML (+ or -)	+	-	+	-	+	-	+	-	+	-	+	-
Band Intensity	8689.59	11351.68	2137.79	7635.93	2891.14	8376.38	2987.14	6982.58	3927.96	7679.39	4881.11	8545.85
Intact fragment (%)		76.55		28.00		34.52		42.78		51.15		57.12
Damage (%)		23.45		72.00		65.48		57.22		48.85		42.88
Repair (%)				0.00		9.05		20.53		32.16		40.44

Expt 2	U		0		1		2		3		4	
ML (+ or -)	+	-	+	-	+	-	+	-	+	-	+	-
Band Intensity	2123.39	2012.58	984.22	3911.45	1015.47	3288.81	1452.70	3389.39	1553.07	3223.29	1921.58	3655.45
Intact fragment (%)		105.51		25.16		30.88		42.86		48.18		52.57
Damage (%)		-5.51		74.84		69.12		57.14		51.82		47.43
Repair (%)				0.00		7.64		23.65		30.76		36.62

Expt 3	U		0		1		2		3		4	
ML (+ or -)	+	-	+	-	+	-	+	-	+	-	+	-
Band Intensity	70421.87	68642.40	8680.87	44821.46	13540.95	46140.13	16878.07	45589.91	34697.01	70371.40	38504.39	72359.30
Intact fragment (%)		102.59		19.37		29.35		37.02		49.31		53.21
Damage (%)		-2.59		80.63		70.65		62.98		50.69		46.79
Repair (%)				0.00		12.38		21.89		37.13		41.97

Summary	0	1	2	3	4
Mean Repair (%)	0.00	9.69	22.02	33.35	39.68
Standard Deviation	0.00	2.43	1.56	3.35	2.76

rpd3 mutant, NTS

Expt 1	U		0		1		2		3		4	
ML (+ or -)	+	-	+	-	+	-	+	-	+	-	+	-
Band Intensity	54568.34	67688.94	14542.37	41415.45	17958.92	45838.80	22035.39	44727.92	25036.33	43731.87	26248.46	38934.59
Intact fragment (%)		80.62		35.11		39.18		49.27		57.25		67.42
Damage (%)		19.38		64.89		60.82		50.73		42.75		32.58
Repair (%)				0.00		6.26		21.81		34.12		49.78

Expt 2	U		0		1		2		3		4	
ML (+ or -)	+	-	+	-	+	-	+	-	+	-	+	-
Band Intensity	7143.03	7286.48	1492.61	3788.96	1962.88	4449.98	2349.28	4155.16	5854.72	9657.34	5894.90	8079.59
Intact fragment (%)		98.03		39.39		44.11		56.54		60.62		72.96
Damage (%)		1.97		60.61		55.89		43.46		39.38		27.04
Repair (%)				0.00		7.78		28.29		35.03		55.38

Expt 3	U		0		1		2		3		4	
ML (+ or -)	+	-	+	-	+	-	+	-	+	-	+	-
Band Intensity	18223.20	18202.96	2665.84	12125.83	4469.71	13007.61	5031.13	11619.30	9014.36	19186.01	12744.19	21323.90
Intact fragment (%)		100.11		21.98		34.36		43.30		46.98		59.76
Damage (%)		-0.11		78.02		65.64		56.70		53.02		40.24
Repair (%)				0.00		15.87		27.32		32.04		48.43

Summary	0	1	2	3	4
Mean Repair (%)	0.00	9.97	27.13	33.73	51.20
Standard Deviation	0.00	5.17	5.23	1.53	3.69

hda1 mutant, TS

Expt 1	U		0		1		2		3		4	
ML (+ or -)	+	-	+	-	+	-	+	-	+	-	+	-
Band Intensity	12429.55	12909.44	3325.33	8307.33	5297.31	11524.35	6392.64	12533.55	7614.14	12482.82	9162.69	12318.73
Intact fragment (%)		96.28		40.03		45.97		51.00		61.00		74.38
Damage (%)		3.72		59.97		54.03		49.00		39.00		25.62
Repair (%)				0.00		9.90		18.30		34.96		57.28

Expt 2	U		0		1		2		3		4	
ML (+ or -)	+	-	+	-	+	-	+	-	+	-	+	-
Band Intensity	6814.88	8276.47	1045.76	2617.37	1499.48	3008.32	2478.86	4499.80	2134.02	3626.70	3918.16	5752.12
Intact fragment (%)		82.34		39.95		49.84		55.09		58.84		68.12
Damage (%)		17.66		60.05		50.16		44.91		41.16		31.88
Repair (%)				0.00		16.47		25.20		31.46		46.90

Expt 3	U		0		1		2		3		4	
ML (+ or -)	+	-	+	-	+	-	+	-	+	-	+	-
Band Intensity	51447.16	55403.23	16806.80	46621.53	21743.32	47886.88	31835.01	53533.35	37792.79	55655.96	33738.93	48211.27
Intact fragment (%)		92.86		36.05		45.41		59.47		67.90		69.98
Damage (%)		7.14		63.95		54.59		40.53		32.10		30.02
Repair (%)				0.00		14.63		36.62		49.81		53.06

Expt 4	U		0		1		2		3		4	
ML (+ or -)	+	-	+	-	+	-	+	-	+	-	+	-
Band Intensity	16254.23	20193.67	4765.93	15243.11	7650.81	18649.63	8269.93	18564.74	13191.22	25353.14	9843.52	16536.61
Intact fragment (%)		80.49		31.27		41.02		44.55		52.03		59.53
Damage (%)		19.51		68.73		58.98		55.45		47.97		40.47
Repair (%)				0.00		14.20		19.32		30.21		41.11

Expt 5	U		0		1		2		3		4	
ML (+ or -)	+	-	+	-	+	-	+	-	+	-	+	-
Band Intensity	79473.79	55337.58	24443.93	89339.17	22754.46	67448.33	43856.32	121329.10	68564.38	121733.57	57505.03	89194.77
Intact fragment (%)		143.62		27.36		33.74		36.15		56.32		64.47
Damage (%)		-43.62		72.64		66.26		63.85		43.68		35.53
Repair (%)				0.00		8.78		12.10		39.87		51.09

Summary	0	1	2	3	4
Mean Repair (%)	0.00	12.79	22.31	37.26	49.89
Standard Deviation	0.00	3.29	9.25	7.95	6.17

hda1 mutant, NTS

Expt 1	U		0		1		2		3		4	
ML (+ or -)	+	-	+	-	+	-	+	-	+	-	+	-
Band Intensity	98539.94	92060.07	15195.14	32907.16	9218.33	17404.28	15986.41	24380.34	20651.56	29941.75	14307.59	18685.10
Intact fragment (%)		107.04		46.18		52.97		65.57		68.97		76.57
Damage (%)		-7.04		53.82		47.03		34.43		31.03		23.43
Repair (%)				0.00		12.62		36.03		42.35		56.47

Expt 2	U		0		1		2		3		4	
ML (+ or -)	+	-	+	-	+	-	+	-	+	-	+	-
Band Intensity	19120.07	19524.66	6698.78	16994.58	10229.83	19939.25	10826.88	18918.85	13665.06	21090.41	17772.43	26755.62
Intact fragment (%)		97.93		39.42		51.30		57.23		64.79		66.43
Damage (%)		2.07		60.58		48.70		42.77		35.21		33.57
Repair (%)				0.00		19.62		29.40		41.89		44.58

Expt 3	U		0		1		2		3		4	
ML (+ or -)	+	-	+	-	+	-	+	-	+	-	+	-
Band Intensity	20413.05	16251.96	8077.06	22852.83	8200.66	17790.80	13834.78	26150.54	17756.78	30479.07	15813.09	22431.88
Intact fragment (%)		125.60		35.34		46.09		52.90		58.26		70.49
Damage (%)		-25.60		64.66		53.91		47.10		41.74		29.51
Repair (%)				0.00		16.63		27.16		35.44		54.36

Summary	0	1	2	3	4
Mean Repair (%)	0.00	16.29	32.97	37.79	51.80
Standard Deviation	0.00	3.51	8.20	3.57	6.34

DY 6445 (*rpd3hos1hos2* mutant), TS

Expt 1	U		0		1		2		3		4	
ML (+ or -)	+	-	+	-	+	-	+	-	+	-	+	-
Band Intensity	56575.65	61807.73	1339.08	4326.73	2064.80	4497.17	19250.44	35015.81	35264.51	43350.43	37184.95	41540.61
Intact fragment (%)		91.53		30.95		45.91		54.98		81.35		89.51
Damage (%)		8.47		69.05		54.09		45.02		18.65		10.49
Repair (%)				0.00		21.67		34.80		72.99		84.82

Expt 2	U		0		1		2		3		4	
ML (+ or -)	+	-	+	-	+	-	+	-	+	-	+	-
Band Intensity	59586.45	68858.40	9385.82	32611.00	22955.57	49681.59	51552.51	78227.50	31947.45	44295.99	2187.62	2499.20
Intact fragment (%)		86.53		28.78		46.02		65.90		72.12		87.53
Damage (%)		13.47		71.22		53.98		34.10		27.88		12.47
Repair (%)				0.00		24.21		52.12		60.86		82.49

Expt 3	U		0		1		2		3		4	
ML (+ or -)	+	-	+	-	+	-	+	-	+	-	+	-
Band Intensity	5837.49	6035.82	3829.95	7280.21	3026.04	4539.07	3105.88	4183.33	3611.25	4614.50	4668.64	5576.11
Intact fragment (%)		96.71		52.61		66.67		74.24		78.26		83.73
Damage (%)		3.29		47.39		33.33		25.76		21.74		16.27
Repair (%)				0.00		29.66		45.65		54.12		65.66

Summary	0	1	2	3	4
Mean Repair (%)	0.00	25.18	44.19	62.65	77.66
Standard Deviation	0.00	4.08	8.76	9.56	10.46

DY 6445 (*rpd3hos1hos2* mutant), NTS

Expt 1	U		0		1		2		3		4	
ML (+ or -)	+	-	+	-	+	-	+	-	+	-	+	-
Band Intensity	5714.19	4963.77	518.59	2623.61	1831.62	3872.69	164.19	296.25	2974.28	4906.23	2059.75	3221.47
Intact fragment (%)		115.12		19.77		47.30		55.42		60.62		63.94
Damage (%)		-15.12		80.23		52.70		44.58		39.38		36.06
Repair (%)				0.00		34.31		44.44		50.92		55.05

Expt 2	U		0		1		2		3		4	
ML (+ or -)	+	-	+	-	+	-	+	-	+	-	+	-
Band Intensity	12490.83	14950.61	189.96	785.88	4501.36	9347.87	571.41	951.38	7521.86	9952.58	8270.54	9185.26
Intact fragment (%)		83.55		24.17		48.15		60.06		75.58		90.04
Damage (%)		16.45		75.83		51.85		39.94		24.42		9.96
Repair (%)				0.00		31.63		47.33		67.79		86.87

Expt 3	U		0		1		2		3		4	
ML (+ or -)	+	-	+	-	+	-	+	-	+	-	+	-
Band Intensity	138810.16	174499.84	155523.35	499835.54	139780.85	278749.38	319708.66	531954.88	291513.67	450676.41	279414.20	398330.81
Intact fragment (%)		79.55		31.11		50.15		60.10		64.68		70.15
Damage (%)		20.45		68.89		49.85		39.90		35.32		29.85
Repair (%)				0.00		27.63		42.08		48.73		56.66

Expt 4	U		0		1		2		3		4	
ML (+ or -)	+	-	+	-	+	-	+	-	+	-	+	-
Band Intensity	11429.28	15950.10	14117.69	33583.87	20737.26	38142.54	21389.32	31438.05	21131.13	27825.41	22350.27	25301.92
Intact fragment (%)		71.66		42.04		54.37		68.04		75.94		88.33
Damage (%)		28.34		57.96		45.63		31.96		24.06		11.67
Repair (%)				0.00		21.27		44.86		58.49		79.87

Summary	0	1	2	3	4
Mean Repair (%)	0.00	28.71	44.68	56.48	69.61
Standard Deviation	0.00	5.67	2.15	8.62	16.15

DY 6446 (*rpd3hos1hda1* mutant), TS

Expt 1	U		0		1		2		3		4	
ML (+ or -)	+	-	+	-	+	-	+	-	+	-	+	-
Band Intensity	70060.58	82823.00	28187.95	64203.98	34504.01	59632.39	36022.26	55396.21	55356.96	76347.56	61968.32	82119.66
Intact fragment (%)		84.59		43.90		57.86		65.03		72.51		75.46
Damage (%)		15.41		56.10		42.14		34.97		27.49		24.54
Repair (%)				0.00		24.88		37.65		50.99		56.26

Expt 2	U		0		1		2		3		4	
ML (+ or -)	+	-	+	-	+	-	+	-	+	-	+	-
Band Intensity	1523.40	1839.51	1092.49	2668.01	1369.24	2497.95	1325.44	2088.77	1316.88	1807.57	1369.72	1750.79
Intact fragment (%)		82.82		40.95		54.81		63.46		72.85		78.23
Damage (%)		17.18		59.05		45.19		36.54		27.15		21.77
Repair (%)				0.00		23.48		38.12		54.03		63.14

Expt 3	U		0		1		2		3		4	
ML (+ or -)	+	-	+	-	+	-	+	-	+	-	+	-
Band Intensity	536.65	673.62	286.33	699.99	276.68	500.12	342.31	558.97	330.32	459.47	297.55	353.64
Intact fragment (%)		79.67		40.91		55.32		61.24		71.89		84.14
Damage (%)		20.33		59.09		44.68		38.76		28.11		15.86
Repair (%)				0.00		24.40		34.41		52.43		73.16

Summary	0	1	2	3	4
Mean Repair (%)	0.00	24.25	36.73	52.48	64.18
Standard Deviation	0.00	0.71	2.02	1.52	8.50

DY 6446 (*rpd3hos1hda1* mutant), TS

Expt 1	U		0		1		2		3		4	
ML (+ or -)	+	-	+	-	+	-	+	-	+	-	+	-
Band Intensity	1618.81	1225.31	504.51	893.58	639.60	880.53	667.42	857.76	1094.00	1370.88	1200.41	1448.16
Intact fragment (%)		132.11		56.46		72.64		77.81		79.80		82.89
Damage (%)		-32.11		43.54		27.36		22.19		20.20		17.11
Repair (%)				0.00		37.16		49.03		53.61		60.71

Expt 2	U		0		1		2		3		4	
ML (+ or -)	+	-	+	-	+	-	+	-	+	-	+	-
Band Intensity	2028.93	1862.24	1049.30	2269.87	1858.92	3227.91	1932.89	2811.53	2895.07	3894.41	2932.88	3594.50
Intact fragment (%)		108.95		46.23		57.59		68.75		74.34		81.59
Damage (%)		-8.95		53.77		42.41		31.25		25.66		18.41
Repair (%)				0.00		21.13		41.88		52.28		65.77

Expt 3	U		0		1		2		3		4	
ML (+ or -)	+	-	+	-	+	-	+	-	+	-	+	-
Band Intensity	33826.07	37540.96	8125.17	18608.81	12704.14	23676.44	12904.13	19085.55	11809.50	15957.07	16382.93	21177.95
Intact fragment (%)		90.10		43.66		53.66		67.61		74.01		77.36
Damage (%)		9.90		56.34		46.34		32.39		25.99		22.64
Repair (%)				0.00		17.74		42.51		53.86		59.81

Summary	0	1	2	3	4
Mean Repair (%)	0.00	25.34	44.47	53.25	62.10
Standard Deviation	0.00	10.37	3.96	0.85	3.21

A III.4 NER of CPDs at *MFA2*, at the level of the nucleotide – high resolution analysis

Full data sets for two experiments per strain, for the TS and NTS are provided. Due to the large number of gels, the remaining data are summarised in table AIII.4-7, giving the mean time taken to repair 50% of CPDs at each specified position for the *MFA2* TS and NTS of each strain, with standard deviations.

AIII.4-1 W303 (wild type), TS

(i) Band density values (peak area)

CPD	Expt 1					CPD	Expt 2				
Position	0	1	2	3	4	Position	0	1	2	3	4
Top Bands	62990	47945	14223	11558	136877	Top Bands	117730	89422	40183	20444	9272
481	1969	2427	1785	1491	3498	481	3169	2025	863	221	119
453	1111	1659	1170	912	1694	453	902	624	145	192	111
434	2428	2649	1478	1105	3017	434	2332	1381	636	236	185
404	1163	1135	730	596	1619	404	4625	3079	1118	610	298
370	3148	3000	1477	1056	2549	370	1939	1170	392	260	82
316	352	331	175	142	337	316	6362	4325	1529	472	219
238	913	763	318	337	557	238	5016	3872	1486	474	263
224	2136	2334	1071	805	1601	224	968	723	324	118	76
177	2787	2122	1138	797	1547	177	1143	836	361	170	73
135	1153	1417	766	680	1865	135	297	204	82	58	24
122	1661	1845	1080	851	1824	122	1175	864	297	128	71
100	608	711	483	445	995	100	943	755	204	132	85
88	542	551	450	195	435	88	1527	1009	237	163	83
82	1027	750	429	309	824	82	2850	2369	744	345	168
71	488	431	259	166	255	71	2519	2179	550	271	137
42	951	646	264	180	275	42	667	557	210	93	46
27	2065	1985	1195	823	1875	27	9893	6738	2029	904	397
6	1474	1662	877	705	1492	6	2752	1573	475	145	78
-5	403	534	327	196	493	-5	11637	7904	2402	956	578
-65	228	145	63	84	478	-65	2164	1496	518	188	101
-77	6109	6952	3510	2296	4994	-77	3208	2198	667	184	121
-89	2217	2052	942	642	1464	-89	3626	2460	686	245	183
-115	7427	7797	3996	2581	5811	-115	938	755	258	144	83
-122	1659	1605	951	720	1783	-122	1321	1031	350	186	102
-130	2670	2108	951	661	1311	-130	4478	4049	1463	530	289
-150	1895	2325	1313	752	1559	-150	1911	1665	661	434	400
-156	686	793	462	255	743	-156	864	1063	491	420	268
-164	268	132	121	133	952	-164					
-172	552	753	586	394	863	-172					
-188	3458	3790	2227	1617	2927	-188					
-190	1456	1206	799	635	1277	-190					
-213						-213					
Total	117997	104558	45615	34119	187791	Total	196957	146325	59360	28723	13913
Ratio	1.00	0.89	0.39	0.29	1.59	Ratio	1.00	0.74	0.30	0.15	0.07

(ii) Adjusted band density values

CPD Position	Expt 1					CPD Position	Expt 2				
	0	1	2	3	4		0	1	2	3	4
481	1969	2739	4618	5155	2198	481	3169	2726	2864	1513	1682
453	1111	1873	3026	3155	1064	453	902	840	481	1313	1573
434	2428	2990	3823	3821	1896	434	2332	1859	2112	1619	2618
404	1163	1281	1888	2060	1018	404	4625	4145	3711	4183	4225
370	3148	3386	3820	3653	1602	370	1939	1574	1300	1783	1157
316	352	374	452	492	212	316	6362	5821	5073	3237	3097
238	913	861	823	1164	350	238	5016	5212	4930	3253	3728
224	2136	2634	2770	2782	1006	224	968	973	1075	806	1075
177	2787	2395	2944	2756	972	177	1143	1125	1196	1162	1031
135	1153	1599	1983	2352	1172	135	297	274	274	401	344
122	1661	2082	2793	2944	1146	122	1175	1163	985	880	1004
100	608	802	1250	1539	625	100	943	1017	678	907	1203
88	542	622	1164	676	274	88	1527	1359	785	1114	1181
82	1027	847	1109	1069	518	82	2850	3188	2468	2369	2376
71	488	486	670	576	160	71	2519	2933	1824	1856	1945
42	951	730	682	621	173	42	667	749	696	638	650
27	2065	2241	3090	2845	1178	27	9893	9069	6731	6202	5623
6	1474	1876	2268	2440	938	6	2752	2118	1577	993	1110
-5	403	603	846	677	310	-5	11637	10639	7969	6553	8187
-65	228	164	163	291	300	-65	2164	2014	1719	1287	1429
-77	6109	7846	9080	7939	3138	-77	3208	2958	2213	1263	1709
-89	2217	2315	2438	2221	920	-89	3626	3311	2275	1683	2592
-115	7427	8799	10337	8926	3652	-115	938	1016	855	987	1176
-122	1659	1812	2460	2492	1120	-122	1321	1387	1162	1278	1441
-130	2670	2379	2460	2286	824	-130	4478	5450	4853	3635	4091
-150	1895	2624	3397	2601	979	-150	1911	2241	2194	2975	5657
-156	686	895	1195	881	467	-156	864	1431	1629	2882	3791
-164	268	148	314	460	598	-164					
-172	552	850	1515	1364	543	-172					
-188	3458	4277	5760	5593	1839	-188					
-190	1456	1361	2067	2195	802	-190					
-213						-213					
Total	55007	63890	81204	78026	31991	Total	79227	76593	63628	56775	65696

(iii) Signal remaining (%)

CPD Position	Expt 1					T50%	CPD Position	Expt 2					T50%
	0	1	2	3	4			0	1	2	3	4	
481	100	139	235	262	112	4.6	481	100	86	90	48	53	3.8
453	100	169	272	284	96	4.4	453	100	93	53	146	174	
434	100	123	157	157	78	4.5	434	100	80	91	69	112	
404	100	110	162	177	87	4.7	404	100	90	80	90	91	
370	100	108	121	116	51	4.1	370	100	81	67	92	60	
316	100	106	128	140	60	4.3	316	100	91	80	51	49	3.6
238	100	94	90	128	38	4.1	238	100	104	98	65	74	5.2
224	100	123	130	130	47	4.1	224	100	100	111	83	111	
177	100	86	106	99	35	4.1	177	100	98	105	102	90	
135	100	139	172	204	102	4.7	135	100	92	92	135	116	
122	100	125	168	177	69	4.4	122	100	99	84	75	85	
100	100	132	206	253	103	4.7	100	100	108	72	96	128	
88	100	115	215	125	50	4	88	100	89	51	73	77	
82	100	82	108	104	50	4	82	100	112	87	83	83	
71	100	100	137	118	33	4.1	71	100	116	72	74	77	
42	100	77	72	65	18	3.3	42	100	112	104	96	97	
27	100	109	150	138	57	4.1	27	100	92	68	63	57	4.2
6	100	127	154	165	64	4.2	6	100	77	57	36	40	2..3
-5	100	149	210	168	77	4.3	-5	100	91	68	56	70	4.8
-65	100	72	71	128	132		-65	100	93	79	59	66	4.8
-77	100	128	149	130	51	4.1	-77	100	92	69	39	53	3.4
-89	100	104	110	100	42	3.8	-89	100	91	63	46	71	2.8
-115	100	118	139	120	49	4	-115	100	108	91	105	125	
-122	100	109	148	150	68	4.2	-122	100	105	88	97	109	
-130	100	89	92	86	31	3.6	-130	100	122	108	81	91	
-150	100	138	179	137	52	4.1	-150	100	117	115	156	296	
-156	100	130	174	128	68	4.2	-156	100	166	189	334	439	
-164	100	55	117	172	223		-164						
-172	100	154	274	247	98		-172						
-188	100	124	167	162	53	4.1	-188						
-190	100	93	142	151	55	4.1	-190						
-213							-213						
Total	100	116	148	142	58	4.1	Total	100	97	80	72	83	

AIII.4-2 W303 (wild type), NTS

(i) Band density values (peak area)

CPD Position	Expt 1					CPD Position	Expt 2				
	0	1	2	3	4		0	1	2	3	4
Top Bands	66691	54366	54072	45207	42289	Top Bands	66848	48709	27009	6994	7444
-220	3777	3386	3145	1879	756	-220	5995	3861	1874	432	220
-222	572	493	278	170	84	-222	704	357	105	43	26
-85	2798	2496	2414	1367	868	-85	476	356	141	66	38
-45	814	717	704	418	268	-45	1123	767	419	154	127
14	973	826	924	512	298	14	731	440	263	74	46
38	5498	5299	5090	3502	2170	38	1767	1045	366	86	69
63	286	278	294	160	57	63	1768	1042	389	144	114
92	1475	1435	1234	648	340	92	3481	2238	1176	335	205
126	171	190	195	140	98	126	4607	2667	1538	455	182
160	463	379	81	239	453	160	3023	1846	1004	286	121
196	2194	2100	1966	1525	1051	196	2434	1550	888	259	125
230	2511	2217	2069	1371	798	230	2249	1411	746	200	113
260	222	303	193	133	138	260	985	559	278	73	34
270	308	305	298	296	283	270	324	223	99	40	24
280	559	388	407	250	446	280	1555	787	303	75	69
296	689	859	753	573	369	296	1800	1159	583	178	92
310	2139	1714	1783	1341	920	310	5321	3040	1370	344	181
329	464	432	450	364	237	329	3822	2466	1176	344	200
339	328	269	266	218	166	339	265	145	62	34	23
350	2340	2127	2144	1451	950	350	557	242	109	42	27
380	2373	2097	1933	1357	853	380	581	235	102	35	40
390	377	458	435	311	199	390	971	652	244	110	74
400	4471	3665	3125	1902	993	400	4651	2617	1225	347	167
406	129	98	46	78	120	406	671	308	126	57	42
412	529	635	561	373	229	412	1719	1049	389	173	123
418	551	408	362	281	174	418	460	186	73	86	59
424	565	777	710	465	295	424	1449	708	323	127	67
432	442	367	272	199	141	432	1069	636	292	206	133
448	955	700	527	453	370	448	2357	1316	639	171	98
456	278	162	130	85	61	456	905	438	262	117	109
472	3098	2466	1600	991	688	472	477	322	311	188	258
477	2759	2576	2430	1905	1151	477	579	346	257	169	151
495						495	1579	841	548	365	300
Total	111802	94990	90888	70165	58313	Total	130195	86148	45322	13086	11338
Ratio	1.00	0.85	0.81	0.63	0.52	Ratio	1.00	0.66	0.35	0.10	0.09

(ii) Adjusted band density values

CPD Position	Expt 1 0	1	2	3	4	CPD Position	Expt 2 0	1	2	3	4
-220	3777	3985	3868	2994	1450	-220	5995	5835	5383	4302	2525
-222	572	580	342	271	161	-222	704	539	301	430	299
-85	2798	2938	2970	2178	1664	-85	476	538	406	658	442
-45	814	844	866	665	514	-45	1123	1160	1203	1530	1463
14	973	973	1136	816	572	14	731	665	756	738	532
38	5498	6237	6261	5580	4160	38	1767	1579	1052	860	793
63	286	327	362	255	109	63	1768	1574	1116	1433	1311
92	1475	1689	1518	1032	651	92	3481	3382	3378	3333	2352
126	171	224	240	224	188	126	4607	4030	4418	4528	2089
160	463	446	99	381	868	160	3023	2791	2885	2850	1385
196	2194	2471	2418	2430	2014	196	2434	2343	2551	2579	1438
230	2511	2609	2545	2185	1531	230	2249	2132	2142	1994	1293
260	222	357	237	212	265	260	985	844	798	725	395
270	308	359	367	471	543	270	324	337	283	397	277
280	559	456	501	398	855	280	1555	1189	871	750	787
296	689	1011	927	913	708	296	1800	1752	1675	1775	1060
310	2139	2018	2193	2136	1763	310	5321	4594	3934	3422	2082
329	464	509	553	579	455	329	3822	3727	3377	3419	2299
339	328	317	327	347	319	339	265	219	178	343	260
350	2340	2503	2637	2313	1821	350	557	365	313	416	307
380	2373	2469	2378	2162	1636	380	581	356	293	345	460
390	377	539	535	496	381	390	971	986	700	1090	849
400	4471	4313	3844	3031	1904	400	4651	3955	3518	3455	1915
406	129	115	57	125	230	406	671	465	362	566	481
412	529	747	690	595	439	412	1719	1585	1116	1719	1408
418	551	480	445	448	334	418	460	281	209	852	673
424	565	914	873	740	566	424	1449	1070	929	1263	768
432	442	432	334	317	270	432	1069	961	840	2045	1529
448	955	824	648	722	709	448	2357	1989	1835	1698	1130
456	278	191	160	136	116	456	905	662	753	1165	1246
472	3098	2903	1969	1580	1320	472	477	487	893	1874	2957
477	2759	3032	2989	3035	2207	477	579	522	739	1679	1736
495						495	1579	1271	1574	3629	3444
Total	45112	47814	45288	39768	30723	Total	63346	56581	52606	60615	44716

(iii) Signal remaining (%)

CPD Position	Expt 1 0	1	2	3	4	T50%	CPD Position	Expt 1 0	1	2	3	4	T50%
-220	100	106	102	79	38	3.7	-220	100	97	90	72	42	3.7
-222	100	101	60	47	28	2.8	-222	100	77	43	61	42	2.5
-85	100	105	106	78	59	4.2	-85	100	113	85	138	93	
-45	100	104	106	82	63	4.3	-45	100	103	107	136	130	
14	100	100	117	84	59	4.2	14	100	91	103	101	73	5.2
38	100	113	114	101	76	4.2	38	100	89	60	49	45	2.8
63	100	114	127	89	38	3.8	63	100	89	63	81	74	
92	100	115	103	70	44	3.8	92	100	97	97	96	68	4.8
126	100	131	140	131	110		126	100	87	96	98	45	4.1
160	100	96	21	82	188	1.7	160	100	92	95	94	46	4
196	100	113	110	111	92		196	100	96	105	106	59	4.4
230	100	104	101	87	61	4.3	230	100	95	95	89	57	4.4
260	100	161	107	95	119		260	100	86	81	74	40	3.7
270	100	116	119	153	176		270	100	104	87	123	85	
280	100	82	90	71	153		280	100	76	56	48	51	2.8
296	100	147	134	133	103	5	296	100	97	93	99	59	4.5
310	100	94	103	100	82		310	100	86	74	64	39	3.6
329	100	110	119	125	96		329	100	98	88	89	60	4.6
339	100	97	100	106	97		339	100	83	67	130	98	
350	100	107	113	99	78	4.9	350	100	66	56	75	55	4.5
380	100	104	100	91	69	4.7	380	100	61	50	59	79	2
390	100	143	142	132	101		390	100	101	72	112	87	
400	100	96	86	68	43	3.7	400	100	85	76	74	41	3.7
406	100	90	44	97	179	1.9	406	100	69	54	84	72	
412	100	141	130	112	83	4.5	412	100	92	65	100	82	
418	100	87	81	81	61		418	100	61	45	185	146	
424	100	162	154	131	100		424	100	74	64	87	53	5.1
432	100	98	76	72	61		432	100	90	79	191	143	
448	100	86	68	76	74	2.7	448	100	84	78	72	48	3.9
456	100	69	58	49	42	2.5	456	100	73	83	129	138	
472	100	94	64	51	43	3	472	100	102	187	393	620	
477	100	110	108	110	80		477	100	90	128	290	300	
495								100	80	100	230	218	
Total	100	106	100	88	68	4.6	Total	100	89	83	96	71	

AIII.4-3 DY 6445 (*rpd3hos1hos2* mutant), TS

(i) Band density values (peak area)

CPD Position	Expt 1					CPD Position	Expt 2				
	0	1	2	3	4		0	1	2	3	4
Top Bands	13683	8814	40239	35675	18318	Top Bands	21078	13245	24531	16576	38310
481	1009	693	2029	1064	348	481	662	474	919	403	634
453	590	337	871	368	108	453	120	82	140	52	79
434	690	544	1371	749	249	434	324	189	319	142	170
404	189	126	360	304	155	404	834	638	1010	450	554
370	843	571	1363	741	244	370	71	76	62	44	42
316	92	61	219	89	60	316	51	34	34	21	16
238	328	199	445	190	63	238	86	75	133	59	38
224	728	420	1187	555	117	224	269	146	274	164	223
177	572	498	891	489	201	177	889	647	826	358	401
135	403	270	732	554	233	135	109	129	151	73	76
122	478	392	1066	610	220	122	129	100	167	75	82
100	190	167	417	236	135	100	360	193	342	122	161
88	168	109	322	116	66	88	1406	825	1447	574	741
82	256	206	362	169	95	82	421	317	497	257	376
71	144	87	140	75	42	71	581	434	784	400	542
42	281	195	238	119	72	42	185	162	231	135	177
27	390	220	574	279	44	27	269	172	344	141	172
6	289	174	384	221	64	6	326	200	264	123	154
-5	126	92	178	97	42	-5	305	187	312	118	157
-65	101	89	133	128	59	-65	359	230	327	163	155
-77	1768	1006	2127	1127	337	-77	723	359	567	285	338
-89	642	375	813	504	118	-89	805	463	533	244	309
-115	2143	1270	2640	1280	393	-115	234	180	244	143	150
-122	526	395	646	435	103	-122	2263	1517	2079	970	1127
-130	661	320	745	575	98	-130	681	370	476	214	246
-150	692	437	723	265	153	-150	1839	1218	1968	744	818
-156	181	130	250	138	76	-156	519	279	502	266	382
-164	55	42	190	186	48	-164	738	384	547	204	240
-172	171	115	294	156	85	-172	618	543	641	354	270
-188	841	572	1351	667	234	-188	239	194	179	160	118
-190	411	263	657	517	401	-190	268	344	410	226	293
-213						-213					
Total	29643	19188	63956	48679	22981	Total	37760	24407	41259	24260	47550
Ratio	1.00	0.65	2.16	1.64	0.78	Ratio	1.00	0.65	1.09	0.64	1.26

(ii) Adjusted band density values

CPD Position	Expt 1					CPD Position	Expt 2				
	0	1	2	3	4		0	1	2	3	4
481	1009	1070	940	648	449	481	662	734	841	627	504
453	590	521	404	224	139	453	120	127	129	81	63
434	690	841	636	456	321	434	324	293	292	221	135
404	189	195	167	185	200	404	834	987	924	700	440
370	843	881	632	451	315	370	71	117	57	69	33
316	92	94	101	54	78	316	51	53	31	32	13
238	328	307	206	116	81	238	86	116	121	91	30
224	728	649	550	338	151	224	269	226	251	256	177
177	572	769	413	298	259	177	889	1000	756	557	318
135	403	416	339	337	300	135	109	199	138	114	60
122	478	605	494	371	283	122	129	154	153	116	65
100	190	258	193	143	174	100	360	299	313	190	128
88	168	168	149	71	85	88	1406	1276	1325	893	589
82	256	318	168	103	122	82	421	490	455	400	299
71	144	134	65	46	54	71	581	671	718	623	430
42	281	301	110	72	93	42	185	251	211	210	141
27	390	340	266	170	57	27	269	266	315	219	136
6	289	269	178	135	83	6	326	309	241	191	123
-5	126	141	82	59	54	-5	305	290	285	184	125
-65	101	138	62	78	76	-65	359	355	299	254	123
-77	1768	1555	986	686	435	-77	723	555	519	444	268
-89	642	580	377	307	152	-89	805	716	488	379	246
-115	2143	1961	1224	780	507	-115	234	278	223	222	119
-122	526	610	300	265	133	-122	2263	2347	1903	1510	895
-130	661	494	345	350	126	-130	681	573	435	333	195
-150	692	674	335	161	197	-150	1839	1885	1801	1159	649
-156	181	200	116	84	98	-156	519	432	459	414	303
-164	55	64	88	114	62	-164	738	594	500	317	191
-172	171	178	136	95	109	-172	618	840	587	551	214
-188	841	884	626	406	302	-188	239	301	164	249	93
-190	411	407	305	315	517	-190	268	533	376	351	232
-213						-213					
Total	15960	16026	10993	7919	6015	Total	16682	17269	15309	11960	7337

(iii) Signal remaining (%)

CPD Position	Expt 1					T50%	CPD Position	Expt 2					T50%
	0	1	2	3	4			0	1	2	3	4	
481	100	106	93	64	44	3.7	481	100	111	127	95	76	
453	100	88	68	38	24	2.6	453	100	106	107	67	52	3.9
434	100	122	92	66	47	3.7	434	100	90	90	68	42	3.7
404	100	103	88	98	106		404	100	118	111	84	53	4.1
370	100	105	75	54	37	3.2	370	100	165	80	97	46	4.1
316	100	102	110	59	84	3.2	316	100	104	62	63	25	3.2
238	100	94	63	35	25	2.5	238	100	135	141	106	35	3.8
224	100	89	76	46	21	2.9	224	100	84	94	95	66	
177	100	134	72	52	45	3.3	177	100	113	85	63	36	3.5
135	100	103	84	84	74		135	100	183	127	105	55	4.3
122	100	127	103	78	59	4.1	122	100	119	118	90	51	4.1
100	100	136	101	75	91		100	100	83	87	53	36	3.2
88	100	100	89	42	50	2.9	88	100	91	94	64	42	3.6
82	100	124	65	40	48	2.6	82	100	116	108	95	71	4.5
71	100	93	45	32	38	2.1	71	100	116	124	107	74	
42	100	107	39	26	33	2	42	100	136	114	114	76	
27	100	87	68	44	15	2.7	27	100	99	117	82	51	4
6	100	93	62	47	29	2.8	6	100	95	74	59	38	3.4
-5	100	112	65	47	43	2.8	-5	100	95	93	60	41	3.5
-65	100	136	61	77	75		-65	100	99	83	71	34	3.5
-77	100	88	56	39	25	2.3	-77	100	77	72	61	37	3.4
-89	100	90	59	48	24	2.7	-89	100	89	61	47	31	2.8
-115	100	92	57	36	24	2.3	-115	100	119	95	95	51	4.1
-122	100	116	57	50	25	3	-122	100	104	84	67	40	3.6
-130	100	75	52	53	19	2.5	-130	100	84	64	49	29	2.9
-150	100	97	48	23	28	2	-150	100	103	98	63	35	3.5
-156	100	111	64	46	54	2.8	-156	100	83	89	80	58	4.7
-164	100	118	161	208	114		-164	100	81	68	43	26	2.7
-172	100	104	80	56	64		-172	100	136	95	89	35	3.7
-188	100	105	74	48	36	2.9	-188	100	126	68	104	39	4
-190	100	99	74	77	126		-190	100	199	140	131	87	
-213							-213						
Total	100	100	69	50	38	3	Total	100	104	92	72	44	3.8

AIII.4-4 DY 6445 (*rpd3hos1hos2* mutant), NTS

(i) Band density values (peak area)

CPD Position	Expt 1					CPD Position	Expt 2				
	0	1	2	3	4		0	1	2	3	4
Top Bands	7987	5054	7860	8026	8573	Top Bands	12488	8771	15015	14592	24610
-220	607	327	400	352	208	-220	82	92	127	39	24
-222	103	59	56	52	48	-222	232	225	343	236	287
-85	469	262	311	168	228	-85	225	212	276	224	339
-45	117	67	89	55	66	-45	1224	1192	1517	1105	1182
14	84	56	69	43	58	14	242	182	235	104	106
38	950	507	629	501	401	38	150	152	185	115	159
63	27	19	16	17	20	63	301	297	409	280	374
92	423	158	126	63	34	92	85	104	90	86	77
126	77	33	32	15	22	126	195	197	257	216	215
160	349	42	227	57	108	160	586	539	667	379	331
196	273	173	243	205	188	196	547	436	508	305	236
230	347	174	260	158	119	230	1323	1177	1300	856	799
260	53	62	41	43	39	260	1064	326	429	367	413
270	474	56	96	52	69	270	202	191	292	214	230
280	214	87	104	73	152	280	410	322	419	297	343
296	200	135	161	104	119	296	558	448	622	489	513
310	280	132	194	151	145	310	556	409	511	385	343
329	79	49	75	56	39	329	200	155	169	109	92
339	117	49	47	49	57	339	310	160	160	91	74
350	374	177	187	131	101	350	369	305	386	285	239
380	413	240	276	203	165	380	430	343	322	196	190
390	68	67	53	44	35	390	710	492	599	295	288
400	688	389	382	226	156	400	787	711	737	418	437
406	94	27	79	22	57	406	216	145	132	102	74
412	178	95	91	51	40	412	1181	982	989	633	527
418	106	54	51	45	33	418	187	109	109	75	51
424	227	130	88	32	29	424	538	300	428	178	202
432	81	56	59	38	39	432	321	206	234	110	120
448	491	113	118	87	81	448	217	94	141	81	79
456	44	26	22	13	22	456	872	608	621	323	343
472	586	293	237	125	139	472					
477	643	534	610	377	445	477					
495						495					
Total	17220	9701	13286	11637	12036	Total	26808	19884	28229	23183	33297
Ratio	1.00	0.56	0.77	0.68	0.70	Ratio	1.00	0.74	1.05	0.86	1.24

(ii) Adjusted band density values

CPD Position	Expt 1					CPD Position	Expt 2				
	0	1	2	3	4		0	1	2	3	4
-220	607	581	518	520	297	-220	82	125	121	45	19
-222	103	105	72	78	68	-222	232	303	325	273	231
-85	469	465	404	248	326	-85	225	285	263	259	273
-45	117	118	115	82	95	-45	1224	1607	1441	1277	952
14	84	99	89	64	83	14	242	246	223	120	85
38	950	900	816	741	574	38	150	204	175	133	128
63	27	34	21	25	29	63	301	400	389	323	301
92	423	280	163	94	49	92	85	141	85	100	62
126	77	59	41	22	31	126	195	266	244	250	173
160	349	75	294	84	155	160	586	727	633	438	267
196	273	306	315	303	269	196	547	588	482	353	190
230	347	308	337	234	170	230	1323	1587	1234	990	644
260	53	109	53	64	56	260	1064	439	407	424	332
270	474	99	124	77	98	270	202	258	277	248	186
280	214	154	135	108	217	280	410	435	398	343	276
296	200	240	209	154	170	296	558	604	591	566	413
310	280	233	252	224	208	310	556	552	485	445	276
329	79	88	97	83	56	329	200	209	161	127	74
339	117	87	61	73	81	339	310	215	152	105	59
350	374	314	242	194	145	350	369	411	367	329	192
380	413	426	357	301	237	380	430	463	306	226	153
390	68	120	69	66	51	390	710	664	569	342	232
400	688	691	495	335	223	400	787	959	700	483	352
406	94	47	102	33	81	406	216	196	125	117	60
412	178	169	118	75	58	412	1181	1324	940	732	424
418	106	96	66	67	47	418	187	147	104	86	41
424	227	231	114	48	41	424	538	405	406	206	162
432	81	99	77	56	56	432	321	277	223	127	97
448	491	200	152	129	116	448	217	127	133	94	63
456	44	46	28	20	31	456	872	820	590	373	276
472	586	520	307	185	199	472					
477	643	947	790	558	637	477					
495						495					
Total	9233	8248	7033	5343	4955	Total	14320	14984	12549	9934	6994

(iii) Signal remaining (%)

CPD Position	Expt 1					T50%	CPD Position	Expt 2					T50%
	0	1	2	3	4			0	1	2	3	4	
-220	100	96	85	86	49	4	-220	100	151	146	54	23	3.1
-222	100	101	70	75	66		-222	100	130	140	117	99	
-85	100	99	86	53	69	3.1	-85	100	127	117	115	121	
-45	100	101	99	70	81	3.6	-45	100	131	118	104	78	
14	100	118	107	76	99	3.5	14	100	102	92	50	35	3
38	100	95	86	78	60	4.6	38	100	137	117	89	86	
63	100	125	76	93	106		63	100	133	129	108	100	
92	100	66	38	22	12	1.6	92	100	166	100	118	73	5
126	100	76	53	28	41	2.3	126	100	136	125	128	89	
160	100	21	84	24	44		160	100	124	108	75	45	3.8
196	100	112	115	111	99		196	100	107	88	64	35	3.5
230	100	89	97	67	49	3.9	230	100	120	93	75	49	3.9
260	100	206	100	121	106		260	100	41	38	40	31	2
270	100	21	26	16	21	0.6	270	100	128	137	123	92	
280	100	72	63	51	102	3	280	100	106	97	84	67	4.6
296	100	120	104	77	85	3.5	296	100	108	106	101	74	4.8
310	100	83	90	80	74		310	100	99	87	80	50	4.1
329	100	111	122	105	71	4.5	329	100	104	80	63	37	3.5
339	100	74	52	62	69		339	100	70	49	34	19	2
350	100	84	65	52	39	3.1	350	100	111	99	89	52	4.1
380	100	103	87	73	57	4.3	380	100	108	71	53	36	3.1
390	100	176	102	96	74	4.3	390	100	93	80	48	33	3.2
400	100	100	72	49	32	2.9	400	100	122	89	61	45	3.6
406	100	51	109	35	87		406	100	91	58	54	28	2.9
412	100	95	67	42	32	2.7	412	100	112	80	62	36	3.5
418	100	91	63	63	44	3.6	418	100	79	56	46	22	2.5
424	100	102	50	21	18	2	424	100	75	76	38	30	2.7
432	100	123	95	69	69	4.5	432	100	87	69	40	30	2.6
448	100	41	31	26	24	0.9	448	100	59	62	43	29	2.6
456	100	104	64	45	71	2.7	456	100	94	68	43	32	2.7
472	100	89	52	32	34	2.1	472						
477	100	147	123	87	99	5	477						
495						4.1							
Total	100	89	76	58	54	495	Total	100	105	88	69	49	3.9

AIII.4-5 DY 6446 DY 6446 (*rpd3hos1hda1* mutant), TS

(i) Band density values (peak area)

CPD Position	Expt 1					CPD Position	Expt 2				
	0	1	2	3	4		0	1	2	3	4
Top Bands	30877	23945	5034	41394	31255	Top Bands	42332	18302	45024	55211	57103
481	1969	950	94	1665	453	481	761	420	777	532	291
453	1296	617	47	893	271	453	91	43	103	90	37
434	1488	1310	167	1004	1070	434	346	231	265	189	89
404	656	436	92	510	437	404	1061	639	1062	754	511
370	1609	1331	155	1202	761	370	480	243	465	372	270
316	198	167	35	115	88	316	944	525	859	715	440
238	541	408	60	282	197	238	105	0	120	93	47
224	1372	982	125	761	551	224	24	9	25	33	21
177	1076	925	156	752	470	177	37	26	30	27	36
135	716	591	90	611	386	135	155	114	158	117	90
122	836	779	128	707	584	122	378	291	309	196	150
100	227	210	69	196	209	100	797	528	674	422	258
88	192	207	27	149	85	88	968	470	770	533	318
82	476	347	64	349	223	82	711	326	735	614	398
71	270	160	25	143	48	71	770	421	707	640	409
42	479	274	35	180	172	42	251	146	278	226	146
27	1136	678	110	651	398	27	121	66	116	123	71
6	906	592	92	582	301	6	128	88	129	107	93
-5	295	211	42	246	127	-5	251	164	264	188	127
-65	148	134	30	93	56	-65	88	42	76	71	30
-77	3323	2377	400	2547	1336	-77	89	67	89	70	51
-89	1190	830	115	694	404	-89	204	120	107	43	37
-115	3803	3038	441	2841	1624	-115	65	36	51	25	10
-122	961	801	133	760	423	-122	160	63	163	88	71
-130	1277	907	107	715	444	-130	257	118	219	144	104
-150	1358	1021	134	731	484	-150	299	222	202	175	123
-156	435	373	65	400	225	-156	678	307	496	375	212
-164	172	102	33	218	151	-164	652	315	543	378	189
-172	435	389	82	392	322	-172	135	67	134	89	60
-188	1902	1447	273	1742	1097	-188	26	42	90	177	25
-190	630	563	267	846	691	-190	2079	1273	1712	1492	872
-213						-213	5196	4074	5466	5717	3189
Total	62248	47102	8726	64371	45345	Total	60638	29795	62220	70028	65880
Ratio	1.00	0.76	0.14	1.03	0.73	Ratio	1.00	0.49	1.03	1.15	1.09

(ii) Adjusted band density values

CPD Position	Expt 1					CPD Position	Expt 2				
	0	1	2	3	4		0	1	2	3	4
481	1969	1255	674	1610	622	481	761	854	758	461	268
453	1296	815	335	864	372	453	91	88	100	78	34
434	1488	1731	1192	971	1469	434	346	471	259	163	82
404	656	576	656	493	600	404	1061	1301	1035	653	470
370	1609	1759	1109	1162	1045	370	480	494	453	322	249
316	198	221	252	112	120	316	944	1069	837	619	405
238	541	539	428	273	270	238	105	0	117	81	44
224	1372	1298	889	736	757	224	24	18	25	29	19
177	1076	1222	1116	727	646	177	37	52	29	23	33
135	716	782	643	591	530	135	155	232	154	101	83
122	836	1030	914	684	802	122	378	592	301	170	138
100	227	277	490	190	287	100	797	1074	656	366	238
88	192	273	193	144	116	88	968	956	750	462	293
82	476	459	458	338	306	82	711	663	717	531	366
71	270	212	178	139	67	71	770	856	689	554	377
42	479	362	246	174	236	42	251	296	271	196	135
27	1136	896	784	630	547	27	121	135	113	106	66
6	906	783	653	562	414	6	128	180	126	93	85
-5	295	279	298	238	174	-5	251	333	258	163	117
-65	148	177	213	90	77	-65	88	86	74	61	28
-77	3323	3142	2852	2463	1834	-77	89	135	87	60	47
-89	1190	1096	821	671	555	-89	204	244	104	37	34
-115	3803	4015	3146	2748	2229	-115	65	72	50	22	9
-122	961	1059	947	735	580	-122	160	128	158	76	65
-130	1277	1198	765	691	610	-130	257	240	214	125	95
-150	1358	1350	953	707	665	-150	299	453	197	151	114
-156	435	493	460	387	309	-156	678	625	483	324	195
-164	172	135	235	210	207	-164	652	641	529	328	174
-172	435	514	583	379	442	-172	135	136	130	77	55
-188	1902	1912	1946	1685	1506	-188	26	85	88	153	23
-190	630	744	1908	818	948	-190	2079	2590	1669	1292	803
-213						-213	5196	8290	5327	4950	2935
Total	31371	30603	26337	22220	19342	Total	18306	23391	16759	12830	8079

(iii) Signal remaining (%)

CPD Position	Expt 1					T50%	CPD Position	Expt 2					T50%
	0	1	2	3	4			0	1	2	3		
481	100	64	34	82	32	2.5	481	100	100	100	61	35	3.6
453	100	63	26	67	29	1.7	453	100	97	100	86	37	3.8
434	100	116	80	65	99	3.3	434	100	100	75	47	24	3.2
404	100	88	100	75	92		404	100	100	98	62	44	3.7
370	100	109	69	72	65		370	100	100	94	67	52	4.0
316	100	112	127	56	61	4	316	100	100	89	66	43	3.7
238	100	100	79	50	50	3.7	238	100		100	77	42	3.8
224	100	95	65	54	55		224	100	73	100	100	80	
177	100	114	104	68	60	4.1	177	100	100	81	64	90	
135	100	109	90	82	74		135	100	100	100	66	54	3.9
122	100	123	109	82	96		122	100	100	80	45	37	3.5
100	100	122	216	84	127		100	100	100	82	46	30	3.3
88	100	142	100	75	61	4.3	88	100	99	78	48	30	3.2
82	100	96	96	71	64	4.6	82	100	93	100	75	51	4.0
71	100	78	66	51	25	2.8	71	100	100	90	72	49	3.9
42	100	76	51	36	49	2	42	100	100	100	78	54	4.0
27	100	79	69	55	48	3.6	27	100	100	94	88	54	4.1
6	100	86	72	62	46	3.7	6	100	100	99	73	67	4.2
-5	100	95	101	81	59	4.3	-5	100	100	100	65	47	3.8
-65	100	119	144	61	52	4.2	-65	100	98	84	69	32	3.5
-77	100	95	86	74	55	4.2	-77	100	100	97	68	53	3.8
-89	100	92	69	56	47	3.6	-89	100	100	51	18	17	2.5
-115	100	106	83	72	59	4.3	-115	100	100	77	34	14	2.9
-122	100	110	99	76	60	4.2	-122	100	80	99	48	41	3.5
-130	100	94	60	54	48	3.5	-130	100	93	83	49	37	3.3
-150	100	99	70	52	49	3.6	-150	100	100	66	51	38	3.4
-156	100	113	106	89	71	4.6	-156	100	92	71	48	29	3.0
-164	100	79	137	122	120		-164	100	98	81	50	27	3.2
-172	100	118	134	87	102		-172	100	100	97	57	41	3.6
-188	100	101	102	89	79		-188	100	100	100	100	88	
-190	100	118	303	130	151		-190	100	100	80	62	39	3.5
-213							-213						
Total	100	98	84	71	62	4.6	Total	100	100	92	70	44	4

AIII.4-6 DY 6446 DY 6446 (*rpd3hos1hda1* mutant), NTS

(i) Band density values (peak area)

CPD Position	Expt 1					CPD Position	Expt 2				
	0	1	2	3	4		0	1	2	3	4
Top Bands	10350	11286	27287	19386	18841	Top Bands	22982	10685	27607	39235	43119
-220	270	755	1501	594	272	-220	408	181	463	459	370
-222	201	133	163	94	73	-222	425	218	411	416	309
-85	736	594	1138	686	550	-85	1369	937	1458	1157	814
-45	255	244	464	239	244	-45	208	168	183	127	98
14	241	235	500	222	185	14	253	146	238	181	134
38	1397	1318	2840	1397	1115	38	460	232	503	399	341
63	76	70	93	58	30	63	105	37	95	54	66
92	400	407	590	249	147	92	260	111	280	273	202
126	67	87	153	89	69	126	99	61	120	133	85
160	103	124	325	134	261	160	391	267	396	275	168
196	575	490	1403	762	672	196	124	92	170	151	126
230	695	653	1467	626	528	230	51	48	44	42	12
260	134	108	173	76	103	260	196	109	162	134	80
270	92	127	226	154	182	270	711	481	651	485	310
280	427	252	239	241	271	280	483	369	513	393	252
296	359	281	356	244	299	296	608	367	673	568	350
310	723	502	1125	563	444	310	263	195	310	276	135
329	149	89	166	108	79	329	58	37	35	17	14
339	150	95	156	77	103	339	92	63	101	93	61
350	886	636	1082	583	561	350	695	408	653	472	330
380	836	504	1069	559	419	380	743	400	758	668	444
390	205	180	270	152	160	390	600	308	635	466	291
400	1428	1021	1611	965	769	400	310	211	278	172	88
406	38	45	98	48	83	406	111	109	134	98	84
412	271	213	305	174	157	412	328	283	238	130	103
418	214	154	213	146	161	418	537	382	535	371	178
424	346	210	338	233	249	424	410	279	378	257	130
432	168	135	148	130	159	432	626	406	578	338	182
448	409	380	496	367	345	448	803	572	761	543	318
456	76	66	75	49	53	456	43	37	50	32	49
472	1415	726	965	602	529	472	78	77	75	73	87
477	1032	1021	992	705	808	477	84	110	71	34	40
495						495	2924	2909	2910	2087	1418
Total	24722	23141	48026	30711	28921	Total	37840	21297	42468	50611	50787
Ratio	1.00	0.94	1.94	1.24	1.17	Ratio	1.00	0.56	1.12	1.34	1.34

(ii) Adjusted band density values

CPD Position	Expt 1					CPD Position	Expt 2				
	0	1	2	3	4		0	1	2	3	4
-220	270	806	773	478	232	-220	408	322	413	343	276
-222	201	142	84	75	62	-222	425	388	366	311	230
-85	736	634	586	552	470	-85	1369	1666	1299	865	606
-45	255	261	239	193	208	-45	208	298	163	95	73
14	241	251	257	178	158	14	253	259	212	135	100
38	1397	1408	1462	1125	953	38	460	413	448	298	254
63	76	74	48	46	25	63	105	66	85	41	49
92	400	435	304	201	126	92	260	198	250	204	150
126	67	93	79	71	59	126	99	108	107	99	63
160	103	133	167	108	223	160	391	474	353	206	125
196	575	524	722	613	574	196	124	164	151	113	94
230	695	698	755	504	452	230	51	85	39	32	9
260	134	115	89	61	88	260	196	193	145	100	59
270	92	136	116	124	156	270	711	855	580	363	231
280	427	270	123	194	231	280	483	656	457	294	188
296	359	300	183	196	255	296	608	652	600	425	261
310	723	536	579	453	379	310	263	346	276	206	100
329	149	95	86	87	67	329	58	65	31	13	10
339	150	101	80	62	88	339	92	112	90	69	46
350	886	679	557	470	480	350	695	725	582	353	246
380	836	538	550	450	358	380	743	711	676	500	331
390	205	192	139	122	136	390	600	547	566	348	217
400	1428	1091	829	776	657	400	310	376	248	129	65
406	38	48	50	39	71	406	111	194	120	73	62
412	271	228	157	140	135	412	328	503	212	97	77
418	214	165	109	117	138	418	537	679	476	277	133
424	346	224	174	187	213	424	410	496	337	192	97
432	168	145	76	105	136	432	626	721	515	253	136
448	409	406	255	295	295	448	803	1017	678	406	237
456	76	71	39	40	45	456	43	66	44	24	37
472	1415	775	497	485	452	472	78	137	67	54	65
477	1032	1091	511	567	691	477	84	195	63	25	30
495						495	2924	5170	2593	1560	1057
Total	14372	12665	10676	9117	8617	Total	14859	18855	13241	8506	5714

(iii) Signal remaining (%)

CPD Position	Expt 1					T50%	CPD Position	Expt 2					T50%
	0	1	2	3	4			0	1	2	3	4	
-220	100	299	286	177	86		-220	100	79	100	84	68	5.2
-222	100	70	42	37	31	1.7	-222	100	91	86	73	54	4.3
-85	100	86	80	75	64		-85	100	100	95	63	44	3.7
-45	100	102	93	75	82		-45	100	100	78	46	35	3.3
14	100	104	107	74	66	4.4	14	100	100	84	54	39	3.5
38	100	101	105	81	68	4.6	38	100	90	97	65	55	4.1
63	100	98	63	61	34	3.2	63	100	63	81	38	47	3.2
92	100	109	76	50	31	3	92	100	76	96	78	58	4.6
126	100	138	117	106	88	4.8	126	100	100	100	100	64	
160	100	129	163	105	217		160	100	100	90	53	32	3.4
196	100	91	126	107	100		196	100	100	100	92	76	5.3
230	100	100	109	73	65	4.4	230	100	100	76	62	17	3.2
260	100	86	67	45	66	2.8	260	100	98	74	51	30	3.1
270	100	147	126	134	169		270	100	100	82	51	32	3.2
280	100	63	29	45	54	1.4	280	100	100	95	61	39	3.5
296	100	84	51	55	71		296	100	100	99	70	43	3.7
310	100	74	80	63	52	4.5	310	100	100	100	78	38	3.7
329	100	64	57	59	45	3	329	100	100	54	23	18	2.4
339	100	68	54	42	59	2.3	339	100	100	97	75	50	4
350	100	77	63	53	54		350	100	100	84	51	35	3.4
380	100	64	66	54	43	3.1	380	100	96	91	67	45	3.7
390	100	94	68	60	67		390	100	91	94	58	36	3.5
400	100	76	58	54	46	3.1	400	100	100	80	42	21	3.1
406	100	128	134	103	189		406	100	100	100	66	56	4.1
412	100	84	58	52	50	3.2	412	100	100	65	30	23	2.7
418	100	77	51	55	65		418	100	100	89	52	25	3.2
424	100	65	50	54	62	2.2	424	100	100	82	47	24	3.1
432	100	86	45	62	81	1.9	432	100	100	82	40	22	3
448	100	99	62	72	72		448	100	100	84	51	30	3.2
456	100	93	51	52	59		456	100	100	100	56	84	
472	100	55	35	34	32	1.2	472	100	100	86	70	84	
477	100	106	49	55	67	2	477	100	100	75	30	36	3
Total	100	88	74	63	60	4.6	Total	100	100	89	57	38	3.6

AIII.4-7 Mean T50% values and standard deviation at each CPD position in the W303 (wild type), DY 6445 (*rpd3hos1hos2* mutant) and DY 6446 (*rpd3hos1hda1* mutant) strains

(i) TS

CPD Position	W303		DY 6445		DY 6446	
	Mean T50%	Standard Deviation	Mean T50%	Standard Deviation	Mean T50%	Standard Deviation
481				0.6	3.5	
453	4.6		3.2	0.6	3.2	1.0
434	4.8	0.5	3.2	0.7	2.4	0.6
404	3.9		1.6			
370	4.1	0.8	3.2	0.7	3.1	0.8
316	3.5		2.9	1.1	3.5	0.4
224	5.4	0.9	3.3	1.0	3.7	
177	4.0	0.7	3.0	0.4	3.1	0.7
135	3.6	0.8	3.1	1.5	3.3	0.6
122	3.4	1.0	2.4	0.9	2.7	0.7
100	4.0	0.7	3.2	0.7	3.2	0.7
88	4.8	0.4	4.0	1.0	4.6	0.8
82	3.7					
71	4.0	1.0	3.9	1.2	4.0	0.3
42	4.0	0.8	3.7	1.0	3.9	0.9
27	3.9	0.6	2.8	1.0	3.3	0.6
6	4.2	0.6	3.2	1.0	2.8	1.0
-5	3.6	0.8	2.3	0.7	2.6	0.7
-65	4.1	0.6	7.4	0.6	3.3	9.3
-77	4.4	0.9	2.7	0.6	3.3	0.2
-89	4.3	0.8	3.2	0.9	3.7	0.7
-115	3.9	0.7	2.9	1.0	3.4	0.5
-122	3.6	0.7	2.5	0.7	3.0	0.4
-130	3.9	0.7	2.8	0.8	3.4	0.6
-150	4.1	0.5	3.4	0.9	3.5	1.0
-156	3.6	0.6	2.4	0.8	3.0	0.3
-164	3.3	1.0	2.6	0.6	3.1	0.7
-172	3.5	1.1	3.1	0.7	3.8	0.8
-190	4.4	0.7	3.6	0.6	4.1	1.0
-213	4.4	0.9	3.6	0.6	4.2	0.6
-220	4.4	0.4			3.0	

(ii) NTS

CPD Position	W303 Mean T50%	W303 Standard Deviation	DY 6445 Mean T50%	DY 6445 Standard Deviation	DY 6446 Mean T50%	DY 6446 Standard Deviation
-222			2.6	0.7	4.1	1.4
-85	2.6	1.6	3.1	2.1	4.5	0.3
-45	3.8		4.1	0.6	3.7	0.4
14	3.8	1.7	3.1	1.9	2.2	0.6
38	3.7	2.8	3.7	1.7	3.3	0.3
63	4.8		3.4	1.8	4.5	0.3
92	5.4	0.3	5.3	0.4	4.0	0.6
126	2.8		4.1	0.1	4.1	0.5
160	4.5	0.5	3.5	0.5	4.1	0.8
196	3.8	1.4	3.2	0.4	3.6	0.5
230	4.1		4.4	0.5	3.9	0.5
260	4.0		4.3	0.4	3.4	0.7
270	4.4		4.5	0.5	4.0	0.2
280	4.5	0.1	4.0	0.4	3.7	0.4
296	4.5	1.0	3.3	1.4	3.0	0.7
310	3.2	1.5	2.4	1.4	2.4	1.1
329	4.2	0.5	3.9	0.5	3.1	1.2
339	4.0	0.4	2.8	0.2	3.0	0.4
350	4.9	0.4	3.5	0.4	3.3	0.6
380	3.1	1.3	2.2	0.6	3.2	0.9
390	4.0	0.6	3.1	0.5	2.9	0.3
400	3.9	0.4	2.3	1.3	2.0	0.7
406	4.6		2.1	0.5	2.6	0.7
412	4.8	0.7	3.2	1.2	3.0	1.8
418	4.7		3.2	1.5	2.8	1.1
424	4.6	0.8	2.6	1.9	2.4	0.6
432	4.4		3.9	1.5	3.3	0.7
448			3.1	1.8	2.8	0.4
456					3.9	
472					3.9	0.1
477					3.9	

Appendix IV

Data from experiments presented in Chapter 5

A IV.1 Cell survival following UV treatment.

W303α (wild type), 10^{-4} dilution

Experiment 1

UV Dose (J/m²)	Colonies/Plate Plate 1	Plate 2	Plate 3	Average	% S.D.	% Survival
0	122	95	88	101.667	17.954	100.000
20	86	75	97	86.000	11.000	84.590
40	36	45	50	43.667	7.095	42.951
80	6.2	3.7	5.2	5.033	1.258	4.951
120	0.19	0.17	0.37	0.243	0.110	0.239
160	0.01	0.02	0	0.010	0.010	0.010

Summary

UV Dose (J/m²)	Mean % Survival	Mean % St Dev
0	100	26.14369
20	87.81144	15.71559
40	41.3076	13.26683
80	5.026531	3.834623
120	0.506044	0.263953
160	0.032572	0.010816

Experiment 2

UV Dose (J/m²)	Colonies/Plate Plate 1	Plate 2	Plate 3	Average	% S.D.	% Survival
0	316	191	238	248.333	63.137	100.000
20	266	209	231	235.333	28.746	94.765
40	107	133	113	117.667	13.614	47.383
80	10.1	2.6	16.7	9.800	7.055	3.946
120	0.99	0.76	1.36	1.037	0.303	0.417
160	0.029	0.04	0.053	0.041	0.012	0.016

Experiment 3

UV Dose (J/m²)	Colonies/Plate Plate 1	Plate 2	Plate 3	Average	% S.D.	% Survival
0	108	97	93	99.333	7.767	100.000
20	90	91	114	98.333	13.577	98.993
40	30	29	76	45.000	26.851	45.302
80	1.2	9		5.100	5.515	5.134
120	0	0.14	0.11	0.083	0.074	0.084
160	0.005	0.011	0.011	0.009	0.003	0.009

Experiment 4

UV Dose (J/m²)	Colonies/Plate Plate 1	Plate 2	Plate 3	Average	% S.D.	% Survival
0	90	121	110	107.000	15.716	100.000
20	72	73	89	78.000	9.539	72.897
40	29	38	28	31.667	5.508	29.595
80	4.9	7.9	6.7	6.500	1.510	6.075
120	1.02	2.03	1.07	1.373	0.569	1.283
160	0.089	0.122	0.094	0.102	0.018	0.095

JDY22α (*hta1-S129stop/hta2-S129stop*), 10^{-4} dilution

Experiment 1

UV Dose (J/m²)	Colonies/Plate			Average	% S.D.	% Survival
	Plate 1	Plate 2	Plate 3			
0	77	70	155	100.667	47.184	100.000
20	78	65	52	65.000	13.000	64.570
40	21	52	103	58.667	41.405	58.278
80	2.7	5	2.2	3.300	1.493	3.278
120	0.28	0.13	0.16	0.190	0.079	0.189
160	0.015	0.014	0.008	0.012	0.004	0.012

Summary

UV Dose (J/m²)	Mean % Survival	Mean % St Dev
0	100.00	26.14
20	87.81	15.72
40	41.31	13.27
80	5.03	3.83
120	0.51	0.26
160	0.03	0.01

Experiment 2

UV Dose (J/m²)	Colonies/Plate			Average	% S.D.	% Survival
	Plate 1	Plate 2	Plate 3			
0	243	220	184	215.667	29.738	100.000
20	142	129	131	134.000	7.000	62.133
40	29	69	88	62.000	30.116	28.748
80	4.7	4	5.4	4.700	0.700	2.179
120	0.13	0.26	0.08	0.157	0.093	0.073
160	0.006	0.011	0.02	0.012	0.007	0.006

Experiment 3

UV Dose (J/m²)	Colonies/Plate			Average	% S.D.	% Survival
	Plate 1	Plate 2	Plate 3			
0	135	237	290	220.667	78.780	100.000
20	280	238	186	234.667	47.089	106.344
40	138	110	85	111.000	26.514	50.302
80	2.6	7	3.2	4.267	2.386	1.934
120	0.35	0.54	0.63	0.507	0.143	0.230
160	0.005	0.009	0.04	0.018	0.019	0.008

Experiment 4

UV Dose (J/m²)	Colonies/Plate			Average	% S.D.	% Survival
	Plate 1	Plate 2	Plate 3			
0	92	104	105	100.333	7.234	100.000
20	60	62	39	53.667	12.741	53.488
40	28	30	27	28.333	1.528	28.239
80	4.9	6.5	5.3	5.567	0.833	5.548
120	0.21	0.28	0.33	0.273	0.060	0.272
160	0.021	0.014	0.037	0.024	0.012	0.024

JHY2 (wild type), 10^{-4} dilution

Experiment 1

UV Dose (J/m²)	Colonies/Plate Plate 1	Plate 2	Plate 3	Average	% S.D.	% Survival
0	20	18	17	18.333	1.528	100.000
20	12	7	15	11.333	4.041	61.818
40	4	9		6.500	3.536	35.455
80	13.9	16.3	17.5	15.900	1.833	86.727
120	1.08	1.4	1.26	1.247	0.160	6.800
160	0.08	0.26	0.1	0.147	0.099	0.800

Summary

UV Dose (J/m²)	Mean % Survival	Mean % St Dev
0	100.00	52.72
20	88.33	30.86
40	52.22	27.90
80	27.81	3.69
120	2.45	0.61
160	0.25	0.08

Experiment 2

UV Dose (J/m²)	Colonies/Plate Plate 1	Plate 2	Plate 3	Average	% S.D.	% Survival
0	358	344	381	361.000	18.682	100.000
20	418	350	321	363.000	49.790	100.554
40	55	60	103	72.667	26.388	20.129
80	9.1	4.9		7.000	2.970	1.939
120	0.43	0.58	0.6	0.537	0.093	0.149
160	0.017	0.033	0.038	0.029	0.011	0.008

Experiment 3

UV Dose (J/m²)	Colonies/Plate Plate 1	Plate 2	Plate 3	Average	% S.D.	% Survival
0	96		317	206.500	156.271	100.000
20	181	247	280	236.000	50.408	114.286
40	170	178	246	198.000	41.761	95.884
80	11.2	17.2	28.9	19.100	9.002	9.249
120	2.2	2.15	2.49	2.280	0.184	1.104
160	0.178	0.064	0.054	0.099	0.069	0.048

Experiment 4

UV Dose (J/m²)	Colonies/Plate Plate 1	Plate 2	Plate 3	Average	% S.D.	% Survival
0	244	186	183	204.333	34.385	100.000
20	174	160	136	156.667	19.218	76.672
40	100	89	163	117.333	39.929	57.423
80	27.6	28	26.2	27.267	0.945	13.344
120	5.88	2.5	2.27	3.550	2.021	1.737
160	0.268	0.424	0.175	0.289	0.126	0.141

JHY3 (hta_1-$S_{129}A$/HTB_1), 10^{-4} dilution

Experiment 1

UV Dose (J/m²)	Colonies/Plate Plate 1	Plate 2	Plate 3	Average	% S.D.	% Survival
0	126	131	126	127.667	2.887	100.000
20	133	86	172	130.333	43.062	102.089
40	46	46	97	63.000	29.445	49.347
80	10.7	10	11.5	10.733	0.751	8.407
120	1.89	1.31	1.19	1.463	0.374	1.146
160	0.069	0.17	0.101	0.113	0.052	0.089

Summary

UV Dose (J/m²)	Mean % Survival	Mean % St Dev
0	100.00	35.30
20	81.60	49.30
40	50.96	21.72
80	9.12	5.34
120	1.04	0.69
160	0.07	0.05

Experiment 2

UV Dose (J/m²)	Colonies/Plate Plate 1	Plate 2	Plate 3	Average	% S.D.	% Survival
0	268	230	242	246.667	19.425	100.000
20	223	153	181	185.667	35.233	75.270
40	81	72	107	86.667	18.175	35.135
80	26.2	16	17.3	19.833	5.552	8.041
120		1.38	1.77	1.575	0.276	0.639
160	0.082	0.099	0.098	0.093	0.010	0.038

Experiment 3

UV Dose (J/m^2)	Colonies/Plate			Average	% S.D.	% Survival
	Plate 1	Plate 2	Plate 3			
0	146	312	284	247.333	88.867	100.000
20	124	330	216	223.333	103.196	90.296
40	216	186	152	184.667	32.021	74.663
80	12.7	12.6	29	18.100	9.440	7.318
120	1.5	3.14	1.74	2.127	0.886	0.860
160	0.178	0.064	0.054	0.099	0.069	0.040

Experiment 4

UV Dose (J/m^2)	Colonies/Plate			Average	% S.D.	% Survival
	Plate 1	Plate 2	Plate 3			
0	239	188	186	204.333	30.039	100.000
20	113	109	138	120.000	15.716	58.728
40	96	83	95	91.333	7.234	44.698
80	31.6	20.4	26	26.000	5.600	12.724
120	2.5	4.5	2.24	3.080	1.237	1.507
160	0.21	0.145	0.272	0.209	0.064	0.102

JHY9 (*HTA1/htb1-S125**), 10^{-4} dilution

Experiment 1

UV Dose (J/m^2)	Colonies/Plate			Average	% S.D.	% Survival
	Plate 1	Plate 2	Plate 3			
0	100	96	83	93.000	8.888	100.000
20	68	47		57.500	14.849	61.828
40	27	30	28	28.333	1.528	30.466
80	4.5	2.3	3.2	3.333	1.106	3.584
120	0.23	0.67	0.23	0.377	0.254	0.405
160	0.014	0.005	0.003	0.007	0.006	0.008

Summary

UV Dose (J/m^2)	Mean % Survival	Mean % St Dev
0	100.00	40.73
20	63.64	52.68
40	32.11	26.24
80	4.61	3.43
120	0.29	0.22
160	0.01	0.01

Experiment 2

UV Dose (J/m^2)	Colonies/Plate			Average	% S.D.	% Survival
	Plate 1	Plate 2	Plate 3			
0	276	447	296	339.667	93.490	100.000
20	243	226	155	208.000	46.680	61.237
40	96	194	125	138.333	50.342	40.726
80	12.7	16.4	10.8	13.300	2.848	3.916
120	0.53	0.72	0.56	0.603	0.102	0.178
160	0.022	0.013	0.008	0.014	0.007	0.004

Experiment 3

UV Dose (J/m^2)	Colonies/Plate			Average	% S.D.	% Survival
	Plate 1	Plate 2	Plate 3			
0	406	404	324	378.000	46.776	100.000
20	110	242	232	194.667	73.494	51.499
40	66	76	143	95.000	41.869	25.132
80	7.5	12	12.3	10.600	2.689	2.804
120	0.24	0.18	0.14	0.187	0.050	0.049
160	0.012	0.007	0.009	0.009	0.003	0.002

Experiment 4

UV Dose (J/m^2)	Colonies/Plate			Average	% S.D.	% Survival
	Plate 1	Plate 2	Plate 3			
0	290	272	263	275.000	13.748	100.000
20	184	169	307	220.000	75.717	80.000
40	91	76	98	88.333	11.240	32.121
80	15.6	21.9	29.7	22.400	7.063	8.145
120	1.44	0.97	1.93	1.447	0.480	0.526
160	0.051	0.12	0.041	0.071	0.043	0.026

FHY10 (wild type), 10^{-4} dilution

Experiment 1

UV Dose (J/m²)	Colonies/Plate			Average	% S.D.	% Survival
	Plate 1	Plate 2	Plate 3			
0	219	249	212	226.667	8.671	100.000
20	174	200	196	190.000	6.176	83.824
40	88	105	88	93.667	4.330	41.324
80	17.3	22.5	23.3	21.033	1.437	9.279
120	3.54	2.06	2.02	2.540	0.382	1.121
160	0.468	0.392	0.39	0.417	0.020	0.184

Summary

UV Dose (J/m²)	Mean % Survival	Mean % St Dev
0	100.00	11.13
20	77.02	4.73
40	55.53	4.62
80	14.11	1.56
120	2.95	0.70
160	0.23	0.02

Experiment 2

UV Dose (J/m²)	Colonies/Plate			Average	% S.D.	% Survival
	Plate 1	Plate 2	Plate 3			
0	249	235	237	240.333	3.151	100.000
20	211	203	203	205.667	1.922	85.576
40	130	137	125	130.667	2.508	54.369
80	26	35.8	30.2	30.667	2.046	12.760
120	7.04	7.42	9.94	8.133	0.656	3.384
160	0.414	0.465	0.449	0.443	0.011	0.184

Experiment 3

UV Dose (J/m²)	Colonies/Plate			Average	% S.D.	% Survival
	Plate 1	Plate 2	Plate 3			
0	115	180	143	146.000	22.331	100.000
20	110	91	105	102.000	6.746	69.863
40	65	53	65	61.000	4.745	41.781
80	21	16.1	19.6	18.900	1.729	12.945
120	0.76	0.98	0.48	0.740	0.172	0.507
160	0.028	0.027	0.049	0.035	0.009	0.024

Experiment 4

UV Dose (J/m²)	Colonies/Plate			Average	% S.D.	% Survival
	Plate 1	Plate 2	Plate 3			
0	518	614	454	528.667	15.233	100.000
20	430	374	361	388.333	6.935	73.455
40	227	269	235	243.667	4.218	46.091
80	68	57.4	48	57.800	1.893	10.933
120	13.2	9.04	6.4	9.547	0.648	1.806
160	1.092	1.354	0.922	1.123	0.041	0.212

Experiment 5

UV Dose (J/m²)	Colonies/Plate			Average	% S.D.	% Survival
	Plate 1	Plate 2	Plate 3			
0	494	458	480	477.333	3.802	100.000
20	372	396	366	378.000	3.326	79.190
40	362	362	420	381.333	7.015	79.888
80	95.2	91.6	96.8	94.533	0.558	19.804
120	21.92	33.94	31.36	29.073	1.326	6.091
160	2.24	2.224	2.536	2.333	0.037	0.489

FHY14 (*hta1-S129A/HTB1*), 10^{-4} dilution

Experiment 1

UV Dose (J/m²)	Colonies/Plate Plate 1	Plate 2	Plate 3	Average	% S.D.	% Survival
0	153	150	143	148.667	3.452	100.000
20	82	74	82	79.333	3.107	53.363
40	26	29	36	30.333	3.452	20.404
80	3	3	3.5	3.167	0.194	2.130
120	0.28	0.27	0.32	0.290	0.018	0.195
160	0.026	0.036	0.029	0.030	0.003	0.020

Summary

UV Dose (J/m²)	Mean % Survival	Mean % St Dev
0	100.00	12.98
20	75.04	15.80
40	36.54	4.00
80	6.81	1.11
120	0.55	0.32
160	0.02	0.01

Experiment 2

UV Dose (J/m²)	Colonies/Plate Plate 1	Plate 2	Plate 3	Average	% S.D.	% Survival
0	119	110	126	118.333	6.778	100.000
20	105	65	88	86.000	16.965	72.676
40	38	35	36	36.333	1.291	30.704
80	4.6	5.5	6	5.367	0.600	4.535
120	0.26	0.37	0.26	0.297	0.054	0.251
160	0.029	0.015	0.018	0.021	0.006	0.017

Experiment 3

UV Dose (J/m²)	Colonies/Plate Plate 1	Plate 2	Plate 3	Average	% S.D.	% Survival
0	91	82	95	89.333	7.453	100.000
20	55	70	53	59.333	10.401	66.418
40	34	23	26	27.667	6.365	30.970
80	6.8	9	5.9	7.233	1.785	8.097
120	1.24	0.17	0.14	0.517	0.701	0.578
160	0.002	0.014	0	0.005	0.008	0.006

Experiment 4

UV Dose (J/m²)	Colonies/Plate Plate 1	Plate 2	Plate 3	Average	% S.D.	% Survival
0	162	192	303	219.000	33.916	100.000
20		146	108	127.000	12.269	57.991
40	56	67	62	61.667	2.515	28.158
80	7.3	9.2	10.5	9.000	0.735	4.110
120	0.2	0.74	0.28	0.407	0.133	0.186
160	0.016	0.007	0.02	0.014	0.003	0.007

Experiment 5

UV Dose (J/m²)	Colonies/Plate Plate 1	Plate 2	Plate 3	Average	% S.D.	% Survival
0	358	347	332	345.667	3.776	100.000
20	449	296	324	356.333	23.567	103.086
40	198	173	213	194.667	5.846	56.316
80	31.4	40.3	37.1	36.267	1.304	10.492
120	3.11	5.6	3.49	4.067	0.388	1.176
160	0.113	0.142	0.206	0.154	0.014	0.044

FHY25 (*htb1-K123R-S125A-S126A*), 10^{-4} dilution

Experiment 1

UV Dose (J/m²)	Colonies/Plate			Average	% S.D.	% Survival
	Plate 1	Plate 2	Plate 3			
0	Contaminated					
20						
40						
80						
120						
160						

Summary

UV Dose (J/m²)	Mean % Survival	Mean % St Dev
0	100.00	12.78
20	62.76	9.84
40	35.29	5.21
80	7.56	1.97
120	0.52	0.11
160	0.04	0.01

Experiment 2

UV Dose (J/m²)	Colonies/Plate			Average	% S.D.	% Survival
	Plate 1	Plate 2	Plate 3			
0	285	295	262	280.667	6.029	100.000
20	130	148	89	122.333	10.774	43.587
40	86	68	63	72.333	4.310	25.772
80	10.4	8.4	8.1	8.967	0.445	3.195
120	0.59	0.45	0.29	0.443	0.053	0.158
160	0.015	0.045	0.046	0.035	0.006	0.013

Experiment 3

UV Dose (J/m²)	Colonies/Plate			Average	% S.D.	% Survival
	Plate 1	Plate 2	Plate 3			
0	235	253	218	235.333	7.437	100.000
20	138	110	109	119.000	6.995	50.567
40	66	60	53	59.667	2.765	25.354
80	6.7	10.3	5.5	7.500	1.061	3.187
120	0.26	0.38	0.16	0.267	0.047	0.113
160	0.003	0.011	0.004	0.006	0.002	0.003

Experiment 4

UV Dose (J/m²)	Colonies/Plate			Average	% S.D.	% Survival
	Plate 1	Plate 2	Plate 3			
0	382	223	366	323.667	27.048	100.000
20	240	191	234	221.667	8.258	68.486
40	139	116	102	119.000	5.772	36.766
80	24	18.7	34.7	25.800	2.518	7.971
120	1.11	1.72	1.14	1.323	0.106	0.409
160	0.101	0.076	0.068	0.082	0.005	0.025

Experiment 5

UV Dose (J/m²)	Colonies/Plate			Average	% S.D.	% Survival
	Plate 1	Plate 2	Plate 3			
0	297	367	329	331.000	10.587	100.000
20	301	332	245	292.667	13.322	88.419
40	188	146	195	176.333	8.007	53.273
80	57.8	61.8	38	52.533	3.850	15.871
120	3.87	5.49	4.64	4.667	0.245	1.410
160	0.372	0.419	0.46	0.417	0.013	0.126

FHY47 (*hta*$_1$-$S_{122}A$), 10^{-4} dilution

Experiment 1

UV Dose (J/m^2)	Colonies/Plate Plate 1	Plate 2	Plate 3	Average	% S.D.	% Survival
0	26	31	36	31.000	16.129	100.000
20	24	21	27	24.000	9.677	77.419
40	16	10	13	13.000	9.677	41.935
80	1.3	0.3	1.6	1.067	2.196	3.441
120	0.13	0.05	0.03	0.070	0.171	0.226
160	0.003	0.002	0.003	0.003	0.002	0.009

Summary

UV Dose (J/m^2)	Mean % Survival	Mean % St Dev
0	100.00	14.89
20	73.41	8.29
40	46.54	14.70
80	6.04	1.65
120	0.72	0.10
160	0.07	0.01

Experiment 2

UV Dose (J/m^2)	Colonies/Plate Plate 1	Plate 2	Plate 3	Average	% S.D.	% Survival
0	47	60	50	52.333	13.007	100.000
20	33	44	36	37.667	10.865	71.975
40	18	17	10	15.000	8.329	28.662
80	1.6	0.4	1.1	1.033	1.152	1.975
120	0.12	0.15	0.05	0.107	0.098	0.204
160	0.013	0.02	0.007	0.013	0.012	0.025

Experiment 3

UV Dose (J/m^2)	Colonies/Plate Plate 1	Plate 2	Plate 3	Average	% S.D.	% Survival
0	34	42	35	37.000	11.781	100.000
20	12	11	15	12.667	5.626	34.234
40	9	8	10	9.000	2.703	24.324
80	1.1	0.6	0.4	0.700	0.974	1.892
120	0.09	0.02	0.05	0.053	0.095	0.144
160	0.001	0.003	0.002	0.002	0.003	0.005

Experiment 4

UV Dose (J/m^2)	Colonies/Plate Plate 1	Plate 2	Plate 3	Average	% S.D.	% Survival
0	119	152	215	162.000	30.108	100.000
20	136	140	142	139.333	1.886	86.008
40	79	63	71	71.000	4.938	43.827
80	12.8	12.5	10.9	12.067	0.631	7.449
120	0.66	0.56	0.68	0.633	0.040	0.391
160	0.073	0.068	0.031	0.057	0.014	0.035

Experiment 5

UV Dose (J/m^2)	Colonies/Plate Plate 1	Plate 2	Plate 3	Average	% S.D.	% Survival
0	198	212	204	204.667	3.432	100.000
20	183	231	184	199.333	13.402	97.394
40	117	157	303	192.333	47.836	93.974
80	30	39	25.7	31.567	3.316	15.423
120	5.42	5.56	5.12	5.367	0.110	2.622
160	0.558	0.528	0.667	0.584	0.036	0.286

A IV.2 Genome-wide NER analysis – Immuno Slot-blot assay

FHY10 (wild type)

	Repair time (hours)	U	0	1	2	3	4
Exp 1	*Volume*						
	Adjusted Volume	0	427570	407028	315524	279844	262291
	% Vol (damage)		100	95	74	65	61
	% Repair		0	5	26	35	39
Exp 2	Volume	163049	786104	719209	601831	524323	494646
	Adjusted Volume	0	623055	556160	438782	361274	331596
	% Vol (damage)		100	89	70	58	53
	% Repair		0	11	30	42	47
Exp 3	Volume	103965	883514	794374	603427	572086	454742
	Adjusted Volume	0	779549	690409	499462	468121	350777
	% Vol (damage)		100	89	64	60	45
	% Repair		0	11	36	40	55
		Mean	0	9.42	30.57	38.84	46.81
		St Dev	0	4.12	4.94	3.85	8.17

FHY14 mutant (*HTA1/htb1-S125**)

	Repair time (hours)	U	0	1	2	3	4
Exp 1	Volume	16397	214368	202017	169632	149291	121182
	Adjusted Volume	0	197971	185619	153235	132893	104785
	% Vol (damage)		100	94	77	67	53
	% Repair		0	6	23	33	47
Exp 2	Volume	89264	712277	646698	542010	466010	447981
	Adjusted Volume	0	623013	557435	452746	376747	358717
	% Vol (damage)		100	89	73	60	58
	% Repair		0	11	27	40	42
Exp 3	Volume	75145	719702	655401	625487	483319	418767
	Adjusted Volume	0	644557	580256	550342	408174	343622
	% Vol (damage)		100	90	85	63	53
	% Repair		0	10	15	37	47
		Mean	0	8.91	21.51	36.36	45.39
		St Dev	0	2.33	6.43	3.34	2.58

A IV.3 NER at the level of the gene – Southern blotting analysis of removal of CPDs following UV irradiation

FHY10 (wild type), TS

Expt 1	U		0		1		2		3		4	
ML (+ or -)	+	-	+	-	+	-	+	-	+	-	+	-
Band Intensity	14670	13754	2245	7610	5483	15712	9816	20592	11165	17069	13988	19728
Intact fragment (%)		107		29		35		48		65		71
Damage (%)		-7		71		65		52		35		29
Repair (%)				0.00		7.66		25.77		50.94		58.73

Expt 2	U		0		1		2		3		4	
ML (+ or -)	+	-	+	-	+	-	+	-	+	-	+	-
Band Intensity	2872	2885	700	2837	1711	5096	2500	5835	2620	5287	2837	4954
Intact fragment (%)		100		25		34		43		50		57
Damage (%)		0		75		66		57		50		43
Repair (%)				0.00		11.79		24.10		33.01		43.27

Expt 3	U		0		1		2		3		4	
ML (+ or -)	+	-	+	-	+	-	+	-	+	-	+	-
Band Intensity	1461	1214	563	1645	745	2128	1616	2897	1645	2597	1558	2210
Intact fragment (%)		120		34		35		56		63		71
Damage (%)		-20		66		65		44		37		29
Repair (%)				0.00		1.22		32.79		44.30		55.16

Expt 4	U		0		1		2		3		4	
ML (+ or -)	+	-	+	-	+	-	+	-	+	-	+	-
Band Intensity	17614	14759	5585	19856	9245	26828	17541	33326	19122	29300	17655	25684
Intact fragment (%)		119		28		35		53		65		69
Damage (%)		-19		72		65		47		35		31
Repair (%)				0.00		9.18		34.10		51.67		56.51

Expt 5	U		0		1		2		3		4	
ML (+ or -)	+	-	+	-	+	-	+	-	+	-	+	-
Band Intensity	11479	13145	2838	11538	7314	18749	10093	25430	9532	18182	9303	17145
Intact fragment (%)		87		25		39		40		52		54
Damage (%)		13		75		61		60		48		46
Repair (%)				0.00		19.11		20.01		36.90		39.34

Expt 6	U		0		1		2		3		4	
ML (+ or -)	+	-	+	-	+	-	+	-	+	-	+	-
Band Intensity	5933	6723	1328	5319	2840	8280	2178	4789	7286	12461	6105	9856
Intact fragment (%)		88		25		34		45		58		62
Damage (%)		12		75		66		55		42		38
Repair (%)				0.00		12.45		27.33		44.65		49.27

Expt 7	U		0		1		2		3		4	
ML (+ or -)	+	-	+	-	+	-	+	-	+	-	+	-
Band Intensity	14648	16010	2679	9028	5775	12089	4712	8957	14739	21522	14941	19867
Intact fragment (%)		91		30		48		53		68		75
Damage (%)		9		70		52		47		32		25
Repair (%)				0.00		25.74		32.61		55.19		64.74

Mean Repair (%)	0.00	12.45	28.10	45.24	52.43
Standard Deviation	0.00	7.97	5.26	8.10	8.95

FHY10 (wild type), NTS

Expt 1	U		0		1		2		3		4	
ML (+ or -)	+	-	+	-	+	-	+	-	+	-	+	-
Band Intensity	62457	56641	10370	29452	22159	51658	33378	63732	29348	43098	39849	53839
Intact fragment (%)		110		35		43		52		68		74
Damage (%)		-10		65		57		48		32		26
Repair (%)				0.00		11.86		26.49		50.76		59.89

Expt 2	U		0		1		2		3		4	
ML (+ or -)	+	-	+	-	+	-	+	-	+	-	+	-
Band Intensity	2096	2051	653	1990	1155	3483	1859	3598	1823	3062	1799	3009
Intact fragment (%)		102		33		33		52		60		60
Damage (%)		-2		67		67		48		40		40
Repair (%)				0.00		0.46		28.05		39.73		40.14

Expt 3	U		0		1		2		3		4	
ML (+ or -)	+	-	+	-	+	-	+	-	+	-	+	-
Band Intensity	2494	2080	1233	2812	2016	3662	3424	4962	3079	3937	3446	4363
Intact fragment (%)		120		44		55		69		78		79
Damage (%)		-20		56		45		31		22		21
Repair (%)				0.00		19.97		44.81		61.20		62.56

Expt 4	U		0		1		2		3		4	
ML (+ or -)	+	-	+	-	+	-	+	-	+	-	+	-
Band Intensity	1997	2041	531	1598	675	1515	1542	2976	2029	3024	2108	2933
Intact fragment (%)		98		33		45		52		67		72
Damage (%)		2		67		55		48		33		28
Repair (%)				0.00		16.97		27.80		50.74		57.84

Expt 5	U		0		1		2		3		4	
ML (+ or -)	+	-	+	-	+	-	+	-	+	-	+	-
Band Intensity	1108	1396	389	1154	989	2167	1406	2828	1111	1917	1229	1893
Intact fragment (%)		79		34		46		50		58		65
Damage (%)		21		66		54		50		42		35
Repair (%)				0.00		17.99		24.13		36.59		47.06

Expt 6	U		0		1		2		3		4	
ML (+ or -)	+	-	+	-	+	-	+	-	+	-	+	-
Band Intensity	3816	4133	973	2477	1948	4040	1752	2810	5237	6974	5208	6131
Intact fragment (%)		92		39		48		62		75		85
Damage (%)		8		61		52		38		25		15
Repair (%)				0.00		14.71		38.01		58.97		75.19

Expt 7	U		0		1		2		3		4	
ML (+ or -)	+	-	+	-	+	-	+	-	+	-	+	-
Band Intensity	24487	26968	5536	21118	9845	25282	8801	16000	33941	55488	32164	44684
Intact fragment (%)		91		26		39		55		61		72
Damage (%)		9		74		61		45		39		28
Repair (%)				0.00		17.25		39.02		47.37		62.03

Mean Repair (%)	0.00	16.47	32.34	49.34	57.82
Standard Deviation	0.00	2.81	8.16	9.09	11.36

FHY14 (htb_1-S_{125}*) mutant, TS

Expt 1	U		0		1		2		3		4	
ML (+ or -)	+	-	+	-	+	-	+	-	+	-	+	
Band Intensity	22318	25065	9864	29068	7823	14037	11954	19312	21520	31979	21463	29152.71
Intact fragment (%)		89		34		56		62		67		74
Damage (%)		11		66		44		38		33		26
Repair (%)				0		32.99		42.33		50.49		60.07

Expt 2	U		0		1		2		3		4	
ML (+ or -)	+	-	+	-	+	-	+	-	+	-	+	-
Band Intensity	1430	1382	515	1335	617	1357	813	1273	1346	1870		
Intact fragment (%)		104		39		45		64		72		
Damage (%)		-4		61		55		36		28		
Repair (%)				0		11.19		41.15		54.36		

Expt 3	U		0		1		2		3		4	
ML (+ or -)	+	-	+	-	+	-	+	-	+	-	+	-
Band Intensity												
Intact fragment (%)												
Damage (%)												
Repair (%)												

Expt 4	U		0		1		2		3		4	
ML (+ or -)	+	-	+	-	+	-	+	-	+	-	+	-
Band Intensity	16761	15947	4918	14288	5323	14258	7095	13199	13392	19910	1708	1768
Intact fragment (%)		105		34		37		54		67		97
Damage (%)		-5		66		63		46		33		3
Repair (%)				0.00		4.44		29.48		50.08		94.86

Expt 5	U		0		1		2		3		4	
ML (+ or -)	+	-	+	-	+	-	+	-	+	-	+	-
Band Intensity	9281	9560	1789	8184	2522	7788	6622	14562	8490	14311	8660	13464
Intact fragment (%)		97		22		32		45		59		64
Damage (%)		3		78		68		55		41		36
Repair (%)				0.00		13.46		30.22		47.94		54.33

Expt 6	U		0		1		2		3		4	
ML (+ or -)	+	-	+	-	+	-	+	-	+	-	+	-
Band Intensity	18626	15415	3316	10253	5005	12504	7393	14776	15369	25365	9967	14328
Intact fragment (%)		121		32		40		50		61		70
Damage (%)		-21		68		60		50		39		30
Repair (%)				0.00		11.37		26.14		41.76		55.22

Mean Repair (%)	0	14.69	33.862	48.924	56.54
Standard Deviation	0	10.77889	7.365295	4.6262	3.089288

FHY14 (*htb1-S125**) mutant, NTS

Expt 1	U		0		1		2		3		4	
ML (+ or -)	+	-	+	-	+	-	+	-	+	-	+	
Band Intensity	68624	75417	27575	85897	23498	43777	37370	60565	66571	90892	65759	88676.9
Intact fragment (%)		91		32		54		62		73		74
Damage (%)		9		68		46		38		27		26
Repair (%)				0		31.77		43.60		60.59		61.94

Expt 2	U		0		1		2		3		4	
ML (+ or -)	+	-	+	-	+	-	+	-	+	-	+	-
Band Intensity												
Intact fragment (%)												
Damage (%)												
Repair (%)												

Expt 3	U		0		1		2		3		4	
ML (+ or -)	+	-	+	-	+	-	+	-	+	-	+	-
Band Intensity	1936	2174	665	2016	1058	1946	1169	1698	2035	2788	221	306
Intact fragment (%)		89		33		54		69		73		72
Damage (%)		11		67		46		31		27		28
Repair (%)				0.00		31.93		53.52		59.68		58.33

Expt 4	U		0		1		2		3		4	
ML (+ or -)	+	-	+	-	+	-	+	-	+	-	+	-
Band Intensity	2213	2517	802	2320	2655	5364	2044	4009	2276	3724	2320	3547
Intact fragment (%)		88		35		50		51		61		65
Damage (%)		12		65		50		49		39		35
Repair (%)				0.00		22.80		25.09		40.53		47.12

Expt 5	U		0		1		2		3		4	
ML (+ or -)	+	-	+	-	+	-	+	-	+	-	+	-
Band Intensity	1085	1151	321	932	374	858	970	1668	1133	1627	1145	1651
Intact fragment (%)		94		34		44		58		70		69
Damage (%)		6		66		56		42		30		31
Repair (%)				0.00		13.90		36.11		53.70		53.23

Expt 6	U		0		1		2		3		4	
ML (+ or -)	+	-	+	-	+	-	+	-	+	-	+	-
Band Intensity	5501	4656	1349	3474	2152	3800	3100	5105	5675	7907	3414	5182
Intact fragment (%)		118		39		57		61		72		66
Damage (%)		-18		61		43		39		28		34
Repair (%)				0.00		29.13		35.80		53.86		44.22

Mean Repair (%)	0.00	25.71	38.82	53.67	54.10
Standard Deviation	0.00	8.06	10.53	8.01	7.45

References

Aboussekhra, A. and Thoma, F. (1999). TATA-binding protein promotes the selective formation of UV-induced (6-4) photoproducts and modulates DNA repair in the TATA box. *EMBO J*, **18**, 433-443.

Abraham, R.T. (2001). Cell cycle checkpoint signaling through the ATM and ATR kinases. *Genes Dev*, **15**. 2177-2196.

Adimoolam, S. and Ford, J.M. (2003). p53 and regulation of DNA damage recognition during nucleotide excision repair. *DNA Repair*, **2**. 947–954.

Allard, S., Masson, J.Y. and Cote, J. (2004). Chromatin remodeling and the maintenance of genome integrity. *Biochim Biophys* **1677** (1-3). 158-164.

Allfrey, V.G. (1977). Post-synthetic modifications of histone structure: a mechanism for the control of chromosome structure by the modulation of histone-DNA interactions. In *Chromatin and Chromosome Structure* (Li, H.J. and Eckhardt, R. Eds). Academic Press, New York. pp 167-191.

Ananthaswamy, H.N. (1997). Ultraviolet light as a carcinogen. In *Comprehensive Toxicology*, **12**. Chemical Carcinogens and Anticarcinogens (Bowden, G.T. and Fischer, S.M. Eds). Pergamon, Oxford. pp. 255-279.

Andressoo, J.O. and Hoeijmakers, J.H. (2005). Transcription-coupled repair and premature ageing. *Mutat Res*, **577**. 179–194.

Araujo, S.J., Nigg, E.A. and Wood, R.D. (2001). Strong Functional Interactions of TFIIH with XPC and XPG in Human DNA Nucleotide Excision Repair, without a Preassembled Repairosome. *Mol Cell Biol*, **21** (7). 2281–2291.

Balajee, A.S. (2006). *DNA Repair and Human Disease*. Landes Bioscience, Georgetown, TX.

Balajee, A.S. and Bohr, V.A. (2000). Genomic heterogeneity of nucleotide excision repair. *Gene*, **250**. 15-30.

Balajee, A.S., May, A. and Bohr, V.A. (1999). DNA repair of pyrimidine dimers and 6-4 photoproducts in the ribosomal DNA. *Nucleic Acids Res*, **27**. 2511-2520.

Barnes, D.E. & Lindahl, T. (2004). Repair and genetic consequences of endogenous DNA base damage in mammalian cells. *Annu Rev Genet*, **38**. 445–476.

Becker, P.B. and Horz, W. ATP-dependent nucleosome remodelling. *Annu Rev Biochem*, **71**. 247-273.

Benchimol, S. (2001). p53-dependent pathways of apoptosis. *Nature*, **8** (11). 1049-1051.

Bernstein, B.E., Tong, J.K. and Schreiber, S.L. (2000). Genomewide studies of histone deacetylase function in yeast. *Proc Natl Acad Sci USA*, **97** (25).13708-13713.

Bhatia, P.K., Verhage, R.A., Brouwer, J. and Friedberg, E.C. (1996). Molecular cloning and characterization of *Saccharomyces cerevisiae RAD28*, the yeast homolog of the human Cockayne syndrome A (CSA) gene. *J Bacteriol*, **178** (20). 5977-5988.

Bohr, V.A., Smith, C.A., Okumoto, D.S. and Hanawalt, P.C. (1985). DNA repair in an active gene: removal of pyrimidine dimers from the DHFR gene of CHO hamster cells is much more efficient than in the genome overall. *Cell*, **40**. 359-369.

Bootsma, D., Kraemer, K.H., Cleaver, J.E. and Hoeijmakers, J.H.J. (2001). Nucleotide excision repair syndromes: Xeroderma pigmentosum, Cockayne syndrome and trichothiodystrophy. In *The*

Metabolic and Molecular Basis of Inherited Disease, Vol 1 (Scriver, C.R., Beaudet, A.L., Sly, W.S., Valle, D., Vogelstein, B. and Kinzler, K.W. Eds) McGraw-Hill.

Brand, M., Moggs, J.G., Oulad-Abdelghani, M., Lejeune, F., Dilworth, F.J., Stevenin, J., Almouzni, G. and Tora, L. (2001). UV-damaged DNA-binding protein in the TFTC complex links DNA damage recognition to nucleosome acetylation. *EMBO J,* **20**. 3187-3196.

Braunstein, M., Sobel, R.E., Allis, C.D., Turner, B.M. and Broach, J.R. (1996). Efficient transcriptional silencing in *Saccharomyces cerevisiae* requires a heterochromatin histone acetylation pattern. *Mol Cell Biol,* **16**. 4349-4356.

Brown, T.A. (1999). *Genomes.* BIOS Scientific Publishers Ltd., Oxford, UK.

Brownell, J.E., Zhou, J., Ranalli, T., Kobayashi, R., Edmondson, D.G., Roth, S.Y. and Allis, C.D. (1996). Tertrahymena histone acetyltransferases A: A homologue to yeast Gcn5p linking histone acetylation to gene activation. *Cell,* **84**. 843-851.

Brownell, J.E. and Allis, C.D. (1996). Special HATs for special occasions: linking histone acetylation to chromatin assembly and gene activation. *Curr Opin Genet Dev,* **6**. 176-184.

Bucheli, M. and Sweder, K. (2004). In UV-irradiated *Saccharomyces cerevisiae,* overexpression of Swi2/Snf2 family member Rad26 increases transcription coupled repair and repair of the non-transcribed strand. *Mol Microbiol,* **52** (6). 1653-1663.

Burgess, S.M., Ajimura, M. and Kleckner, N. (1999). *GCN5*-dependent histone H3 acetylation and *RPD3*-dependent histone H4 deacetylation have distinct, opposing effects on *IME2* transcription, during meiosis and during vegetative growth, in budding yeast. *Proc Natl Acad Sci USA,* **96**. 6835-6840.

Carey, N. and La Thangue, N.B. (2006). Histone deacetylase inhibitors: gathering pace. *Curr Opin Pharmacol,* **6** (4). 369-375.

Carmen, A.A., Rundlett, S.E. and Grunstein, M. (1996). HDA1 and HDA3 are components of a yeast histone deacetylase (HDA) complex. *J Biol Chem,* **271**. 15837-15844.

Chen, H., Tini, M. and Evans, R.M. (2001). HATs on and beyond chromatin. *Curr Opin Cell Biol,* **13**. 218-224.

Cheung, P., Tanner, K.G., Cheung, W.L., Sassone-Corsi, P., Denu, J.M. and Allis, C.D. (2000). Synergistic coupling of histone H3 phosphorylation and acetylation in response to epidermal growth factor stimulation. *Mol Cell,* **5**. 905–915.

Citterio, E., Vermeulen, W. and Hoeijmakers, J.H. (2000). Transcriptional healing. *Cell,* **101**. 447-450.

Cleaver, J.E. (1968). Defective repair replication of DNA in xeroderma pigmentosum. *Nature,* **218**. 652–656.

Cockayne, E.A (1936). Dwarfism with retinal atrophy and deafness. *Arch Dis Child,* **11**. 1–8.

Constantinou, A., Gunz, D., Evans, E., Lalle, P., Bates, P.A, Wood, R.D. and Clarkson, S.G. (1999). Conserved residues of human XPG protein important for nuclease activity and function in nucleotide excision repair. *J Biol Chem,* **274**. 5637–5648.

Conconi, A. (2005). The yeast rDNA locus: A model system to study DNA repair in chromatin. *DNA Repair (Amst),* **4** (8). 897-908.

Conconi, A., Bespalov, V.A., Fahy, D. and Smerdon, M.J. (2005). DNA repair in RNA polymerase I transcribed genes. In: *Comprehensive Series in Photosciences: From DNA photolesions to mutations, skin cancer and cell death,* Sage, E., Drouin, R., and Rouabhia, M. (eds). pp.123-147. RS-C Publishers, UK.

Conconi, A., Bespalov, V.A. and Smerdon, M.J. (2002). Transcription-coupled repair in RNA polymerase I-transcribed genes of yeast. *Proc Natl Acad Sci USA,* **99** (2). 649-654.

Cooper, P.K. (1982). Characterisation of long-patch excision repair of DNA in ultraviolet-irradiated *Escherichia coli*: an inducible function under *rec-lex* control. *Mol Gen Genet,* 185. 189-197.

Cooper, J.P., Roth, S.Y., and Simpson, R.T. The global transcriptional regulators, SSN6 and TUP1, play distinct roles in the establishment of a repressive chromatin structure. (1994). *Genes Dev,* **8.** 1400–1410.

Cosgrove, M.S., Boeke, J.D. and Wolberger, C. (2004). Regulated nucleosome mobility and the histone code. *Nat Struct Mol Biol,* **11**(11). 1037-1043.

Cosgrove, M.S. and Wolberger, C. (2005). How does the histone code work?. *Biochem Cell Biol,* **83.** 468-476.

Dahmus, M.E. (1994). The role of multisite phosphorylation in the regulation of RNA polymerase II activity. *Prog Nucleic Acid Res Mol Biol,* **48.** 143–179.

Daniel, J.A., Torok, M.S., Sun, Z.W., Schieltz, D., Allis, C.D., Yates, J.R. 3rd and Grant, P.A. (2004). Deubiquitination of histone H2B by a yeast acetyltransferase complex regulates transcription. *J Biol Chem,* **279** (3). 1867-1871.

Davie, J.K., Edmondson, D.G., Coco, C.B. and Dent, S.Y. (2003). Tup1-Ssn6 interacts with multiple class I histone deacetylases *in vitro*. *J Biol Chem,* **278** (50). 50158-50162.

Davie, J.K., Trumbly, R.J. and Dent, S.Y. (2002). Histone-dependent association of Tup1-Ssn6 with repressed genes in vivo. *Mol Cell Biol,* **22** (3). 693-703.

de Boer, J. and Hoeijmakers, J.H. (2000) Nucleotide excision repair and human syndromes. *Carcinogenesis,* **21** (3). 453-460.

Deckert, J. and Struhl, K. (2002). Targeted recruitment of Rpd3 histone deacetylase represses transcription by inhibiting recruitment of Swi/Snf, SAGA, and TATA-binding protein. *Mol Cell Biol,* **22** (18). 6458-6470.

de Laat, W.L., Jaspers, N.G. and Hoeijmakers, J.H. (1999). Molecular mechanism of nucleotide excision repair. *Genes Dev,* **13** (7). 768-785.

Demple, B., Herman, T. and Chen, D.S. (1991). Cloning and expression of APE, the cDNA encoding the major human apurinic endonuclease: definition of a family of DNA repair enzymes. *Proc Natl Acad Sci USA,* **88**. 11450–11454.

den Dulk, B., Brandsma, J.A., Brouwer, J. (2005). The Rad4 homologue YDR314C is essential for strand-specific repair of RNA polymerase I-transcribed rDNA in Saccharomyces cerevisiae. *Mol Microbiol,* **56** (6). 1518-1526.

den Dulk, B., Sun, S.M., de Ruijter, M., Brandsma, J.A. and Brouwer, J. (2006). Rad33, a new factor involved in nucleotide excision repair in Saccharomyces cerevisae. *DNA Repair (Amst),* **5** (6). 683-692

Denu, J.M. (2003). Linking chromatin function with metabolic networks: Sir2 family of NAD(+)-dependent deacetylases. *Trends Biochem Sci,* **28** (1). 41-48.

De Haan, H. (1993). Solar UV-light penetration and photodegradation of humic substances in peaty lake water. *Lmnol Oceanogr,* **38** (5). 1072-1076.

De Rubertis, F., Kadosh, D., Henchoz, S., Pauli, D., Reuter, G., Struhl, K. and Spierer, P. (1996). The histone deacetylase RPD3 counteracts genomic silencing in Drosophila and yeast. *Nature.*, **384**. 589-591.

De Ruijter, A.J., Van Gennip, A.H., Caron, H.N., Kemp, S. and Van Kuilenberg, A.B. (2003). Histone deacetylases: characterisation of the classical HDAC family. *Biochem J*, **370** (3). 737-749.

Dilworth, F.J., Fromental-Ramain, C., Yamamoto, K. and Chambon, P. (2000). ATP-driven chromatin remodelling activity and histone acetyltransferases act sequentially during transactivation by RAR/RXR *in vitro*. *Mol Cell*, **6**. 1049-1058.

Downs, J.A., Allard, S., Jobin-Robitaille, O., Javaheri, A., Auger, A., Bouchard, N., Kron, S.J., Jackson, S.P. and Cote, J. (2004). Binding of chromatin-modifying activities to phosphorylated histone H2A at DNA damage sites. *Mol Cell*, **16**. 979–990.

Downs, J.A., Kosmidou, E., Morgan, A. and Jackson, S.P. (2003). Suppression of homologous recombination by the *Saccharomyces cerevisiae* linker histone. *Mol Cell*, **11**. 1685-1692.

Downs, J.A., Lowndes, N.F. and Jackson, S.P. (2000). A role for Saccharomyces cerevisiae histone H2A in DNA repair. *Nature*, **408**. 1001–1004.

Drapkin, R., Reardon, J.T., Ansari, A., Huang, J.C., Zawe,l L., Ahn, K., Sancar, A. and Reinberg, D. (1994). Dual role of TFIIH in DNA excision repair and in transcription by RNA polymerase II. *Nature*, **368** (6473). 769–772.

Dulbecco, R. (1949). Reactivation of ultraviolet-inactivated bacteriophage by visible light. *Nature*, **162**. 949-950.

Durocher, D. and Jackson, S.P. (2001). DNA-PK, ATM and ATR as sensors of DNA damage: variations on a theme? *Curr Opin Cell Biol*, **13**. 225–231.

Dvir, A., Garrett, K.P., Chalut, C., Egly, J.M., Conaway, J.W. and Conaway, R.C. (1996). A role for ATP and TFIIH in activation of the RNA polymerase II preinitiation complex prior to transcription initiation. *J Biol Chem*, **271**. 7245–7248.

Dvir, A., Conaway, R.C. and Conaway, J.W. (1997). A role for TFIIH incontrolling the activity of early RNA polymerase II elongation complexes. *Proc Nat. Acad. Sci. USA*, **94**. 9006–9010.

Edmondson, D.G. and Roth, S.Y. (1996). Chromatin and transcription. *FASEB J*, **10**. 1173-1182.

Edmondson, D.G., Smith, M.M., and Roth, S.Y. (1996). Repression domain of the yeast global repressor Tup1 interacts directly with histones H3 and H4. *Genes Dev*, **10**. 1247–1259.

Edmondson, D.G., Zhang, W., Watson, A., Xu, W., Bone, J.R., Yu, Y., Stillman, D. and Roth, S.Y. (1998). In vivo functions of histone acetylation/deacetylation in Tup1p repression and Gcn5p activation. *Cold Spring Harb Symp Quant Biol*, **63**. 459-468.

Edmondson, D.G., Davie, J.K., Zhou, J., Mirnikjoo, B., Tatchell, K. and Dent, S.Y. (2002). Site-specific loss of acetylation upon phosphorylation of histone H3. *J Biol Chem*, **277** (33). 29496-29502.

Ehrenhofer-Murray, A.e. (2004). Chromatin dynamics at DNA replication, transcription and repair. *Eur J Biochem*, **271**. 2335–2349.

Eker, A.P.M., Kooiman, P., Hessels, J.K.C., and Yasui, A. (1990) DNA photoreactivating enzyme from the cyanobacterium Anacystis nidulans. *J Biol Chem*, **265**. 8009-8015.

Ekwall, K., Olsson, T., Turner, B.M., Cranston, G. and Allshire, R.C. (1997). Transient inhibition of histone deacetylation alters the structural and functional imprint at fission yeast centromeres. *Cell*, **91**. 1021-1032.

Elledge, S.J. (1996). Cell cycle checkpoints: preventing an identity crisis. *Science*, **274**. 1664-1672.

Emr, S.D., Schekman, R., Flessel, M.C. and Thorner, J. (1983). An MF alpha 1-SUC2 (alpha-factor-invertase) gene fusion for study of protein localization and gene expression in yeast. *Proc Natl Acad Sci USA*, **80** (23). 7080-7084.

Enomoto, S. and Berman, J. (1998). Chromatin assembly factor I contributes to the maintenance, but not the re-establishment, of silencing at the yeast silent mating loci. *Genes Dev*, **12**. 219-232.

Fangman, W.L. and Brewer, B.J. (1992). A question of time – replication origins of eukaryotic chromosomes.*Cell*, **71**. 363-366.

Fazzio, T.G., Kooperberg, C., Goldmark, J.P., Neal, C., Basom, R., Delrow, J. and Tsukiyama, T. (2001). Widespread collaboration of Isw2 and Sin3-Rpd3 chromatin remodeling complexes in transcriptional repression. *Mol Cell Biol*, **21**. 6450–6460.

Feaver, W.J., Svejstrup, J.Q. and Bardwell, L. (1993). Dual roles of a multiprotein complex from S. cerevisiae in transcription and DNA repair. *Cell*, **75** (7). 1379–1387.

Fernandez-Capetillo, O. and Nussenzweig, A. (2004). Linking histone deacetylation with the repair of DNA breaks. *Proc Natl Acad Sci USA*, **101** (6). 1427-1428.

Ferreiro, J.A., Powell, N.G., Karabetsou, N., Kent, N.A., Mellor, J. and Waters, R. (2004). Cbf1p modulates chromatin structure, transcription and repair at the *Saccharomyces cerevisiae* MET16 locus. *Nucl Acids Res*, **32**. 1617-1626.

Fields, S. and Herskowitz, I. (1985). The yeast *STE12* product is required for expression of two sets of cell-type specific genes. *Cell*, **42** (3). 923-930.

Fischle, W., Wang, Y. and Allis, C.D. (2003). Binary switches and modification cassettes in histone biology and beyond. *Nature*, **425**. 475-479.

Fisher, A.L. and Caudy, M. (1998). Groucho proteins: transcriptional corepressors for specific subsets of DNA-binding transcription factors in vertebrates and invertebrates. *Genes Dev*, **12**. 1931-1940.

Fleming, A.B., and Pennings, S. (2001). Antagonistic remodelling by Swi-Snf and Tup1-Ssn6 of an extensive chromatin region forms the background for *FLO1* gene regulation. *EMBO J*, **20**. 5219–5231.

Foster, E.R. and Downs, J.A. (2005). Histone H2A phosphorylation in DNA double-strand break repair. *FEBS J*, **272**. 3231-3240.

Freidkin, I. and Katcoff, D.J. (2001). Specific distribution of the Saccharomyces cerevisiae linker histone homolog HHO1p in the chromatin. *Nucleic Acids Res*, **29** (19). 4043-4051.

Friedberg, E.C., (1996a). Relationships between DNA repair and transcription. *Ann Rev Biochem*, **65**. 15-42.

Friedberg, E.C., (1996b). Cockayne syndrome: a primary defect in DNA repair, transcription, both or neither?. *BioEssays*. **18**. 731-738.

Friedberg, E.C., (2001). How nucleotide excision repair protects against cancer. *Nat Rev Cancer*. **1** (1). 22-27.

Friedberg, E.C., (2003). DNA damage and repair. *Nature.* **421**. 436-440.

Friedberg, E.C., Walker, G.C., Siede, W., Wood, R.D., Schultz, R.A. and Ellenberger, T. (2005). *DNA Repair and Mutagenesis,* 2nd edition, ASM Press, Washington DC.

Fromme, J.C. and Verdine, G.L. (2004). *DNA repair and replication.* Yang, W. (ed). **69**. 1-41. Elsevier, San Diego, CA.

Fuss, J.O. and Cooper, P.K. (2006). DNA Repair: Dynamic defenders against cancer and aging. *PLoS Biol,* **4** (6). e203.

Gaillard, P.H., Martini, E.M., Kaufman, P.D., Stillman, B., Moustacchi, E. and Almouzni, G. (1996). Chromatin assembly coupled to DNA repair: a new role for chromatin assembly factor 1. *Cell,* **86**. 887-896.

Gale, J.M., Nissen, K.A. and Smerdon, M.J. (1987). UV-induced formation of pyrimidine dimers in nucleosome core DNA is strongly modulated with a periodicity of 10.3 bases. *Proc Natl Acad Sci USA*, **84**. 6644-6648.

Gale, J.M. and Smerdon, M.J. (1990). UV-induced 6-4 photoproducts are distributed differently than cyclobutane pyrimidine dimers in nucleosomes. *Photochem Photobiol*, **51** (4). 411-417.

Gao, L., Cueto, M.A., Asselbergs, F.and Atadja, P. (2002). Cloning and functional characterization of HDAC11, a novel member of the human histone deacetylase family. *J Biol Chem,* **277** (28). 25748-25755.

Gietz, D., St Jean, A., Woods, R.A., Schiestl, R.H. (1992). Improved method for high efficiency transformation of intact yeast cells. *Nucl Acids Res,* **20**. 1425.

Giglia-Mari, G., Coin, F., Ranish, J.A., Hoogstraten, D., Theil, A., Wijgers, N., Jaspers, N.G., Raams, A., Argentini, M., van der Spek, P.J., Botta, E., Stefanini, M., Egly, J.M., Aebersold, R., Hoeijmakers, J.H. and Vermeulen, W. (2004) A new, tenth subunit of TFIIH is responsible for the DNA repair syndrome trichothiodystrophy group A. *Nat Genet,* **36**. 714–719.

Giglia-Mari, G., Miquel, C., Theil, A.F., Mari, P.O., Hoogstraten, D., Ng, J.M., Dinant, C., Hoeijmakers, J.H. and Vermeulen, W. (2006). Dynamic interaction of TTDA with TFIIH is stabilized by nucleotide excision repair in living cells. *PLoS Biol,* **4**. e156.

Gimble, F.S. and Sauer, R.T. (1989). Lambda repressor mutants that are better substrates for RecA-mediated cleavage. *J Mol Biol,* **206**. 29-39.

Gong, F., Kwon, Y.H. and Smerdon, M.J. (2005). Nucleotide excision repair in chromatin and the right of entry. *DNA Repair (Amst),* **4** (8). 884-896.

Gontijo, A.M., Green, C.M. and Almouzni, G. (2003). Repairing DNA damage in chromatin. *Biochimie,* **85**. 1133-1147.

Gordon, L.K. and Haseltine, W.A. (1982). Quantitation of cyclobutane pyrimidine dimer formation in double- and single-stranded DNA fragments of defined sequence. *Radiat Res,* **89**. 99-112.

Graftstrom, R.H., Park, L. and Grossman, L. (1982). Enzymatic repair of pyrimidine dimer-containing DNA. A 5' dimer DNA glycosylase: 3'-apyrimidinic endonuclease mechanism from Micrococcus luteus. *J Biol Chem,* **257**. 13465-13474.

Grant, P.A. (2001). A tale of histone modifications. *Genome Biol,* **2** (4). Reviews0003.1-0.0003.6, Epub.

Grant, P.A. and Berger, S.L. (1999). Histone acetyltransferase complexes. *Semin Cell Dev Biol,* **10**. 169-177.

Grant, P.A., Duggan, L., Cote, J., Roberts, S.M., Brownell, J.E., Candau, R., Ohba, R., Owen-Hughes, T., Allis, C.D., Winston, F., Berger, S.L. and Workman, J.L. (1997). Yeast Gcn5 functions in two multisubunit complexes to acetylate nucleosomal histones: characterisation of an Ada complex and the SAGA (Spt/Ada) complex. *Genes Dev,* **11**. 1640-1650.

Gray, S.G. and Elkstrom, T.J. (2001). The human histone deacetylase family. *Exp Cell Res,* **262** (2). 75-83.

Grbavec, D., Lo, R., Liu, Y., Greenfield, A. and Stifani, S. (1999). Groucho/transducin-like enhancer of split (TLE) family members interact with yeast transcriptional co-repressor SSN6 and mammalian SSN6-related proteins: Implications for evolutionary conservation of transcription repression mechanisms. *Biochem J,* **337**. 13-17.

Green, C.M., and Almouzni, G. (2002). When repair meets chromatin. *EMBO Rep,* **3** (1). 28-33.

Green, C.M., and Almouzni, G. (2003). Local action of the chromatin assembly factor CAF-1 at sites of nucleotide excision repair *in vivo*. *EMBO J,* **22** (19). 5163-5174.

Green, S.R., and Johnson, A.D. (2004). Promoter-dependent roles for the Srb10 Cyclin-dependent kinase and the Hda1 deacetylase in Tup1-mediated repression in *Saccharomyces cerevisiae*. *Mol Biol Cell,* **15** (4). 1999-2009.

Grozinger, C.M., Hassig, C.A. and Schreiber, S.L. (1999). Three proteins define a class of human histone deacetylases related to yeast Hda1p. *Proc Natl Acad Sci USA,* **96**. 4868-4873.

Grunstein, M. (1990). Histone function in transcription. *Annu Rev Cell Biol,* **6**. 643-678.

Grunstein, M. (1997). Histone acetylation in chromatin structure and transcription. *Nature,* **389**. 349-352.

Guoqing, C., Joseph, F., Sheenah, M., and Albert, C. (1999). A functional interaction between the histone deacetylase Rpd3 and the corepressor Groucho in *Drosophila* development. *Genes & Dev,* **13**. 2218-2230.

Guldener, U., Heck, S., Fielder, T., Beinhauer, J. and Hegemann, J.H. (1996). A new efficient gene disruption cassette for repeated use in budding yeast. *Nucleic Acids Res,* **24**. 2519-2524.

Guzder, S.N., Habraken, Y., Sung, P., Prakash, L. and Prakash, S. (1995). Reconstitution of yeast nucleotide excision repair with purified Rad proteins, replication protein A, and transcription factor TFIIH. *J Biol Chem,* **270** (22). 12973-12976.

Guzder, S.N., Habraken, Y., Sung, P., Prakash, L. and Prakash, S. (1996a). *RAD26*, the yeast homolog of human Cockayne's syndrome group B gene, encodes a DNA dependent ATPase. *J Biol Chem,* **271**. 18314-18317.

Guzder, S.N., Sung, P., Prakash, L. and Prakash, S. (1996b). Nucleotide excision repair in yeast is mediated by sequential assembly of repair factors and not by a pre-assembled repairosome. *J Biol Chem,* **271** (15). 8903-8910.

Guzder, S.N., Sung P., Prakash, L. and Prakash, S. (1997). Yeast Rad7-Rad16 complex, specific for the nucleotide excision repair of the non-transcribed DNA strand, is an ATP-dependent DNA damage sensor. *J Biol Chem,* **272** (35). 21665-21668.

Guzder, S.N., Sung P., Prakash, L. and Prakash, S. (1998). The DNA-dependent ATPase activity of yeast nucleotide excision repair factor 4 and its role in DNA damage recognition. *J Biol Chem,* **273** (11). 6292-6296.

Haber, J.E. (1998). Mating-type gene switching in *Saccharomyces cerevisiae*. *Annu Rev Genet,* **32**. 561-599.

Hafe, B.D. and Robertson, S.J. (2000). DNA mismatch repair and genetic instability. *Annu Rev Genet,* **34**. 359-399.

Hampsey, M. (1998). Molecular genetics of the RNA polymerase II general transcriptional machinery. *Microbiol Mol Biol Rev,* **62** (2). 465-503.

Hanawalt, P.C. (2002). Subpathways of nucleotide excision repair and their regulation. *Oncogene,* **21**. 8949-8956.

Hara, R., Mo, J. and Sancar, A. (2000). DNA damage in the nucleosome core is refractory to repair by human excision nuclease. *Mol Cell Biol,* **20**. 9173-9181.

Harvey, A.C., Jackson, S.P. and Downs, J.A. (2005). Saccharomyces cerevisiae histone H2A Ser122 facilitates DNA repair. *Genetics,* **170** (2). 543-553.

Hassan, A.H., Neely, K.E., Vignali, M., Reese, J.C. and Workman, J.L. (2001). Promoter targeting of chromatin-modifying complexes. *Front Biosci,* **6**. 1054-1064.

Hassan, A.H., Neely, K.E. and Workman, J.L. (2001b). Histone acetyltransferase complexes stabilise swi/snf binding to promoter nucleosomes. *Cell,* **104**. 817-827.

He, Z. and Ingles, C.J. (1997). Isolation of human complexes proficient in nucleotide excision repair. *Nucleic Acid Res,* **25** (6). 1136-1141.

Hebra, F. and Kaposi, M. (1874). *On diseases of the skin, including the exanthemata.* Vol 16 (translated by Tay, W., London). New Sydenham Society, London. pp 252-258.

Heinen, C.D., Schmutte, C., and Fishel, R. (2002). DNA repair and tumorigenesis: lessons from hereditary cancer syndromes. *Cancer Biol Ther,* **1** (5). 477-485.

Herskowitz, I. (1989). A regulatory hierarchy for cell specialization in yeast. *Nature,* **342**. 749-757.

Hicks, J., Strathern, J. & Herskowitz, I. (1977) in *DNA Insertion Elements, Plasmids and Episomes.* Bukhari, A. I., Shapiro, J. A. and Adhya, S. L. (Eds). (Cold Spring Harbor Laboratory, Cold Spring Harbor, NY), pp. 457-462.

Hirschhorn, J.N., Bortvin, A.L., Ricupero-Hovasse, S.L., and Winston, F. (1995). A new class of histone H2A mutations in *Saccharomyces cerevisiae* causes specific transcriptional defects in vivo. *Mol Cell Biol,* **15**. 4191-4202.

Hoeijmakers, J.H.J. (1994). Human nucleotide excision repair syndromes: molecular clues to unexpected intricacies. *Eur J Cancer,* **30A**. 1912-1921.

Hoeijmakers, J.H.J. (2001). Genome maintenance mechanisms for preventing cancer. *Nature,* **411**. 366-374.

Hollaender, A. and Curtis, J.T. (1936). Effect of sublethal doses of monochromatic ultraviolet radiation on bacteria in liquid suspension. *Proc Soc Exp Biol Med,* **33**. 61-62.

Holstege, F.C., Jennings, E.G., Wyrick, J.J., Lee, T.I., Hengartner, C.J., Green, M.R., Golub, T.R., Lander, E.S. and Young, R.A. (1998). Dissecting the regulatory circuitry of a eukaryotic genome. *Cell,* **95** (5). 717-728.

Holstege, F.C., van der Vliet, P.C, and Timmers, H.T. (1996). Opening of an RNA polymerase II promoter occurs in two distinct steps and requires the basal transcription factors IIE and IIH. *EMBO J,* **15**. 1666–1677.

Hoogstraten, D., Nigg, A.L., Heath, H., Mullenders, L.H., van Driel, R., Hoeijmakers, J.H., Vermeulen, W. and Houtsmuller, A.B. (2002) Rapid switching of TFIIH between RNA polymerase I and II transcription and DNA repair in vivo. *Mol Cell,* **10**. 1163–1174.

Horibata, K., Iwamoto, Y., Kuraoka, I., Jaspers, N.G., Kurimasa, A., Oshimura, M., Ichihashi, M. and Tanaka, K. (2004). From the cover: Complete absence of Cockayne syndrome group B gene product gives rise to UV-sensitive syndrome but not Cockayne syndrome. *Proc Natl Acad Sci USA*, **101**. 15410–15415.

Horn, P.J. and Peterson, C.L. (2002). Molecular biology. Chromatin higher order folding – wrapping up transcription. *Science*, **297** (5588). 1824-1827.

Howard-Flanders, P., Boyce, R.P., and Theriot, L. (1966). Three loci in *Escherichia coli* K-12 that control the excision of pyrimidine dimers and certain other mutagen products from DNA. *Genetics*, **53** (5). 1119-1136.

Herouy, Y., Krutmann, J., Norgauer, J. and Schopf, E. (2003). Xerderma pigmentosum: children of the moon. *J Dtsch Dermatol Ges*, **1** (3). 191-198.

Huang, L., Zhang, W., and Roth, S.Y. (1997). Amino termini of histones H3 and H4 are required for a1-alpha2 repression in yeast. *Mol Cell Biol*, **17**. 6555–6562.

Husain, I., Griffith, J. and Sancar, A. (1988). Thymine dimers bend DNA. *Proc Natl Acad Sci USA*. **85**. 2558-2562.

Jaskelioff, M., and Peterson, C.L. (2003). Chromatin and transcription: Histones continue to make their marks. *Nat Cell Biol*, **5**. 395–399.

Jazayeri, A., McAinsh, A.D. and Jackson, S.P. (2004). Saccharomyces cerevisiae Sin3p facilitates DNA double-strand break repair. *Proc Natl Acad Sci USA*, **101** (6). 1644-1649.

Jensen, K.A. and Smerdon, M.J. (1990). DNA repair within nucleosome cores of UV-irradiated human cells. *Biochemistry*, **29**. 4773-4782.

Jiricny, J. (2006). The multifaceted mismatch repair system. *Nat Rev Mol Cell Biol*, 7(5). 335-46.

Johnson, A.D. (1995). Molecular mechanisms of cell-type determination in budding yeast. *Curr Opin Genet Dev*, **5** (5). 552-558.

Johnson, C.N., Adkins, N.L., Georgel, P. (2005). Chromatin remodeling complexes: ATP-dependent machines in action. *Biochem Cell Biol*, **83** (4). 405-417.

Jun, S.H., Kim, T.G. and Ban, C. (2006). DNA mismatch repair system: Classical and fresh roles. *FEBS J*, **273** (8). 1609-1619.

Kadosh, D. and Struhl, K (1997). Repression by Ume6 includes recruitment of a complex containing Sin3 corepressor and Rpd3 histone deacetylases to target promoters. *Cell*, **89**. 365-371.

Kadosh, D. and Struhl, K (1998). Targeted recruitment of the Sin3-Rpd3 histone deacetylases complex generates a highly localized domain of repressed chromatin in vivo. *Mol Cell Biol*, **18**. 5121-5127.

Kaufman, P.D., Kobayashi, R. and Stillman, B. (1997). Ultraviolet radiation sensitivity and reduction of telomeric silencing *Saccharomyces cerevisiae* cells lacking chromatin assembly factor-I. *Gene Dev*, **11**. 345-357.

Keeney, S., Chang, G.J. and Linn, S. (1993). Characterization of a human DNA damage binding protein implicated in xeroderma pigmentosum E. *J Biol Chem*, **268**. 21293-21300.

Kelly, T.J., Qin, S., Gottschling, D.E. and Parthun, M.R. (2000) Type B histone acetyltransferase participates in telomeric silencing. *Mol Cell Biol*, **20**. 7051-7058.

Kelner, A. (1949). Effect of visible light on the recovery of *Streptomycin griseus canidia* from ultraviolet irradiation injury. *Proc Natl Acad Sci USA*, **35**. 73-79.

Khader, A., Gritli, S., Boussen, I., Oueslati, Z., Ferjaoui, M., Nouira, R., Ladgham, A. and Boussen, H. (2005). Topical and systemic chemotherapy with 5-fluouracil in facial carcinoma secondary to xeroderma pigmentosum. *Tunis Med*, **83** (11). 672-674.

Kim, J.K., Patel, D. and Choi, B.S. (1995). Contrasting structural impacts induced by *cis-syn* cyclobutane pyrimidine dimer and (6-4) adduct in DNA duplex decamers: implication in mutagenesis and repair activity. *Photochem Photobiol*, **62** (1). 44-50.

Kingston, R.E. and Narlikar, G.J. (1999). ATP-dependent remodeling and acetylation as regulators of chromatin fluidity. *Genes Dev*, **13**. 2339-2352.

Kolodner, R.D. (1996). Biochemistry and genetics of eukaryotic mismatch repair. *Genes Dev*, **10**. 1433-1442.

Komachi, K., Redd, M.J. and Johnson. (1994). The WD repeats of Tup1 interact with the homeo domain protein alpha 2. *Genes Dev*, **8**. 2857-2867.

Kornberg, R.D. (1977). Structure of chromatin. *Ann Rev Biochem*, **46**. 931-954.

Kraemer, K.H., Myung, M.L. and Scotto, J. (1987). Xeroderma pigmentosum. Cutaneous, ocular and neurologic abnormalities in 830 published cases. *Arch derm*, **123**. 241-250.

Krokan, H.E., Standal, R. and Slupphaug, G. (1997). DNA glycosylases in the base excision repair of DNA. *Biochem J*, **325**. 1–16.

Kruszewski, M. and Szumiel, I. (2005). Sirtuins (histone deacetylases III) in the cellular response to DNA damage – facts and hypotheses. *DNA Repair*, **4**. 1306-1313.

Kunkel, T.A. and Erie, D.A. (2005). DNA mismatch repair. *Annu Rev Biochem*, **74**. 681-710.

Kunkel, T.A. and Wilson, S.H. (1996). Push and pull of base flipping. *Nature*, **384**. 25-26.

Kuo, M.-H. and Allis, C.D. (1998). Roles of histone acetyltransferases and deacetylases in gene regulation. *Bioessays*, **20**. 615-626.

Kuo, M.-H., Zhou, J., Jambeck, P., Churchill, M.E.A. and Allis, C.D. (1998). Histone acetyltransferase activity of yeast Gcn5p is required for the activation of target genes in vivo. *Genes Dev*, **12**. 627-639.

Kurdistani, S.K., Tavazoie, S. and Grunstein, M. (2004). Mapping global histone acetylation patterns to gene expression. *Cell*, **117**. 721-733.

Kyrylenko, S., Kyrylenko, O., Suuronen, T. and Salminen, A. (2003). Differential regulation of the Sir2 histone deacetylase gene family by inhibitors of class I and II histone deacetylases. *Cell Mol Life Sci*, **60** (9). 1990-1997.

La Thangue, N.B. (2004). Histone deacetylase inhibitors and cancer therapy. *J Chemother*, **16** (4). 64-67.

Lamers, M.H., Winterwerp, H.H. and Sixma, T.K. (2003). The alternating ATPase domains of MutS control DNA mismatch repair. *EMBO J*, **22** (3). 746-756.

Landry, J., Sutton, A., Tafrov, S.T., Heller, R.C., Stebbins, J., Pillus, L. and Sternglanz, R. (2000). The silencing protein SIR2 and its homologs are NAD-dependent protein deacetylases. *Proc Natl Acad Sci USA*, **97** (11). 5807-5811.

Lauder, S., Bankman, M., Guzder, S.N., Sung, P., Prakash, L. and Prakash, S. (1996). Dual requirement for the yeast *MMS19* gene in DNA repair and RNA polymerase II transcription. *Mol Cell Biol*, **16** (12). 6783–6793.

Leach, F.S., Nicolaides, N.C., Papadopoulos, B., Liu, B., Jen, J., Parsons, R., Peltomaki, P., Sistonen, P., Aaltonen, L.A., Nystrom-Lahti, M., Guan, X.-Y., Zhang, J., Meltzer, P.S., Yu, J.-W., Kao, F.-T., Chen, D.J., Cerosaletti, K.M., Fournier, R.E.K., Todd, S., Lewis, T., Leach, R.J., Naylor, S.L., Weissenbach, J.-P., Mecklin, Jarvinen, H., Petersen, G.M., Hamilton, S.R., Green, J., Jass, J., Watson, P., Lynch, H.T., Trent, J.M., de la Chapelle, A., Kinzler, K.W. and Vogelstein, B. (1993). Mutations of a *mutS* homolog in hereditary nonpolyposis colorectal cancer. *Cell,* **75**. 1215-1225.

Lebbink, J.H., Georgijevic, D., Natrajan, G., Fish, A., Winterwerp, H.H., Sixma, T.K. and de Wind, N. (2006). Dual role of MutS glutamate 38 in DNA mismatch discrimination and in the authorization of repair. *EMBO J,* **25** (2). 409-419.

Lee, D.Y., Hayes, J.J., Pruss, D. and Wolffe, A.P. (1993). A positive role for histone acetylation in transcription factor access to nucleosomal DNA. *Cell,* **72**. 73-84.

Lee, S.-K., Yu, S.-L., Prakash, L. and Prakash, S. (2001). Requirement for yeast *RAD26*, a homolog of the human *CSB* gene, in elongation by RNA polymerase II. *Mol Cell Biol,* **21**. 8651-8656.

Lehmann, A. R. (2001). The xeroderma pigmentosum group D (*XPD*) gene: one gene, two functions, three diseases. *Genes Dev,* **15**. 15-23.

Lewin, B. (2000). *Genes VII.* Oxford University Press Inc., New York.

Lewis, L.K. and Resnick, M.A. (2000). Tying up loose ends: nonhomologous end-joining in Saccharomyces cerevisiae, *Mutat Res,* **451**. 71–89.

Levanon, D., Goldstein, R.E., Bernstein, Y., Tang, H., Goldenberg, D., Stifani, S., Paroush, Z. and Groner, Y. (1998). Transcriptional repression by AML1 and LEF-1 is mediated by the TLE/Groucho corepressors. *Proc Natl Acad Sci USA,* **95**. 11590-11595.

Li, B., and Reese, J.C. (2001). Ssn6-Tup1 Regulates *RNR3* by Positioning Nucleosomes and Affecting the Chromatin Structure at the Upstream Repression Sequence. *J Biol Chem,* **276**. 33788–33797.

Li, G.M. (2003). DNA mismatch repair and cancer. *Front Biosci,* **8**. 997-1017.

Li, S. and Smerdon, M.J. (2002). Rpb4 and Rpb9 mediate subpathways of transcription-coupled DNA repair in *Saccharomyces cerevisiae. EMBO J,* **21** (21). 5921–5929.

Li, S. and Smerdon, M.J. (2002b). Nucleosome structure and repair of N-methylpurines in the GAL1-10 genes of *Saccharomyces cerevisiae. J Biol Chem,* **277**. 44651-44659.

Li, S. and Smerdon, M.J. (2004). Dissecting transcription-coupled repair and global genomic repair in the chromatin of yeast *GAL1-10* genes. *J Biol Chem,* **279** (14). 14418-14426.

Lieberman, M.W., Smerdon, M.J., Tlsty, T.D. and Oleson, F.B. (1979). The role of chromatin structure in DNA repair in human cells damaged with chemical carcinogens and ultraviolet radiation. In *Environmental Carcinogenesis.* (Emmelot, P. and Kriek, E. Eds). Elsevier/North Holland Biomedical Press, Amsterdam. pp. 345-363.

Lin, H.Y., Chen, C.S., Lin, S.P., Weng, J.R. and Chen C.C. (2006). Targeting histone deacetylase in cancer therapy. *Med Res Rev,* **26** (4). 397-413.

Lindahl, T. (1993). Instability and decay of the primary structure of DNA. *Nature.* **362**. 709-715.

Lindahl, T. and Wood, R.D. (1999). Quality control by DNA repair. *Science.* **286**. 1897-1905.

Lindenbaum, Y., Dickson, D., Rosenbaum, P., Kraemer, K., Robbins, I. and Rapin, I. (2001). Xeroderma pigmentosum/Cockayne syndrome complex: first neuropathological study and review of eight other cases. *Eur J Paediatr Neurol,* **5** (6). 225-242.

Lo, W.S., Trievel, R.C., Rojas, J.R., Duggan, L.,Hsu, J.Y., Allis, C.D., Marmorstein, R. and Berger, S.L. (2000). Phosphorylation of serine 10 in histone H3 is functionally linked in vitro and in vivo to Gcn5-mediated acetylation at lysine 14. *Mol Cell*, **5**. 917-926.

Lodish, H., Berk, A., Zipursky, L., Matsudaira, P., Baltimore, D. and Darnell, J. (2000). *Molecular Cell Biology (4th Edition)*. W.H. Freeman and Company, Basingstoke.

Lowndes, N.F. and Murguia, J.R. (2000). The DNA damage-dependent checkpoints of yeast and human cells. *Curr Opin Genet Dev*, **10**. 17-25.

Luger, K. (2006). Dynamic nucleosomes. *Chromosome Res*, **14** (1). 5-16.

Luger, K., Mader, A.W., Richmond, R.K., Sargent, D.F. and Richmond, T.J, (1997). Crystal Structure of the Nucleosome Core Particle at 2.8 Å Resolution. *Nature*, **389** (6648). 251-260.

Lynch, H.T. and de la Chapelle, A. (1999). Genetic susceptibility to non-polyposis colorectal cancer. *J Med Genet*, **36**. 801-818.

Magnaldo, T. and Sarasin, A. (2004). Xeroderma pigmentosum: from symptoms and genetics to gene-based skin therapy. *Cells Tissues Organs*, **177** (3). 189-198.

Mai, A., Massa, S., Rotili, D., Cerbara, I., Valente, S., Pezzi, R., Simeoni, S. and Ragno, R. (2005). Histone deacetylation in epigenetics: an attractive target for anticancer therapy. *Med Res Rev*, **25** (3).261-309.

Malhotra, K., Kim, S.T., Walsh, C. and Sancar, A. (1992). Roles of FAD and 8-hydroxy-5-deazaflavin chromophores in photoreactivation by Anacystis nidulans DNA photolyase. *J Biol Chem*, **267** (22). 15406-15411.

Mallet, L., Bussereau, F. and Jacquet, M. (1995). A 43.5Kb segment of yeast chromosome XIV, which contains MFA2, MEP2, CAP/SRV2, NAM9, FKB1/FRP1/RBP1, MOM22 and CPT1, predicts an adenosine deaminase gene and 14 new open reading frames. *Yeast*, **11**. 1195-1209.

Mandal, T.N., Mahdi, A.A., Sharples, G.J. and Lloyd, R.G. (1993). Resolution of Holliday intermediates in recombination and DNA repair: indirect suppression of *ruvA*, *ruvB* and *ruvC* mutations. *J Bacteriol*, **175**. 4325-4334.

Mankovich, J.A., McIntyre, C.A. and walker, G.C. (1989). Nucleotide sequence of the *Salmonella typhimurium mutL* gene required for mismatch repair; homology of *mutL* to *hexB* of *Streptococcus pneumoniae* and to *PMS1* of the yeast *Saccharomyces cerevisiae*. *J Bacteriol*, **171**. 5325-5331.

Marks, P.A. and Dokmanovic, M. (2005). Histone deacetylase inhibitors: discovery and development as anticancer agents. *Expert Opin Investig Drugs*, **14** (12). 1497-1511.

Martini, E., Roche, D.M.J., Marheineke, K., Verreault, A. and Almouzni, G. (1998). Recruitment of phosphorylated Chromatin Assembly Factor 1 to chromatin following UV irradiation of human cells. *J Cell Biol*, **143**. 563-575.

Matsumura, Y. and Ananthaswamy, H.N. (2002). Structure of the major UV-induced photoproducts in DNA. *Expert reviews in molecular medicine*. Cambridge University Press.

Meier, A., Livingstone-Zatchej and Thoma, F. (2002). Repair of active and silenced rDNA in yeast: the contributions of transcription-coupled nucleotide excision repair. *J Biol Chem*, **277**. 11845-11852.

Meijer, M. and Smerdon, M.J. (1999). Accessing DNA damage in chromatin: insights from transcription. *BioEssays*, **21**. 596-603.

Mellon, I. (2005). Transcription-coupled repair: a complex affair. *Mutat Res*, **577** (1-2). 155-161.

Mellon, I., Hanawalt, P.C., (1989). Induction of *Escherichia coli* lactose operon selectively increases repair of its transcribed DNA strand. *Nature*, **342**. 95-98.

Mellon, I., Spivak, G., Hanawalt, P.C., (1987). Selective removal of transcription-blocking DNA damage from the transcribed strand of the mammalian DHFR gene. *Cell*, **51**. 241-249.

Michaelis, S. and Herskowitz, I. (1988). The a-factor pheromone of *Saccharomyces cerevisiae* is essential for mating. *Mol Cell Biol*, **8**. 1309-1318.

Millar, C.B. and Grunstein, M. (2006). Genome-wide patterns of histone modifications in yeast. *Nat Rev Mol Cell Biol*, 7, 657-666.

Mitchell, D.L.. (1988). The relative cytotoxicity of (6-4) photoproducts and cyclobutane pyrimidines dimers in mammalian cells. *Photochem Photobiol*, **48**. 51-57.

Mitchell, D.L. and Nairn, R.S. (1989). The biology of the (6-4) photoproduct. *Photochem Photobiol* **49**. 805-819.

Mitchell, D.L., Nguyen, T.D. and Cleaver, J.E. (1990). Non-random induction of pyrimidine-pyrimidone (6-4) photoproducts in ultraviolet irradiated human chromatin. *J Biol Chem*, **265**. 5353-5356.

Mitchell, J.R., Hoeijmakers, J.H.J. and Niedernhofer, L.J. (2003). Divide and conquer: nucleotide excision repair battles cancer and ageing. *Curr Opin Cell Biol*, **15**. 232-240.

Mitra, D., Parnell, E.J., Landon, J.W., Yu, Y. and Stillman, D.J. (2006). SWI/SNF binding to the HO promoter requires histone acetylation and stimulates TATA-binding protein recruitment. *Mol Cell biol*, **26** (11). 4095-4110.

Modrich, P. and Lahue, R. (1996). Mismatch repair in replication fidelity, genetic recombination and cancer biology. *Annu Rev Biochem*, **65**. 101-133.

Moggs, J.G. and Almouzni, G. (1999). Chromatin rearrangements during nucleotide excision repair. *Biochimie*, **81**. 45-52.

Morales, V., Giamarchi, C., Chailleux, C., Moro, F., Marsaud, V., Le Ricousse, S. and Richard-Foy, H. (2001). Chromatin structure and dynamics; functional implications. *Biochimie*, **83** (11-12). 1029-1039.

Mork, C.N., Faller, D.V. and Spanjaard, R.A. (2005). A mechanistic approach to anticancer therapy: targeting the cell cycle with histone deacetylase inhibitors. *Curr Pharm Des*, **11** (9). 1091-1104.

Morrison, A.J. and Shen, X. (2005). DNA repair in the context of chromatin. *Cell Cycle*, **4** (4). 568-571.

Mu, D. and Sancar, A. (1997). Model for XPC-independent transcription coupled repair of pyrimidine dimers in humans. *J Biol Chem*, **272**. 7570-7573.

Mullenders, L.H.F., Stary, A. and Sarasin, A. (2001). Nucleotide excision repair. *Atlas Genet Cytogenet Oncol Haematol.*
(URL : http://AtlasGeneticsOncology.org/Deep/ExcisRepairID20014.html)

Nasmyth, K.A. (1982). Molecular genetics of yeast mating type. *Annu Rev Genet*, **16**. 439-500.

Nasmyth K, Stillman, D. and Kipling, D. (1987). Both positive and negative regulators of HO transcription are required for mother-cell-specific mating-type switching in yeast. *Cell* **48** (4):579-587.

Natrajan, G., Lamers, M.H., Enzlin, J.H., Winterwerp, H.H., Perrakis, A. and Sixma, T.K. (2003). Structures of Escherichia coli DNA mismatch repair enzyme MutS in complex with different

mismatches: a common recognition mode for diverse substrates. *Nucleic Acids Res,* **31** (16). 4814-4821.

Neely, K.E. and Workman, J.L. (2002). Histone acetylation and chromatin remodelling: which comes first? *Mol Genet Metab,* **76**. 1-5.

Nusinzon, I. and Horvath, C.M. (2005). Histone Deacetylases as Transcriptional Activators? Role Reversal in Inducible Gene Regulation. *Sci. STKE* 2005, re11.

Nusinzon, I. and Horvath, C.M. (2006). Positive and Negative Regulation of the Innate Antiviral Response and Beta Interferon Gene Expression by Deacetylation. *Mol Cell Biol,* **26** (8). 3106-3113.

O'Brien, T., Hardin, S., Greenleaf, A. and Lis, J.T. (1994). Phosphorylation of RNA polymerase II C-terminal domain and transcriptional elongation. *Nature,* **370**. 75–77.

Ogryzko, V.V., Schlitz, R.L., Russanova, V., Howard, B.H. and Katatani, Y. (1996). The transcription coactivators p300 and CBP are histone acetyltransferases. *Cell,* **87**. 953-959.

Olsson, M. and Lindahl, T. (1980). Repair of alkylated DNA in *Escherichia coli*. Methyl group transfer from O^6-methylguanine to a protein cysteine residue. *J Biol Chem,* **255**. 10569-10571.

Papamichos-Chronakis, M., Conlan, R.S., Gounalaki, N., Copf, T. and Tzamarias, D. (2000). Hrs1/Med3 is a Cyc8-Tup1 corepressor target in the RNA polymerase II holoenzyme. *J Biol Chem,* **275**. 8397-8403.

Park, H., Zhang, K., Ren, Y., Nadji, S., Sinha, N., Taylor, J.S. and Kang, C. (2002). Crystal structure of a DNA decamer containing a *cis-syn* thymine dimer. *Proc Natl Acad Sci USA,* **99**. 15965-15970.

Parsons, J.L., Dianova, I.I. and Dianov, G.L. (2004). APE1 is the major 3'-phosphoglycolate activity in human cell extracts. *Nucleic Acids Res,* **32** (12). 3531-3536.

Parsons, R., Li, G.-M., Longley, M.J., Fang, W.-H., Papadopoulos, N., Jen, J., de la Chapelle, A., Kinzler, K.W., Vogelstein, B. and Modrich, P. (1993). Hypermutability and mismatch repair of in RER^+ tumour cells. *Cell,* **75**. 1227-1236.

Patterton, H.G., Landel, C.C., Landsman, D. Peterson, C.L. and Simpson, R.T. (1998). The biochemical and phenotypic characterization of Hho1p, the putative linker histone H1 of Saccharomyces cerevisiae. *J Biol Chem,* **273** (13). 7268-7276.

Patterton, H.G. and Simpson, R.T. (1994). Nucleosomal location of of the STE6 TATA box and Mat alpha 2p-mediated repression. *Mol Cell Biol,* **14** (6). 4002-4010.

Paulovich, A.G. and Hartwell, L.H. (1995). A checkpoint regulates the rate of progression through S phase in *S. cerevisiae* in response to DNA damage. *Cell,* **82**. 841-847.

Pearlman, D.A., Holbrook, S.R., Pirkle, D.H. and Kim, S.H. (1985). Molecular models for DNA damaged by photoreaction. *Science,* **227**. 1304-1308.

Pehrson, J.R. (1989). Photo footprint of nucleosome core DNA in intact chromatin having different structural states. *J Mol Biol,* **204**. 949-958.

Pehrson, J.R. (1995). Probing the conformation of nucleosome linker DNA in situ with pyrimidine dimer formation. *J Biol Chem,* **270** (38). 22440-22444.

Pérez-Martin, J. (1999). Chromatin and transcription in *Saccharomyces cerevisiae*. *FEMS Microbiol Rev,* **23**. 503-523.

Peterson, C.L. and Cote, J. (2004). Cellular machineries for chromosomal DNA repair. *Genes Dev,* **18**. 602-616.

Peterson, C.L. and Laniel, M.A. (2004). Histones and histone modifications. *Curr Biol,* **14**. 546-551.

Petit, C. and Sancar, A. (1999). Nucleotide excision repair: from *E. coli* to man. *Biochimie,* **81**. 15-25.

Philippe, T.G. and Hansen, J.C. (2001). Linker histone function in chromatin: Dual mechanisms of action. *Biochem Cell Biol,* **79** (3). 313–316.

Pokholok, D.K., Harbison, C.T., Levine, S., Cole, M., Hannett, N.M., Lee, T.I., Bell, G.W., Walker, K., Rolfe, P.A., Herbolsheimer, E., Zeitlinger, J., Lewitter, F., Gifford, D.K. and Young, R.A. (2005). Genome-wide map of nucleosome acetylation and methylation in yeast. *Cell,* **122** (4). 517-527.

Politi, A., Mone, M.J., Houtsmuller, A.B., Hoogstraten, D., Vermeulen, W., Heinrich, R. and van Driel, R. (2005). Mathematical modeling of nucleotide excision repair reveals efficiency of sequential assembly strategies. *Mol Cell,* **19** (5). 679-90.

Pollitt, R.J., Jenner, F.A. and Davies, M. (1968). Sibs with mental and physical retardation and trichorrhexis nodosa with abnormal amino acid composition of the hair. *Arch Dis Child,* **43**. 211–216.

Powell, N.G., Ferreiro, J.A., Karabetsou, N., Mellor, J. and Waters, R. (2003). Transcription, nucleosome positioning and protein binding modulate nucleotide excision repair of the *Saccharomyces cerevisiae* MET17 promoter. *DNA Repair (Amst),* **2**. 375-386.

Prakash, S. and Prakash, L. (2000). Nucleotide excision repair in yeast. *Mutat Res,* **451** (1-2). 13-24.

Prakash, S., Sung, P. and Prakash, L. (1993). DNA repair genes and proteins of *Saccharomyces cerevisiae*. *Annu Rev Genet,* **27**. 33-70.

Pray-Grant, M.G., Schieltz, D., McMahon, S.J., Wood, J.M., Kennedy, E.L., Cook, R.G., Workman, J.L., Yates, J.R. III and Grant, P.A. (2002). The novel SLIK histone acetyltransferase complex functions in the yeast retrograde response pathway. *Mol Cell Biol,* **22**. 8774–8786.

Prolla, T.A., Christie, D.-M. and Liskay, R.M. (1994). Dual requirement in yeast DNA mismatch repair for *MLH1* and *PMS1*, two homologs of the bacterial *mutL* gene. *Mol Cell Biol,* **14**. 407-415.

Qin, J. and Li, L. (2003). Molecular anatomy of the DNA damage and replication checkpoints. *Radiat Res,* **159**(2). 139-148.

Ramanathan, B. and Smerdon, M.J. (1989). Enhanced DNA repair synthesis in hyperacetylated nucleosomes. *J Biol Chem,* **264**. 11026-11034.

Ranish, J.A., Hahn, S., Lu, Y., Yi, E.C., Li, X.J., Eng, J. and Aebersold, R.. (2004). Identification of TFB5, a new component of general transcription and DNA repair factor IIH. *Nat Genet,* **36** (7). 707-713.

Rapin, I., Lindenbaum, Y., Dickson, D.W., Kraemer, K.H. and Robbins, J.H. (2000). Cockayne syndrome and xeroderma pigmentosum: DNA repair disorders with overlaps and paradoxes. *Neurology,* **55** (10). 1442-1449.

Redd, M.J., Arnaud, M.B. and Johnson, A.D. (1997). A complex composed of tup1 and ssn6 represses transcription in vitro. *J Biol Chem,* **272**. 11193-11197.

Redon, C., Pilch, D.R., Rogakou, E., Orr, A.H., Lowndes, N.F. and Bonner, W.M. (2003). Yeast histone 2A serine 129 is essential for the efficient repair of checkpoint-blind DNA damage. *EMBO Rep,* **4**. 678–684.

Reed, S.H. (2005). Nucleotide excision repair in chromatin: the shape of things to come. *DNA Repair (Amst),* **4** (8). 909-918.

Reed, S.H., You, Z. and Friedberg,E.C. (1998). The yeast *RAD7* and *RAD16* genes are required for postincision events during nucleotide excision repair. *In vitro* and *in vivo* studies with *rad7 and rad16* mutants and purification of a Rad7/Rad16-containing protein complex. *J Biol Chem,* **273** (45). 29481-29488.

Ridgway, P. and Almouzni, G. (2000). CAF-1 and the inheritance of chromatin states: at the crossroads of DNA replication and repair. *J Cell Sci,* **113** (15). 2647-2658.

Robert, F., Pokholok, D.K., Hannett, N.M., Rinaldi, N.J., Chandy, M., Rolfe, A., Workman, J.L., Gifford, D.K. and Young, R.A. (2004). Global position and recruitment of HATs and HDACs in the yeast genome. *Mol Cell,* **16** (2). 199-209.

Roberts, R.J. and Cheng, X. (1998). Base flipping. *Annu Rev Biochem,* **67**. 181-198.

Robyr, D., Suka, Y., Xenarios, I., Kurdistani, S.K. and Wang, A. (2002). Microarray deacetylation maps determine genome-wide functions for yeast histone deacetylases. *Cell,* **109**. 437-446.

Rodriguez, K., Talamantez, J., Huang, W., Reed, S.H., Wang, Z., Chen, L., Feaver, W.J., Friedberg, E.C. and Tomkinson, A.E. (1998). Affinity purification and partial characterization of a yeast multiprotein complex for nucleotide excision repair using histidine-tagged Rad14 protein. *J Biol Chem,* **273** (51). 34180-34189.

Rogakou, E.P., Pilch, D.R., Orr, A.H., Ivanova, V.S. and Bonner, W.M. (1998). DNA double-stranded breaks induce histone H2AX phosphorylation on serine 139. *J Biol Chem,* **273.** 5858–5868.

Roth, S.Y., Dean, A., and Simpson, R.T. (1990). Yeast alpha 2 repressor positions nucleosomes in TRP1/ARS1 chromatin. *Mol Cell Biol,* **10.** 2247–2260.

Roth, S.Y., Denu, J.M. and Allis, C.D. (2001). Histone acetyltransferases. *Annu Rev Biochem,* **70**. 81-120.

Rouse, J. and Jackson, S.P. (2002). Interfaces between the detection, signalling, and repair of DNA damage. *Science,* **297**. 547-551.

Rubbi, C.P. and Milner, J. (2003). p53 is a chromatin accessibility factor for nucleotide excision repair of DNA damage. *EMBO J,* **22**. 975-986.

Rundlett, S.E., Carmen, A.A., Kobayashi, R., Bavykin, S., Turner, B.M. and Grunstein, M. (1996). HDA1 and RPD3 are members of distinct yeast histone deacetylases complexes that regulate silencing and transcription. *Proc Natl Acad Sci USA,* **93**. 14503-14508.

Rundlett, S.E., Carmen, A.A., Suka, N., Turner, B.M. and Grunstein, M. (1998). Transcriptional repression by UME6 involves deacetylation of lysine 5 of histone H4 by RPD3. *Nature,* **392**. 831-835.

Rupert, C.S., Goodgal, S. and Herriott, R.M. (1958). Photoreactivation *in vitro* of ultraviolet inactivated *Hemophilus influenzae* transforming factor. *J Gen Physiol,* **41**. 451-471.

Rupert, C.S. (1960). Photoreactivation of transforming DNA by an enzyme from baker's yeast. *J Gen Physiol,* **43**. 573-595.

Saha, A., Wittmeyer, J. and Cairns, B.R. (2006). Chromatin remodelling: the industrial revolution of DNA around histones. *Nat Rev Mol Cell Biol,* **7** (6). 437-447.

Sancar, A. (1996). DNA excision repair. *Annu Rev Biochem,* **65.** 43-81.

Sancar, A. and Sancar, G.B. (1988). DNA repair enzymes. *Annu Rev Biochem,* **57.** 29-67.

Sancar, G.B. (1990). DNA photolyases: Physical properties, action mechanism, and roles in dark repair. *Mutat Res,* **236** (2-3). 147-160.

Sancar, G.B. (2000). Enzymatic photoreactivation: 50 years and counting. *Mutat Res,* **451.** (1-2). 25-37.

Schleicher, E., Heßling, B., Illarionova, V., Bacher, A., Weber, S., Richter, G. and Gerwert, K. (2005). Light-induced reactions of Escherichia coli DNA photolyase monitored by Fourier transform infrared spectroscopy. *FEBS J,* **272.** 1855–1866.

Scicchitano, D.A. and Mellon, I. (1997). Transcription and DNA Damage: A Link to a Kink. *Environ Health Perspect,* **105** (1). 145-153.

Seeberg, E., Eide, L. and Bjoras, M. (1995). The base excision repair pathway. *Trends Biochem Sci,* **20.** 391-397.

Selby, C.P. and Sancar, A. (1991). Gene- and strand-specific repair *in vitro:* partial purification of a transcription-repair coupling factor. *Proc Natl Acad Sci USA,* **88.** 8232-8236.

Selby, C. P., and Sancar, A. (1994). Mechanisms of transcription-repair coupling andmutation frequency decline. *Mut Res,* **58.** 317-329.

Selby, C. P., and Sancar, A. (1997). Cockayne syndrome group B protein enhances elongation by RNA polymerase II. *Proc Natl Acad Sci USA,* **94.** 11205-11209.

Selby, C.P., Witkin, E.M. and Sancar, A. (1991). *Escherichia coli mfd* mutant deficient in "mutation frequency decline" lacks strand-specific repair: *in vitro* complementation with purified coupling factor. *Proc Natl Acad Sci USA,* **88.** 11574-11578.

Shimizu, M., Roth, S.Y., Szent-Gyorgyi, C. and Simpson, R.T. (1991). Nucleosomes are positioned with base pair precision adjacent to the alpha 2 operator in Saccharomyces cerevisiae. *EMBO J,* **10** (10). 3033-3041.

Shiota, S. and Nakayama, H. (1997). UV endonuclease of *Micrococcus luteus,* a cyclobutane pyrimidine dimer-DNA glycosylase/abasic lyase: Cloning and characterisation of the gene. *Proc Natl Acad Sci USA,* **94.** 593-598.

Shivji, M.K.K., Podust, V.N., Hubscher, U. and Wood, R.D. (1995). Nucleotide excision repair DNA synthesis by DNA polymerase epsilon in the presence of PCNA, RFC and RPA. *Biochemistry,* **34.** 5011-5017.

Smerdon, M. J. and Conconi, A. (1999). Modulation of DNA damage and DNA repair in chromatin. *Prog Nucleic Acid Res Mol Biol.* **62,** 227-255.

Smerdon, M.J., Lan, S.Y., Calza, R.E. and Reeves, R. (1982). Sodium butyrate stimulates DNA repair in UV-irradiated normal and xeroderma pigmentosum human fibroblasts. *J Biol Chem,* **257.** 13441-13447.

Smerdon, M.J. and Lieberman, M.W. (1978). Nucleosome rearrangement in human chromatin during UV-induced DNA-repair synthesis. *Proc Natl acad Sci USA,* **75.** 4238-4241.

Smerdon, M.J. and Lieberman, M.W. (1980). Distribution within chromatin of deoxyribonucleic acid repair synthesis occurring at different times after ultraviolet radiation. *Biochemistry,* **19.** 2992-3000.

Smerdon, M.J., Thoma, F., (1990). Site-specific DNA repair at the nucleosome level in a yeast minichromosome. *Cell,* **61.** 675-684.

Smith, R.L., Redd, M.J. and Johnson, A.D. (1995). The tetratricopeptide repeats of Ssn6 interact with the homeodomain of alpha 2. *Genes Dev,* **9.** 2903-2910.

Smith, R.L. and Johnson, A.D. (2000). Turning genes off by Ssn6-Tup1: a conserved system of transcriptional repression in eukaryotes. *Trends Biochem Sci*, **25** (7). 325-330.

Sobel, R.E., Cook, R.G., Perry, C.A., Annunziato, A.T. and Allis, C.D. (1995). Conservation of deposition-related acetylation sites in newly synthesized histones H3 and H4. *Proc Natl Acad Sci USA*, **92** (4). 1237-1241.

Stefanini, M., Lagomarsini, P., Arlett, C.F., Marinoni, S., Borrone, C., Crovato, F., Trevisan, G., Cordone, G., Nuzzo, F. (1986). Xeroderma pigmentosum (complementation group D) mutation is present in patients affected by trichothiodystrophy with photosensitivity. *Hum Genet*, **74**. 107–112.

Sternberg, P.W., Stern, M.J., Clark, I. and Herskowitz, I. (1987). Activation of the yeast *HO* gene by release from multiple negative controls. *Cell*, **48**. 567-577.

Stillman, B. (1996). Cell cycle control of DNA replication. *Science*, **274**. 1659-1664.

Strahl, B.D. and Allis, C.D. (2000). The language of covalent histone modifications. *Nature*, **403**. 41-45.

Strathern, J.N., Klar, A.J., Hicks, J.B., Abraham, J.A., Ivy, J.M., Nasmyth, K.A. and McGill, C. (1982). Homothallic switching of yeast mating type cassettes is initiated by a double-stranded cut in the MAT locus. *Cell*, **1**. 183–192.

Struhl, K. (1998). Histone acetylation and transcriptional regulatory mechanisms. *Genes Dev*, **12**. 599-606.

Sugasawa, K., Masutani, C. and Hanaoka, F. (2003). Cell-free repair of UV-damaged simian virus 40 chromosomes in human cell extracts. I. Development of a cell-free system detecting excision repair of UV-irradiated SV40 chromosomes. *J Biol Chem*, **268** (12). 9098-9104.

Sugasawa, K., Ng, J.M., Masutani, C., Iwai, S., van der Spek, P.J., Eker, A.P., Hanaoka, F., Bootsma, D. and Hoeijmakers, J.H. (1998). Xeroderma pigmentosum group C protein complex is the initiator of global genome nucleotide excision repair. *Mol Cell*, **2**. 223-232.

Sugasawa, K., Okamoto, T., Shimizu, Y., Masutani, C., Iwai, S and Hanaoka, F. (2001). A multistep damage recognition mechanism for global genomic nucleotide excision repair. *Genes Dev*, **15** (5). 507-21.

Sun, Z.W. and Allis, C.D. (2002). Ubiquitination of histone H2B regulates H3 methylation and gene silencing in yeast. *Nature*, **418**. 104-108.

Sung, J.-S. and Demple, B. (2006). Roles of base excision repair subpathways in correcting oxidized abasic sites in DNA. *FEBS J*, **273**. 1620–1629.

Sutherland, B.M., Harber, L.C. and Kochevar, I.E. (1980). Pyrimidine dimer formation and repair in human skin. *Cancer Res*, **40**. 3181-3185.

Svejstrup, J.Q., Wang, Z., Feaver, W.J., Wu, X., Bushnell, D.A., Donahue, D.F., Friedberg, E.C. and Kornberg, R.D. (1995). Different forms of TFIIH for transcription and DNA repair: holo-TFIIH and a nucleotide excision repairosome. *Cell*, **80** (1). 21-28.

Sweeney, F.D., Yang, F., Chi, A., Shabanowitz, J., Hunt, D.F. and Durocher, D. (2005). Saccharomyces cerevisiae Rad9 Acts as a Mec1 Adaptor to Allow Rad53 Activation. *Curr Biol*, **15** (15). 1364-1375.

Syntichaki, P., Topalidou, I. and Thireos, G. (2000). The Gcn5 bromodomain co-ordinates nucleosome remodelling. *Nature*, **404**. 414-417.

Taddei, Maison, C., Roche, D. and Almouzni, G. (2001). Reversible disruption of pericentric heterochromatin and centromere function by inhibiting deacetylases in mammals. *Nat Cell Biol,* **4**. 114-120.

Tan, S. and Richmond, T.J. (1998). Crystal structure of the yeast MATalpha2/MCM1/DNA ternary complex. *Nature,* **391** (6668). 660-666.

Tang, J.Y., Hwang, B.J., Ford, J.M., Hanawalt, P.C. and Chu, G. (2000). Xeroderma pigmentosum p48 gene enhances global genomic repair and suppresses UV-induced mutagenesis. *Mol Cell,* **5**. 737-744.

Tanny, J.C. and Moazed, D. (2001). Coupling of histone deacetylation to NAD breakdown by the yeast silencing protein Sir2: evidence for acetyl transfer from substrate to and NAD breakdown product. *Proc Natl Acad Sci USA,* **98** (2). 415-420.

Taunton, J., Hassig, C.A. and Schreiber, S.L. (1996). A mammalian histone deacetylase related to yeast transcriptional regulator Rpd3p. *Science,* **272**. 408-411.

Taylor, A.M.R., Oxford, J.M. and Metcalfe, J.A. (1981). Spontaneous cytogenetic abnormalities in lymphocytes from 13 patients with ataxia telangiectasia. *Int J Cancer,* **27**. 311-319.

Teng, Y., Li, S., Waters, R. and Reed, S.H. (1997). Excision repair at the level of the nucleotide in the Saccharomyces cerevisiae MFA2 gene: mapping of where enhanced repair in the transcribed strand begins or ends and identification of only a partial rad16 requisite for repairing upstream control sequences. *J Mol Biol,* **267**. 324-337.

Teng, Y., Longhese, M., McDonough, G. and Waters, R. (1998). Mutants with changes in different domains of yeast replication protein A exhibit differences in repairing the control region, the transcribed strand and the non-transcribed strand of the *Saccharomyces cerevisiae MFA2* gene. *J Mol Biol,* **280** (3). 355-363.

Teng, Y. and Waters, R. (2000). Excision repair at the level of the nucleotide in the upstream control region, the coding sequence and in the region where transcription terminates of the *Saccharomyces cerevisiae MFA2* gene and the role of *RAD26. Nucleic Acids Res,* **28** (5). 1114-1119.

Teng, Y., Yu, S. and Waters, R. (2001). The mapping of nucleosomes and regulatory protein binding sites at the *Saccharomyces cerevisiae MFA2* gene: a high resolution approach. *Nucleic Acids Res,* **29** (13). e64.

Teng, Y., Yu, Y., Ferreiro, J.A. and Waters, R. (2005). Histone acetylation, chromatin remodelling, transcription and nucleotide excision repair in *S. cerevisiae*: studies with two model genes. *DNA Repair (Amst),* **4** (8). 870-883.

Teng, Y., Yu, Y. and Waters, R. (2002). The *Saccharomyces cerevisiae* histone acetyltransferase Gcn5 has a role in the photoreactivation and nucleotide excision repair of UV-induced cyclobutane pyrimidine dimers in the MFA2 gene. *J Mol Biol,* **316**. 489-499.

Terleth, C., van Sluis, C.A. and van de Putte, P. (1989). Differential repair of UV damage in *Saccharomyces cerevisiae. Nucleic Acids Res,* **17** (12). 4433-4439.

Thoma, F. (1999). Light and dark in chromatin repair: repair of UV-induced DNA lesions by photolyase and nucleotide excision repair. *EMBO J,* **18** (23). 6585-6595.

Thoma, F. (2005). Repair of UV lesions in nucleosomes – intrinsic properties and remodelling. *DNA Repair (Amst),* **4** (8). 855-869.

Tijsterman, M. and Brouwer, J. (1999). Rad26, the yeast homolog of the Cockayne syndrome B gene product, counteracts inhibition of DNA repair due to RNA polymerase II transcription. *J Biol Chem,* **274** (3). 1199-1202.

Tijsterman, M., de Pril, R., Tasseron-de Jong, J.G. and Brouwer, J. (1999). RNA polymerase II transcription suppresses nucleosomal modulation of UV-induced (6-4) photoproduct and cyclobutane pyrimidine dimer repair in yeast. *Mol Cell Biol,* **19**. 934-940.

Todo, T., Kim, S.T., Hitomi, K., Otoshi, E., Inui, T., Morioko, H., Kobayashi, H, Ohtsuka, E., Toh, H. and Ikenaga, M. (1997). Flavin adenine dinucleotide as a chromophore of the *Xenopus* (6-4) photolyase. *Nucleic Acids Res,* **25** (4). 764-768.

Todo, T., Ryo, H., Yamamoto, K., Toh, H., Inui, T., Ayaki, H., Nomura, T and Ikenaga, M. (1996). Similarity among the *Drosophila* (6-4) photolyase, a human photolyase homolog and the DNA photolyase-blue-light phororeceptor family. *Science,* **272** (5258). 109-112.

Toh, G.W., Lowndes, N.F. (2003). Role of the Saccharomyces cerevisiae Rad9 protein in sensing and responding to DNA damage. *Biochem Soc Trans,* **31** (1). 242-246.

Tong, J.K., Hassig, C.A., Schnitzler, G.R., Kingston, R.E. and Schreiber, S.L. (1998). Chromatin deacetylation by an ATP-dependent nucleosome remodelling complex. *Nature,* **395** (6705). 917-21.

Tornaletti, S. and Hanawalt, P.C. (1999). Effect of DNA lesions on transcription elongation. *Biochimie,* **81**. 139-146.

Tsutakawa, S.E. and Cooper, P.K. (2000). Transcription-coupled repair of oxidative damage in human cells: mechanisms and consequences. *Cold Spring Harbor Symp Quant Biol,* **65**. 201-215.

Turner, B.M. (1993). Decoding the nucleosome. *Cell,* **75**. 5-8.

Ura, K., Araki, M., Saeki, H., Masutani, C., Ito, T., Iwai, S., Mizukoshi, T., Kaneda, Y. and Hanaoka, F. (2001). ATP-dependent chromatin remodelling facilitates nucleotide excision repair of UV-induced DNA lesions in synthetic dinucleosomes. *EMBO J,* **20** (8). 2004-2014.

Ura, K. and Hayes, J.J. (2002). Nucleotide excision repair and chromatin remodelling. *Eur J Biochem,* **269**. 2288-2293.

Ushinsky, S.C., Bussey, H., Ahmed, A.A., Wang, Y, Friesen, J., Wulliams, B.A. and Storms, R.K. (1997). Histone H1 in Saccharomyces cerevisiae. *Yeast,* **13** (2). 151-61.

van den Boom, V., Jaspers, N.G.J. and Vermeulen, W. (2002). When machines get stuck: obstructed RNA polymerase II: displacement. *Bioessays,* **24**. 780-784.

van Gool, A.J., Verhage, R., Swagemakers, S.M., van de Putte, P., Brouwer, J, Troelstra, C., Bootsma, D. and Hoeijmakers, J.H. (1994). *RAD26,* the functional *S. cerevisiae* homolog of the Cockayne syndrome B gene. *EMBO J,* **13** (22). 5361-5369.

van Houten, B. (1990). Nucleotide excision repair in *Escherichia coli. Microbiol Rev,* **54**. 18-51.

Van Hoffen, A., Venema, J., Meschini, R., van Zeeland, A.A. and Mullenders, L.H.F. (1995). Transcription coupled repair removes both cyclobutane pyrimidine dimers and 6-4 photoproducts with equal efficiency and in a sequential way from transcribed DNA in Xeroderma pigmentosum group C fibroblasts. *EMBO J,* **14**. 360-367.

Verdin, E., Dequiedt, F. and Kasler, H.G. (2003). Class II histone deacetylases: versatile regulators. *Trends Genet,* **19** (5). 286-293.

Verhage, R., Zeeman, A.M., de Groot, N., Gleig, F., Bang, D.D., van de Putte, P. and Brouwer, J. (1994). The *RAD7* and *RAD16* genes, which are essential for pyrimidine dimer removal from the silent mating type loci, are also required for repair of the non-transcribed strand of an active gene in *Saccharomyces cerevisiae. Mol Cell Biol,* **14** (9). 6135-6142.

Verhage, R.A., Van de Putte, P. and Brouwer, J. (1996). Repair of rDNA in *Saccharomyces cerevisiae*: RAD4-independent strand-specific nucleotide excision repair of RNA polymerase I transcribed genes. *Nucleic Acids Res*, **24**. 1020-1025.

Verhage, R.A., Heyn, J., van de Putte, P. and Brouwer, J. (1997) Transcription elongation factor S-II is not required for transcription-coupled repair in yeast. *Mol Gen Genet*, **254** (3). 284-290.

Verhage, R.A., Tijsterman, M., van de Putte, P. and Brouwer, J. (1998). Transcription-coupled and global genome nucleotide excision repair. In: *Nucleic Acids and Molecular Biology*, Vol **12**. Eckstein, F. and Lilley, D.M.J. (eds). 157-172. Springer-Verlag, Berlin, Germany.

Veron, M., Zou, Y., Yu, Q., Bi, X., Selmi, A., Gilson, E. and Defossez, P.A. (2006). Histone H1 of Saccharomyces cerevisiae inhibits transcriptional silencing. *Genetics*, **173** (2). 579-587.

Vettese-Dadey, M., Grant, P.A., Hebbes, T.R., Crane-Robinson, C., Allis, C.D. and Workman, J.L. (1996). Acetylation of Histone H4 Plays a Primary Role in Enhancing Transcription Factor Binding to Nucleosomal DNA *in vitro*. *EMBO J*, **15**. 2508-2518.

Vidal, M., Strich, R., Esposito, R.E. and Gaber, R.F. (1991). *RPD1* (*SIN3/UME4*) is required for maximal activation and repression of diverse yeast genes. *Mol Cell Biol*, **11**, 6306–6316.

Voelter-Mahlknecht, S., Ho, A.D. and Mahlknecht, U. (2005). Chromosomal organization and localization of the novel class IV human histone deacetylase 11 gene. *Int J Mol Med*, **16** (4). 589-598.

Vogelauer, M., Wu, J., Suka, N. and Grunstein, M. (2000). Global histone acetylation and deacetylation in yeast. *Nature*, **408** (6811). 495-498.

Volker, M., Mone, M.J., Karmakar, P., van Hoffen, A., Schul W., Vermeulen W., Hoeijmakers J.H., van Driel R., van Zeeland A.A. and Mullenders L.H. (2001). Sequential assembly of the nucleotide excision repair factors in vivo. *Mol Cell*, **8** (1). 213-24.

Wade, P.A. (2001). Transcriptional control at regulatory checkpoints by histone deacetylases: molecular connections between cancer and chromatin. *Hum Mol Genet*, **10**. 693-698.

Wade, P.A., Pruss, D. and Wolffe, A.P. (1997). Histone acetylation: chromatin in action. *TIBS*, **22**. 128-132.

Waga, S. and Stillman, B. (1998). The DNA replication fork in eukaryotic cells. *Annu Rev Biochem*, **67**. 721-751.

Wagner, E.K., Rice, M. and Sutherland, B.M. (1975). Photoreactivation of herpes simplex virus in human fibroblasts. *Nature* (London), **254**. 627-628.

Wahi, M. and Johnson, A.D. (1995). Identification of genes required for alpha 2 repression in Saccharomyces cerevisiae. *Genetics*, **140** (1).79-90.

Wakasugi, M., Reardon, J.T., Sancar, A. (1997). The non-catalytic function of XPG protein during dual incision in human nucleotide excision repair. *J Biol Chem*, **272**. 16030–16034.

Walia, H., Chen, H.Y., Sun, J.-M., Holth, L.T. and Davie, J.R. (1998). Histone acetylation is required to maintain the unfolded nucleosome structure associated with transcribing DNA. *J Biol Chem*, **273** (23). 14516-14522.

Walker, G.C. (2000). Understanding the complexity of an organism's responses to DNA damage. *Cold Spring Harbour Symp Quantit Biol*, **65**. 1-10.

Wang, A., Kurdistani, S.K. and Grunstein, M. (2002). Requirement of Hos2 histone deacetylase for gene activity in yeast. *Science*, **298** (5597). 1412-1414.

Wang, C.I. and Taylor, J.S. (1991). Site-specific effect of thymine dimer formation on dAn.dTn tract bending and its biological implications. *Proc Natl Acad Sci USA*, **88**. 9072-9076.

Wang, J.Y. (1998). Cellular responses to DNA damage. *Curr Opin Cell Biol*, **10** (2). 240-247.

Wang, W. (2003). The SWI/SNF family of ATP-dependent chromatin remodelers: similar mechanisms for diverse functions. *Curr Top Microbiol Immunol*, **274**. 143-169.

Wang, Z., Svejstrup, J.Q., Feaver, W.J., Wu, X., Kornberg, R.D. and Friedberg, E.C. (1994). Transcription factor b (TFIIH) is required during nucleotide-excision repair in yeast. *Nature*, **368** (6466). 74-76.

Wang, Z., Buratowski, S., Svejstrup, J.Q., Feaver, W.J., Wu, X., Kornberg, R.D., Donahue, T.F. and Friedberg, E.C. (1995). The yeast TFB1 and SSL1 genes, which encode subunits of transcription factor IIH, are required for nucleotide excision repair and RNA polymerase II transcription. *Mol Cell Biol*, **15** (4). 2288-2293.

Wang, Z., Wei, S., Reed, S.H., Wu, X., Svejstrup, J.Q., Feaver, W.J., Kornberg, R.D. and Friedberg, E.C. (1997). The *RAD7, RAD16* and *RAD23* genes of *Saccharomyces cerevisiae:* requirement for transcription-independent nucleotide excision repair *in vitro* and interactions between the gene products. *Mol Cell Biol*, **17** (2). 635-643.

Wang, Z.G., Wu, X.H. and Friedberg, E.C. (1991). Nucleotide excision repair of DNA by human cell extracts is repressed in reconstituted nucleosomes. *J Biol Chem*, **266**. 22472-22478.

Waters, R.W. (2006). Maintaining genome integrity

Watson, A. D., Edmonson, D.G., Bone, J.R., Mukai, Y., Yu, Y., Du, W., Stillman, D.J. and Roth, S.Y. (2000). Ssn6-Tup1 interacts with class I histone deacetylases required for repression. *Genes & Dev*, **14**. 2737-2744.

Watson, J..D. and Crick, F.H.C. (1953a). A structure for deoxyribose nucleic acid. *Nature*. **171**. 737-738.

Watson, J..D. and Crick, F.H.C. (1953b). Genetic implications of the structure of deoxyribose nucleic acid. *Nature*. **171**. 964-967.

Weeda, G., Eveno, E., Donker, I., Vermeulen, W., Chevallier-Lagente, O., Taieb, A., Stary, A., Hoeijmakers, J.H., Mezzina, M. and Sarasin, A. (1997). A mutation in the XPB/ERCC3 DNA repair transcription gene, associated with trichothiodystrophy. *Am J Hum Genet*, **60**. 320–329.

Weinert, T.A. and Hartwell, L.H. (1990). Characterization of RAD9 of Saccharomyces cerevisiae and evidence that its function acts posttranslationally in cell cycle arrest after DNA damage. *Mol Cell Biol*, **10** (12). 6554-6564.

Wellinger, R.E. and Thoma, F. (1997). Nucleosome structure and positioning modulate excision repair in the non-transcribed strand of an active gene. *EMBO J*, **16**. 5046-5056.

Widom, J. (1998). Structure, dynamics and function of chromatin in vitro. *Annu Rev Biophys Biomol Struct*, **27**. 285-327.

Williams, J.I. and Friedberg, E.C. (1982). Increased levels of unscheduled DNA synthesis in UV-irradiated human fibroblasts pretreated with sodium butyrate. *Photochem Photobiol*, **36**. 423-427.

Wilson, K.L. and Herskowitz, I. (1984). Negative regulation of *STE6* gene expression by the alpha 2 product of *Saccharomyces cerevisiae*. *Mol Cell boil*, **4** (11). 2420-2427.

Wolffe, A.P. (1998). *Chromatin structure and function*. (3rd Edn). Academic Press, New York.

Wolffe, A.P. and Hansen, J.C. (2001). Nuclear visions: functional flexibility from structural instability. *Cell,* **104**. 631-634.

Wolffe, A.P. and Hayes, J.J. (1999). Chromatin disruption and modification. *Nucleic Acids Res,* **27** (3). 711-720.

Woo, R.A. and Poon, R.Y. (2003). Cyclin-dependent kinases and S phase control in mammalian cells. *Cell Cycle.* **2**(4). 316-324.

Wood, R..D. (1997). Nucleotide excision repair in mammalian cells. *J Biol Chem.* **272** (38). 23465-23468.

Wood, R..D. (1999). Genetic DNA damage recognition during nucleotide excision repair in mammalian cells. *Biochimie.* **81**. 39-44.

Wittschieben, B.O., Iwai, S. and Wood, R.D. (2005). DDB1-DDB2 (xeroderma pigmentosum group E) protein complex recognizes a cyclobutane pyrimidine dimer, mismatches, apurinic/apyrimidinic sites, and compound lesions in DNA. *J Biol Chem,* **280** (48). 39982-39989.

Workman, J.L. and Kingston, R.E. (1998). Alteration of nucleosome structure as a mechanism of transcriptional regulation. *Ann Rev Biochem,* **67**. 545-579.

Wu, J. and Grunstein, M. (2000). 25 years after the nucleosome model: chromatin modifications. *Trends Biochem Sci,* **25**. 619-623.

Wu, X., Guo, D., Yuan, F. and Wang, Z. (2001). Accessibility of DNA polymerases to repair synthesis during nucleotide excision repair in yeast cell-free extracts. *Nucleic Acids Res,* **29** (14). 3123-3130.

Wu, J., Suka, N., Carlson, M., and Grunstein, M. (2001b). TUP1 utilises histone H3/H2B-specific HDA1 deacetylase to repress gene activity in yeast. *Mol Cell,* **7,** 117–126.

Wyatt, H.R., Liaw, H., Green, G.R. and Lustig, A.J. (2003) Multiple roles for *Saccharomyces cerevisiae* histone H2A in telomere position effect, Spt phenotypes and double-strand-break repair. *Genetics,* **164**. 47–64.

Yang, X.J. and Grégoire, S. (2005). Class II histone deacetylases: from sequence to function, regulation and clinical implication. *Mol Cell Biol,* **25**. 2873-2884.

Yang, X.J. and Seto, E. (2003). Collaborative spirit of histone deacetylases in regulating chromatin structure and gene expression. *Curr Opin Genet Dev,* **13**. 143–153.

Yasui, A. and Eker, A.P. (1998). DNA photolyases. In Nickoloff, J.A. and Hoekstra, M.F. (Ed), *DNA Damage and Repair.* Vol. 2, *DNA repair in higher eukaryotes.* The Humana Press Inc., Totowa, NJ. 9-32.

Yasui, A., Eker, A.P., Yasuhira, S., Yajima, H., Kobayashi, T., Takao, M. and Oikawa, A. (1994). A new class of DNA photolyases present in various organisms including aplacental mammals. *EMBO J,* **13** (24). 6143-6151.

You, Z., Feaver, W.J. and Friedberg, E.C. (1998). Yeast RNA polymerase II transcription in vitro is inhibited in the presence of nucleotide excision repair: complementation of inhibition by Holo-TFIIH and requirement for *RAD26. Mol Cell Biol,* **18** (5). 2668-2676.

Yu, S., Owen-Hughes, T., Friedberg, E.C., Waters, R. and Reed, S.H. (2004). The yeast Rad7/Rad16/Abf1 complex generates superhelical torsion in DNA that is required for nucleotide excision repair. *DNA Repair (Amst),* **3** (3). 277-287.

Yu, Y., Teng, Y., Liu, H., Reed, S.H. and Waters, R. (2005). UV irradiation stimulates histone acetylation and chromatin remodeling at a repressed yeast locus. *Proc Natl Acad Sci USA,* **102** (24). 8650-8655.

Zaman, Z., Ansari, A.Z., Koh. S.S., Young, R. and Ptashne, M. (2001). Interaction of a transcriptional repressor with the RNA polymerase II holoenzyme plays a crucial role in repression. *Proc Natl Acad Sci USA,* **98**. 2550-2554.

Zhang, Z. and Reese, J.C. (2004). Redundant mechanisms are used by Ssn6-Tup1 in repressing chromosomal gene transcription in Saccharomyces cerevisiae. *J Biol Chem,* **279** (38). 39240-39250.

Zhang, Y., Sun, Z.W., Iratni, R., Erdjument-Bromage, H., Tempst, P., Hampsey, M. and Reinberg, D. (1998). SAP30, a novel protein conserved between human and yeast, is a critical component of a histone deacetylase complex. *Mol Cell,* **1**. 1021-1031.

Zhao, R. et al (2000). Analysis of p53-regulated gene expression patterns using oligonucleotide arrays. *Genes Dev,* **14**. 981-993.

Zhou, B.B. and Elledge, S.J. (2000). The DNA damage response: putting checkpoints in perspective. *Nature,* **408** (6811). 433-439.

Zhou, J. Ahn, J., Wilson, S.H. and Prives, C. (2001). A role for p53 in base excision repair. *EMBO J,* **20**. 914–923.